2014

Syntheses and characterization of isoporphyrins and BODIPYs for PDT and imaging

Haijun Wang
Louisiana State University and Agricultural and Mechanical College, hwang12@tigers.lsu.edu

SYNTHESES AND CHARACTERIZATION OF ISOPORPHYRINS AND BODIPYS FOR PDT AND IMAGING

A Dissertation

Submitted to Graduate Faculty of the
Louisiana State University and
Agricultural and Mechanical College
in partial fulfillment of the
requirements for the degree of
Doctor of Philosophy

in

The Department of Chemistry

by
Haijun Wang
B.S., Northwest University, 2001
M.S., Chinese Academy of Sciences, 2006
May 2014

Dedicated to my parents, my brother and sisters

Acknowledgements

First of all, I want to thank Dr. Kevin M. Smith for taking me as his student and for guiding me throughout my Ph.D. studies. It has been such an honor working with him. He is a tremendous mentor, not only as a chemist but also as an individual person. His passion and enthusiasm for chemistry always spurred me on to greater efforts in the laboratory. He had a many great ideas for my projects. In the meantime, he also gave me enough freedom to work on my own ideas. He has a big heart and a great personality; I was never afraid to venture my ideas and solutions to him. There is so much I want to say here; very last, I want to thank him for the time he spent on my Dissertation. It took a lot of patience to suggest revisions.

I also would like to take this chance to thank Dr. M. Graca H. Vicente for her support. She gave me many suggestions for my projects and always encouraged me. She is so considerate and nice. Working with her was always breezy and joyful. I also want to thank her for the help she gave me in my job search.

Many thanks are also due to my committee members, Dr. William Crowe, Dr. David Spivak and Dr. Ricardo Estrada for their thoughts and for the time they put into supporting my graduate studies. I enjoyed their lectures and learned a lot from their classes. I also want to give my thanks to Dr. Frank R. Fronczek for his efforts to determine crystal structures of my new compounds and to Dr. W. Dale Treleaven and Dr. Thomas Weldegheorghis for their help with the Dep[artmental NMR facilities. I also thank Connie David for mass spectroscopy determinations. Thanks also to Dr. Xiaoke Hu and to Zehua Zhou for their contributions to the cellular studies.

I have spent so much wonderful time with my previous lab-mates: Dr. R. G. Waruna Jinadasa, Dr. Moses I. Ihachi, Dr. Benson G. Ongarora, Dr. N. V. S. Dinesh Bhupathiraju,

Dr. Timsy Uppal, Dr. Alecia M. McCall, Dr. Krystal R. Fontenot and Dr. Javoris V. Hollingsworth. This also goes for my curruent lab-mates Jamie Hayes, Ning Zhao, Elizabeth Okoth, Daniel J. LaMaster, Qianli Meng, Alex L. Nguyen and Tyrslai Williams. There were ups and downs with my research, but laughter with you guys was always a happy and enjoyable part of my lab life.

My family has always been there for me no matter what happens. They are the people who care about me the most in this world. I want to thank my parents, my brother and my sisters for their unconditional love and support.

Table of Contents

Glossary of Abbreviations

Ac Acetyl

Bn……..Benzyl

BOC……..tert-butoxycarbonyl

BODIPY……...4,4-Difluoro-4-bora-3a,4a-diaza-*s*-indacene

BOP-Cl…….Bis(2-Oxo-3-Oxazolidinyl)phosphonic Choride

n-BuLi……n-Butyl lithium

DCM…….Dichloromethane

DCC……..N,N'-dicyclohexylcarbodiimide

1,2-DCE……1,2-Dichloroethane

DDQ…….2,3-Dichloro-5,6-dicyanobenzoquione

DIEA……..N,N-Diisopropylethylamine

DMAP……...4-Dimethylaminopyridine

DME……..Dimethoxyethane

DMF……...N,N-dimethylformamide

DMSO……...Dimethyl sulfoxide

EDC……...1-Ethyl-3-(3-dimethylaminopropyl)carbodiimide

ESI-MS…….....Electrospray Ionization Mass Spectrometry

ER……...Endoplasmic Reticulum

Et……..Ethyl

FMOC…….9-fluorenylmethoxycarbonyl

HATU……..2-(1*H*-7-Azabenzotriazol-1yl)-1,1,3,3-tetramethyl uranium heafluorophosphate

HBTU……...*O*-Benzotriazole-N,N,N’,N’-tetramethyl-uronium hexafluorophosphate

HRMS……..High Resolution Mass Spectrometry

HOBt……Hydroxybenzotriazole

LTA……..Lead(IV) acetate

MALDI……Matrix-assisted Laser Desorption/Ionization

Me……...Methyl

MW…….……Molecular Weight

m/z……..Mass to charge ratio

nm……...Nanometer

NMR……Nuclear Magnetic Resonance

Pc…….Phthalocyanine

Pd/C…….....Palladium on Carbon

PDT…….....Photodynamic Therapy

P^{Me}……...Methyl propionate

Ph……..Phenyl

ppm…….....Parts per Million

PyBOP-PF_6……..Benzotriazol-1yl-oxytripyrrolidinophosphonium hexafluorophosphate

RT…….....Room Temperature

TBTU……O-(Benzotriazol-1yl)-N,N,N',N'-tetramethyluronium tetrafluoroborate

TEA……..Triethylamine

TES……..Triethylsilane

Tf……..Triflate

TFA……..Trifluoroacetic Acid

THF……..Tetrahydrofuran

TLC……..Thin Layer Chromatography

TMS…….....Trimethylsilane

TMOF……..Trimethylorthoformate

TEOF……...Triethylorthoformate

p-TsOH…….....*p*-Toluenesulfonic acid

UV-vis……..Utraviolet-visible spectroscopy

µs…….Microsecond

µm…….....Microlitter

Abstract

This Dissertation is divided into five chapters reporting various aspects of the background to my field of study and the results obtained during my research program.

Chapter 1 gives a very brief introduction to photodynamic therapy including the mechanism of the treatment, the localization of photosensitizer in tumor cells, the pathways leading to tumor death and characteristics of various photosensitizers such as porphyrin-based photosensitizers and non-porphyrin based photosensitizers.

Chapter 2 reports a total synthesis of zinc(II) isoporphyrins by cyclization of b-bilene salt using α-keto esters for the macrocyclization carbon. Functionalization of the resulting zinc(II) isoporphyrins was attempted using different strategies such as direct functionalization of the isoporphyrin after cyclization of the b-bilene salt and introduction of the functional group during the cyclization of b-bilene salt.

Chapter 3 desrcibes a different total synthesis of zinc(II) isoporphyrins by way of the MacDonald 2+2 condensation approach. A serial of zinc(II) isoporphyrins were obtained and further functionalization of these compounds was also attempted by use of various hydrolytic reactions. Functionalization of dipyrromethanes before cyclization was also investigated through hydrolytic and amination reactions.

Chapter 4 explores novel syntheses of BODIPYs using pyrroketones as starting materials. Reactions of pyrroketoned including electropholic alkylation with Meerwein's salt, chlorination using phosgene, and protonation with acids were investigated. The reactivity of the derivatives, especially, 5-chloro-dipyrromethenes and 8-chloro-BODIPYs were also investigated by using replacement (substitution/elimination) and modern

organometallic coupling reactions. Some meso-substituted BODIPYs were obtained and their photophysical properties were studied, including absorption, fluorescence and quantum yields.

Chapter 5 presents a synthesis of tri-chloro-BODIPYs. Global and regioselective Stille coupling reactions were investigated using tri-chloro-BODIPYs. A novel series of new symmetrical and unsymmetrical BODIPYs s were synthesized using this method.

Chapter 1: Introduction

1.1 Photodynamic Therapy (PDT)

Photodynamic therapy (PDT) was discovered in the 19th century and matured as a viable medical technology in the 1980s at several institutions throughout the world, in countries such as Canada, USA and Japan. This treatment involves the use of photochemical reactions mediated by the interaction of a photosensitizing agent, light, and oxygen, to kill malignant tumor cells. Depending on the part of the body being treated, the drug is either injected into the bloodstream or applied to the skin; over time, the drug is preferentially absorbed by cancer cells and clears from normal cells. Then a specific wavelength of light is applied to initiate a photochemical reaction and produce singlet oxygen, the active form of oxygen, and other active oxygen spevcies which can damage the cancer cell (Figure 1.1).[1]

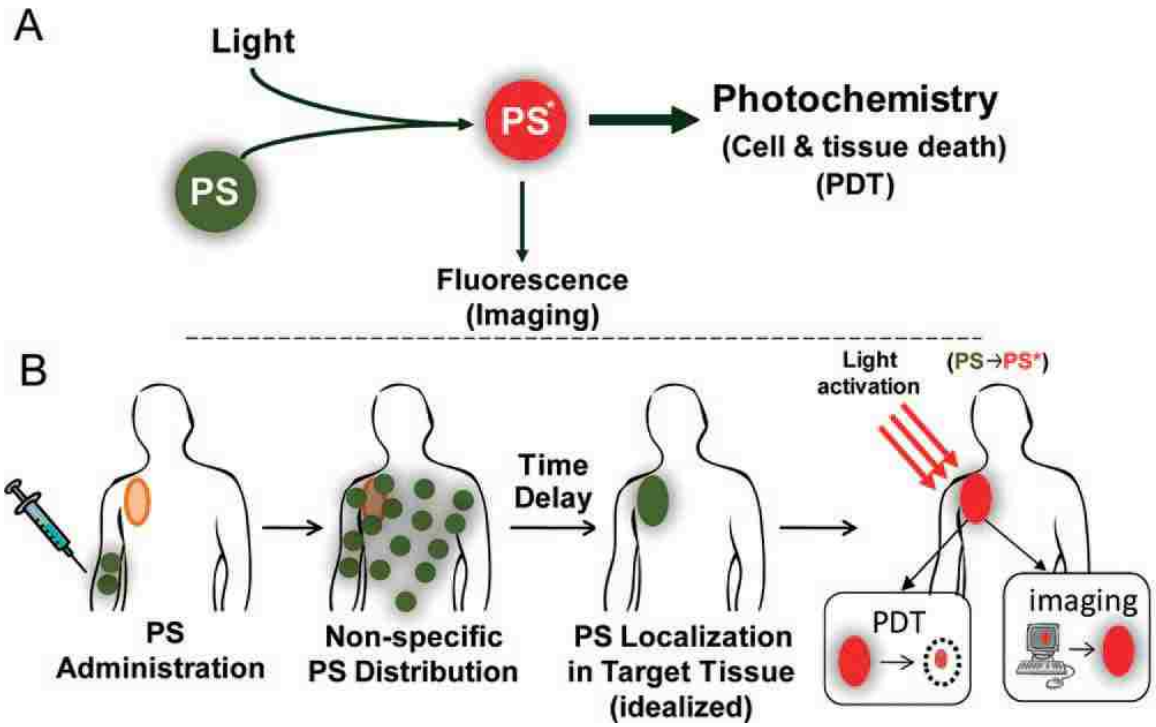

Figure 1.1: The application of photodynamic therapy.[1]

A simplified Jablonski diagram (Figure 1.2) is used to explain what actually happens during the treatment. Once photosensitizers are exposed to a specific wavelength of light, they are promoted from the ground state S_0 to the spin-allowed excited singlet states S_n; from this point, the photosensitizers can undergo several electronic changes.[3] Radiationless deactivation of photosensitizer from upper-lying excited states to the lowest excited state is a very fast process on the picosecond time scale. From the lowest excited state, the photosensitizers can release energy in the form of fluorescence and return to ground state. The pathway which involves intersystem crossing from the lowest excited singlet state to triplet state is the key process for PDT and a high population of triplet state is required to produce toxic $^1O_2$; if the triplet state population is too low, the photosensitizer will return to its ground state with the emission of light as phosphorescence. From triplet state, the photosensitizer can transfer the energy to the

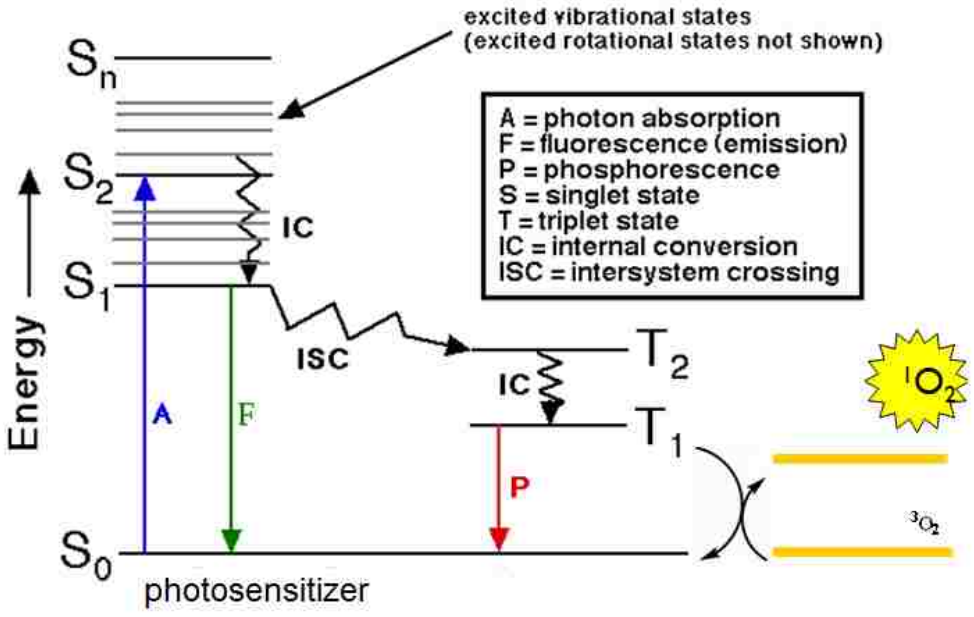

Figure1. 2: Jablonski diagram.

http://www.chemicool.com/img1/chem-ed/quantum/graphics/jablon.gif

nearby molecule triplet oxygen through spin exchange and generate the highly reactive singlet oxygen, which is believed to be one of the key species toxic to cancer cells. The half life of singlet oxygen is less than 0.04 μs and it thus has a migrating radius smaller than 0.02 μm^2, therefore making PDT a very local treatment.

1.2 Localization of Photosensitizer in Tumor Cells

It was discovered that some compounds, especially porphyrins and porphyrin derivatives, can selectively localize in tumor cells compared with normal cells.[4] Although intensive studies have been done to find out the mechanism, there is still no clear result so far. However, it has been found that all the different photosensitizers are bound to serum protein to some degree after injection into the bloodstream.[5] Based on pharmacokinetic studies of photosensitizers,[6] one of the proposals is that photosensitizers prefer to bind to albumin and heavy proteins such as HDL, LDL and VLDL. The assumption in this theory is that the tumor cell can overexpress heavy proteins such as LDL-receptors compared with normal cells since tumor cells grow faster than normal cells and they need more cholesterol to permit the rapid growth of cellular membranes. Therefore, when the photosensitizers circulate in a patient's body, most are absorbed by the tumor cells instead of normal cells. There are some other theories, more related to the structural difference between cancer cells and normal cells. It was found that tumor cells usually have a lower pH environment than do normal cells, and they therefore have affinity for anionic photosensitizers. For example, Thomas and Girotti[7] found that decrease of pH by admistrating glucose into tumor cells can result in a greater accumulation of the sensitizer hematoporphyrin derivatives (HpD). The assumption is that negatively charged photosensitizers are neutralized once protonated and therefore become more lipophilic, which is a very important property during localization since the membrane of tumor cells is also lipophilic. Another theory is related to the vascular

permeability of photosentizers to tumor cell and lymphatic drainage of tumor cells. It is well known that photosensitizers behave as macromolecules because they are either bound to large proteins or form intermolecular aggregates.[8] Vasculature is nonproliferative for adults while the vasculature of tumors has some embryonic vessels and neovasculature which are highly proliferative; the photosensitizers usually have an affinity for proliferative neovaculature[9] over nonproliferative vasculature, therefore increasing the permeability of the photosensitizers to the neovasculature of the tumor. Additionally, the tumor cells have poorly developed lymphatic drainage; the photosensitizers which extravasate from the hyperpermeable tumor neovasculature tend to remain in the extravascular space.

There are some relationships between the structures of photosensitizers and selectivity for the tumor, specifically, in different organelles of tumor cells (Figure 1.3). According to the structures of the photosensitizers, they could be classified into three categories: hydrophilic photosensitizers (such as tetra-sulfonated derivatives of tetraphenylporphine), amphiphilic photosensitizers (like benzoporphyrin derivative monoacid) and hydrophobic photosensitizers (such as unsubstituted phthalocyanines). According to whether or not the photosensitizers carry charges, they could be classified into anionic, cationic or neutral photosensitizers. Depending on the properties of photosensitizers, they can diffuse across the plasma membrane and selectively relocate in one of the organelles of the tumor cell or several of them including mitochondria, lysosomes, Golgi and Endoplasmic Reticulum (ER) or plasma. Some correlations between the characteristic of photosensitizers and their localizations in tumor cell were found through years of studies. The photosensitizers with net negative charges (anionic photosensitizers) tend to localize in the lysosomes, while the photosensitizers with positive charges (cationic photosensitizers) prefer to localize in mitochondria.[10] For example, Woodburn et al. reported the intracellular localization of a series of porphyrin

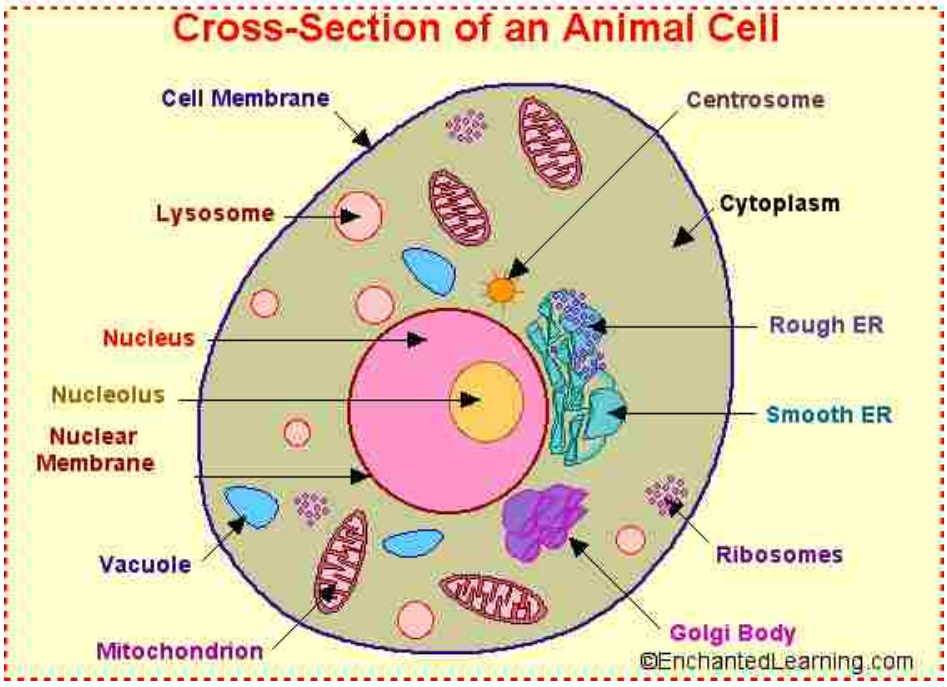

Figure 1.3: The configuration of cell.

Taken from: http://www.enchantedlearning.com/subjects/animals/cell/

derivatives with different properties (Table 1.1) such as hydrophobic, anionic or cationic characters in V79 Chinese hamster lung fibroblasts and C6 glioma cells.[11] The localization results are listed in Table 2. One can see that anionic photosensitizers **2**, 8, and **10** mainly localized in lysosomes and cationic photosensitizer **4**, **6**, **7** and **9** preferred to localize in mitochondria. Lysosomes, and mitochondria are the main subcellular compartment PDT targets. Some photosensitizers localized in the Golgi apparatus and endoplasmic reticulum (ER) instead of lysosomes and mitochondria. For instance, Foscan[12] predominantly localized in Golgi and ER with very weak accumulation in mitochondria. For the amphipathic photosensitizers, there should be a balance between hydrophobic and hydrophilic properties. Hydrophilicities can facilitate the delivery of the photosensitizers through the bloodstream and hydrophobic properties can help with the permeability of the membrane of tumor cells.

Table 1.1. Photosensitizers with Different Properties.

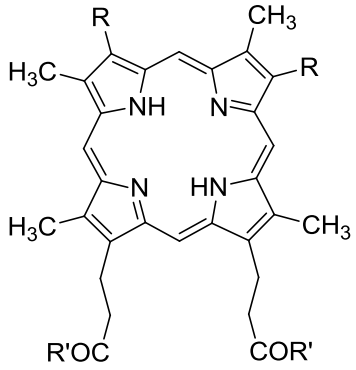

Compound	R	R’
1 (HpD)		
2	$HC(CH_3)OH$	OH
3	$HC(CH_3)OCH_3$	OCH_3
4	$CH=CH_2$	$NH(CH_2)_2N(CH_3)_2$
5	$HC(CH_3)O(CH_2)_2OCH_2CH_3$	OH
6	$HC(CH_3)O(CH_2)_2OCH_2CH_3$	$NH(CH_2)_2N(CH_3)_2$
7	$HC(CH_3)SCH_2CONH(CH_2)_2N(CH_3)_2$	$NH(CH_2)_2N(CH_3)_2$
8	$HC(CH_3)S(CH_2)_2NO$	OH
9	$HC(CH_3)S(CH_2)_2NO$	$NH(CH_2)_2N(CH_3)_2$
10	$HC(CH_3)O(CH_2)_2N(CH_3)_2$	OH

*

Table 1.2. The Localization of Photosensitizers in Different Organelles.

Compound	R	R’	Localization
1(HpD)			Diffuse cytoplasmic plus perinuclear
2	hydrophilic	Anionic	Diffuse cytoplasmic plus lysosomes
3	hydrophobic	Hydrophobic	Diffuse cytoplasmic plus lysosomes
4	hydrophobic	cationic	mitochondria
5	hydrophobic	Anionic	Diffuse cytoplasmic
6	hydrophobic	Cationic	C6; mitochondira → lysosomes V79; mitochondria → lysosomes(vacuolation)
7	Amphipathic	catioic	mitochondira
8	amphipathic	Anionic	cytoplasmic → lysosomes → lysosome engorgement

Table 1.2 continued

.

Compound	R	R'	Localization
9	amphipathic	Cationic	C6; mitochondria ⟶ lysosomes
10	amphipathic	Anionic	V79; mitochondria cytoplasmic ⟶ lysosomes ⟶ lsysosome engorgement

1.3 The Pathways Leading to Tumor Cell Death

The outcome of PDT depends on numerrous factors such as the localization of photosensitizers, tissue types, and PDT dose, etc. There is no single pathway leading to cell death; a combination of factors is necessary to achieve the optimum tumor cures. There are three main independent pathways leading to tumor cell death: (1) subcellular localization-induced apopotosis and necrosis, which is the direct tumor cell death effect of PDT; (2) vasculature destruction is another way to kill tumor cell; and (3) immune system response is the impact after the PDT is completed, and is therefore called the post-PDT effect. Apoptosis is an energy-consuming process through activation of a death receptor or the mitochondrial release of cytochrome;[13] both of these pathways could activate caspase which can cause damage to subcellular organelles such as mitochondira, lysosomes and ER, or initiate DNA fragmentation and cell shrinkage. Apoptosis is the dominant, rapid and intermediate form of tumor cell death during photodynamic therapy. Another pathway that can lead to direct tumor cell death is necrosis. Necrosis[14] has been considered an uncontrolled process caused by physical or chemical damage. It is an intense and rapid form of degeneration that can cause cytoplasmic swelling, damage to organelles and dysfunction of plasma membrane. Therefore the necrosis process really depends on the PDT dose such as high photosensitizer concentration or a high light fluence, or both; the pathway of cell death can switch from apoptotic to necrotic when the PDT dose is excessive. The localization

of photosensitizer can also play a role in the cell death pathway. Mitochondria localizing photosensitizers usually induce apoptosis while plasma membrane localizing photosensitizers are most likely to induce necrosis, which can damage the plasma membrane integrity due to acute inflammation. There are another two pathways leading

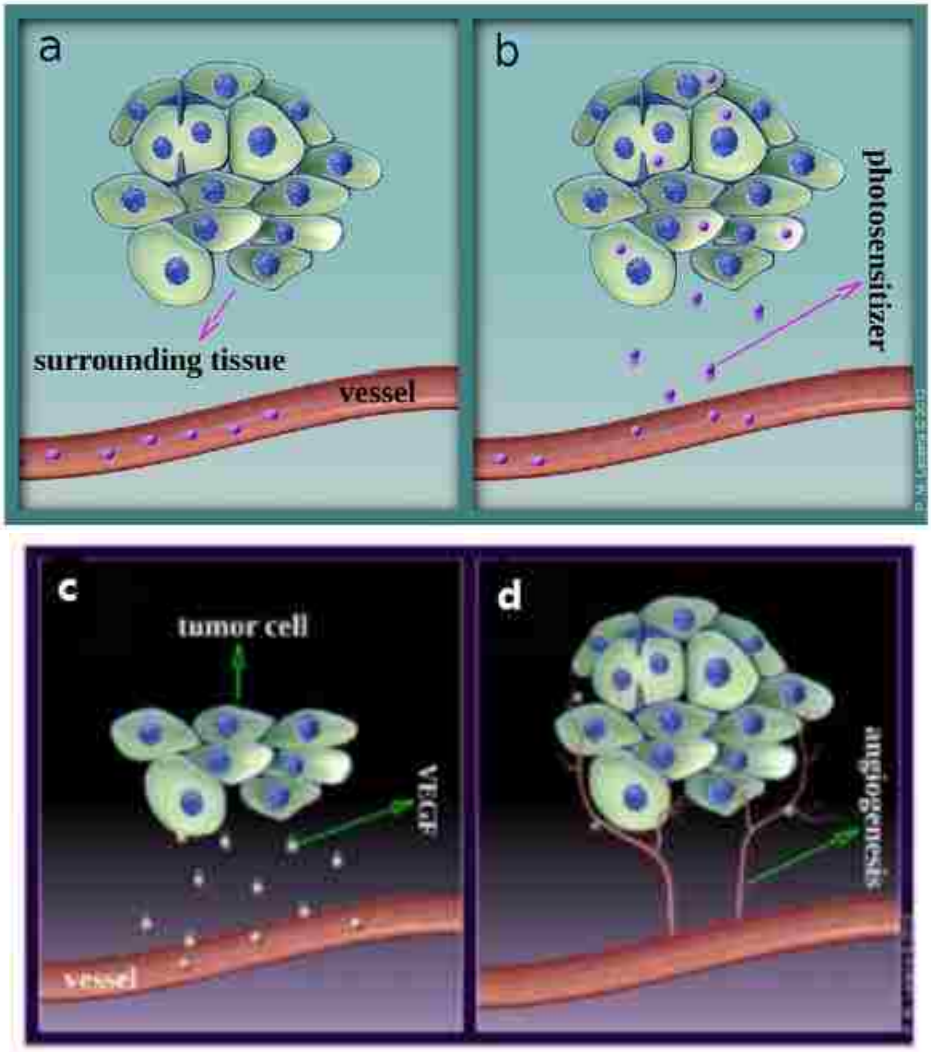

Figure 1.4: The formation of angiogenesis[15] (a) photosensitizer in the vessel at the beginning; (b) photosensitizer diffused into the surrounding tissue gradually as time increases; (c) vascular endothelial growth factor (VEGF); (d) The emergence of new blood vessels accompanied by endothelial cell proliferation and migration.

to tumor cell death beside apoptosis and necrosis. One of them is vascular damage; as was mentioned in discussion of localization in tumor cells, the blood is the medium to deliver the nutrient and oxygen to cells through vessels. Damage to the neovasculature can lead to thrombosis, hemorrhage and tissue hypoxia. Nutrient deprivation and eventual starvation can also cause death of tumor cells[15] (Figure 1.4).

Photodynamic therapy is a local treatment. However, this treatment can also have some systemic attributes since it can induce response of the immune system. PDT induced anti-tumor immunity is due to the acute inflammatory response, exposure and presentation of tumor-specific antigens.[16] With the PDT-induced destruction of the tumor cells, a strong inflammatory reaction occurs locally at the same time and enables the influx of non-affected immune cells into the PDT-site from elsewhere and result in the development of a systemic anti-tumor immune response.[17] In summary, the effect of PDT is the combination of various factors such as subcellular localization of photosensitizers, PDT dose and tissue targets, and these factors cannot be localized independently.

1.4 Lights and Penetration of Tissue.

Light is one of the non-toxic components of photodynamic therapy and is used as an energy form to activate the photosensitizers. Therefore, it is very important to develop light resources in parallel with photosensitizers. Lasers are the mostly common light source used in photodynamic therapy[18] due to their capability of generating a coherent light beam. The light could be directed to the site need to be treated through optical fibers with a 200-400 μm diameter. Figure 1.5 shows the correlation between wavelength of light and the depth of penetration into tumor.[19] Semiconductor lasers such as LED lights will be the preference in the future because they are cheap and easy to handle.

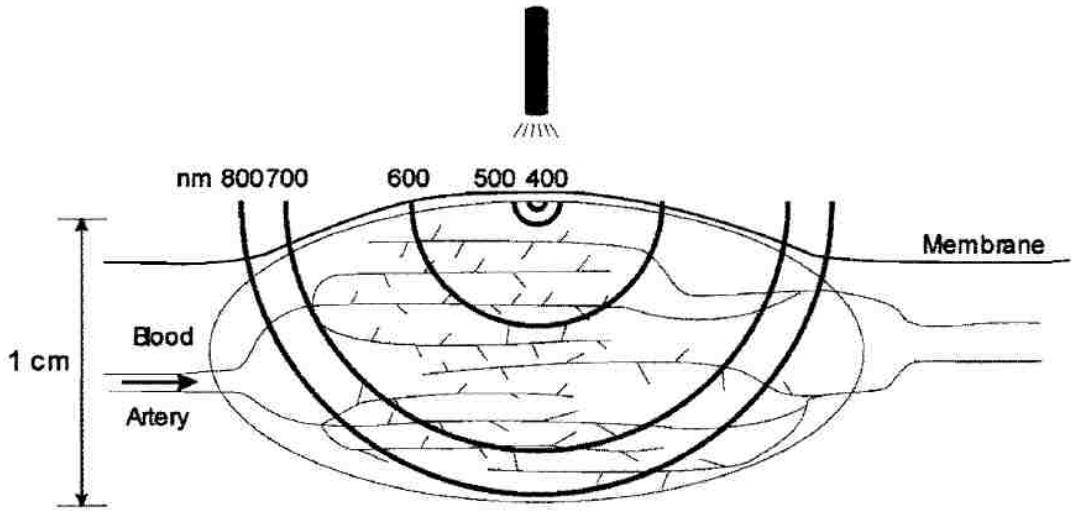

Figure 1.5: The wavelength dependence of depth of penetration of light into a tumor.[19]

1.5 Advantages and Limitations of PDT.

Photodynamic therapy is a very selective treatment of tumor cells over normal cells. It can target the tumor cell very precisely without damage to surrounding tissues due to the short-lived $^1O_2$, which only can migrate within the cell about 0.02 μm. Compared with traditional cancer treatments such as chemotherapy, radiation, and surgery, photodynamic therapy is less invasive, the only invasive operation being the technique that is used with the optical fiber, which is very small and is used to penetrate the tissue to direct the incoming light. Therefore, there is little or no scar left after treatment of superficial tumors. Another advantage of PDT is that this treatment can be used at the same site repeatedly until all cancer cells are killed.

Of course, there are some limitations with this PDT treatment. The main drawback of PDT is that it can be only used to treat early stage cancers. Once the tumor cells spread, it is hard to target any metastases. It cannot be used to treat larger tumors due to the problem of light penetration though tissues. Another inconvenience of this treatment is

that the delay time after injection of photosensitizer can be fairly long from 24 hours to 72 hours. Another complication is that the patients can remain photosensitive after treatment for some time depending on the photosensitizer used. Investigators are developing more mature photodynamic therapies to solve these issues.

1.6. Ideal Photosensitizers

To be an ideal photosensitizer, the compound should meet the following requirements to achieve a good outcome in photodynamic therapy:

1. The compound should have preferential tumor localization over normal cells. The better localization can be achieved by conjugation of biomolecule such as amino acids or sugars to the molecule.

2. The photosensitizer candidate should be able to generate singlet oxygen ($^1O_2$) efficiently which is mostly responsible for the tumor cell death in photodynamic therapy. This requires the compound to have a high quantum yield of the triplet state ($\varphi_T > 0.4$) with a long lifetime ($t > 100$ μs).

3. The photosensitizers should have an absorption region between 630-800 nm (Figure 1.6) with high extinction coefficient. The energy gap between $^3O_2$ and $^1O_2$ can be measured by observing its 1270 nm phosphorescence. By detection of the 1270 nm phosphorescence emission, theoretically, a photosensitizer with a triplet state energy higher than 94kJ/mol (1270 nm) can transfer its energy to ground state $^3O_2$. However, the photosensitizer with long wavelength absorption cannot efficiently generate singlet oxygen. For example, a reported 34-π conjugated porphyrin with absorption at 940 nm did not produce singlet oxygen.[20]

4. The photosensitizer should be nontoxic in the absence of light and have minimal residual skin photosensitivity.

5. The sensitizer should be photostable and biologically stable, and easily to soluble in injectable solvents. This requires the photosensitizer should have some amphiphilic and hydrophobic groups attached.

6. The photosensitizers should be chemically pure so that the subsequent studies such as pharmacokinetics and dose-response correlation can be performed easily.

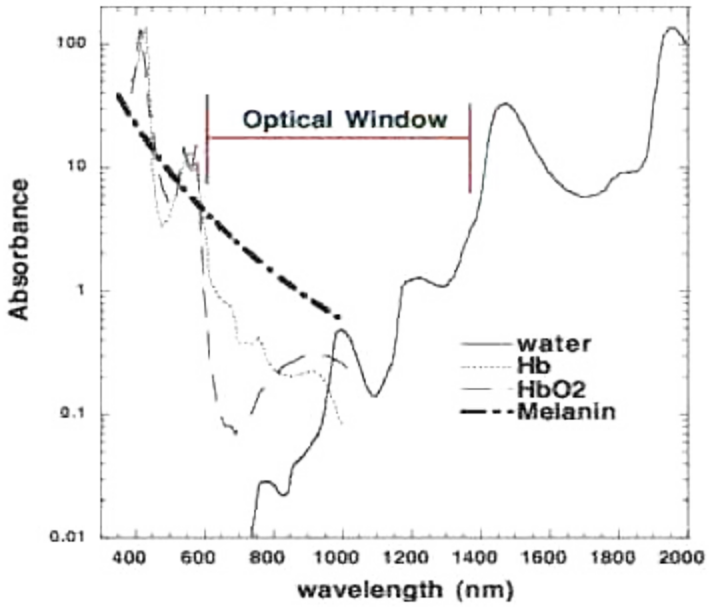

Figure1.6: The therapeutic window of photodynamic therapy.
http://www.photobiology.info/Hamblin.html

1.7. Porphyrin-based Photosensitizers

Porphyrins and their derivatives[21] are a class of very important biological products in nature. Porphyrins are the building blocks of hemoglobin and myoglobin which are the two major oxygen binding proteins in blood. These aromatic macrocyles possess 18-π electrons and have very interesting optical spectra with a Soret absorption band around 400 nm belonging to the π-π* transition and four small Q bands in the visible region. When porphyrins are reduced by breaking a cross-conjugated double bonds without

interruption of the aromaticity of macrocycle, the Q-band is red shifted with a high extinction coefficient[19] (Figure 1.7). This is probably due to perturbation introduced to the planar and symmetrical porphyrin ring and the energy of the HOMO orbital is raised and therefore reduces the energy gap between the HOMO and LUMO orbitals.[22] From the optical spectrum of porphyrins and their derivatives, one can see that their absorption in the visible and IR areas make these molecules very good candidates as potential photosensitizers. Porphyrins also possess some other potentially advantageous features including their localization in tumor cells, ability to produce singlet oxygen, their florescence, low-dark toxicity and high chemical stability. All these properties make porphyrin-based compounds extremely useful for PDT. So far, several porphyrin derivatives have been developed and some of them have been approved in countries such as Canada, the USA, Europe and Japan, for treating various cancers.

Hematoporphyrin derivatives (HpD) and photofrin[23-25] (Figure 1.8) were discovered to have the ability to selectively accumulate in neoplastic tissue and function in various malignant tissues such as carcinomas of the breast, colon, prostate and malignant melanomas. Photofrin is a purified version of hematoporphyrin derivative (HpD) and has been approved by the US FDA to treat lung cancer, esophageal cancer, malignant and nonmalignant skin diseases, and early-stage cervical cancer.[26] Due to the low extinction coefficient of the Q bands, significant dosage or a high concentration of Photofrin was needed to achieve tumor eradication. This caused serious side effects. Chemical modification of hematoporphyrin was performed to overcome the chemical complexity of Photofin by functionalization of the benzylic hydroxyl groups or by introducing different substituents.[27,28] However, the sensitizing efficiency did not change much. Other synthetic porphyrin-based photosensitizers available are meso-tetraphenylporphyrin (TPP), which was synthesized and modified by

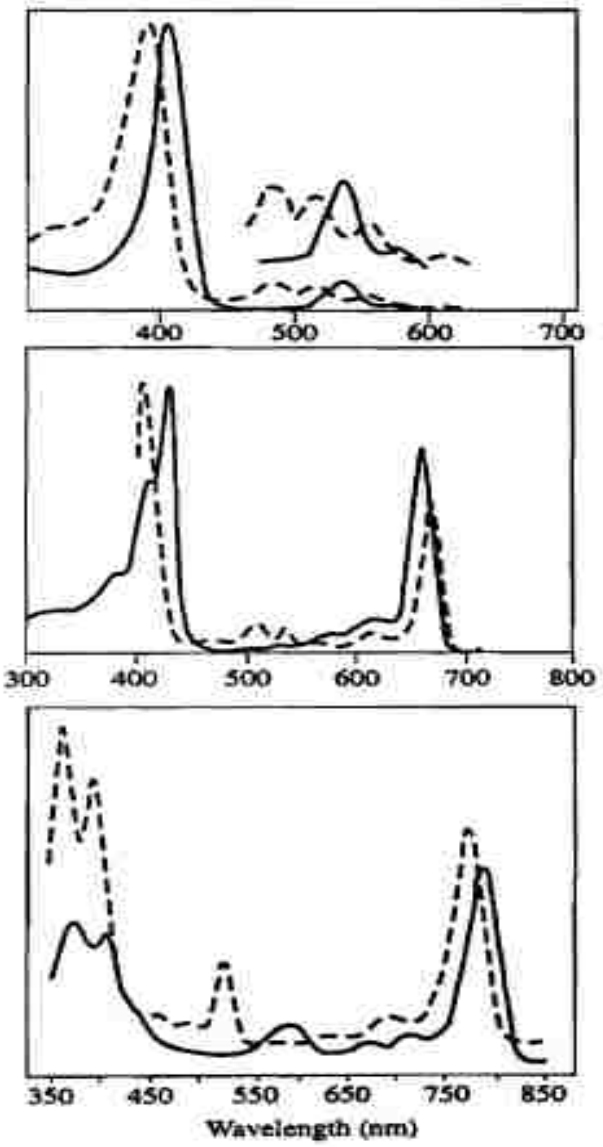

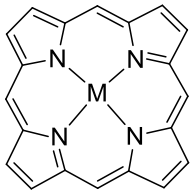

Broken line - Porphyrin (M = 2H)
solid line - metalloporphyrin (M = Metal)

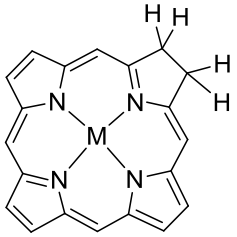

Broken line - Chlorin (M = 2H)
solid line - metallochlorin (M = Metal)

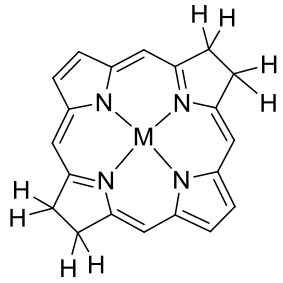

Broken line - Bacteriochlorin (M = 2H)
solid line - metalloporphyrin (M = Metal)

Figure 1.7: Optical spectra of porphyrins, chlorins, bateriochlorins and their metal complexes.[19]

several groups such as those of Hagan, Czuchajowski and Lozynski[29,30] to introduce hydrophilic groups and hydrophobic groups including hydrogen, hydroxyl and sulfonate, and reduced the porphyrin to the dihydroporphyrin (chlorin) level The investigation of biological properties of these porphyrins showed that the o, m, and p-isomers of tetra(hydroxyphenyl)chlorins have very potent activity and tissue selectivity in photo-necrosis. Especially, tetra(m-hydroxy)phenylchlorin was 25-30 times potent than HpD, and this is now marketed as Foscan.

Porphyrins usually can satisfy most of the requirements for effective photosensitizers. However porphyrins only have a small Q band with low molar extinction coefficient compared with their Soret band. The longest wavelength band of porphyrins can reach to around 650 nm. They can not be used to treat deep-seated tumors. Some reduced porphyrins were developed, such as chlorins and bacteriochlorins, to solve the problems associated with first generation porphyrin-based photosensitizers. These photosensitizers are chemically pure and have longer wavelength absorption and less side effects after treatment is completed. Since they absorb at long wavelengths, they can be used to treat large tumors because long wavelength light travels further through tissues. Figure 1.9 lists several chlorin-based photosensitizers.

Temoporfin[31] is bactieriochlorin-based photosensitizer approved in 2001 in Europe to treat neck, and head cancers and was the first sensitizer to be used to treat prostate cancer in 2002. Compared with Photofrin, this compound has a pronounced Q band at 652 nm with a higher molar extinction coefficient, therefore a smaller drug dose is needed in clinic trials and it has mild to moderate skin photosensitivity. Tumor cell death was caused through necrosis and vascular damage. Padoporfin[32,33] (palladium-bacteriopheophorbide) (figure 1.9) is a lipophilic photosensitizer which has a maximum absorption wavelength in the near-infra red region at 763 nm and could be active at a

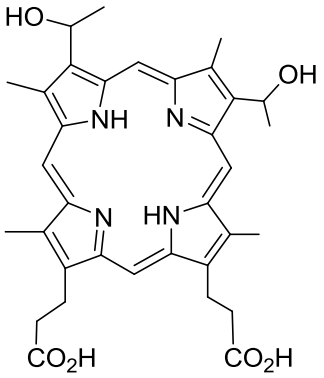

Hematoporphyrin

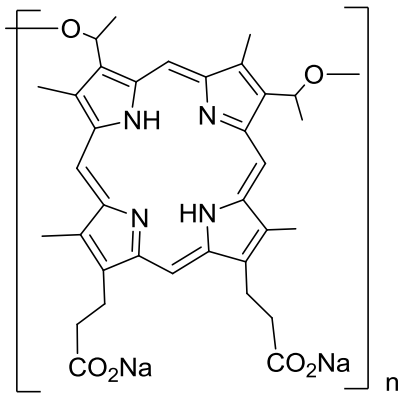

Photofrin

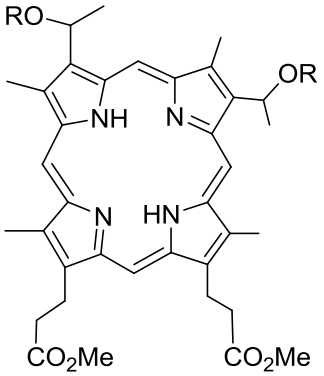

R = alkyl, phytyl

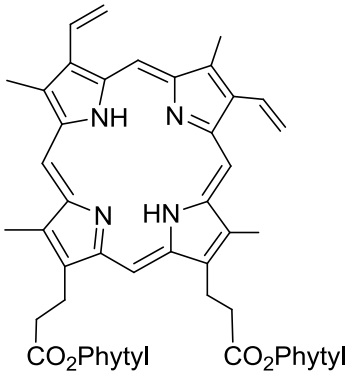

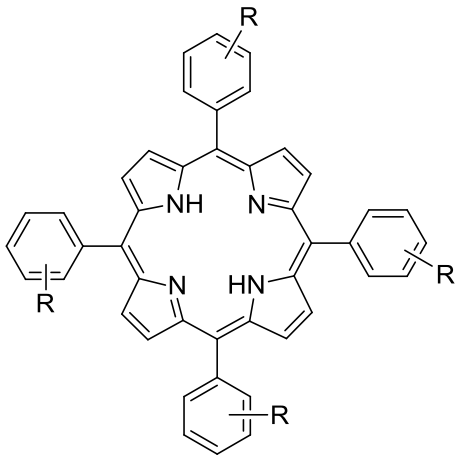

R = H, p-SO_3H, OH, $NHCOCH_3$, OCH_3,

Figure 1.8: Structure of HP, Photofrin, and other porphyrins used in PDT

penetration depth of 4 mm using appropriate light, compared with Photofrin (630 nm, 1.6 mm). Padoporfin is a vascular-acting photosensitizer and was used to treat prostate cancer in clinic studies, which showed that Padoporfin-mediated PDT has a very short drug exposure–light interval and minimal local damage.[34,35] NPe6 (talaporfin, LS II) is a second generation photosensitizer approved for the treatment of lung cancer by the in Japan. NPe6 is a hydrophilic chlorin derivative due to the aspartyl residue and has UV/Visible absorption at 664 nm with a molar extinction coefficient of 4×10^4 $M^{-1}cm^{-1}$. The clinical study[36,37] showed that NPe6 is mainly localized in plasma instead of organelles and the mechanism of tumor cell death was shown to be vascular stasis resulting from direct tumor necrosis. The possibility of using NPe6 to treat other cancers is also under investigation too in clinical trials. Only minimal skin photosensitivity was caused after the treatment. A synthetic chlorin-based photosensitizer Verteporfin was invented by Dolphin and Levy and modified by Callot et al and Pandey et al.[38,39] This compound has a pronounced Q band at 689 nm and has a very efficient generation of singlet oxygen.[40] Verteporfin is a lipophilic photosensitizer used for ocular PDT and approved for age-related macular degeneration since 2000. In vivo studies showed that it prefers to localize in neovascular endotherlium and the localization determined that tumor cell death is through vascular damage and it is 10 times more cytotoxic than hematoporphyrin in human adherent cell lines.[41] Biodistribution studies proved that Verteporfin can accumulate in the vasculature rapidly and clear from a patient's body rapidly after treatment. It is metabolized in a less reactive form and in this way reduced the photosensitivity period.[42]

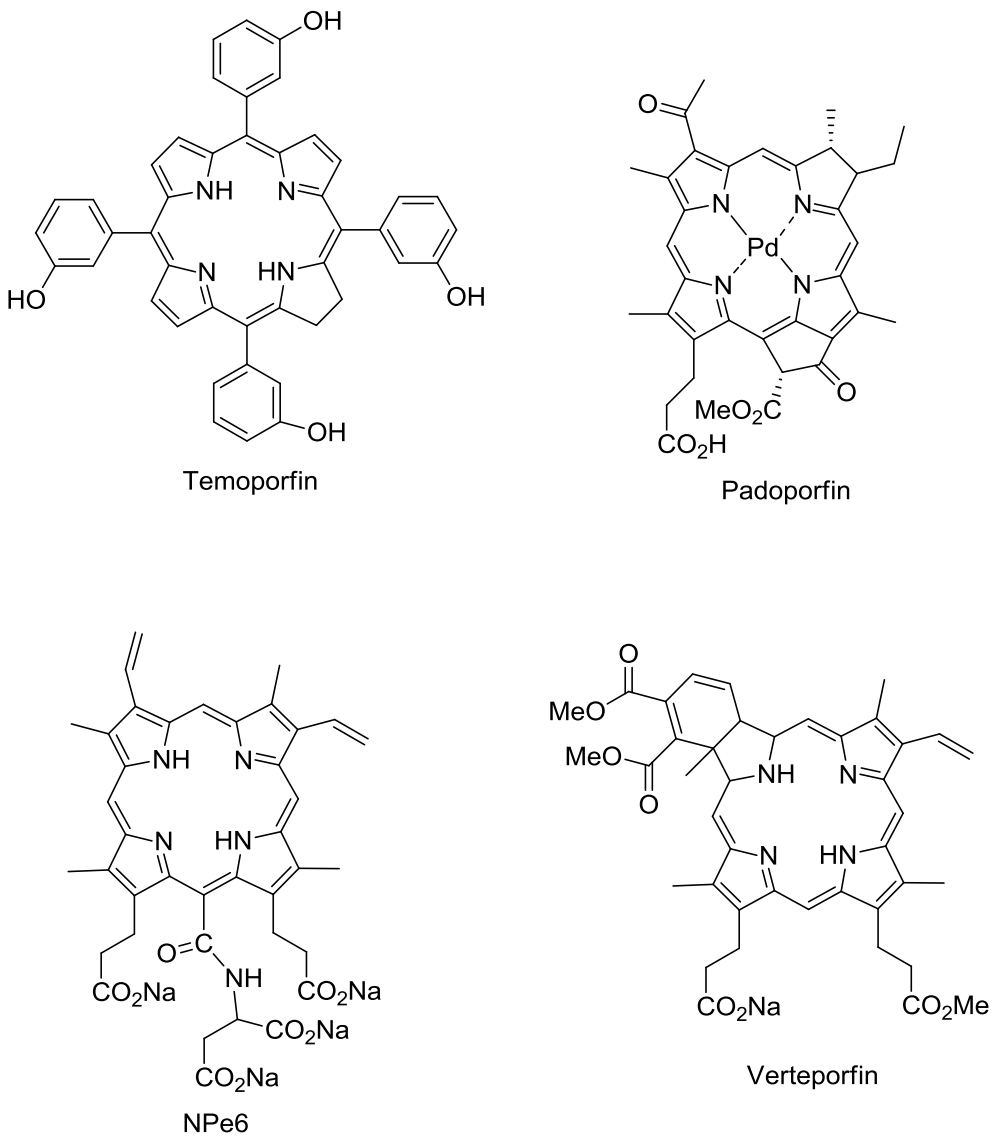

Figure 1.9: Chlorin-based photosensitizers.

Another two porphyrin-type derivatives are phthalocyanine and porphycene (Figure 1.10). Phthalocyanine (Pc) was discovered by Braun and Tcherniac in 1907[43,44] and has been recognized as a PDT agent since 1985. From the structure, Pc can be regarded as tetra-azaporphyrin and it has very strong absorption at 670-770 nm with a molar extinction coefficient around 2.5 x 10^5 $M^{-1}cm^{-1}$; this makes Pc a very good photosensitizer candidate. When chelated with diamagnetic metals such as zinc, aluminum or silicon, Pc

gives excellent singlet oxygen yields even close to 100%.[45,46] Coordination with metals which have valency higher than two, such as silicon, also prevents aggregation by way of axial coordination. Silicon phthalocynies in vitro and in vivo studies have shown that this hydrophobic photosensitizer exclusively localizes in mitochondria, and tumor cell death is mainly caused by the formation of reactive oxygen species. Phthalocyanine is a hydrophobic photosensitizer. However, its structural flexibility allows one to introduce hydrophilic groups to the molecule to modify its amphiphilicity so that the delivery of the drug can be more convenient.

Porphycene is an isomer of porphyrin. Although the structure of porphycene is strained compared with porphyrin, the stability of porphycene is still comparable to that of porphyrin due to hydrogen bonding between the NH and N sites. Porphycene was first synthesized by Vogel et al.,[47,48] and the molecule has absorption around 600 nm with a

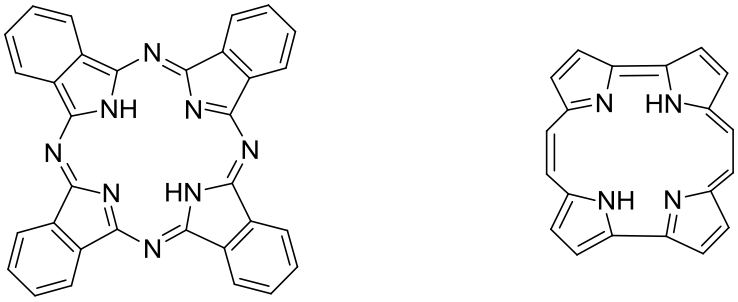

Figure1.10: The structures of phthalocyanine (left) and porphycene (right).

molar extinction coefficient around 5 x 10^4 M^{-1} cm^{-1}. Depending on the structure, porphycenes localize in different compartments of tumor cells such as mitochondria or lysosome,[49,50] Tumor cell death is mediated by apoptotic and necrotic responses.

1.8. Non-porphyrin Based Photosensitizers

There are some non-porphyrin based photosensitizers that have been developed. Most of them are various dyes such as hypericin, methylene blue, and toluidine blue (Figure

11). All these dyes have not succeeded in clinical trials due to drug delivery issues or their low activity against tumor cells. Hypericin[51] has absorption at 590 nm with a molar extinction coefficient around 4.5 x 10^4 M^{-1} cm^{-1} and can generate singlet oxygen very efficiently. This compound attracted attention because it is an inhibitor of protein kinase, which is a key enzyme in the proliferation of tumor cells. Hypericin was found to kill tumor cells through direct tumor cytotoxicity and vascular damage.[52] Methylene blue[53] has been known as an imaging reagent in the clinic for diagnosis of many diseases. It has absorption around 666 nm and a molar extinction coefficient of 8.2 x 10^4 $M^{-1}cm^{-1}$. Methylene blue is not widely used as a PDT agent due to its high reduction potential in tumors cell to give its leuco methylene blue scompound, which is colorless. Therefore the activity is lost. In spite of this, in vitro studies showed that methylene blue can reduce tumor size significantly against human T-cell and B-cell lymphoma.[54] Other dyes used in PDT are aza-BODIPYs, which have absorption at 679 nm with a molar extinction coefficient of 7.5 x $10^4M^{-1}cm^{-1}$. This molecule is improved as a photosensitizer when a halogen is introduced into the structure. The halogen increases the population of triplet states while also reducing the fluorescence due to the heavy atom effect. An *in vivo* study of ADMPM06 (Figure 1.11) showed this molecule has no discernable selectivity to particular cell compartments. Tumor cell death was induced through direct apoptotic and necrotic pathways. A similar strategy was used in BODIPY by introducing halogen to molecules. The first BODIPY investigated as a PDT agent is diiodoBODIPY.[55] This compound has an absorption at 534 nm with a molar coefficient value of 1.1 x 10^5 $M^{-1}cm^{-1}$. The generation of singlet oxygen was observed under IR irradiation when this molecule was excited. The localization of BODIPY depends on the structure. Some localize in mitochondria, ER and some localize in cell membranes.

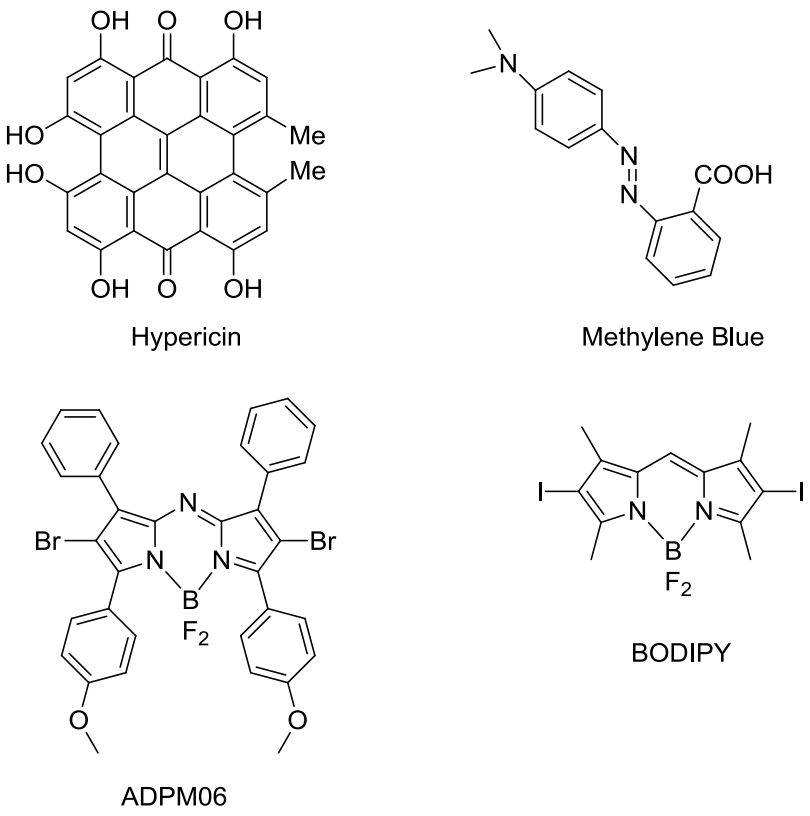

Figure 1.11: Non-porphyrin based photosensitizers.

To achieve better localization in tumor cells over normal cells, researchers have developed various strategies to modify photosensitizers by introducing biomolecules such as amino acids, antibodies, and polyethylene glycols (PEGs). This strategy is based on the fact that malignant tumor cells have cell surface antigens different from normal cells. For example, there is much work focusing on the use of antibodies[56] to direct the photosensitizers to tumor cell over normal cells. A monoclonal antibody (mAB)-PS conjugate is found to specifically bind to the tumor tissue due to its affinity to tumor-associated antigen, which can accumulate up to 10^8 photosensitizers on a tumor. The photosensitizer-biomolecule conjugates are the most promising molecules for photodynamic therapy since enhanced biological specificity provides better photosensitizer delivery to target tissues.

Photodynamic therapy is not only used to treat cancers. This treatment can also be used for many other diseases. For example, many skin diseases can be treated using photodynamic therapy. The photosensitizer Photofrin is used to treat cancers and also was investigated against the HIV virus an *in vitro* study. Verteporfin is used to treat age-related macular degeneration. Scientists including chemists, biologists, physicists and clinicians are collaborating to explore more possibilities for expanding the applications of this treatment.

1.9. References

1. Celli, J. P.; Spring, B. Q.; Rizvi, I.; Evans, C. L.; Samkoe, K. S.;. Verma, S.; Pogue, B. W.; Hasan, T. *Chem. Rev*., **2010**, *110*, 2795.

2. Dolman, D. E. J. G. J.; Fukumura, D.; Jain, R. K. *Nature*, **2003**, *3*, 380.

3. O'Connor, A. E.; William M. Gallagher, W. M.; Byrne, A. T. *Photochem. Photobiol.*, **2009**, 85, 1053.

4. Figge, F. H.; Weiland, G. S.; Manganiello, L. O. *Proc. Soc. Exp. Biol. Med.,* **1948**, *68*, 640.

5. Castano, A. P.; Demidova, T. N.; Hamblin, M. R. *Photodiag. Photodyn. Ther.* **2005**, *2*, 91.

6. Jori, G.; Reddi, E. *Int. J. Biochem*. **1993**, *25*, 1369.

7. Thomas, J. P.; Girotti, A. W. *Photochem. Photobiol*., **1989**, *49*, 241.

8. Hamblin, M. R.; Huang, Y. Y. *Photomedicine*, Taylor & Francis, Boca Raton, **2013**

9. Roberts, W. G.; Hasan, T. *Cancer Res.*, **1992**, *52*, 924.

10. Castano, A. P.; Demidova, T. N.; Hamblin, M. R. *Photodiag. Photodyn. Ther*. **2004**, *1,* 279.

11. Woodburn, K. W.; Vardaxis, N. J.; Hill, J. S.; Kaye, A. H.; Philips, D. R. *Photochem. Photobiol*. **1991**, *54*, 725.

12. Teiten, M. H.; Bezdetnaya, L.; Morliere, P.; Santus, R.; Guillemin, F. *J. Cancer* **2003**, *88*, 146.

13. Mroz, P, Yaroslavsky, A.; Kharkwal, G. B.; Hamblin, M. R. *Cancer,* **2011**, *3*, 2516.

14. Luo, Y.; Kessel, D. *Photochem Photobiol.* **1997***, 66, 479.*

15. Wang, W.; Moriyama, L. T.; Bagnato, V. S. *Laser Phys. Lett*., **2013**, *10*, 1

16. Mroz, P.; Huang, Y. Y.; Hamblin, M. R. *Biophotonics and Immune Responses*, Chen, W. R.;Ed.; SPIE: San Francisco, **2010**, Vol, 5, pp 756503

17. Duijnhoven, F. H. V.; Aalbers, R. I. J. M.; Rovers, J. P.; Terpstra, O. T.; Kuppen, P. J. *Immunobiol*. **2003**, *207*, 105.

18. Wohrle, D.; Hirth, A.; Bogdahn-Rai, T.; Schnurpfeil, G.; Shopova, M. *Russ. Chem. Bull.* **1998**, *47*, 807.

19. Sternberg, E. D.; Dolphin, D. *Tetrahedron*, **1998**, *54*, 4151.

20. Schermann, G.; Schmidt, R.; Volcker, A.; Brauer, H-D.; Mertes, H.; Branck, B. *Photochem. Photobiol*., **1990**, *52*, 741.

21. Hausman, W. *Biochem*istry **1909**, *14*, 275.

22. Pandey, R. K.; Zheng, G. *The Porphyrin Handbook*; Kadish, K. M.; Smith, K. M.; Guildard, R.; Eds.; Academic Press: San Diego, **2000**; Vol. 6, p 173.

23. Lipson, R. L.; Baldes, E. J. *Arch. Dermatol*., **1960**, *82*, 508.

24. Lipson, R. L.; Baldes, E. J.; Gray, M. G. *Cancer*., **1967**, *20*, 2255.

25. Lipson, R. L.; Baldes, E. J.; Olsen, A. M. *J. Natl. Cancer. Inst*. **1961**, *26*, 1.

26. Schuitmaker, J. J.; Baas, P.; Van Leengoed, H. L.; van der Meulen, F. W.; Star, W. M.; Van Zandwijk, N. *J. Photochem. Photobiol. B* **1996**, *34*. 3.

27. Evenson, J. F.; Sommer, S.; Rimington, C.; Moan, J. *Br. J. Cancer.*, **1987**, *55*, 483.

28. Bellnier, D. A.; Henderson, B. W.; Pandey, R. K.; Potter, W. R.; Dougherty, T. J. *J. Photochem. Photobiol*. *B*, **1993**, *20*, 55.

29. Hagan, W. J.; Barber, D. C.; Whitten, D. G.; Kelly, M.; Albrecht, F.; Gibson, S. L.; Hilf, R. *Cancer Res*.**1988**, *48*, 1148.

30. Czuchajowski, L.; Lozynski, M. *J. Heterocycl. Chem*. **1988**, *25*, 349.

31. Mitra, S.; Foster, T. H. *Photochem. Photobiol*., **2005**, *81*, 849.

32. Chen, Q.; Hetzel, F. W.; Clin, J. *Laser Med. Surg*., **1998**, *16*, 9.

33. Chen, Q.; Huang, Z.; Luck, D.; Beckers, J.; Brun, P. H.; Wilson, B. C.; Scherz, A.; Salomon, Y.; Hetzel, F. W. *Photochem. Photobiol.*, **2002**, *76*, 438.

34. Martin, N. E.; Hahn, S. M. *Photodiag. Photodyn. Ther*. 1, **2004**, *1*, 123.

35. Weersink, R. A.; Bobaards, A.; Gertner, M.; Davidson, S. R. H.; Zhang, K.; Netchev, G.; Trachtenberg, T.; Wilson, B. C. *J. Photochem. Photobiol. B*, **2005**, *79*, 211.

36. McMahon, K. S., Wieman, T. J.; Moore, P. H.; Fingar, V. H; *Cancer Res*. **1994**, *54*, 5374.

37. Ferrario, A.; Kessel, D. C.; Gomer, J. *Cancer Res*. **1992**, *52*, 2890.

38. Callot, H. J.; Johnson, A. W.; Sweeney, A. *J. Chem. Soc., Perkin Trans*. *1,* **1973**, 1424.

39. Pandey, R. K.; Jagerovic, N.; Ryan, J. M.; Dougherty, T. J.; Smith, K. M. *Bioorg. Med. Chem. Lett*., **1993**, *13*, 2615.

40. Aveline, B.; Hasan, T.; Redmond, R. W. *Photochem. Photobiol.,* **1994**, *59*, 328.

41. Richter, A. M.; Kelly, B.; Chow, J.; Liu, D. J.; Towers, G. H.; Dolphin, D.; Levy, J. G. *J. Natl. Cancer. Inst.,* **1987**, *79*, 1327.

42. Erfurth, U. S.; Hasan, T. *Surv. Ophthalmol*., **2000**, *45*, 195.

43. Braun, A. J.; Tcherniac. J. *Chem. Ber*., **1907**, *40*, 2709.

44. Linstead, R. R. *J. Chem. Soc.*, **1934**, 1016.

45. Detty, M. R.; Gibson, S. L.; Wagner, S. J. *J. Med. Chem.*, **2004**, 47, 3897.

46. Wainwright, M. *Anti-Cancer Agents Med. Chem*. **2008***, 8,* 280.

47. Vogel, E.; Kocher, M.; Schmickler, H.; Lex, J. *Angew. Chem. Int. Ed. Engl*. **1986**, *25*, 247.

48. Vogel, E.; Broring, M.; Fink, J.; Rosen, D.; Schmickler, H.; Lex, J.; Chan, K. W. K.; Wu, Y-D.; Plattner, D. A.; Nendel, M.; Houk, K. N. *Angew. Chem. Int. Ed. Engl*. **1995**, *34*, 2511.

49. Kessel, D.; Luo, Y. *Cell Death Deffer*., **1999**, *6*, 28.

50. Fickweiler, S.; Abels, C.; Karrer, S.; Bajumler, W.; Landthaler, M.; Hofstadter, F.; Szeimies, R. M. *J. Photochem. Photobiol, B*, **1999**, *48*, 27.

51. Kubin, A.; Wierranni, F.; Burner, U.; Alth, G.; Grunberger, W. *Curr. Pharm. Des*. **2005**, *11*, 233.

52. Brockmoller, J., Reu, T.; Bauer, S.; Kerb, R.; Hubner, W. D.; Roots, I *Pharmacopsychiatry* **1997**, *30*, 94.

53. Jockusch, S.; Lee, D.; Turro, N. J.; Leonard, E. F. *Proc. Natl. Acad. Sci*. U.S.A. **1996**, *93*, 7446.

54. Chen, Y.; Zheng, W.; Li, Y.; Zhong, J.; Shen, P. *Cancer Sci*., **2008**, *99*, 2019.

55. Yogo, T.; Urano, Ishisuka, Y. Y.; Maniwa, F.; Nagano, T. *J. Am, Chem. Soc.*, **2005**, *127*, 12162.

56. Bamias, A.; Keane, P.; Krausz, T.; Williams, G.; Epenetos, A. *Cancer. Res.* **1991**, *51*, 724.

Chapter 2: Total Syntheses and Characterization of Isoporphyrins from b-Bilene Salts

2.1 Introduction

Isoporphyrins **1**[1,2] are tautomeric structures of porphyrins **2** with interrupted macrocyclic conjugation owing to the presence of a saturated meso-carbon atom (Figure 2.1). This interruption of conjugation causes an intense bathochromic shift of the Q-band absorption to around 800 nm, thus making isoporphrins promising potential candidates as photosensitizers in photodynamic therapy (PDT).

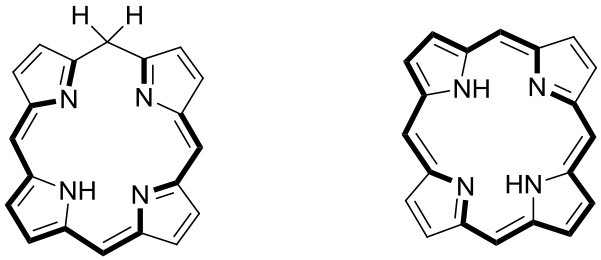

Isoporphyrin
1

porphyrin
2

Figure 2.1: Structure of porphyrin and isoporphyrin

Previous work from our group[3] has shown that zinc isoporphyrins have favorable properties for a photosensitizer, such as relative low dark toxicity, high phototoxicity, and they display multiple localization sites within a cell, especially within mitochiondria. Earlier syntheses of others particularly focused on generating transient isoporphyrins from tetraphenylporphyrin, including electrochemical oxidation,[2] photo-oxidation,[4] and chemical oxidation.[5] However, these isoporphyrins were unstable and easily reverted to their corresponding stable porphyrins. The first thermodynamically stable isoporphyrin was achieved in our laboratory in 1992.[6] The oxidative re-aromatization of isoporphyrins to porphyrins was suppressed by the introduction of suitable geminal substituents at the isoporphyrin sp^3 meso carbon. Yet another alternative synthesis of isoporphyrins was

developed by Smith[3] through cyclization of b-bilene salts by using an α-keto ester for the interpyrrolic carbon, which makes it possible to approach unsymmetrical isoporphyrins.

Based on the previous work from our laboratory,[3] the objectives of this project are to synthesize various zinc(II) isoporphyrins (Figure 2.2) and conjugate them with amino acids and study their biological properties as potential photosentizers. Zinc ions were inserted into isoporphyrins because metalloisoporphyrins are more stable than metal free isoporphyrins and have a significantly more red shifted Q-band (Figure 2.3) compared with metal free analogs, usually have a low toxicity, and the potential of selective uptake in tumors or necrosis. In addition, we hoped to conjugate metalloisoporphyrin with peptides, proteins, PEGs or antibodies to improve the delivery of zinc(II) isoporphyrins to cellular targets for photodynamic therapy.

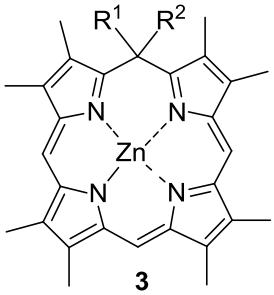

3

R^1 = alkyl, phenyl
R^2 = ester, acetyl,amide

Figure 2.2: Target zinc(II) isoporphyrin molecules.

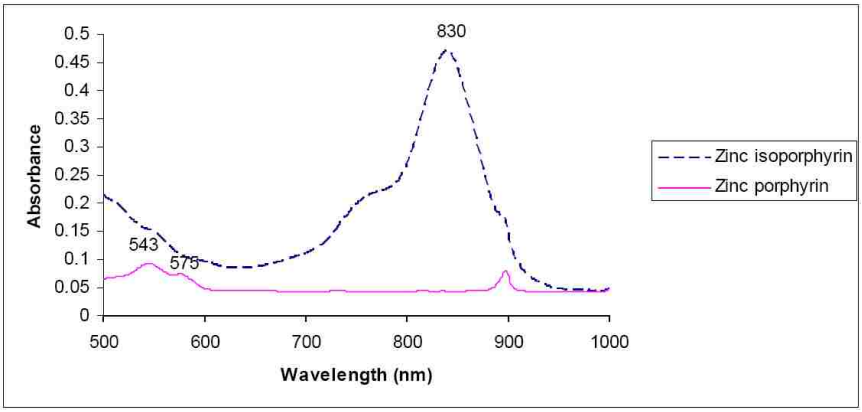

Figure 2.3: UV/Visible spectrum of zinc porphyrin and zinc isoporphyrin in CH_2Cl_2.

2.2 Previous Syntheses

Based on the observed stability of phlorins, which are dihydroporphyrins with a structure similar to isoporphyrins, Woodward postulated the existence of isoporphyrins in 1961.[1] This prediction was confirmed by Dolphin et al.[2] when they reported synthesis of the first metalloisoporphyrin in 1970. This discovery encouraged more efforts on synthesis of isoporphyrins. Generally, the isoporphyrin was obtained by electrochemical oxidation,[2] chemical oxidation[4] or photo-oxidation[5] of tetraphenylporphyrin. However, all these isoporphyrins are unstable and are easily converted into the corresponding fully conjugated porphyrins. The first thermodynamically stable isoporphyrin was obtained by Xie and Smith[6] by use of a variation of the MacDonald method from dipyrromethanes. The introduction of suitable geminal substituents prevented their zinc(II) isoporphyrin from isomerization into zinc(II) porphyrin.

a) Electrochemical oxidation method[2]

Dolphin et. al[2]. reported the first zinc tetraphenylmethoxyisoporphrin **6** as a dark green solid obtained through controlled-potential oxidation of the corresponding zinc *meso*-tetraphenylporphyrin **4** followed by nucleophilic attack of methanol (Scheme 2.1). The optical absorption spectrum exhibited a maximum absorption at 860 nm. This

isoporphyrin could be reduced back to porphyrin **7** with demetalation by addition of KI in glacial acetic acid.

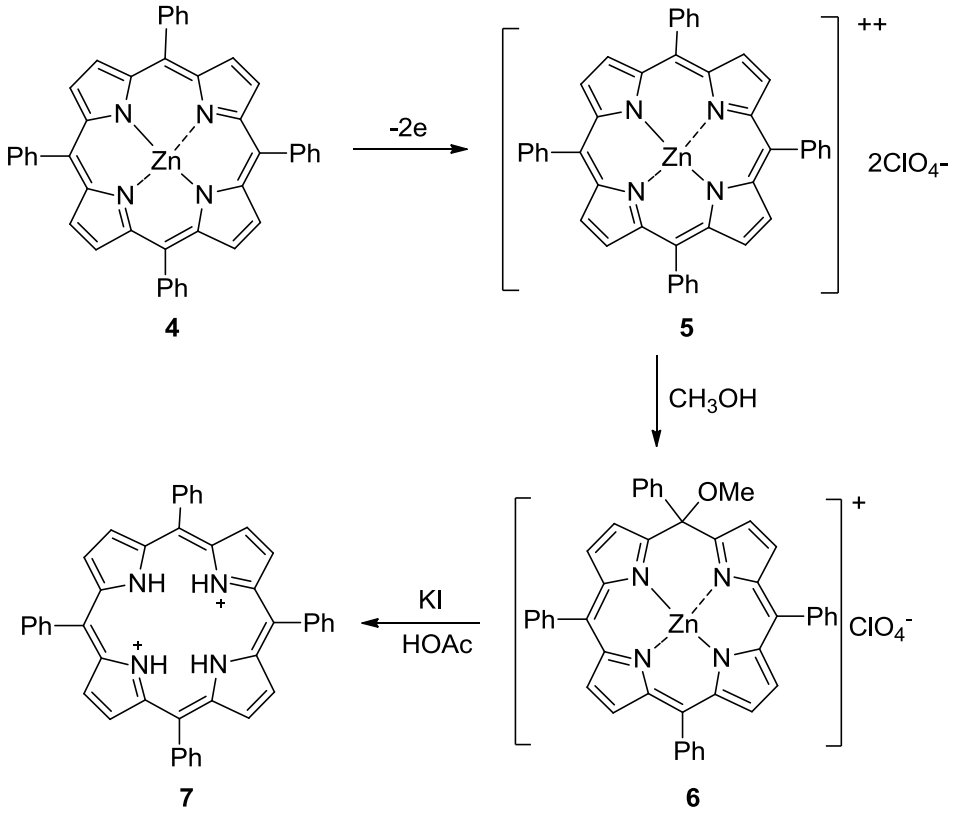

Scheme 2.1: Synthesis of tetraphenylisoporphyrin by electrochemical oxidation.[2]

.

b) Chemical oxidation method[5]

Gold[6a] discovered that isoporphyrins could also be generated by peroxide oxidation of metalloporphyrins (Scheme 2.2). For example, ferric isoporphyrin **8** was obtained as a microcrystalline solid through oxidation of (tetraphenylporphinato) iron(III) complex **9** by t-butyl hydroperoxide. Takeda et al.[5b] also reported synthesis of isoporphyrins by similar methods. Zinc tetraphenylbenzoyloxyisoporphyrin benzoate **10** was obtained by oxidation of the corresponding porphyrin **4** with benzoyl peroxide.

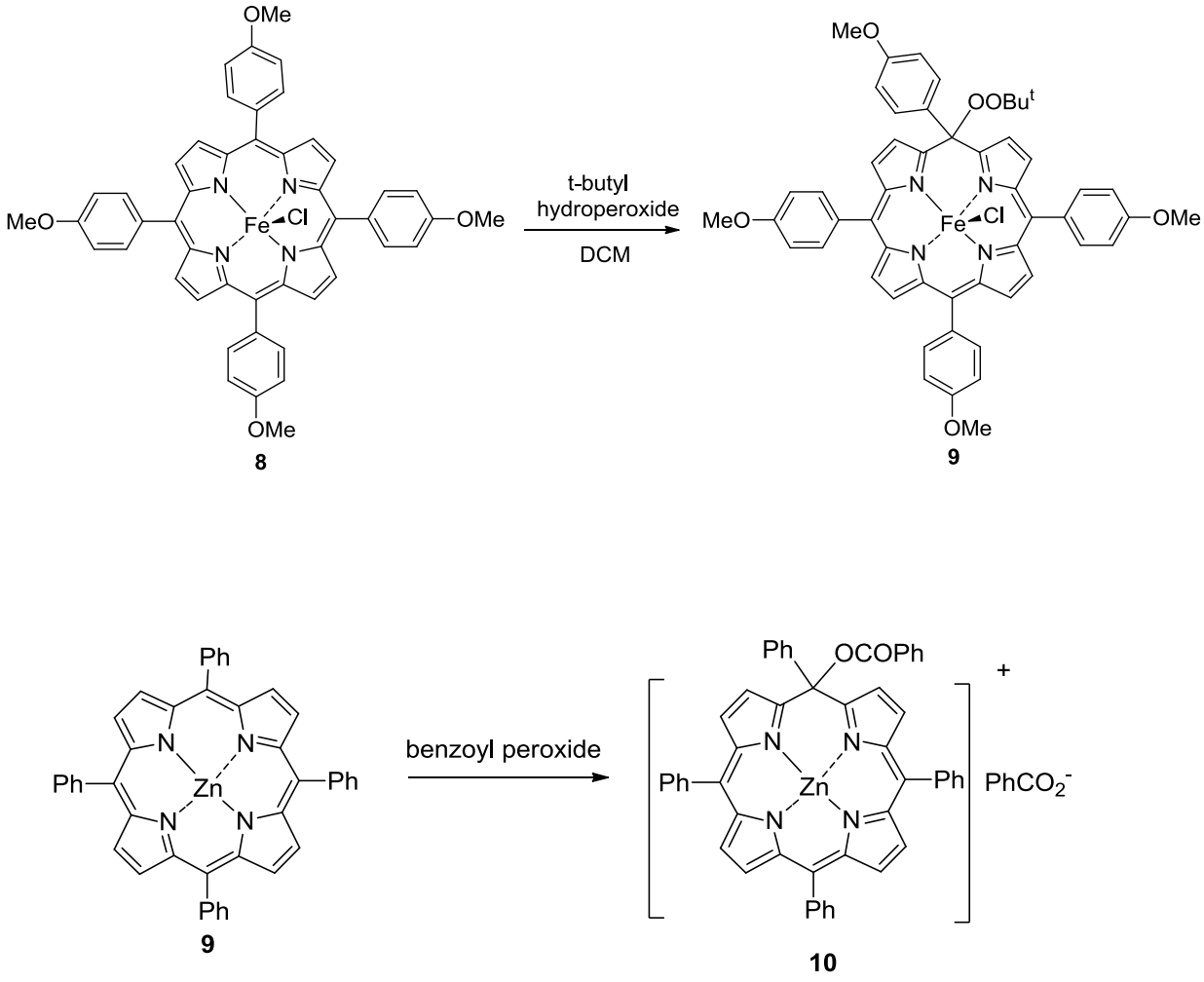

Scheme 2.2: Synthesis of tetraphenylisoporphyrin by chemical oxidation.[5b,6a]

c) Variation of MacDonald method[6]

Xie and Smith[6] successfully achieved the total synthesis of the first thermodynamically stable zinc(II) isoporphyrin **13** by using a variation of the MacDonald '2+2' method through condensation of dipyrromethane dicarboxylic acid **11** and diformydipyrromethane **12** using zinc acetate as a reaction template (Scheme 2.3). The 5,5-dimethyl groups prevent the isoporphyrin core from going back to the corresponding porphyrin.

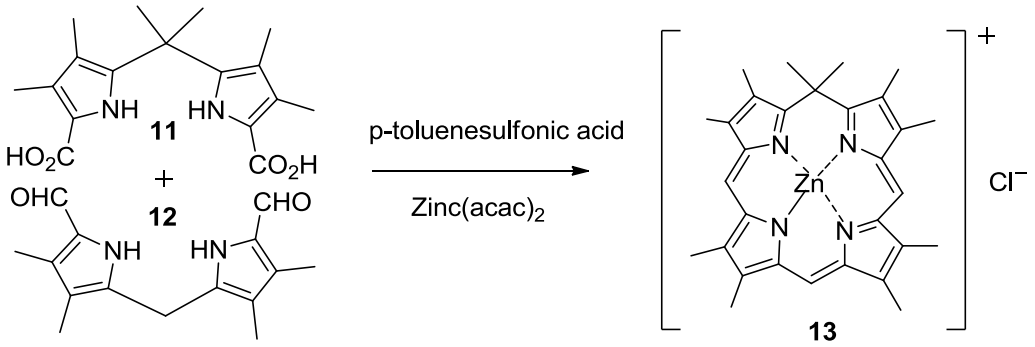

Scheme 2.3: Synthesis of zinc(II) isoporphyrin by the MacDonald approach.[6]

d) Cyclization of b-bilene salts[3]

Smith and coworkers developed another more efficient synthesis of zinc(II) isoporphyrins **15** through cyclization of b-bilene salts **14** using an active α-keto ester reagent (Scheme 2.4). The cyclization mechanism involves a b-bilene to a,c-biladiene transformation. This method provided an alternative pathway to synthesize unsymmetrical zinc(II) isoporphyrins.

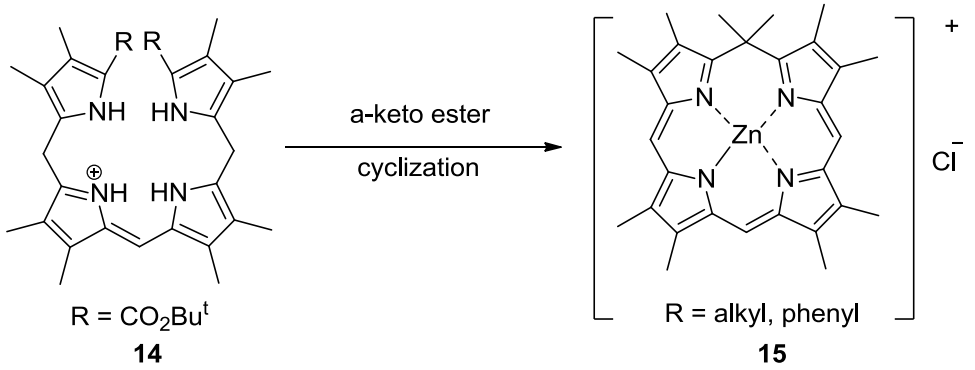

Scheme 2.4: Synthesis of tetraphenylisoporphyrin by cyclization of a b-bilene salt.[3]

Results and Discussion

Isoporphyrins possess special physical and chemical properties, such as unique optical characteristics and redox behavior. However, in the past twenty years, efforts to

synthesize isoporphyrins were hampered in the sense that they are very unstable and are easily converted to more thermodynamically stable porphyrins. Oxidation of porphyrin to isoporphyrin has been known since the 1980s, but this method was only applied to several meso-aryl substituted porphyrins and the resultant isoporphyrins were very unstable. Smith's work[6] provided the first stable zinc(II) isoporphyrin and made it possible to characterize and investigate the chemistry of isoporphyrins.

b-Bilene-1,19-dicarboxylate salts are known intermediates in the synthesis of porphyrins[7] and have also been used to synthesize the isoporphyrin by Smith. The route utilizes crystalline intermediates at all stages, and the method has no inherent symmetry limitations. It could provide an alternative way to synthesize unsymmetrical zinc(II) isoporphyrins. We therefore planned to use this method to approach metalloisoporphyrins, which we would then conjugate with amino acids and evaluate their biological properties as photosensitizers.

2.3 Retrosynthesis

The target molecule can be achieved by cyclization of a 1,19-di-*tert*-butoxycarbonylctamethy-b-bilene hydrochloride, and the b-bilene could be obtained by condensation between a dipyrromethane carboxylic acid and a formyldipyrromethane. Dipyrromethane carboxylic acids and diformyldipyrromethanes are both derived from the corresponding *t*-butyl 9-(benzyloxycarbonyl)-3,4,7,8-tetramethyldipyrromethane-1-carboxylate by hydrogenation and then a Vilsmeier formylation reaction. Dipyrromethanes can be synthesized by condensation of a 5-unsubstituted pyrrole with a 5-acetoxymethylpyrrole (Scheme 2.5).

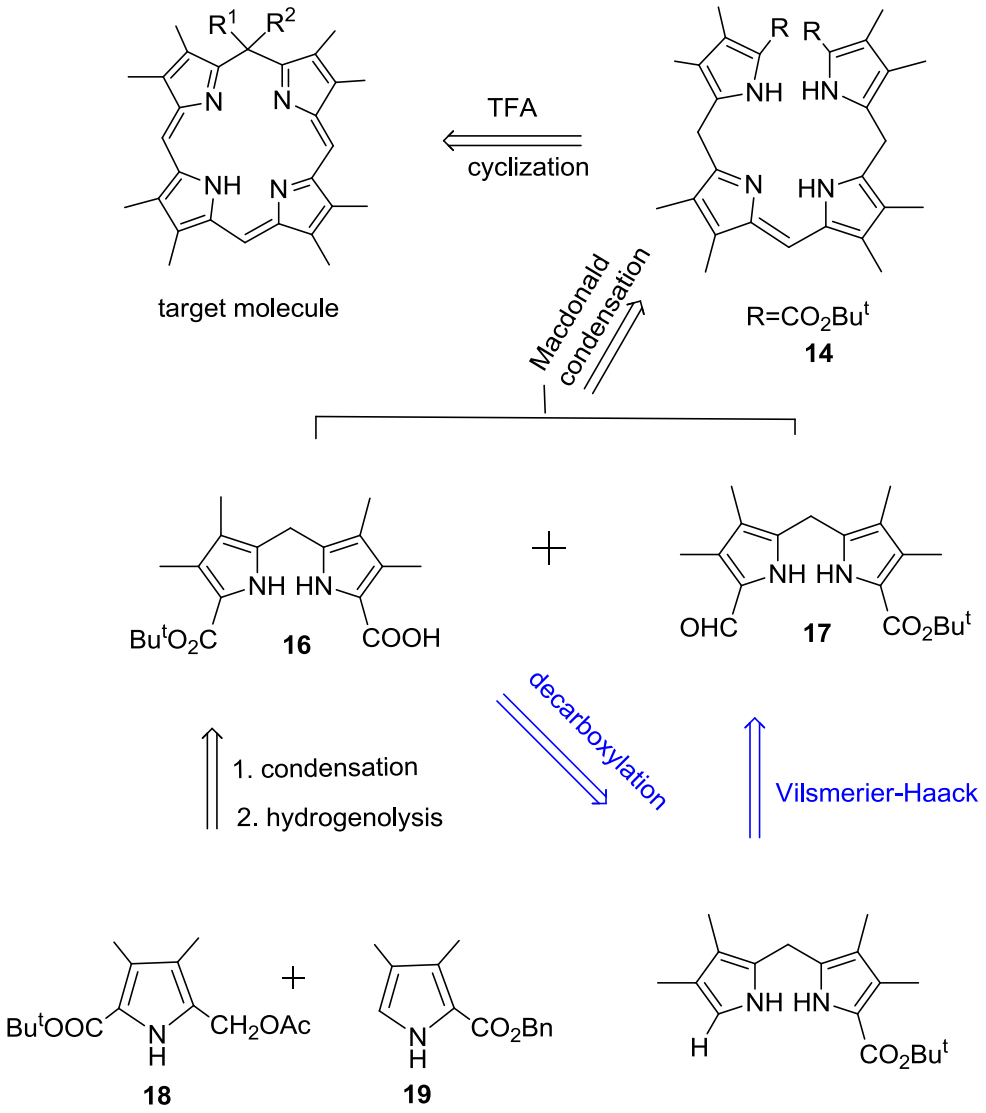

Scheme 2.5: Retrosynthesis of target isoporphyrin molecule.

2.4 Synthesis

The whole synthesis started with only two pyrroles; the 5-acetoxymethylpyrrole **18** was synthesized by using the Johnson[7a] method (Scheme 2.6). Addition of a sodium nitrite solution to *tert*-butyl acetoacetate in acetic acid provided *tert*-butyl oximinoacetoacetate **20.** Condensation between the oximinoacetate and 3-methyl-2,4-pentanedione in acetic acid with portion-wise addition of a mixture of sodium acetate and zinc dust at 70 ℃ furnished *t*-butyl 3,4,5-trimethylpyrrole-2-carboxylate **21** in about 35% yield. Then,

radical oxidation of the α-methyl group by lead tetra-acetate at room temperature led to the 5-acetoxymethylpyrrole **18**.

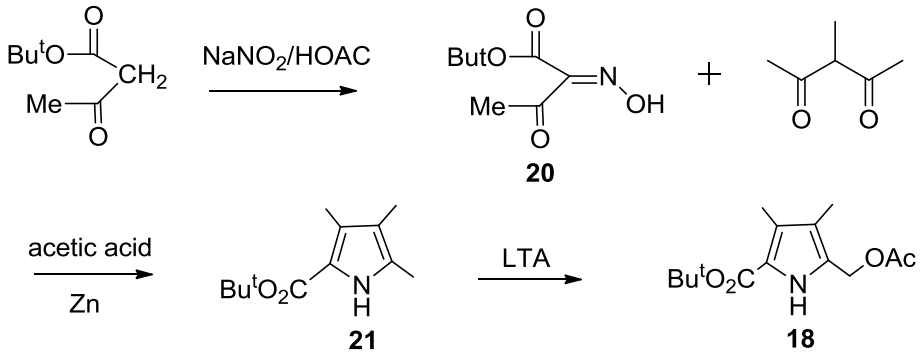

Scheme 2.6: Johnson-type synthesis of pyrrole **18**.

The Barton-Zard[8] reaction was used to synthesize the 5-unsubsituted pyrrole **19** (Scheme 2.7). This reaction utilizes a [3+2] cycloaddition of a nitroalkene with an alkylisocyanoacetate. Central to this method is the ability of the nitro group to depart as nitrite under certain conditions and result in formation of an alkyl 2-unsubstituted pyrrole carboxylate. This method is widely used to synthesize the precursors of dipyrromethanes and has even been extended to the synthesis of β-nitroporphyrins. Henry addition of nitroethane to an aldehyde catalyzed by base, followed by acetylation of the hydroxyl group provided 2-acetoxy-3-nitrobutane **23**, which was condensed with ethyl isocyanoacetate to furnish ethyl ester pyrrole **24** in 80% yield. Here, the acetoxyl group in **23** is a very good leaving group, which is easily eliminated under basic conditions to generate nitroalkene *in situ*. Transformation of the ethyl ester pyrrole to the benzyl ester pyrrole **25** was realized in greater than 90% yield by a transesterification reaction using $PhCH_2ONa$ in benzyl alcohol. The benzyl ester group could be easily removed to give carboxylic acid under neutral conditions through hydrogenation using palladium on activated carbon.

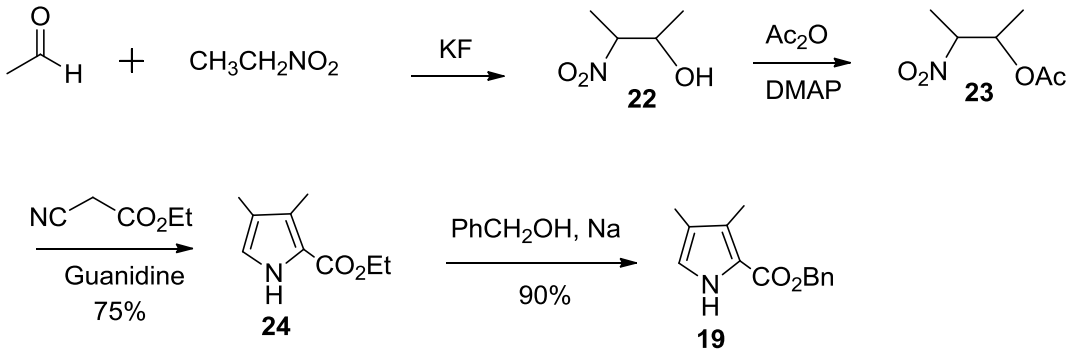

Scheme 2.7: Barton-Zard synthesis of α-free pyrroles **19** and **24**.

The dipyrromethane **25** was constructed by condensation of the 5-acetoxymethylpyrrole **18** and the 5-unsubstituted pyrrole **19** using the Lewis acid Montmorillonite K-10 clay as a catalyst[9] (Scheme 2.8). Almost a 1:1 ratio of these two pyrroles and K-10 clay were added to dry CH_2Cl_2 and the reaction mixture was kept stirring under argon for 24 hours at room temperature. *tert*-Butyl 9-(benzyloxy)carbonyl-3,4,7,8-tetramethyl-dipyrromethane-1-carboxylate **25** was obtained in greater than 90% yield. From the ^1H NMR spectrum the product was shown to be pure enough to go to the next step. Further purification could be done through a flash column (3% MeOH/CH_2Cl_2) or on a regular column (CH_2Cl_2 + a little MeOH) or by recrystallization from CH_2Cl_2/petroleum ether, and then left in the fridge overnight.

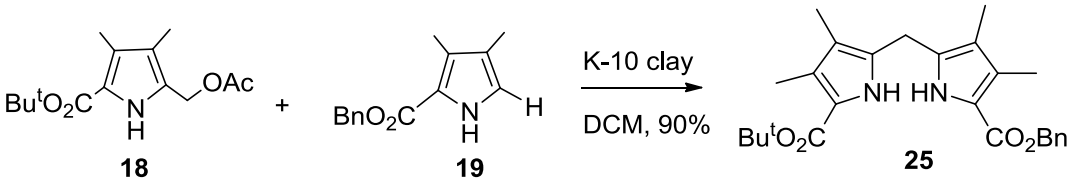

Scheme 2.8: Condensation between 5-acetoxypyrrole **18** and α-free pyrrole **19** in K-10.

Then the precursors of the b-bilene, namely the dipyrromethane carboxylic acid and formydipyrromethane were both derived from the mixed ester dipyrromethane **25**.

Dipyrromethane carboxylic acid **26** was obtained by selectively removing the benzyl group through hydrogenolysis over 10% Pd/C catalyst in excellent yield. Formyldipyrromethane **27** was synthesized using a Vilsmeier-Haack formylation reaction. Decarboxylation was achieved with two equivalents of p-toluenesulfonic acid in CH_2Cl_2 for 2 hours. The resultant unsubstituted dipyrromethane was then treated with the Vilsmeier reagent prepared *in situ*, by mixing of DMF and benzoyl chloride, to give the desired product formyldipyrromethane **27** upon basic hydrolysis, in good yield (Scheme 2.9).

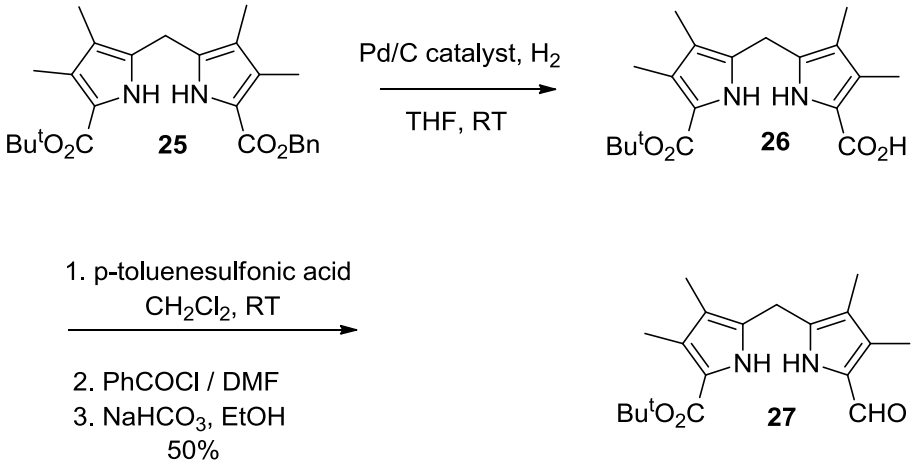

Scheme 2.9: Synthesis of formyldipyrromethane by the Vilsmeier-Haack reaction

Here, benzoyl chloride was used to replace phosphorus oxychoride because it is more moderate compared with the harsh conditions of $POCl_3$/DMF. PhCOCl/DMF generates the same intermediate chloromethyleneiminum salt that $POCl_3$/DMF does (Scheme 2.10). The latter will generate hydrochloric acid because phosphorus can easily release chloride ions in exchange of oxygen and combine with water to produce hydrochloric acid. So, the Vilsmeier-Haack[10] reagent provided an alternative way for formylation of the dipyrromethane, which is sensitive to the action of acetic reagents.

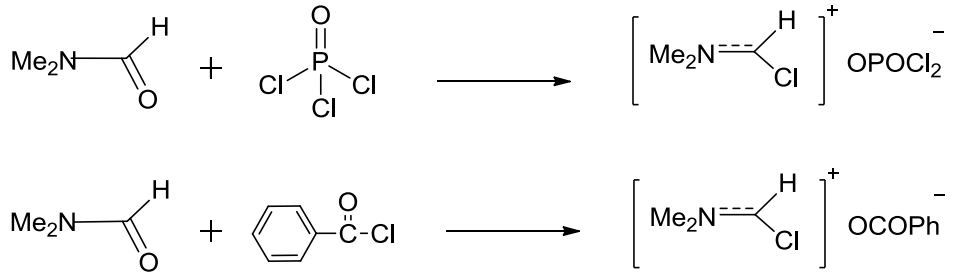

Scheme 2.10: Vilsmeier reagent for formylation of dipyrromethane.

The required b-bilene hydrochloride[11] was obtained by condensation of the two dipyrromethane halves: dipyrromethane carboxylic acid **26** and formyldipyrromethane **27** (Scheme2.11). Condensation of 9-*tert*-butyloxycarbonylpyrromethane-1-carboxylic acid **26** with *tert*-butyl 9-formylpyrromethane-1-carboxylate **27** catalyzed by two equivalents of *p*-tolunesulfonic acid in CH_2Cl_2 furnished the corresponding b-bilene-1,19-di-*tert*-butyl ester as its toluenesulfonic salt **14**. The reaction was monitored by spectrophotometry and the b-bilene salt showed a strong absorption around 500 nm in its UV/Visible spectrum when the reaction was complete. This b-bilene salt was converted into the hydrochloride salt by brief treatment by dry HCl gas in

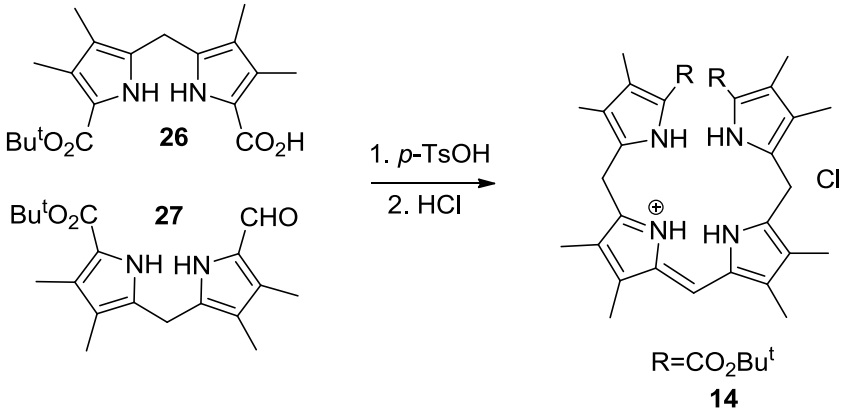

Scheme 2.11: Synthesis of b-bilene hydrochloride salt by condensation of dipyrromethane carboxylic acid **26** and formyldipyrromethane **27**.

distilled CH_2Cl_2 and the solution turned from orange to dark red. Purification of the product was done by recrystallization using CH_2Cl_2/hexane overnight in the fridge to give the crystalline hydrochloride in about 70% yield. The UV-visible spectrum of the b-bilene hydrochloric salt in CH_2Cl_2 showed a strong absorption at 502 nm, as shown in Figure 2.4.

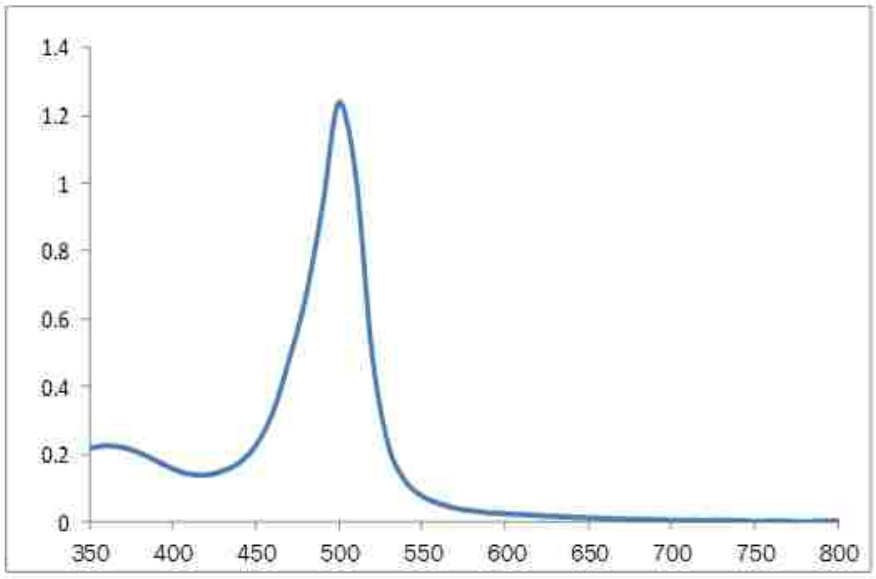

Figure 2.4: UV-visible spectrum of b-bilene hydrochloride salt **14** in CH_2Cl_2

Ring closure of the b-bilene salt is the key step to obtain isoporphyrin. The b-bilene has been already used to synthesize porphyrins, employing trimethyl orthoformate as a one-carbon linking unit.[12] Here, we needed to look for a suitable linking reagent[13] which is able to prevent the isoporphyrin product from going back to corresponding more stable porphyrin. At same time, this reagent must be at least as reactive as trimethyl orthoformate toward electrophilic attack by the b-bilene. So an α-diketone or α-keto ester was selected. The strategy involved cleavage of the *tert*-butyl ester group of the b-bilene hydrochloride using trifluoroacetic acid, then the reaction mixture was diluted with dry CH_2Cl_2 followed by addition

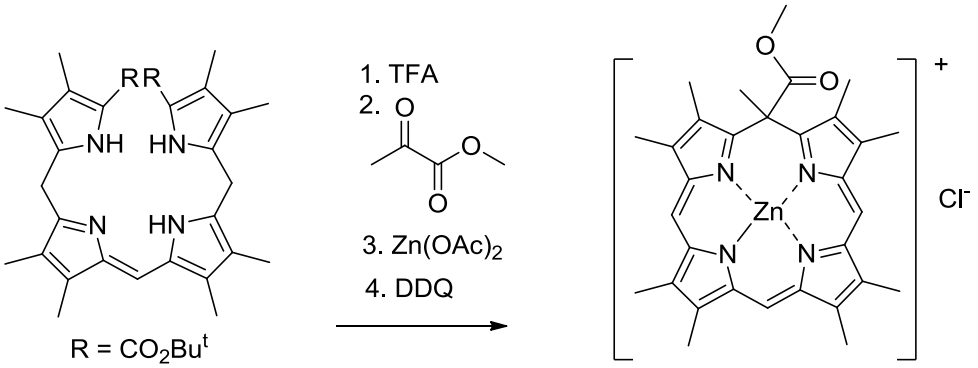

Scheme 2.12: cyclization of b-bilene salt using methyl pyruvate.

methyl pyruvate, and the whole reaction was monitored by spectrophotometry. After one hour, the UV-visible spectrum showed absorptions at 450 and 520 nm, which do not belong to either the starting material b-bilene salt or the product isoporphyrin. These two absorptions actually are characteristic of an open chain and non-conjugated tetrapyrrole. The reaction solution was washed with water containing several drops of aqueous sodium bicarbonate to neutralize excess TFA. The color of the solution changed from red to green. The spectra of UV-visible spectrum indicated two new absorptions at 430 and 790 nm which are very similar to those of isoporphyrins. This may be due to the neutral nature of the solution compared with acidic conditions. Then zinc acetate was added as a reaction template because of its good coordination ability and its partial solubility in organic co-solvents. Zinc acetate changed the greenish color of the solution to red and showed absorptions at 470 and 540 nm as found under acidic conditions. DDQ was added to oxidize the zinc chelated open system to zinc(II) isoporphyrin **28** within ten minutes; characteristic absorptions at 430 and 825 nm appeared in the UV-visible spectrum in CH_2Cl_2. Alternatively, the reaction could be left in the air for several days; the intermediate was oxidized into zinc(II) isoporphyrin **28** (Scheme 2.12). Purification of the product was performed using an alumina column followed by a silica gel

column. Recrystallization of the product was performed using CH_2Cl_2/petroleum ether. The identity of the product was confirmed by mass spectrometry (Figure 2.5) and the UV-visible spectrum of the product is shown in Figure 2.6.

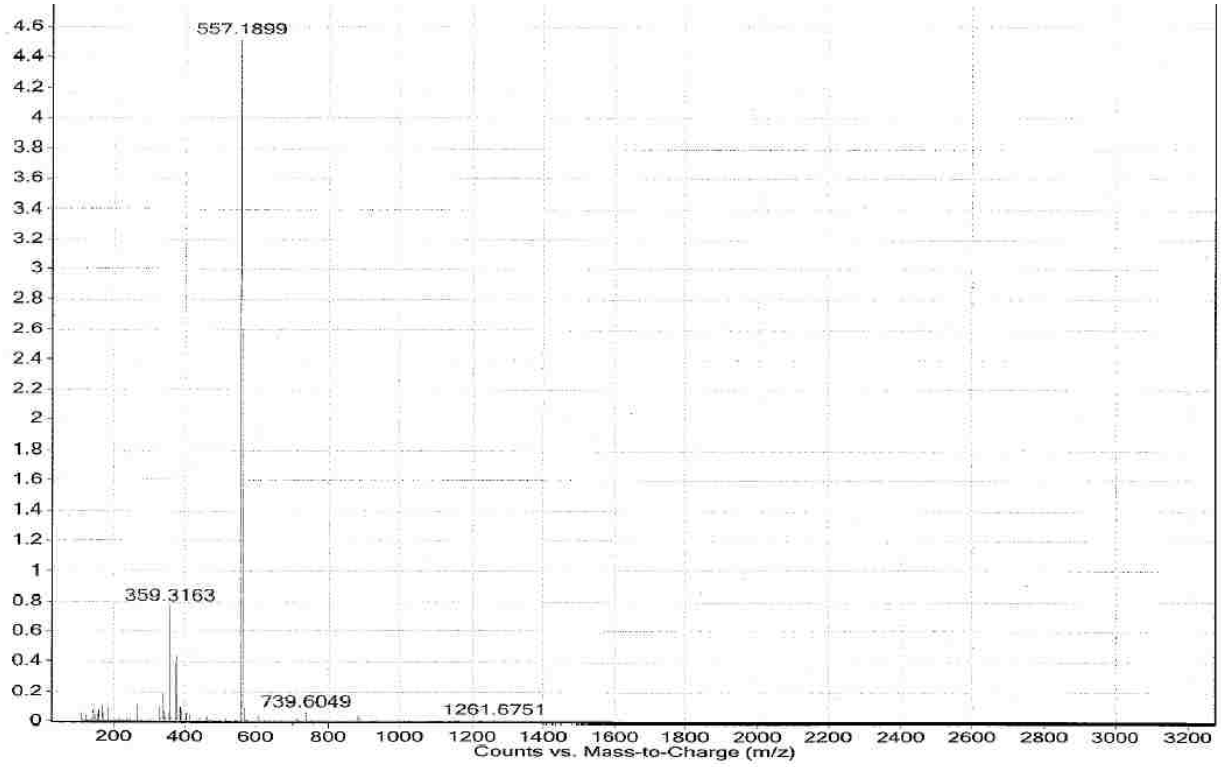

Figure 2.5: The mass spectrum of zinc isoporphyrin **28**.

With the zinc isoporphyrin in hand, it was hoped that saponification of the 5-methyl ester group of the isoporphyrin could provide the corresponding carboxylic acid, which could then be conjugated with organelle-directing peptides so that we can further evaluate its biological properties. The reaction was attempted under basic, acidic and neutral condition. When the reaction was performed using 5% NaOH[14] in dry methanol, the UV-visible spectrum gave a sharp absorption around 400 nm after workup. This is obviously the result of decarboxylation of corresponding

carboxylic acid to give porphyrin. The rearrangement of isoporphyrin led to the more thermodynamically stable porphyrin. Then, ethylenediamine was used as 1.0,

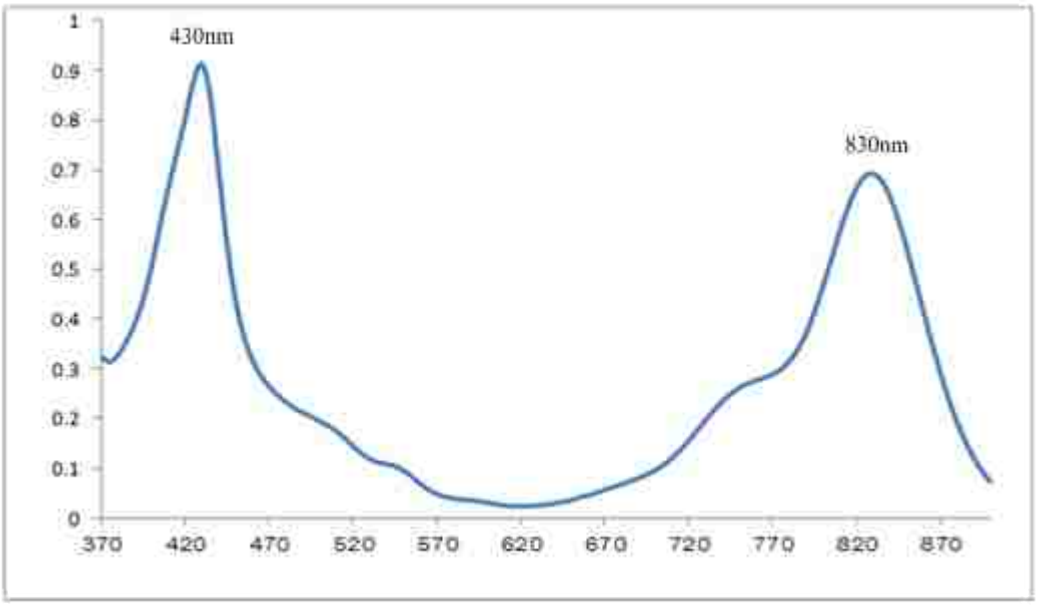

Figure 2.6: UV-visible spectrum of zinc(II) isoporphyrin **28** in CH_2Cl_2.

1.5 and 4.0 equivalents vs. isoporphyrin at room temperature in CH_2Cl_2; the UV-visible spectra showed peaks around 430 and 670 nm which appear to belong to metal-free isoporphyrin. However, these peaks disappeared upon work-up with water or dilute HCl. There is a possibility that ethylenediamine removed the zinc metal from the isoporphyrin through chelation to form a five membered ring and gave metal-free isoporphyrin, which is relatively unstable and decomposed immediately (Scheme 2.13). Lithium iodide[15] was next used for the cleavage of the ester under neutral conditions. The reaction mixture was refluxed in ethyl acetate, DMF and pyridine for 24-48 hours, but the UV-visible and ^{1}H NMR spectra of the zinc(II) isoporphyrin showed no change. This is perhaps due to the sterically hindered isoporphyrin ring system. Therefore, the more active reagent trimethylsilyl iodide[16] was employed instead of LiI. However, UV-visible spectra did not show any peaks above 400 nm. Thus, It appears that the zinc(II) isoporphyrin decomposed

during the reaction. A substitute method to produce TMSI *in situ* by refluxing LiI and TMSCl in CH_3CN solvent did not work either for the hydrolysis step (Scheme 2.14). Lewis acid boron halogens can also be used to cleave relatively simple hindered esters. When the reaction was performed at low temperature (around -25 ^oC), the UV-visible absorptions at 430 and 830 nm of the

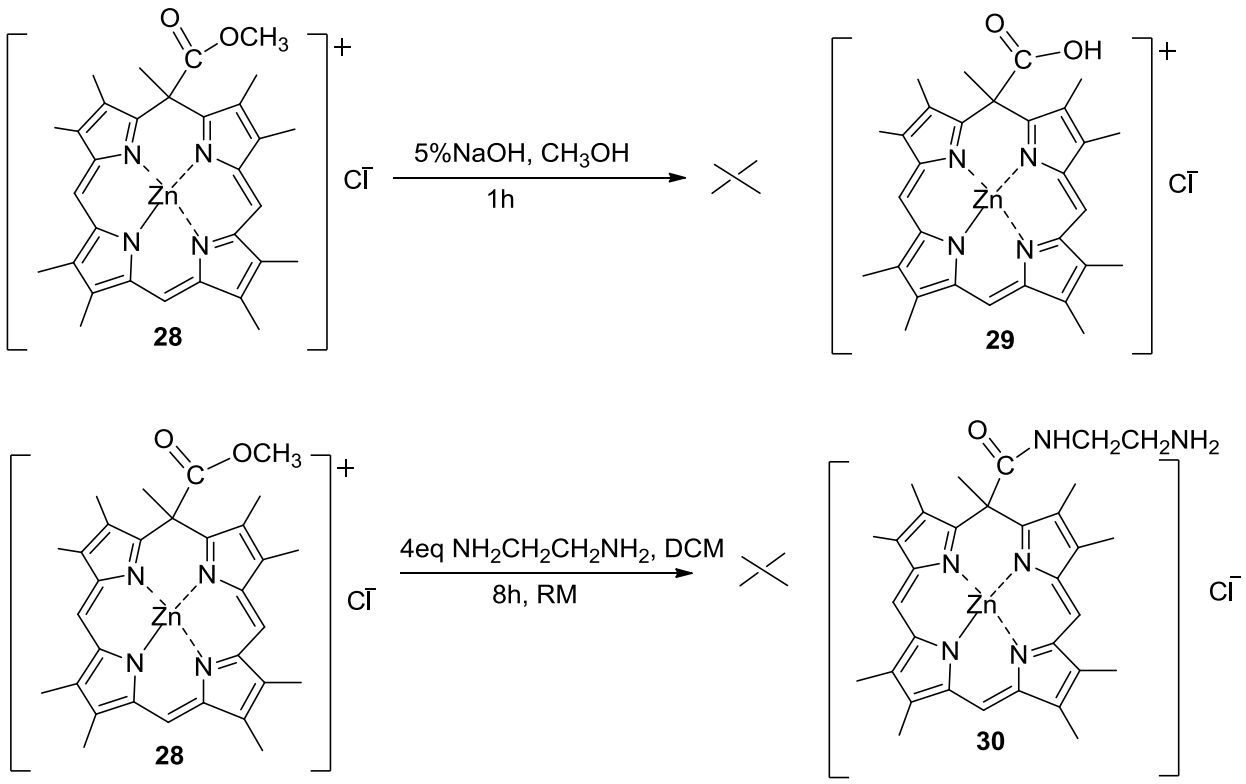

Scheme 2.13: Hydrolysis of methyl ester under basic conditions.

isoporphyrin were present, but these absorptions disappeared after work-up with water, and a strong new absorption at 400 nm belonging to the corresponding porphyrin Soret absorption appeared.

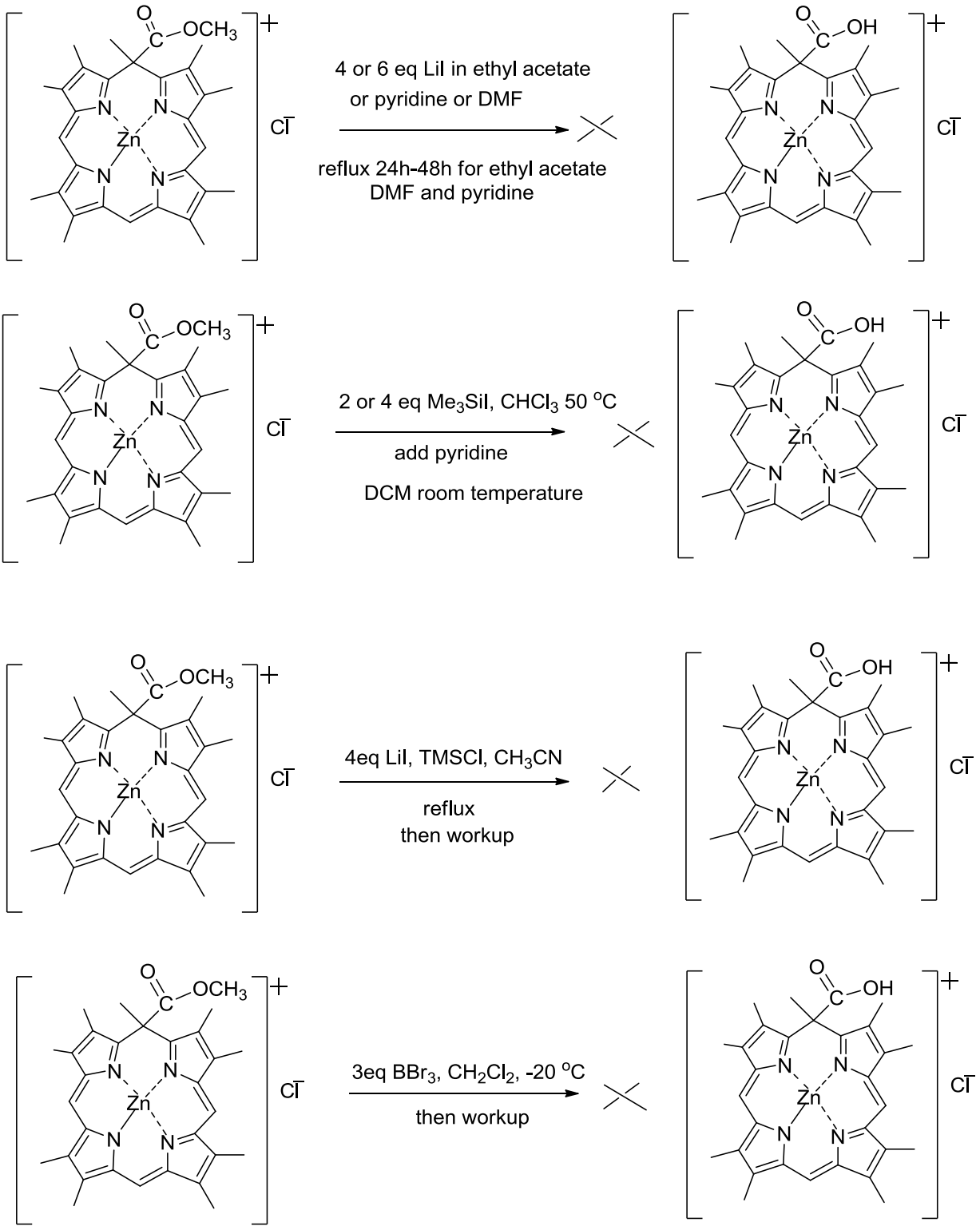

Scheme 2.14: Attempted hydrolyses of zinc(II) isoporphyrin methyl ester under neutral and acidic conditions.

Acidic conditions such as BBr_3[17] were also tried on the zinc(II) isoporphyrin but did not work. Based on the above work, we surmised that zinc(II) isoporphyrins are not stable under harsh acidic or basic condition and even to strong nucleophiles due to the fact that the porphyrin is a good leaving group. Once the ester on isoporphyrin is hydrolyzed, the carboxylic acid group tends to decarboxylate immediately and form the corresponding porphyrin or ring opened system.

To avoid this problem, the following strategies were planned. One choice was to introduce the benzyl ester group during the cyclization so that the ester group can be removed by hydrogenolysis under neutral conditions. Similarly, the b-bilene salt might also be cyclized by using 2,3-butanedione and the resultant acetyl group could possibly be converted into an amine group by an amination reaction (Scheme 2.15). The b-bilene salt was successfully cyclized with benzyl pyruvate or 2,3-butanedione under the same conditions as described above in three steps. The obtained zinc(II) isoporphyrins **31** and **32** have UV-visible absorptions at 431 and 807 nm (Figure 2.7) and 407 and 807 nm (Figure 2.8), respectively.

The benzyl ester substituted zinc(II) isoporphyrin was subjected to hydrogenolysis with Pd/C under hydrogen gas in THF overnight at room temperature; the UV spectrum showed typical peaks around 400, 532 and 668 nm which belong to porphyrin. This assumption is still consistent with a hydrolysis reaction. The carboxylic acid left as a result of decarboxylation and formed the corresponding porphyrin. For the acetyl substituted zinc(II) isoporphyrin, attempts to convert the ketone group into an amine group through reductive amination[18] using BOC-protected ethylenediamine as nucleophile and sodium triacetoxylborohydride as reducing agent failed, probably for similar reasons (Scheme 2.16). The UV/visible

spectrum showed a large peak at 406 nm and no peak around 800 nm, which indicated the zinc(II) isoporphyrin decomposed or was isomerized to porphyrin.

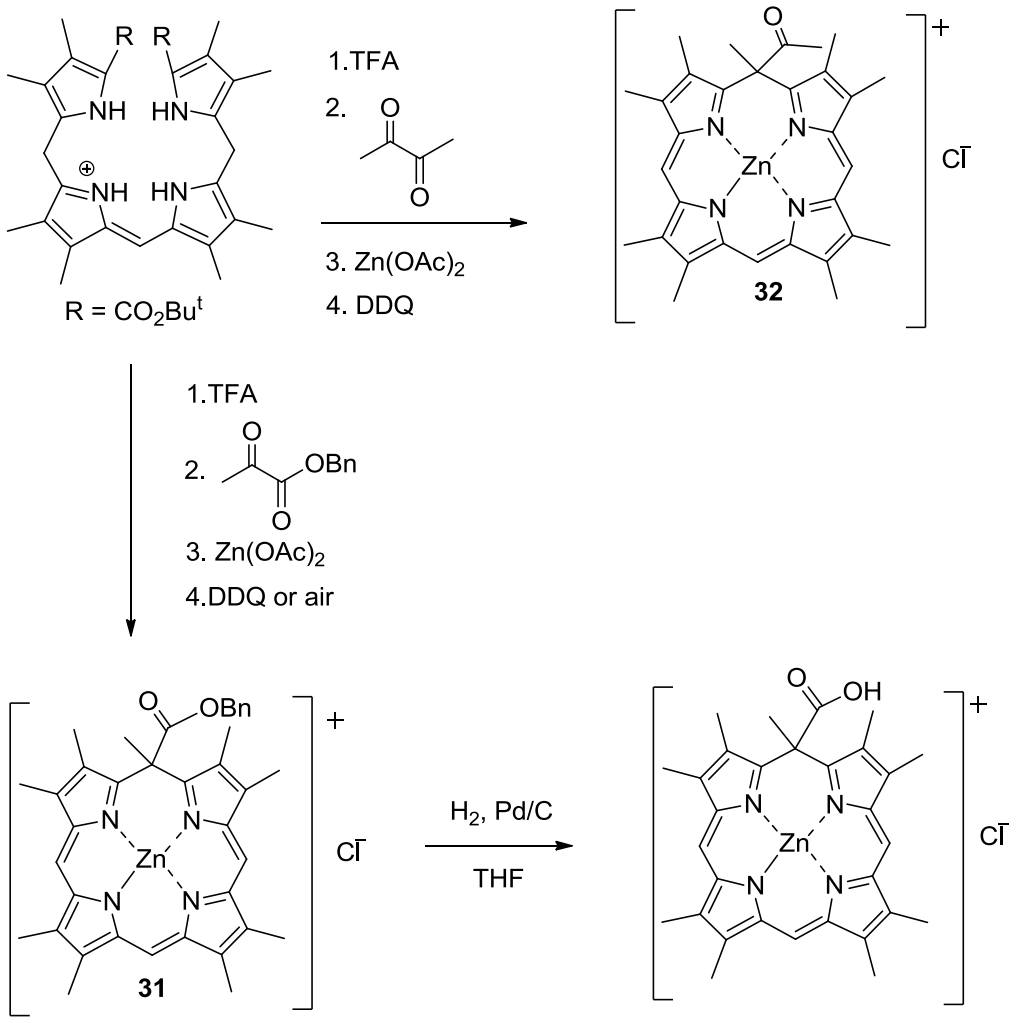

Scheme 2.15: Cyclization of b-bilene salt using benzyl pyruvate or 2,3-butanedione.

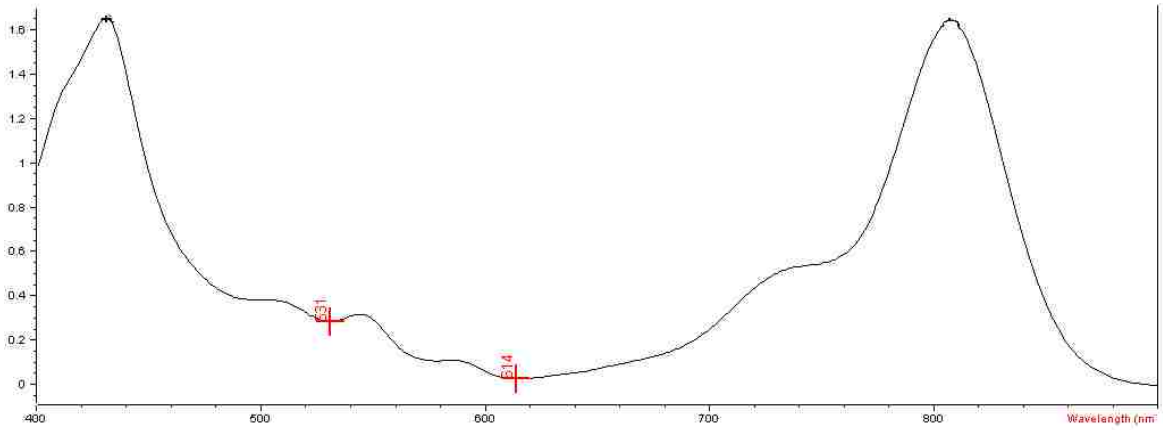

Figure 2.7: UV/visible spectrum in CH_2Cl_2 of zinc(II) isoporphyrin **31** from cyclization of b-bilene salt with benzyl pyruvate.

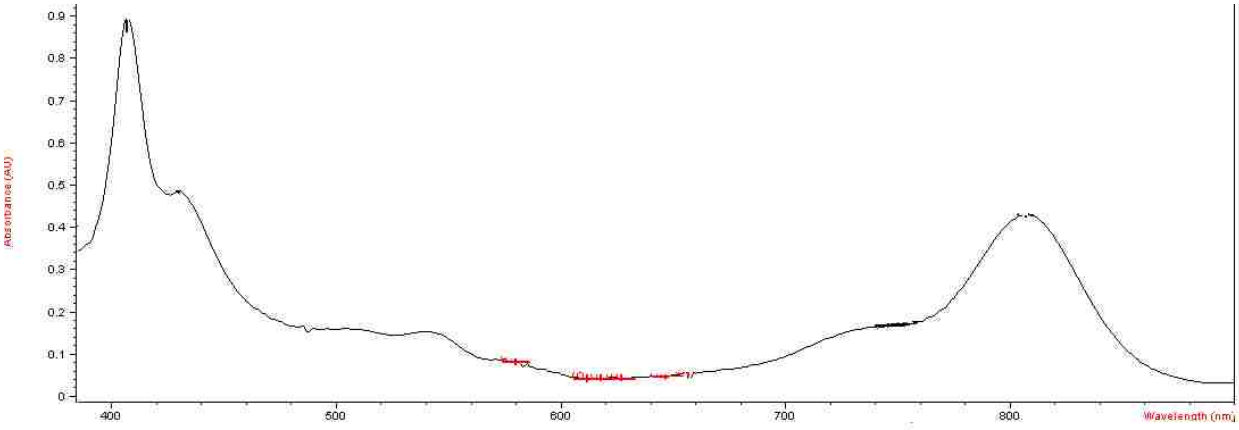

Figure 2.8: UV/visible spectrum in CH_2Cl_2 of zinc(II) isoporphyrin **32** from cyclization of b-bilene salt with 2,3-butanedione.

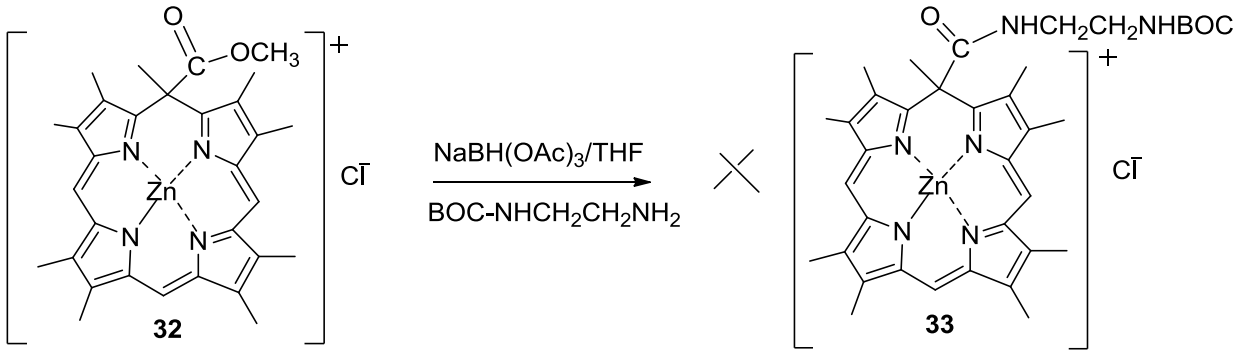

Scheme 2.16: Attempted reductive amination of zinc(II) isoporphyrin **32**.

Another choice was to cyclize the b-bilene salt by using benzyl or ethyl acetoacetate; in the product the resultant carboxylic acid group is separated from the α-position upon hydrolysis to avoid isomerization of isoporphyrin to porphyrin by simple decarboxylation (Scheme 2.17). Both benzyl acetoacetate and ethyl acetoacetate were used to cyclize the b-bilene hbydrochloride, and the reactions were monitored by UV-visible absorption spectroscopy. All the absorption spectra of intermediates are consistent with those intermediates seen during cyclization of the b-bilene salt using methyl pyruvate except for the oxidation step (Figure 2.9). There was no peak around 800 nm after adding DDQ or leaving it in air for a week, which indicated that zinc(II) isoporphyrin was not formed. The possible reason could be that the α-H from benzyl acetoacetate is not acidic enough to facilitate transformation into the intermediate required for cyclization to take place.

From the above attempts to functionalize zinc(II) isoporphyrin such as hydrolysis, amination and aminolysis, it seems that isoporphyrins are sensitive to strong acid, strong base and even nucleophiles such as lithium iodide. Therefore, introducing a functional group such as amine during cyclization would be a good choice for modification of zinc(II) isoporphyrins. In this way functionalization of the isoporphyrin under harsh conditions can be avoided. Pyruvate amide was chosen as a cyclizing reagent with the b-bilene salt,

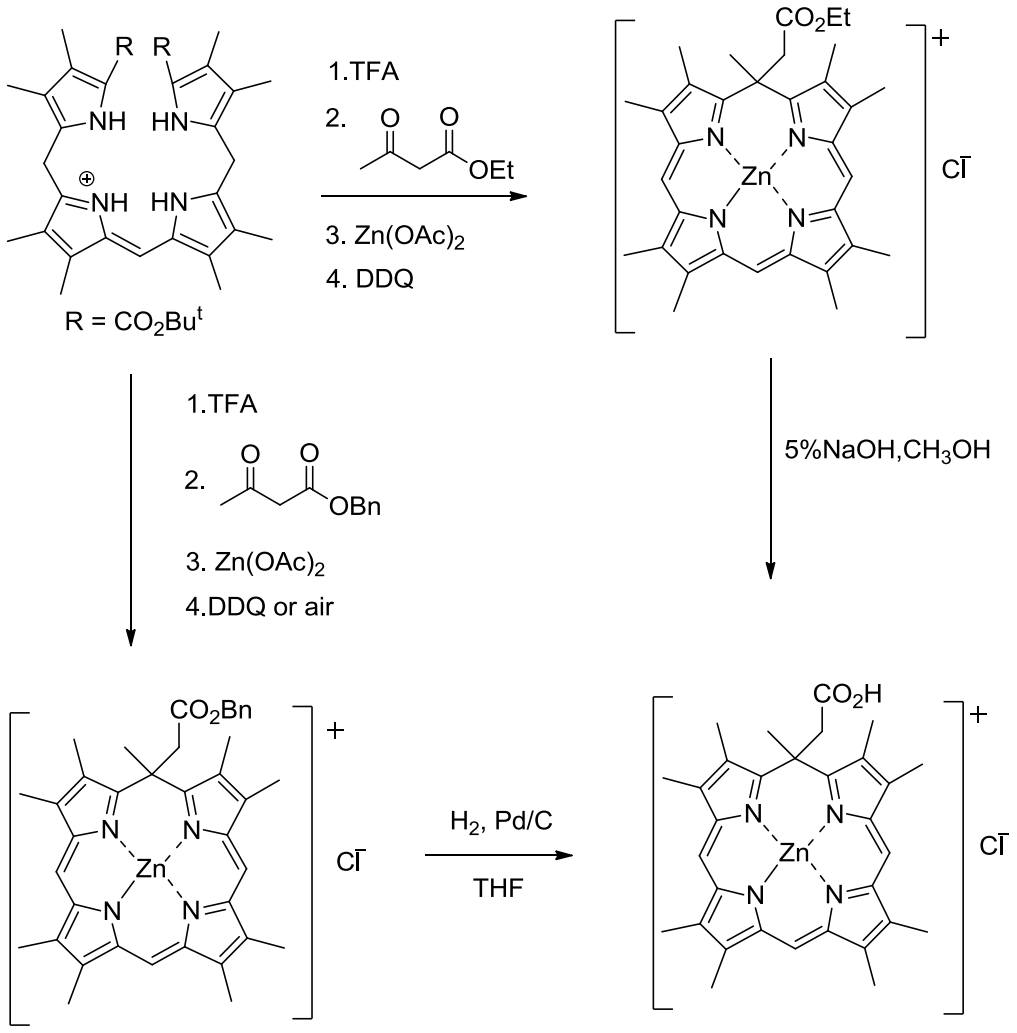

Scheme 2.17: Cyclization of b-bilene hydrochloride using acetoacetate esters.

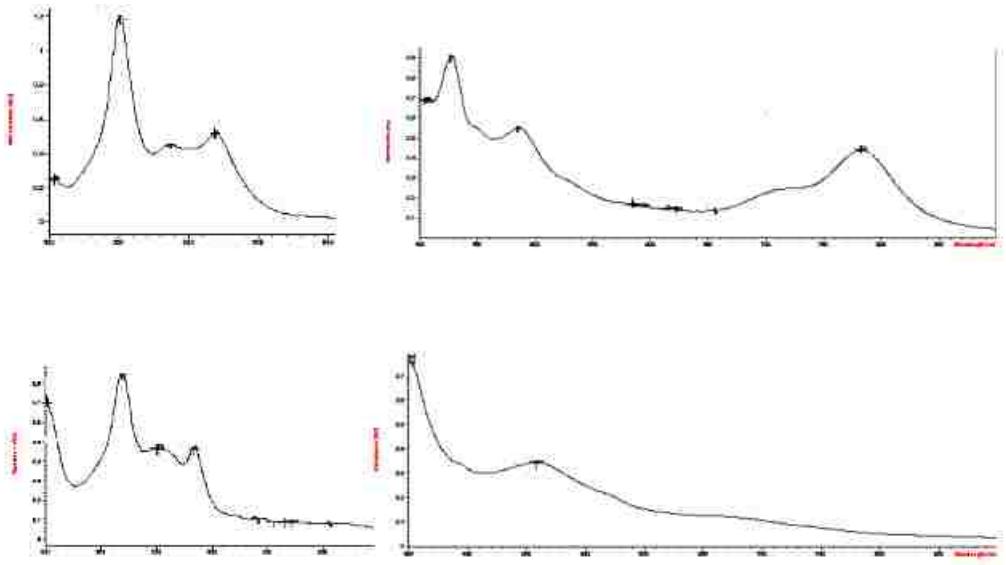

Figure 2.9: UV-Visible spectral changes in CH_2Cl_2 during cyclization of b-bilene hydrochloride **14** with benzyl acetoacetate.

with the intention that the amine group would be employed later to conjugate with biomolecules. Two methods were attempted to make the α-keto amides. One involves a peptidic coupling reaction[19] between α-keto acids and amines in the presence of coupling reagents such as DCC with DMAP，BOP-Cl, PyBOP-PF_6 with TEA and EDC with HOBt (Figure 2.10). The other method involves chlorination of α-keto acids followed by aminolysis with amines. A test reaction between pyruvic acid and hexylamine was examined with different coupling agents and the results are presented in Table 2.1. From this table it can be seen that coupling agents DCC with DMAP, BOPCl or PyBOP with TEA or DIEA only gave trace amount or very low yields of product. In contrast, HOBt with EDC led to an improved yield at 47% with DMF as the solvent. However for similar synthesis of β,γ-unsaturated α-keto amides reported by Rodriguez,[20] both BOPCl/TEA and PyBOP/DIEA gave them quantitive yields.

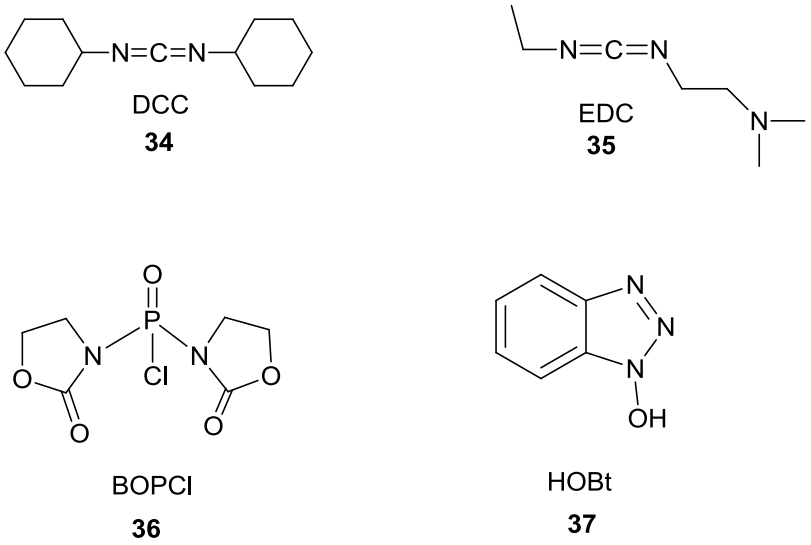

Figure 2.10: The coupling reagents used in reactions.

Table 2.1: The Coupling Reaction Using Different Reagents.

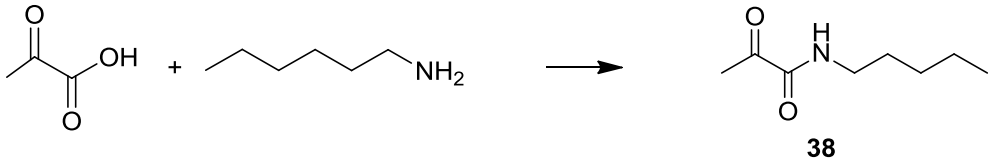

entry	Coupling reagents	Solvent system	yield
1	DCC/DMAP	DCM	trace
2	BOPCl/TEA	DCM	10%
3	PyBOP/TEA	DCM	12%
4	BOPCl or PyBOP/DIEA	DCM	15% and 19%
5	HOBt/EDC	DMF	47%

Meantime, a parallel alternative method was tried that involved chlorination of pyruvic acid with oxalyl chloride in CH_2Cl_2 followed by aminolysis[21] with hexylamine using TEA as base. A catalytic amount of DMF was added to speed up the reaction (Scheme 2.18).

The tedious part of this method is that oxalyl chloride is hard to remove from the reaction after chlorination; the remaining oxalyl chloride reacted with hexylamine to give a symmetrical diamide **39** which was inseparable from the product on a chromatography column. The purification was done by recrystallization using CH_2Cl_2/diethyl ether as the solvent system, to give 52% yield of product **38**.

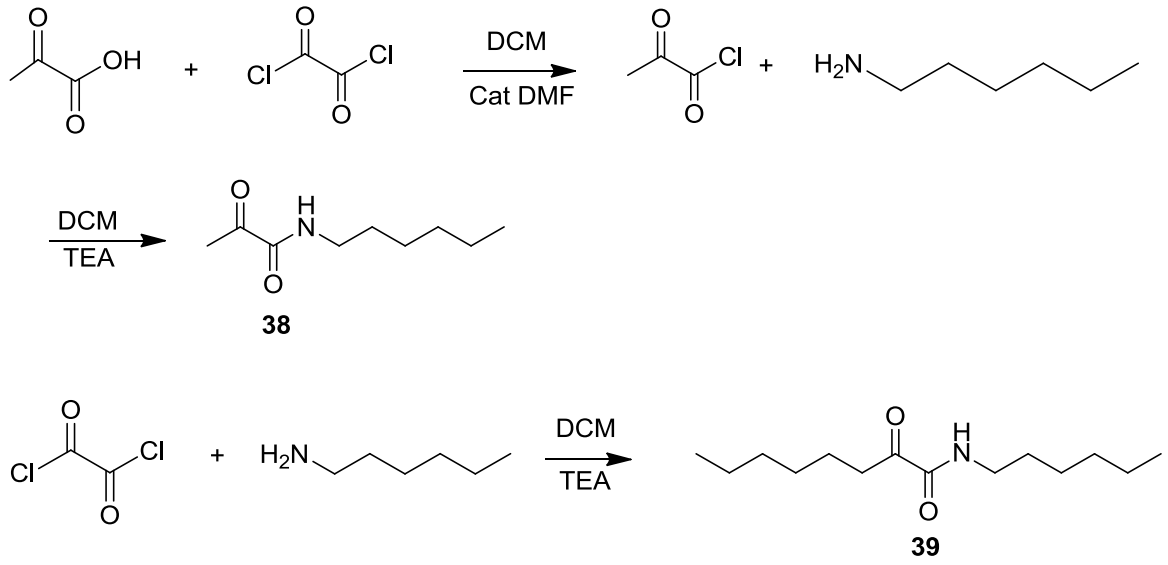

Scheme 2.18: Synthesis of pyruvate amide **38** by aminolysis reaction.

Therefore, the hexyl pyruvatamide was used as a test reagent to see if it was possible to cyclize b-bilene salts using an α-ketoamide. Under the same conditions as previously, a peak around 821 nm in the UV/visible spectrum appeared with time and indicated the formation of zinc(II) isoporphyrin **40** (Scheme 2.19). The hexylpyruvate amide proved that α-keto amides can cyclize with a b-bilene salt, so it was decided to synthesize a *N*-protected α-keto amine so that it can be deprotected later and used as a group to conjugate with amino acids. The similar conjugation reaction between pyruvic acid and mono-BOC protected ethylenediamine was performed with HOBt/EDC as coupling reagents. The product **41** was generated with a slightly lower yield of 41%. Similarly, the BOC-protected lysine was also conjugated with pyruvic acid under the same conditions

with a 32% yield of the product **42** (Scheme 2.20). Both of these two pyruvate amides were used to cyclize b-bilene salts in three steps. For mono-BOC-protected ethylenediamine pyruvate amide, a peak appeared around 826 nm (Figure 2.11) after zinc acetate was added and

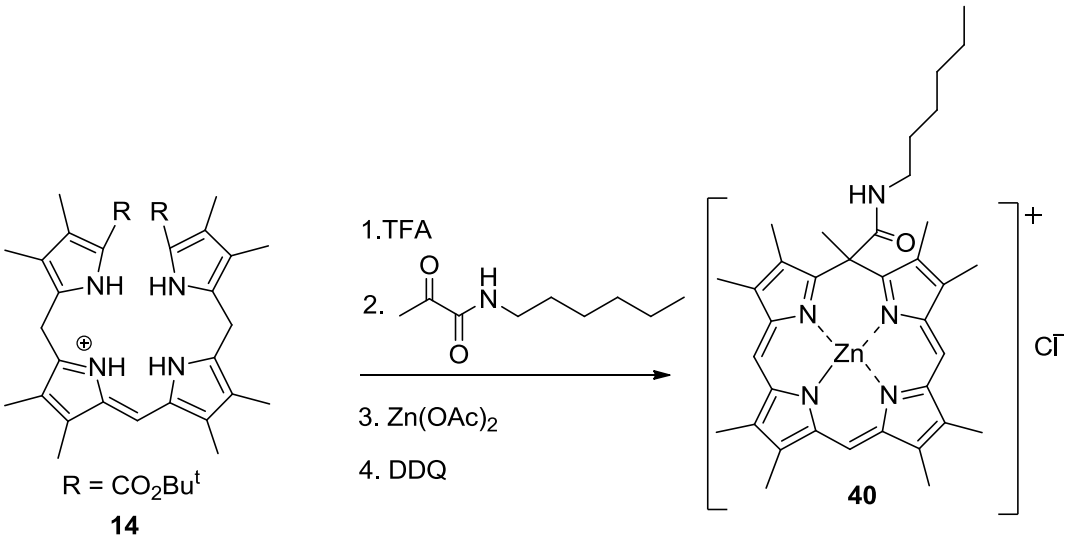

Scheme 2.19: Cyclization of b-bilene salt with hexyamine pyruvate amide.

it was left in air for five minutes, which proved that the macrocycle was formed. However, the peak disappeared with time unexpectedly since it should be increased in size through oxidation by oxygen in air. The assumption is that the cyclization of b-bilene salt into zinc(II) isoporphyrin and cyclization to give porphyrin compete with each other; with a long chain on the meso-carbon of the isoporphyrin, the ring opening is more favored than cyclization, and the open chain compound is cyclized into porphyrin with time. In the case of the BOC-protected lysine pyruvate, the cyclization did not succeed, UV/visible spectrophotometry gave no proof of formation of zinc(II) isoporphyrin. This is probably due to the steric effect from the lysine chain compared with BOC-protected enthylenediamine pyruvate (Scheme 2.21).

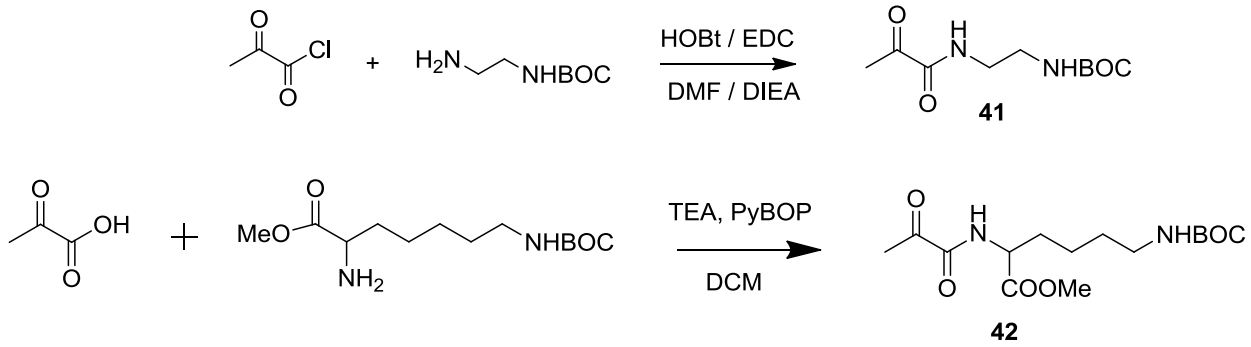

Scheme 2.20: Synthesis of BOC-ethylenediamine and BOC-lysine pyruvate amide **41** and **42**.

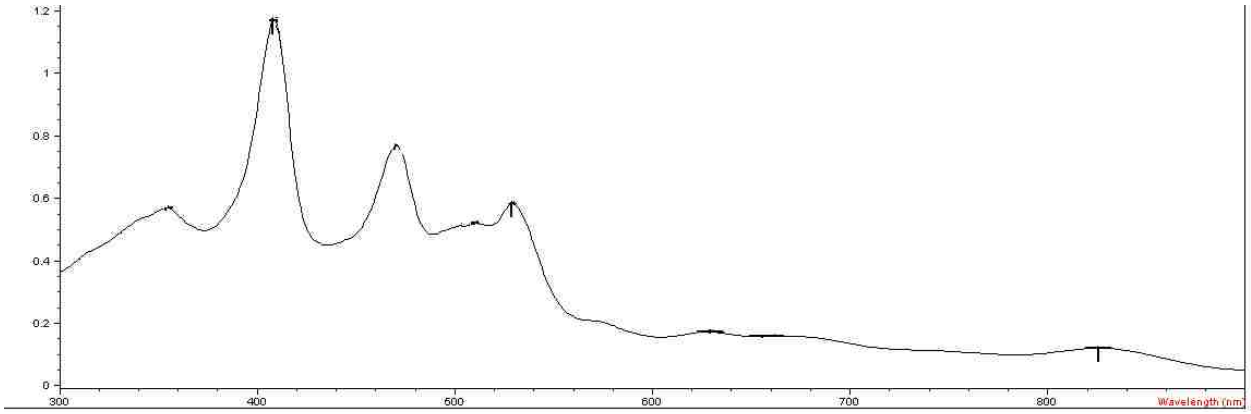

Figure 2.11: The UV/visible spectrum in CH_2Cl_2 of the cyclization of b-bilene salt with BOC-ethylenediame pyruvate amide **42**. The peak at 400 nm indicates porphyrin formation.

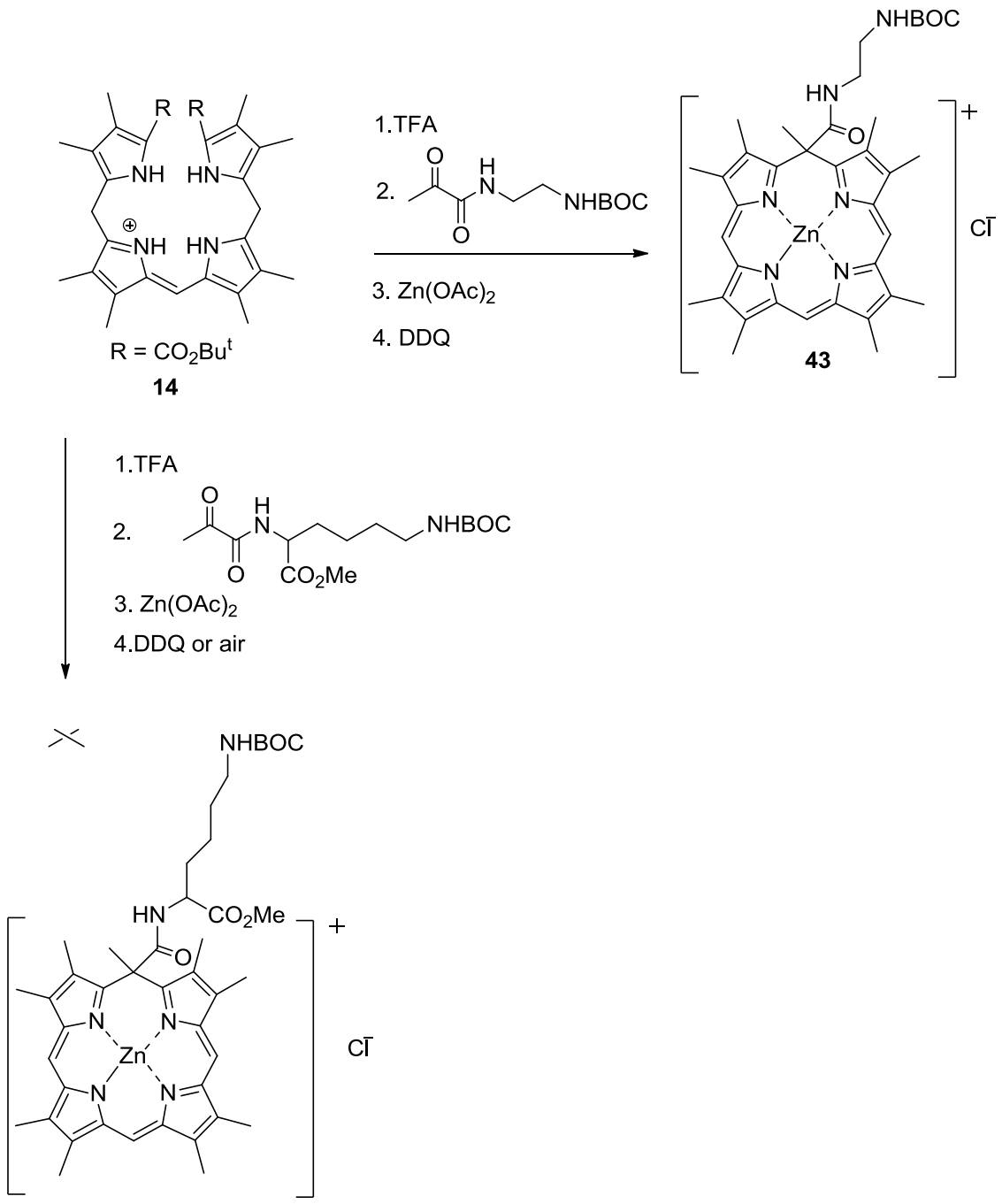

Scheme 2.21: Cyclization of b-bilene salt using BOC-lysine and BOC-ethylenediamine pyruvate amides **41** and **42**.

2.5. Conclusion

Zinc isoporphyrins were synthesized by cyclization of b-bilene salts with active α-keto esters in good yield. The product was characterized using NMR spectroscopy, mass spectroscopy and UV-visible spectroscopy. The resultant zinc(II) decamethylisoporphyrin chloride is stable at room temperature in daylight without decomposition or transformation into porphyrin. Attempts to hydrolyze the 5-methyl ester was so far unsuccessful due to facile decarboxylative conversion into porphyrin during the hydrolysis step. Efforts to introduce functional groups or biomolecules onto the zinc(II) isoporphyrin during cyclization did not solve the problem of isoporphyrin conjugation with biomolecules.

2.6. Experiment Part

tert-Butyl 3,4,5-trimethylpyrrole-2-carboxylate 21

Sodium nitrite (11.5 g, 0.16 mol) in water (40 ml) was added drop-wise with stirring and cooling to t-butyl acetoacetate（26 g, 0.16 mol）in glacial acetic acid (54 ml) at 0 ºC. Stirring was continued for a further 3 h; then the mixture was kept overnight at room temperature. The resultant *t*-butyl oximinoacetate solution was added drop-wise to a solution of 3-methyl-2,4-pentanedione (25 g, 0.22 mol) in acetic acid (88 ml) during portion-wise addition of an intimate mixture of zinc dust (25 g) and sodium acetate (25 g). The addition rate was controlled so that the solution temperature was maintained around 70 ºC. The addition continued for about 1.5 h and the reaction mixture was refluxed for 2 h. The reaction was monitored by TLC. After reaction was complete, the reaction solution was poured into ice/water and a yellow precipitate was filtered and washed with water until neutral. The solid was dissolved in CH_2Cl_2 and dried over anhydrous Na_2SO_4 overnight. The solvent was evaporated and the solid was recrystallized from

CH_2Cl_2/ethanol in the fridge to yield yellow needle crystals. ^{1}H NMR ($CDCl_3$, 400 MHz) δ 8.45 (s, br, 1H), 2.22 (s, 3H), 2.17 (s, 3H), 1.90 (s, 3H), 1.55 (s, 9H).

_t_-Butyl 5-acetoxymethyl-3,4-dimethylpyrrole-2-carboxylate 18

tert-Butyl 3,4,5-trimethylpyrrole-2-carboxylate (1.74 g, 8.3 mmol) was dissolved in acetic acid (39 ml) and acetic anhydride (1.0 ml). Then excess lead tetra-acetate (4.05 g, 9.1 mmol) was added to the solution portion-wise under argon. After addition was complete, the mixture was stirred overnight. The reaction was monitored using TLC. When the reaction was complete, the brown solution was treated drop-wise with 40 ml of ice/water and a yellow precipitate was formed. The solid was filtered and washed with distilled water to remove acetic acid and lead acetate. The solid was dried over anhydrous Na_2SO_4 in CH_2Cl_2 and recrystallization from CH_2Cl_2/hexane in the fridge gave a yellow solid 1.40g (60%). ^{1}H NMR (CDCl3, 400 MHz) δ 8.88 (s, br, 1H), 5.01 (s, 2H, -CH2-O), 2.23 (s, 3H, COCH3), 2.07 (s, 3H), 2.00 (s, 3H), 1.56 (s, 9H).

Ethyl 3,4-dimethylpyrrole-2-carboxylate 24

Acetaldehyde (13.0 ml, 0.465 mol) was stirred into isopropanol (8.5 ml) containing potassium fluoride (0.67 g, 0.023 mol, 0.05 mol eq), and the stirring was continued until the aldehyde had completely dissolved. To the stirred alcoholic solution was then added, drop by drop, nitroethane (16.5 ml, 0.46 mol)in an ice bath during 1 h; after this addition, stirring was continued overnight at room temperature under argon. Then the catalyst was removed by filtration. The residue, upon the removal of solvent, was poured into water and the residual oily matter was extracted with ether. Then the extract was dried over anhydrous Na_2SO_4 and the solvent was removed to give yellow oily product 2-nitro-butanol-3 (21.35 g, 40%).

To a flask was added acetic anhydride (19.2 g, 188 mmol, 1.5 eq), 4-dimethylaminopyridine (DMAP, 0.2 g) and CH_2Cl_2 (10 ml). 2-Nitro-3-butanol (15 g, 126 mmol) was added to the mixture over 20 min. The mixture was allowed to stir for 4 h at room temperature under argon. After reaction was complete, methanol (60 ml) was added to the solution which was stirred for 30 min to destroy excess acetic anhydride. Then, the solution was poured into dilute aqueous $NaHCO_3$ (18 g in 100 ml water) and extracted with CH_2Cl_2 (3 x 40 ml), the organic layer was dried over anhydrous Na_2SO_4 and filtered through a short column of silica gel. Removal of solvent gave the product as yellowish liquid (20.30 g, 49.5%).

To a solution of ethyl isocyanoacetate (2.51 g, 19 mmol, 1.05 eq), and tetramethylguanidine (4.41g, 38 mmol) in 6 ml of THF/Isopropanol (1:1) was added a solution of β-acetoxy-3-nitrobutane (3.0 g, 18.6 mmol) in 18 ml THF/isopropanol (1:1) drop-wise in an ice bath. After addition was complete, the solution was stirred at room temperature overnight under argon. When TLC showed reaction was complete, the resultant solution was concentrated to remove solvent. The oily residue was taken up in CH_2Cl_2 and washed successively with water (6 ml x 3), 5% aqueous HCl (6 ml x 3), water (6 ml x 3), aqueous saturated $NaHCO_3$ (6 ml) and brine (6 ml); then the product was dried over anhydrous Na_2SO_4 and the solvent was removed under vacuum to give the crude product. Recrystallization from CH_2Cl_2/hexane gave the product as a yellowish solid. ^{1}H NMR ($CDCl_3$, 400 MHz) δ 8.65 (s, br,1H), 6.65 (d, 1H), 4.32 (q, 2H, O-CH_2-CH_3), 2.27 (s, 3H), 2.01 (s, 3H), 1.35 (t, 3H, CH_2-CH_3).

Benzyl 3,4-dimethylpyrrole-2-carboxylate 19

Sodium metal (0.168 g, 7.3 mmol) was added to benzyl alcohol (60 ml) under argon. Once all the sodium had reacted, the ethyl ester pyrrole 24 (2.32 g, 14 mmol) was added

and the resultant mixture was heated in an oil bath at 90 ºC for 10 h. The mixture was allowed to stand at room temperature overnight and 1 equiv of acetic acid (0.438 g, 7.3 mmol) was added to neutralize the sodium benzoate. Benzyl alcohol was evaporated to dryness under reduced pressure and the residue was dissolved in CH_2Cl_2, washed with water and treated with decolorizing carbon. After filtration through a Celite cake, the solution was dried over anhydrous $MgSO_4$ and the solvent was evaporated under vacuum to yield a brown solid (1.5 g, 90% yield).^{1}H NMR ($CDCl_3$, 400 MHz) δ 8.70 (s, br, 1H), 7.26-7.41 (m, 5H), 6.65 (d, 1H), 5.30 (s, 2H), 2.28 (s, 3H), 2.01 (s, 3H).

tert-Butyl 9-(benzyloxycarbonyl)-3,4,7,8-tetramethyldipyrromethane-1-carboxylate 25

Montmorillonite clay (K10; 9 g) was added to a solution of 5-acetoxymethylpyrrole **18** (2.72 g, 10 mmol) and 5-unsubstituted pyrrole **19** (2.52 g, 10.1 mmol) under argon in CH_2Cl_2 (100 ml) in a round-bottomed flask. The resultant mixture was stirred vigorously overnight and the reaction was monitored by TLC. After reaction was complete, the clay catalyst was filtered off and washed with CH_2Cl_2 and the solvent was removed on a rotary evaporator. From ^{1}H NMR analysis, the crude product was already pure enough to be used in the next step. Further purification was done on a silica gel column using CH_2Cl_2 containing a little methanol as elution solvent. Alternatively the product could be recrystallized from CH_2Cl_2/petroleum ether in the fridge. ^{1}H NMR ($CDCl_3$, 400 MHz) δ 8.93, 8.68 (s, br,1H each), 7.26-7.35 (m, 5H), 5.27 (s, 2H, CH_2-Ph), 3.81 (s, 2H), 2.26 (s, 3H), 2.22 (s,3H), 1.94 (s, 3H), 1.93 (s, 3H), 1.53 (s, 9H).

1-(_tert_-Butyloxycarbonyl)-2,3,7,8-tetramethyldipyrromethane-9-carboxylic acid 26

A solution of mixed ester dipyrromethane **25** (2.0 g, 46 mmol) in approximately 80 ml of freshly distilled THF was degassed with argon for approximately 15 min. Then to the

solution was added 10% Pd/C (0.13 g) and the suspension was stirred under pressure of hydrogen gas at room temperature for 16 h; when the TLC showed the reaction was complete, the catalyst was removed by filtering through a bed of Celite and washed with THF. The collected filtrate was evaporated and a yellowish foamy solid formed. The product was further dried to give 1.50 g of product **26** (95% yield). δ ^{1}H NMR ($CDCl_3$, 400 MHz) 3.85 (s, 2H), 2.28, 2.18, 2.08, 2.01 (s, 3H each), 1.55 (s, 9H).

***tert*-Butyl 9-formyl-2,3,7,8-tetramethyldipyrromethane-1-carboxylate 27**

To a 100 ml round bottom flask were added dipyrromethane monocarboxylic acid **26** (300 mg, 0.86 mmol) and 40 ml of distilled CH_2Cl_2 under argon. p-Toluenesulfonic acid (328 mg, 1.7 mmol) was added portion-wise. Stirring was continued for 1.5 h until TLC showed completion of reaction. Saturated $NaHCO_3$ was added to neutralize the solution, followed brine, and the organic phase was dried over anhydrous $MgSO_4$. Evaporation of the solvent yielded a brown-reddish semi-solid which was dried under high vacuum to remove any solvents. Dry DMF (1.0 ml) was added to the crude material and the solution was cooled to 0 ºC. Meanwhile, Vilsmeier complex was prepared by adding benzoyl chloride (0.6 ml, 5.1 mmol) drop-wise to dry DMF (0.8 ml, 10.3 mmol) at 0 ºC, with stirring for 30 min. The Vilsmeier complex was added drop-wise to the decarboxylated mixture with stirring and after 15 min, stirring was continued at room temperature for a further 50 min. TLC showed formation of the imine salt. Toluene (10 ml) was added and small grains of precipitate were formed. The toluene was evaporated and the residue was dissolved in ethanol (25 ml), before 1.5 g of $NaHCO_3$ in 25 ml water was added. Stirring was continued overnight at room temperature; the yellowish precipitate was collected, the solid was dissolved in CH_2Cl_2 and washed with water and dried over anhydrous Na_2SO_4. Then the solvent was removed by evaporation and the yellowish solid was chromatographed on a silica gel column eluting with 3% methanol/ CH_2Cl_2 to

afford 171 mg (60%) of the title product. ^{1}H NMR ($CDCl_3$, 400 MHz) δ 10.05(s, br,1H), 9.50 (s, 1H), 9.22 (s, br, 1H), 3.88 (s, 2H), 2.26, 2.24, 1.99, 1.96 (s, CH_3 each), 1.52 (s,9H).

Di-*tert*-butyl 2,3,7,8,12,13,17,18-octamethyl-b-bilene-1,19-dicarboxylate hydrochloride 14

Dipyrromethane monocarboxylic acid **26** (0.14 mmol, 50 mg) and formyldipyrromethane **27** (0.12 mmol, 40 mg) were dissolved in 10 ml of dry CH_2Cl_2 and stirred under argon. p-Toluenesulfonic acid (53.0 mg, 2 equiv) was added portion-wise to the solution and the mixture was kept stirring for 2 h; the reaction was monitored using UV/visible spectroscopy. When a strong absorption at 502 nm was evident, the dark red solution was washed with 5% $NaHCO_3$ solution and water and then dried over anhydrous $MgSO_4$. The solvent was evaporated under reduced pressure to provide the b-bilene intermediate salt, which was dissolved in 5 ml of dry CH_2Cl_2 and hydrogen chloride was bubbled for 30 sec and whereupon the color changed to dark red as the hydrochloride salt formed. The solvent was evaporated and the residue was taken up twice in dry toluene and evaporated to remove any traces of water and HCl. The resultant residue was recrystallized from CH_2Cl_2/hexane and kept in the fridge overnight to give red product (45 mg, 63%). ^{1}H NMR ($CDCl_3$, 400 MHz) 7.07 (1H), 4.22 (CH_2, 4H), 2.22, 2.21, 2.04, 2.02, (each CH_3, 6H), 1.55 (*t*-butyl, 18H).

Zinc(II) 2,3,5,7,8,12,13,17,18-nonamethyl-5-(methoxycarbonyl)isoporphyrin chloride 28

b-Bilene hydrochloride **14**(50 mg, 0.08 ml) was added to a flask and cold TFA (0.3 ml) was added under argon and the reaction was kept stirring for 10 min. The solution was diluted with 20 ml of CH_2Cl_2 and this is followed by addition of methyl pyruvate (8.2 mg,

0.08 mmol). The mixture was stirred another 2 h. whereupon the UV/visible spectrum showed the disappearance of the absorption around 500 nm and new absorptions around 450 and 520 nm. The reaction was stopped and the excess TFA was removed by washing with water and the reddish solution changed to green after work-up, which had absorption maximum around 430 and 790 nm. The green intermediate was dissolved in dry CH_2Cl_2 (30 ml) followed by addition of $Zn(OAc)_2$ (20 mg) in 1 ml of dry methanol under argon. The solution immediately changed back to reddish and new absorptions around 470 and 540 nm were apparent. After about 10 min, DDQ (50 mg, 0.22 mmol) was added to oxidize the product for 30 min, the UV-visible spectrum of the solution then showed absorptions around 430 and 830 nm, these being characteristic absorptions of the zinc(II) isoporphyrin **28**. Then the reaction was kept for about 1 h and washed with water and brine. The product was dried over anhydrous Na_2SO_4. The purification was performed by chromatography on an alumina column eluting with CH_2Cl_2 and the fraction with the absorption of zinc(II) isoporphyrin was collected. Further purification was performed on a silica gel column eluted with CH_2Cl_2/ethyl acetate (7:3) and the product was recrystallized from CH_2Cl_2/petroleum ether. ^{1}H NMR ($CDCl_3$, 400MHz) δ, ppm 7.66 (s, *meso*-H, 1H), 7.58 (s, *meso*-H, 2H), 3.63 (s, 5-OCH_3, 3H), 2.43, 2.41, 2.38, 2.18 (s, β-CH3, 24H), 1.97 (s, 5-CH3, 3H).

Zinc(II) 2,3,5,7,8,12,13,17,18-Nonamethyl-5-benzylcarbonylisoporphyrin chloride 31

This compound was prepared as described above, in 5% yield.^{1}H NMR ($CDCl_3$, 400 MHz) δ ppm 7.63 (s, 2H), 7.59 (s, 1H), 7.01-6.99 (5H), 5.0 (s, 2H), 2.45, 2.41, 2.37, 1.99 (s, β-CH3, 24H), 1.94 (s, 3H).

Zinc(II) 2, 3, 5,8,12,13,17,18-nonamethyl-5-acetylisoporphyrin chloride 32

This compound was prepared as described above, in 20% yield. ^{1}H NMR ($CDCl_3$, 400 MHz) δ ppm 8.11-8.04 (m, 3H), 2.60, 2.57, 2.29, 2.27 (s, β-CH_3, 24H), 1.92 (s, 3H), 1.89 (s, 5-CH_3, 3H).

Hexylpyruvate amide 38

Method I: Pyruvic acid (0.20 g, 2.27 mmol) was dissolved in CH_2Cl_2 (30 ml) and then Et_3N (0.34 g, 0.47 ml) was added under argon. The mixture was cooled down to 0 ^oC, and BOPCl (0.70 g, 2.7 mmol) was added in one portion. The mixture was stirred at 0 ^oC for 30 min and then hexylamine (0.34 g, 3.40 mmol) was added. The mixture was allowed to warm to room temperature and was then stirred overnight. The solution was diluted with CH_2Cl_2 and washed with aqueous 1N HCl, water and then brine. The organic layer was dried over Na_2SO_4 and the product was purified by silica gel column chromatography eluting with 2% MeOH in CH_2Cl_2 to give the product 38.8 mg (10%).

Method 2: Pyruvic acid (0.20 g, 2.27 mmol) was dissolved in CH_2Cl_2 (30ml) and then oxalyl chloride (1.5 ml) was added followed by a drop of DMF; when the mixture stopped bubbling, it was left stirring for 1 h. Then the solvent was removed in vacuo. The residue was dissolved in CH_2Cl_2 (20 ml) and then hexylamine (0.34 g) was added at 0 ^oC, followed by TEA (0.34 g, 0.47 ml). The mixture was stirred overnight at room temperature. Then the solution was washed with 1 N HCl, water, brine and dried over anhydrous Na_2SO_4. The product was purified by crystallization from CH_2Cl_2/ether to give required product (0.20 g, 52%). ^{1}H NMR ($CDCl_3$, 400 MHz) δ ppm 6.94 (s, 1H), 3.30 (t, 2H) 2.47 (s, 3H), 1.53 (m, 2H), 1.29 (m, 6H), 0.89 (t, 3H). HRMS (ESI): *m/z* Calcd for $C_9H_{17}NNaO_2$: 194.1157; found: 194.1152.

BOC-ethylenediamine pyruvate amide 41: This synthesis followed procedure used for compound **38**.

Yield: 37%, ^{1}H NMR ($CDCl_3$, 400MHz): δ ppm 7.49 (s. 1H), 5.0 (s, 1H), 3.40 (t, 2H), 3.28 (t, 2H), 2.43 (s, 3H), 1.39 (s, 9H). HRMS (ESI): *m/z* Calcd for $C_{10}H_{18}N_2NaO_4$: 254.1164; found: 254.1151.

BOC-lysine pyruvate amide 42: The preparation of lysine pyruvate amide followed the procedure used for compound **38**. Yield: 40% ^{1}H NMR ($CDCl_3$, 400MHz): δ, ppm 7.38 (s, 1H), 7.36 (s, 1H) 4.52 (m, 1H), 3.74 (s, 3H), 3.09 (t, 2H) 2.46 (s, 3H), 1.91-1.69 (m, 4H), 1.41(s, 9H), 1.32(m, 2H). HRMS (ESI): *m/z* Calcd for $C_{15}H_{25}N_2O_6$: 329.1713; found: 329.1723.

2.7 Supporting Information

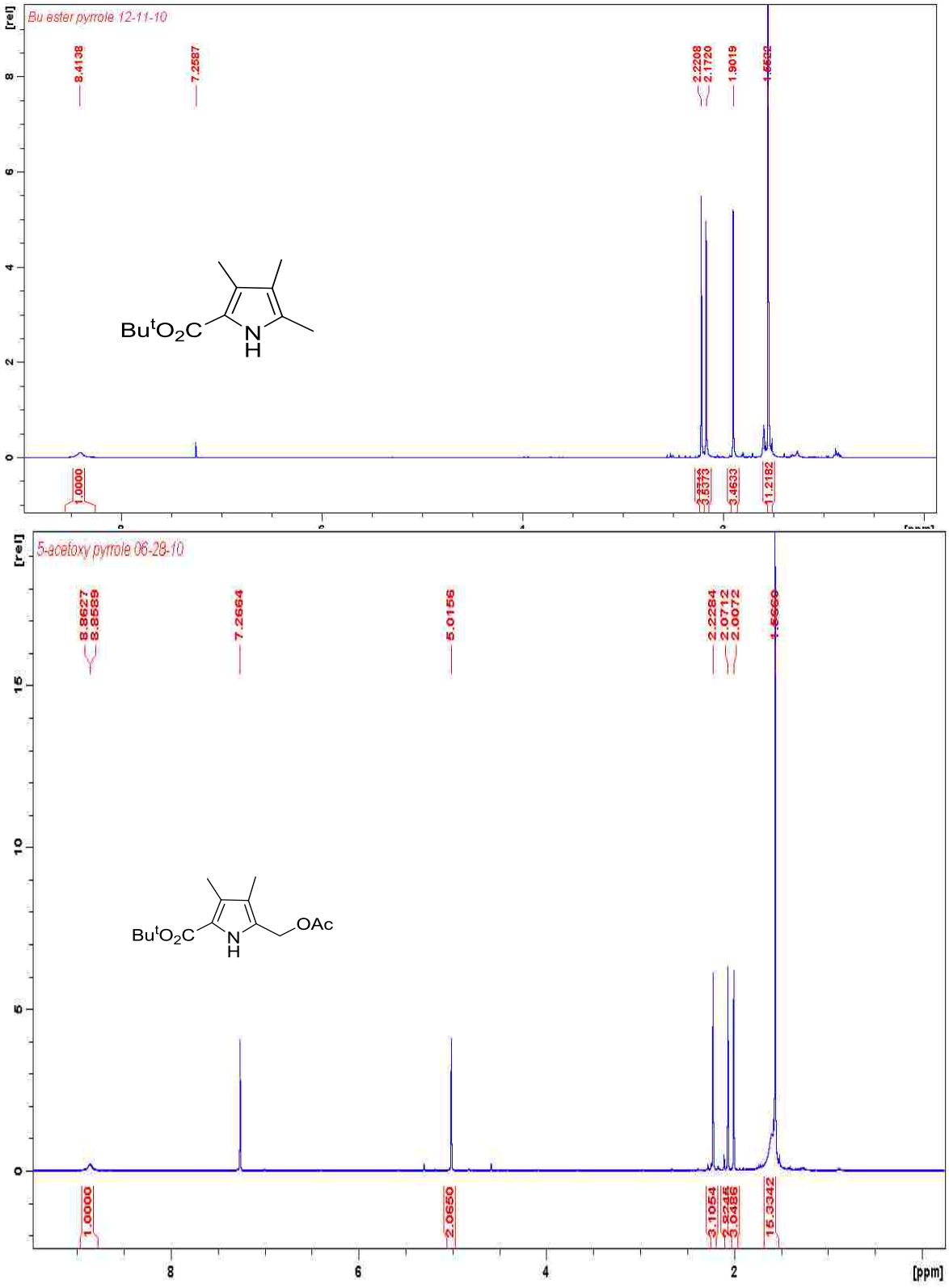

^{1}H NMR spectra of pyrrole **21** and **18** in $CDCl_3$ at 400 MHz.

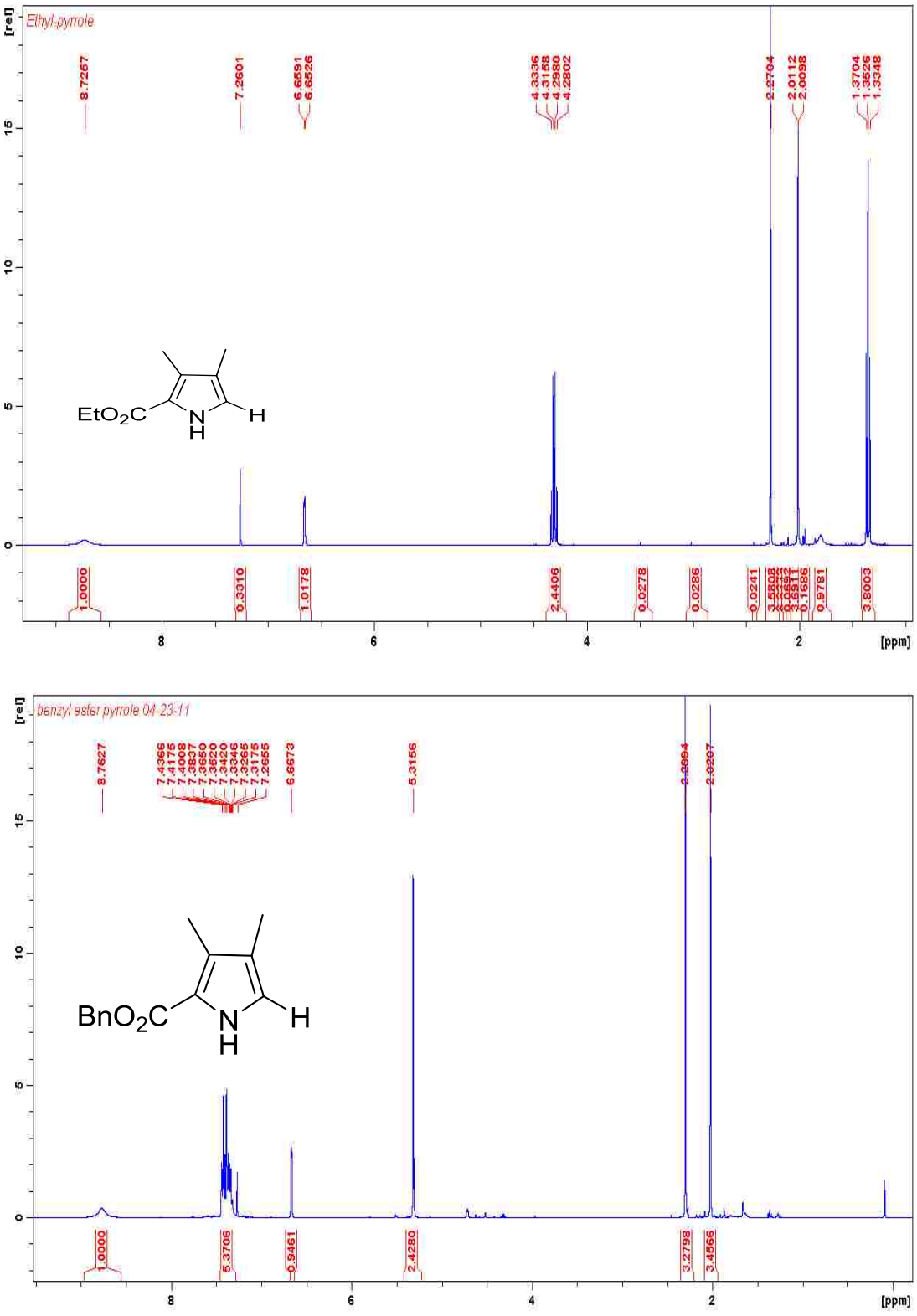

^{1}H NMR spectra of pyrrole **24** and **19** in $CDCl_3$ at 400 MHz.

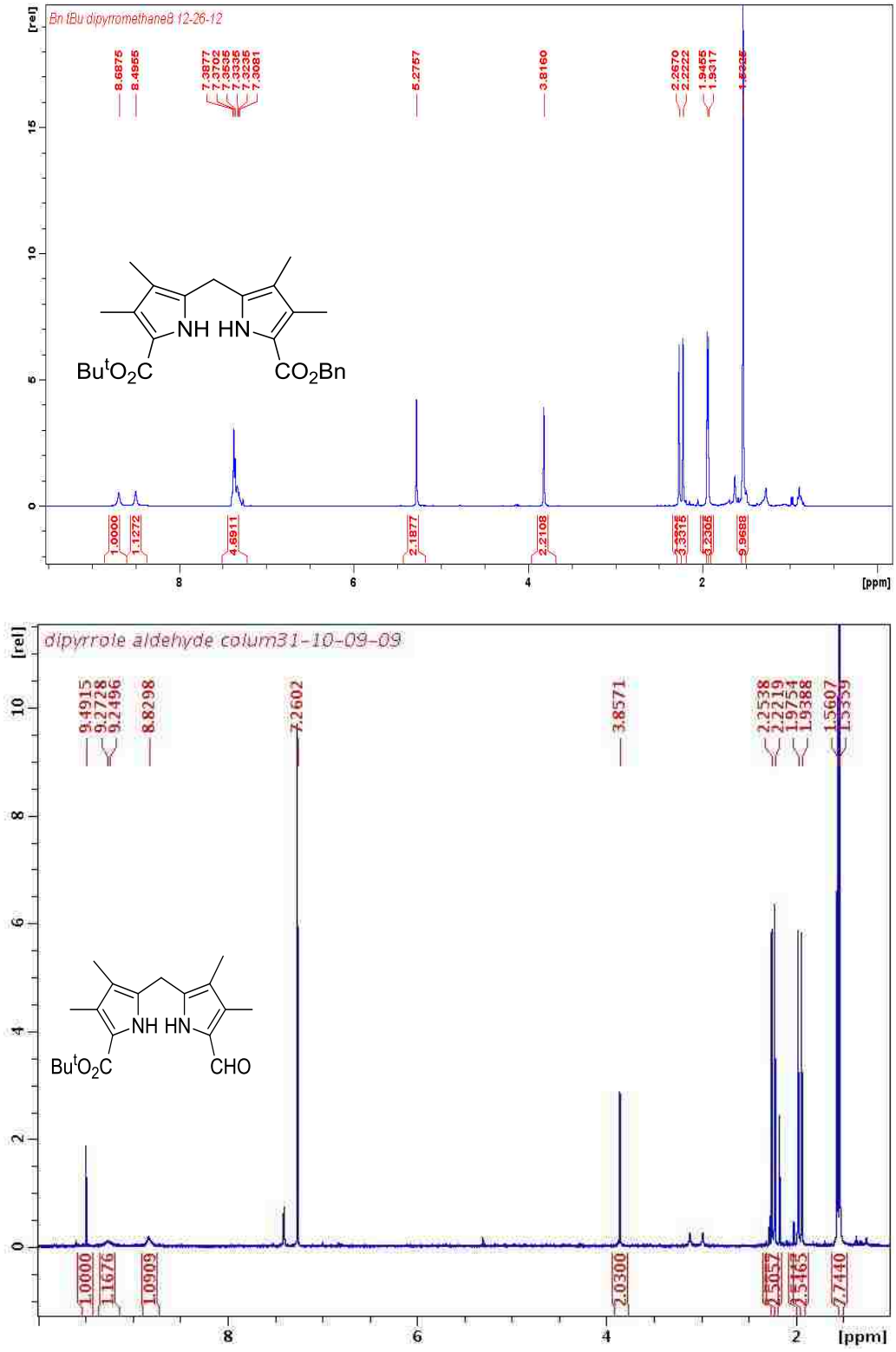

^{1}H NMR spectra of dipyrromethanes **25** and **27** in $CDCl_3$ at 400 MHz.

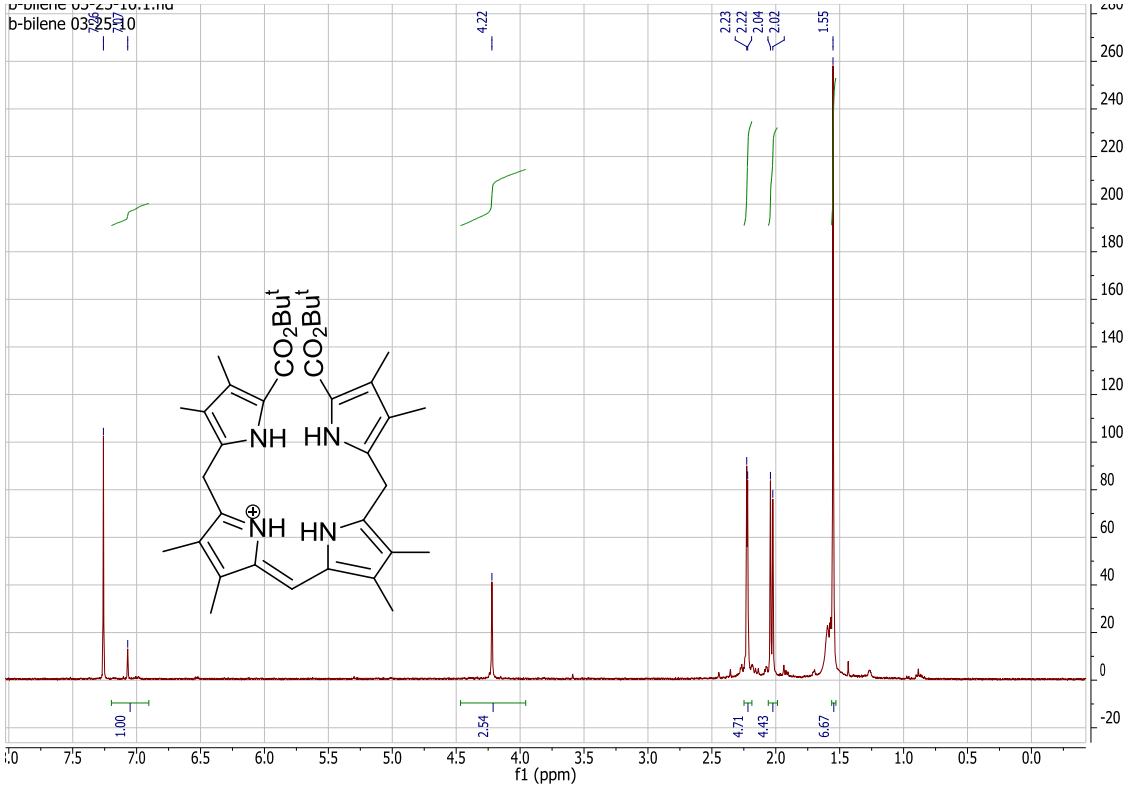

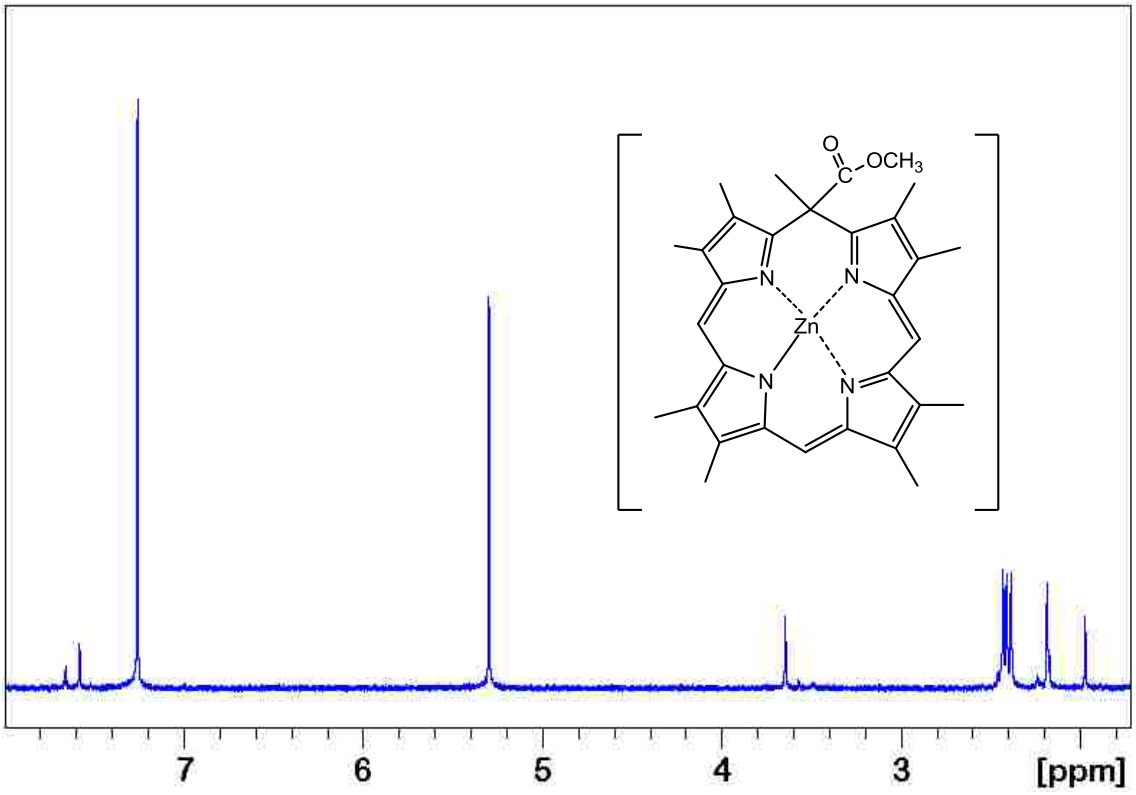

^{1}H NMR spectra of b-bilene salt **14** and isoporphyrin **28** in $CDCl_3$ at 400 MHz.

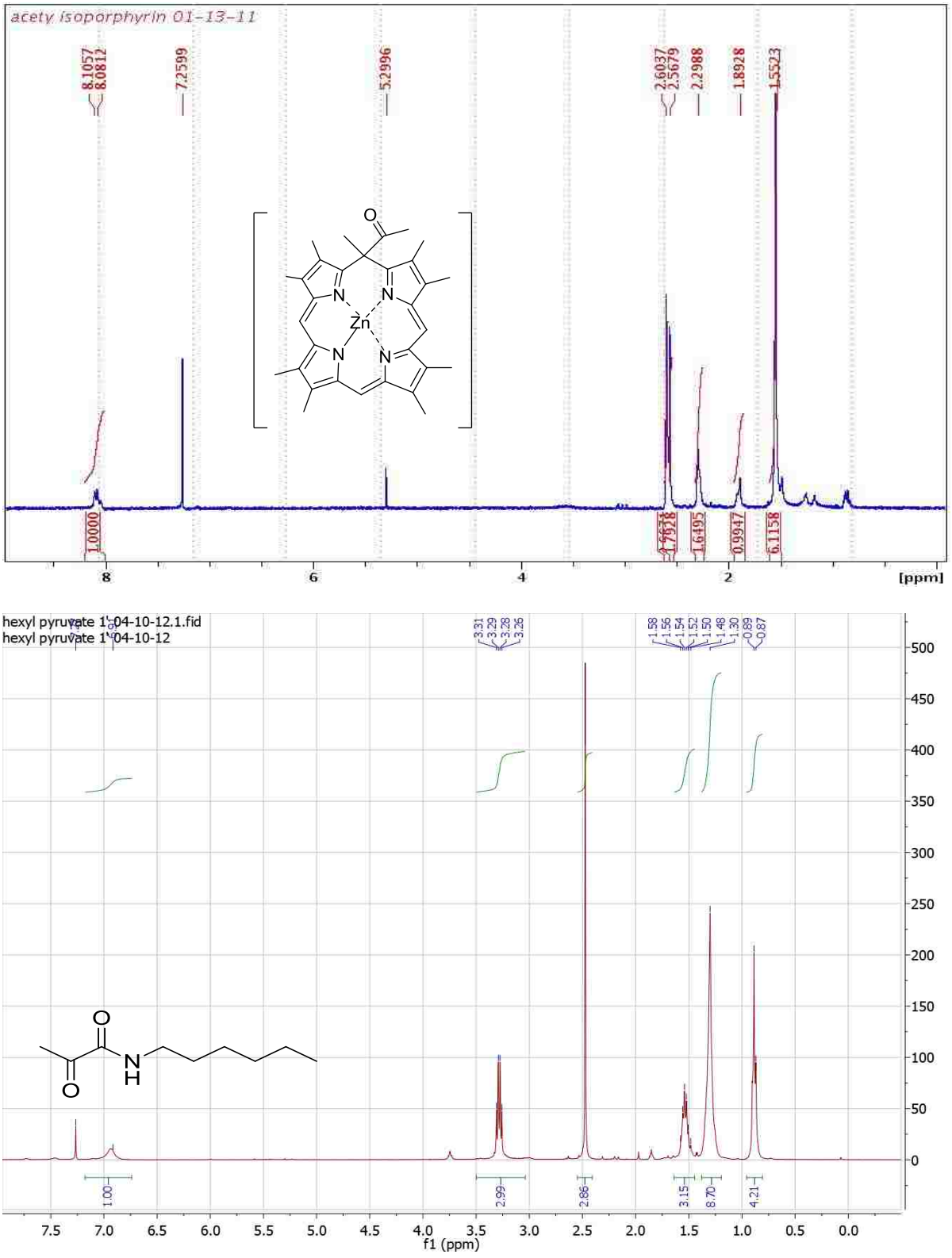

^{1}H NMR spectra of isoporphyrin **32** and pyruvate amide **38** in $CDCl_3$ at 400 MHz.

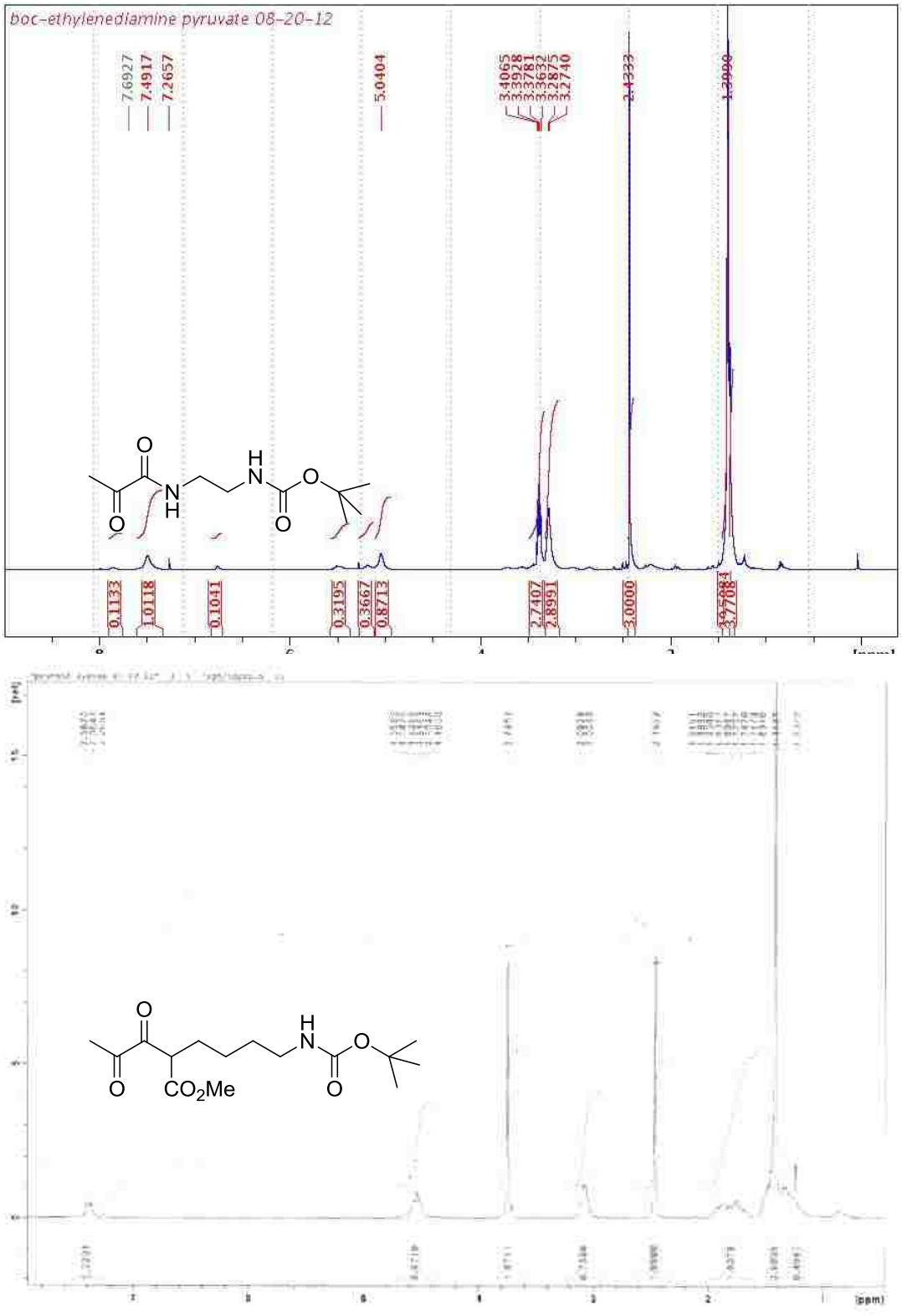

^{1}H NMR spectra of pyruvate amide **41** and **42** in $CDCl_3$ at 400 MHz.

2.8 References

1. Woodward, R. B. *Ind. Chim. Belge.* **1962**, *27*, 1293.

2. Dolphin, D.; Felton, R. H.; Borg, D. C.; Fajer, J.; *J. Am. Chem. Soc.* **1970**, *92*, 743.

3. (a)Mwakwari, C.; Fronczek, F. R.; Smith, K. M.; *Chem. Commun*. **2007**, 2258-60. (b) Mwakwri, C. In *PhD Dissertation*; Louisiana State University: Baton Rouge, **2007**. (c) Gentemann, S.; Leung, S.H.; Smith, K. M.; J. Fajer, J.; Holten, D. *J. Phys. Chem.* **1995**, *99*, 4330.

4. Takeda, Y.; Takahara, S.; Kobayashi, Y.; Misawa, H.; Sakuragi,H.; Tokumaru, K. *Chem. Lett*. **1990**, *11*, 2103.

5. (a) Gold, A.; Ivery, W.; Toney, G. E.; Sangaiah, R.; *Inorg. Chem*. **1984**, *23*, 2932. (b) Takeda, Y.; Takahara, S.; Kobayashi, Y.; Misawa, H.; Sakuragi, H.; Tokumaru, K. *Chem. Lett.* **1990**, *11*, 2103.

6. Xie, H.; Smith, K. M. *Tetrahedron Lett.* **1992**, *33*, 1197.

7. (a) Johnson, A. W.; Markham, E.; Price, W. R.; Shaw, K. B. *J. Chem. Soc.* **1958**, 4254. (b) Cavaleiro, J. A. S.; Kenner, G. W.; Smith, K. M. *J. Chem. Soc., Perkin Trans.* 1, **1973**, 2478.

8. (a) Barton, D. H. R.; Kervagoret, J; Zard, S. Z. *Tetrahedron* **1990**, *46*, 7587. (b) Cavaleiro, J. A. S.; Gonsalves, A. M.; Kenner, G. W.; Smith, K. M. *J. Chem. Soc., Perkin Trans.* 1, **1973**, 2471.

9. Montierth, J. M.; Duran, A. G.; Leung, S. H.; Smith, K. M.; Schore, N. E. *Tetrahedron Lett.* **2000**, 7423.

10. (a) Fox, O.D.; Rolls, T. D.; Drew, M. G. B.; Beer, P. D. *Chem. Commun*. **2001**, 1632. (b) Xie, H.; Smith, *PhD Dissertation*, University of California: Davis, **1992**. (c) Chong, R.; Clezy, P. S.; Liepa, A. J.; Nichol, A. W. *Aust. J. Chem.* **1969**, *22*, 229.

11. (a) Johnson, A. W.; Kay, I. T. *J. Chem. Soc.* **1961***,* 2418*.* (b) Jackson, A. H.; Kenner, G. H.; Smith, K. M. *J. Chem. Soc.* **1971***,* 502. (c) Cox, M. T.; Jackson, A. H.; Kenner, G. W. *J. Chem. Soc.* **1971***,* 1974. (d) Rezzano, I.; Buldain, G.; Frydman, B. *J. Org. Chem.* **1986**, *51*, 3968.

12. Valasinas, A.; Diaz, L.; Friedman, H. C. *J. Org. Chem*. **1985**, *50*, 2328.

13. Theodorou, V.; Skobridis, K.; Tzakos, A. G.; Ragoussis, V. *Tetrahedron Lett*. **2007**, 8230

14. Martin, P.; Mueller, M.; Flubacher, D.; Boudier, A.; Blaser, H-U.; Spielvogel, D. *Org. Pro. Res. Dev.* **2010**, *14*, 799.

15. Mattsson, S.; Dahlström, M.; Karlsson, S. *Tetrahedron Lett.* **2007**, *48*, 2497.

16. (a).Seitza, D. *Syn. Commun.* **1979**, *9*, 931. (b) Mayato, C.; Dorta, R. L.; Vazquez, J. T. *Tetrahedron Lett*. **2008**, *49*,1396. (c) Muller, P.; Siegfried, B. *Helv. Chim. Acta* **1974**, *57*, 987.

17. Felix, A. M. *J. Org. Chem*. **1974**, *39*, 1427.

18. Abdel-Magid, A. F.; Carson, K. G.; Harris, B. D.; Maryanoff, C. A.; Shah, R. D. *J. Org. Chem*, **1996**, 61, 3849.

19. Kende, A. S.; Lan, J.; Fan, J.; *Tetrahedron. Lett*. **2004**, *45*, 133.

20. Allais, C.; Constantieux, T.; Rodriguez, J. *Synthesis* **2009**, *15*, 2523.

21. Jin, H.; Hao, W. *Chem. Eur. J.* **2011**, *17*, 5234.

Chapter 3: Syntheses of Zinc(II) Isoporphyrins through MacDonald Condensation

3.1. Background

Dipyrrolic intermediates including dipyrromethenes[1,2] and dipyrromethanes[3-6] have been used to synthesize porphyrins. Usually the synthesis of the macrocycle involves condensation between one half bearing electrophilic groups such as formyl[7,8] or bromomethyl[9] and the other half which acts as a nucleophile, such as an α-free

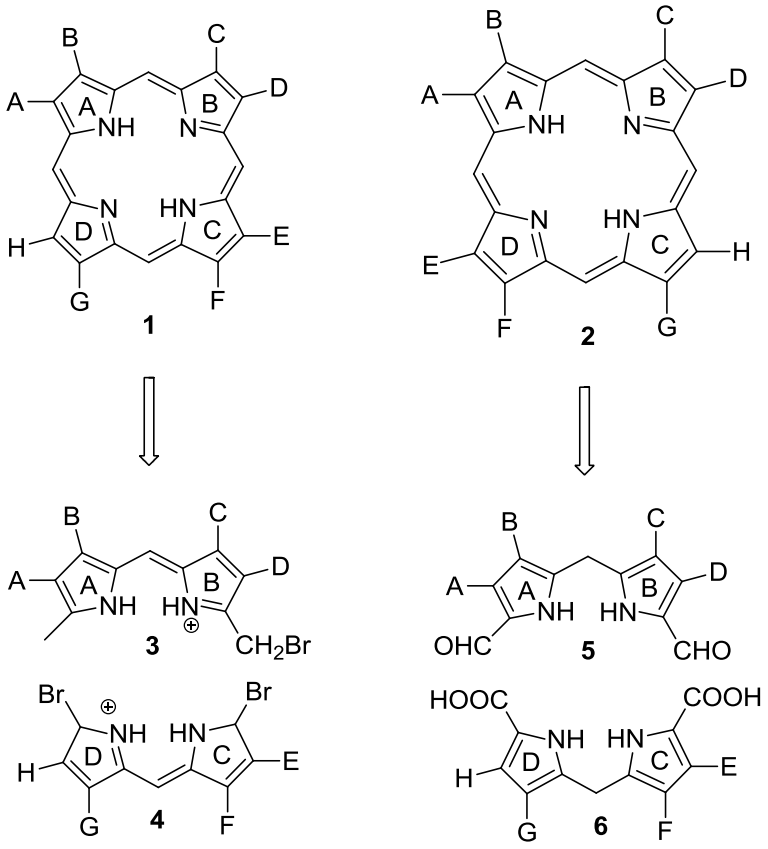

Scheme 3.1: Synthesis of porphyrin by [2+2] dipyrromethene (Fischer, **3**+**4** to 1) and dipyrromethane (MacDonald, **5**+**6** to **2**) condensation.

or bromo substituted dipyrromethenes (Scheme 3.1). This method using dipyrromethenes was developed by Hans Fischer and is an example of a [2+2][10-12] approach, usually only applied to synthesize symmetrical porphyrins[13,14] since this methodology has no selectivity between both ends of the two dipyrrole halves. On the other hand, use of dipyrromethanes (MacDonald approach) also yields porphyrins with

the same limitations as the Fischer approach, but under milder conditions. For asymmetric porphyrins, this method will result a mixture of products due to the selectivity limitation unless one or other of the two dipyrromethenes or two dipyrromethanes is symmetrically substituted about its central methane carbon atom.. The MacDonald dipyrromethane method was expanded successfully to synthesis of symmetrical isoporphyrins by Smith's group,[15-17] and became a fairly universal method to synthesize symmetrical isoporphyrins. The synthesis of zinc(II) isoporphyrin by the [2+2] approach usually involves a condensation reaction between a 1,9-diformyldipyrromethane and 1,9-unsubstituted dipyrromethane, catalyzed by acid (Scheme 3.2). According to the

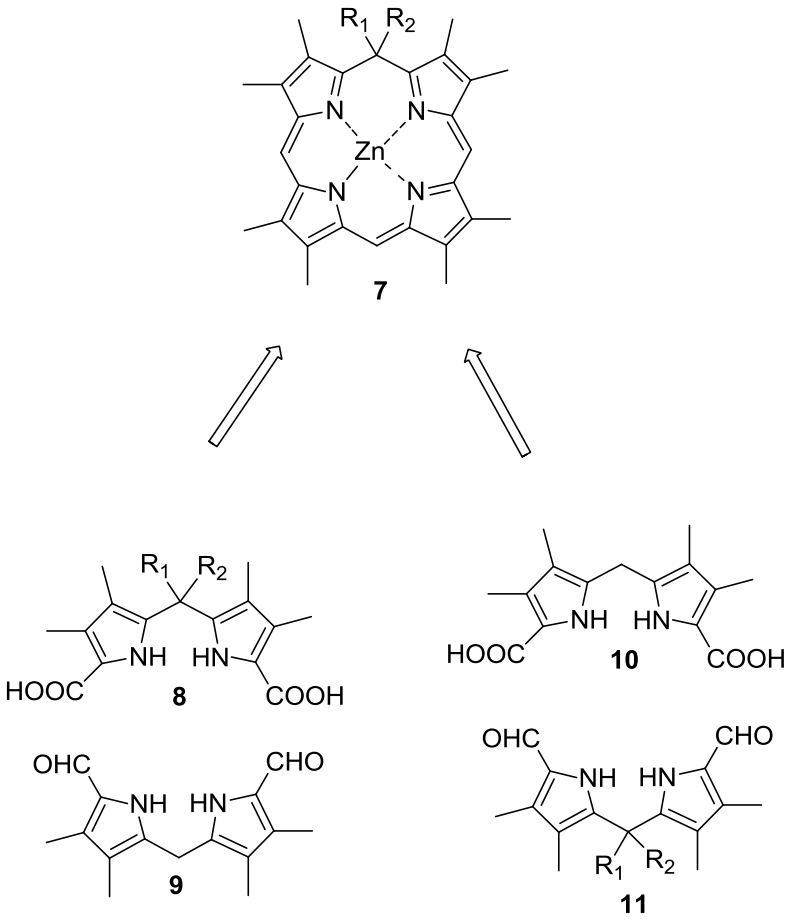

Scheme 3.2: Synthesis of zinc(II) isoporphyrin **7** by MacDonald 2 + 2 condensation.

structure of the target isoporphyrin, one of the dipyrromethane halves should be meso-disubstituted by alkyl or other groups. Metal is necessarily needed to serve as a template and to stabilize the isoporphyrin compounds once formed. In Chapter 2, attempts to introduce functional group such as carboxylate or acetyl group to a meso-carbon during cyclization of a b-bilene were discussed;[18] however, the transformation of these groups into carboxylic acid or amine groups failed when attempts were made to further functionalize the corresponding zinc(II) isoporphyrins after cyclization. The most plausible reason could be due to the fact that porphyrin is a very good and stable leaving group, and once the ester or amide bond on the meso-carbon of the zinc(II) isoporphyrin is cleaved, the decarboxylation takes place leaving a fully aromatic porphyrin as the leaving group. Therefore, to avoid this problem, the isoporphyrin **12** bearing two P^{Me} ($CH_2CH_2CO_2CH_3$) groups on pyrrole subunits was chosen as the target. From the structure we can see the fully conjugated macrocycle is interrupted by one meso-carbon which is saturated by geminal methyl groups.

3.2. Retrosynthesis

According to the MacDonald 2 + 2 condensation, the target molecule can be cyclized by reaction between a 5,5-dimethyldipyrromethane-1,9-dicarboxylate **13** and a 1,9-diformyldipyrromethane **16** in three steps. These two dipyrromethanes can be obtained by debenzylation and and debenzylation and diformylation of the corresponding dipyrromethanes, which were obtained through condensation of pyrrole **15** with acetone (for **13**) and self-condensation of pyrrole **18** (for **16**) (Scheme 3.3). The pyrrole starting materials were synthesized by conventional methods including synthesis of α-free pyrrole **15** by Baton Zard method and Johnson synthesis of pyrrole **18**.

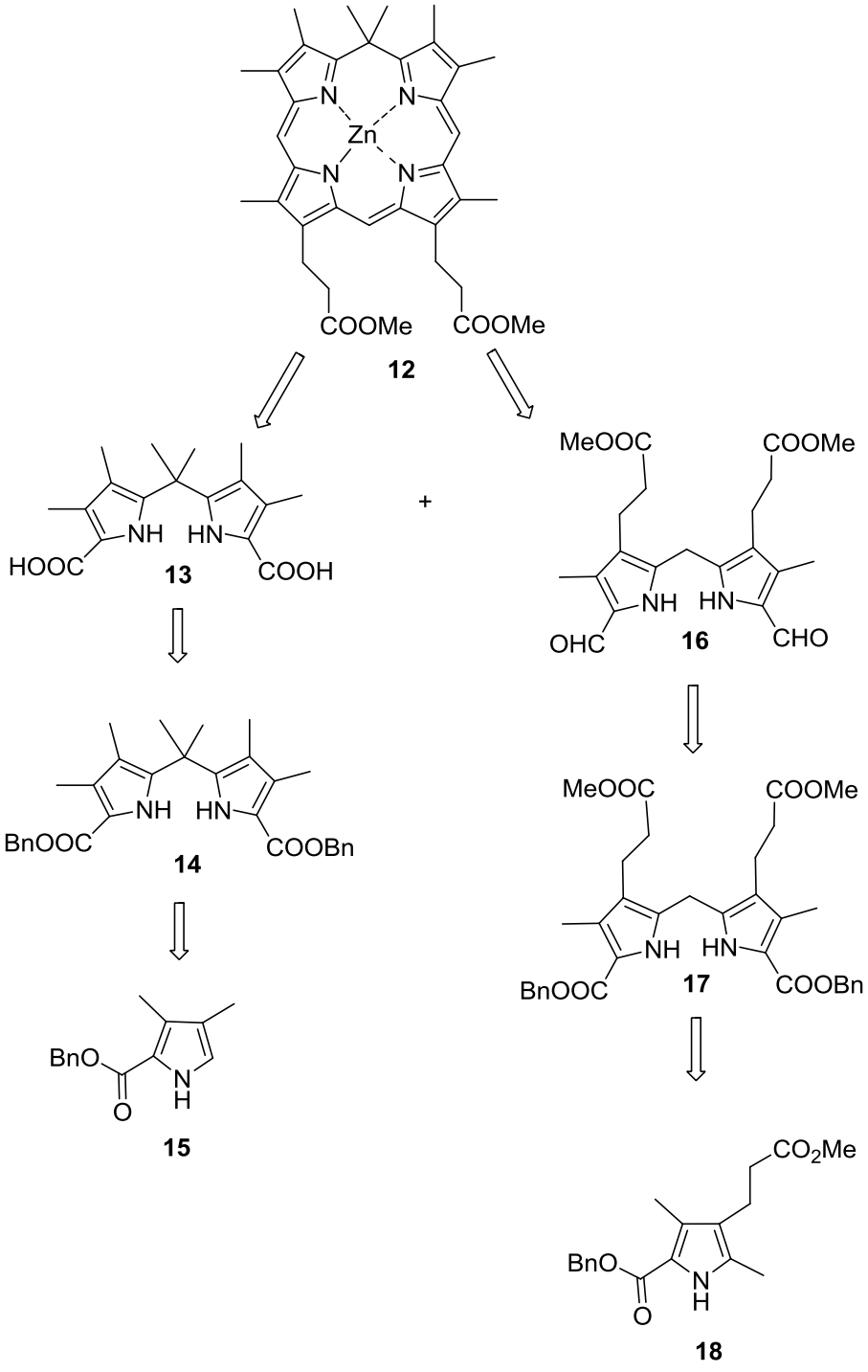

Scheme 3.3: Retrosynthesis of zinc(II) isoporphyrin **12** by the 2+2 MacDonald condensation approach.

3.3. Synthesis of Isoporporphyrins

The synthesis started with pyrroles **18** and **20**. Pyrrole **20** was synthesized, as follows, by Johnson's method.[19,20] Benzyl acetoacetate was treated with sodium nitrite in acetic acid to generate benzyl oximinoacetoacetate **19**, which was condensed with 3-methyl-2,4-pentanedione in glacial acetic acid in the presence of zinc dust and sodium acetate. The mixture was refluxed for one hour and the yellow precipitate was separated and recrystallized from CH_2Cl_2/hexane to give the product in around 65% yield. Pyrrole **18** was synthesized using a similar strategy; the precursor **21** was made by Michael addition of methyl acrylate to 2,4-pentanedione under basic conditions, and this was then condensed with benzyl oximinoacetoacetate, under the same conditions as previously, to afford the pyrrole **18** in around 50% yield. Pyrrole **18** was then treated with bromine in dry ether to give the intermediate 2-bromomethylpyrrole, which was converted into the corresponding symmetrical dipyrromethane **17** through self-condensation by refluxing in methanol.[21] The product was purified by crystallization from cold methanol (Scheme 3.4).

Dipyrromethane **17** was converted into the dicarboxylic acid **22** by catalytic hydrogenation using palladium on activated carbon as catalyst. This dicarboxylic acid was further converted into the 1,9-diformyldipyrromthane **16** by a Vilsmeier-Haack reaction in two steps. Decarboxylation of the dipyrromethane dicarboxylic acid was performed at 160 ^{o}C in DMF for one hour and resulted in the 1,9-di-unsubstituted dipyrromethane, which was treated with a mixture of DMF and benzoyl chloride (Vilsmeier reagent) followed by basic hydrolysis to give the product **16** in 70% yield. The other half, 5,5-dimethyldipyrromethane **14**,[22] was synthesized by condensation between the α-free pyrrole **15** (2 equivalents) and acetone with $BF_3.OEt_2$ as catalyst. Another

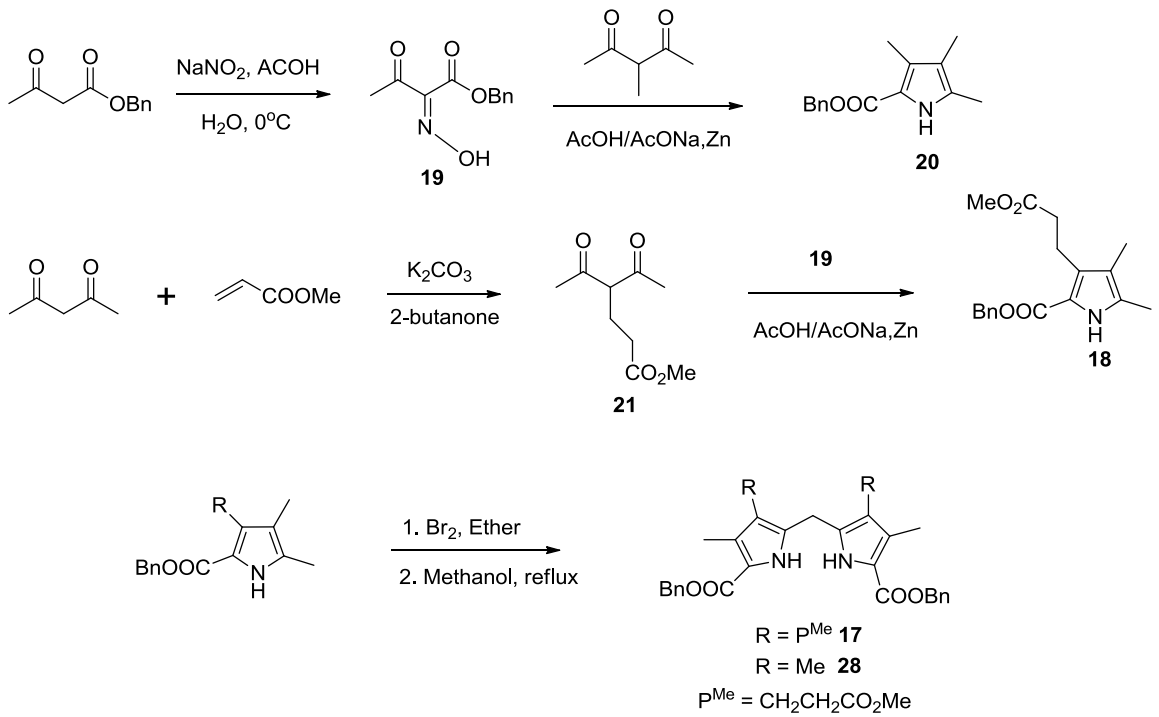

Scheme 3.4: Synthesis of pyrroles **18** and **20** and dipyrromethanes **17** and **28**.

major fraction was separated from chromatography column (running faster than the designed product), which was identified as compound **23** according to ^{1}H NMR (Scheme 3.5). Cyclization to give the zinc(II) isoporphyrin was finished in three steps[15] (Scheme 3.6): (1) The dipyrromethane dicarboxylic acid **13** was treated with toluenesulfonic acid to decarboxylate the two α-positions of the dipyrromethane; (2) The diformydipyrromethane **16**–was added, followed by zinc acetate as a template, and the reaction mixture was kept in the dark for 12 hours; (3) The reaction mixture was opened to air to oxidize the cyclized intermediate. The reaction was monitored by UV/visible absorption spectroscopy (Figure 3.1), with the characteristic peak around 800 nm becoming more pronounced with time, usually reaching a maximum after seven days. The product was purified by chromatography on silica gel, eluted with CH_2Cl_2/MeOH to give a yellowish solid in 20% yield. For zinc(II) isoporphyrin **12**, the Soret band and Q-band showed up at 414 and 799 nm, respectively. The identity of the product was also confirmed by mass spectrometry (m/z at 657.2643).

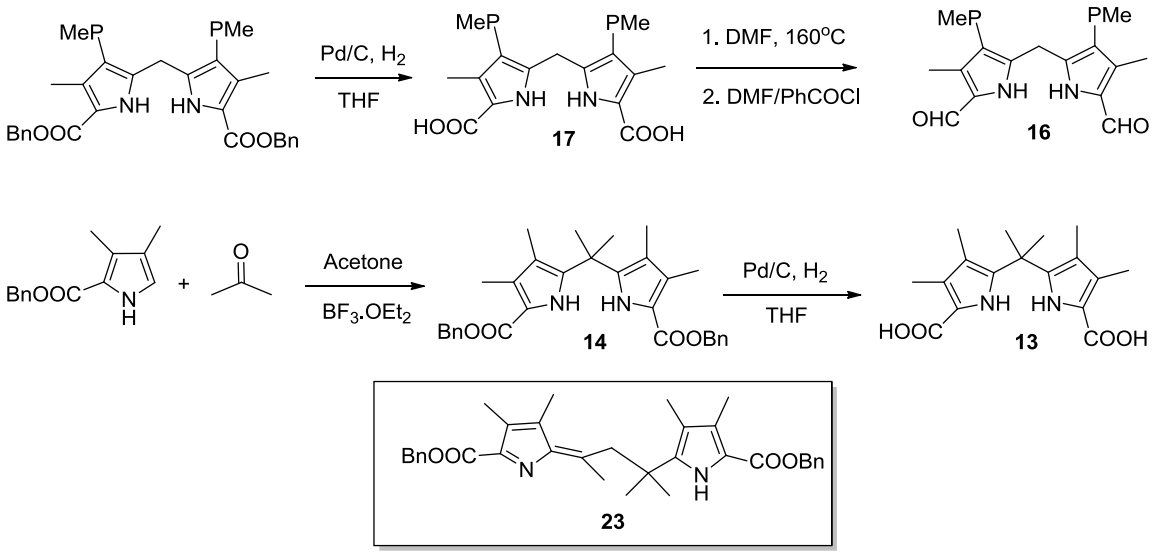

Scheme 3.5: Synthesis of dipyrromethane dicarboxylic acid **13** and diformydipyrromethane **16**.

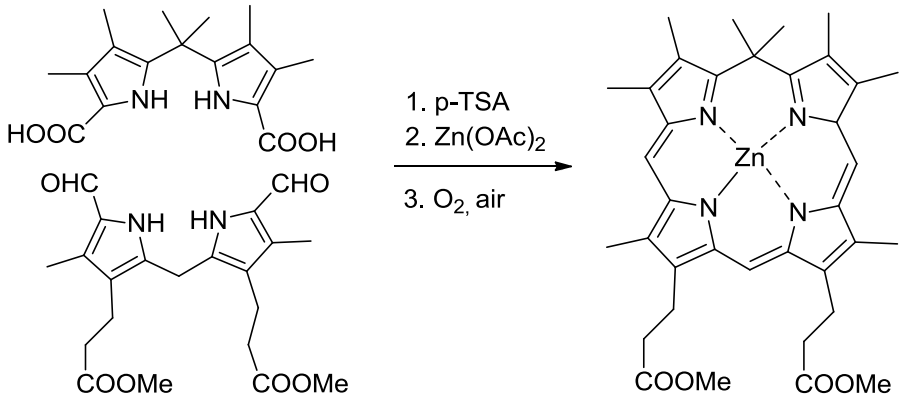

Scheme 3.6: Synthesis of zinc isoporphyrin **12** by 2+2 MacDonald cyclization.

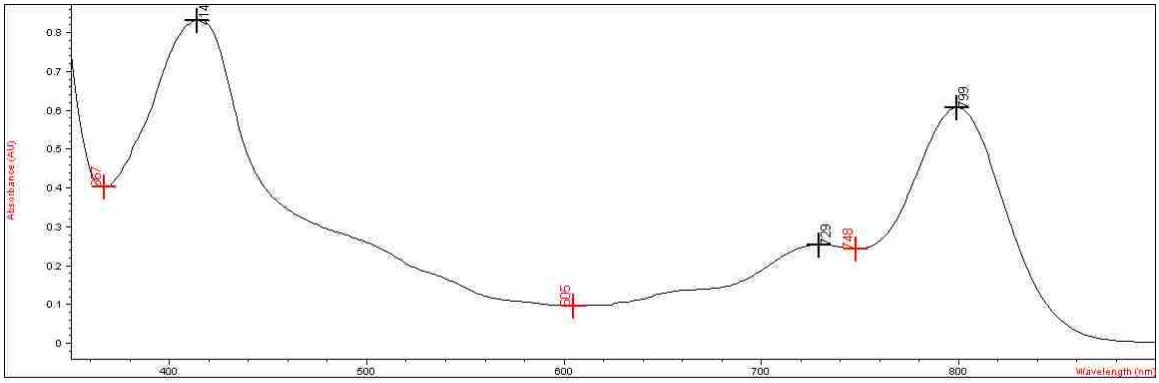

Figure 3.1: Absorption spectrum of zinc(II) isoporphyrin **12** in CH_2Cl_2.

After the success in the synthesis of zinc(II) isoporphyrin **12**, we expanded this method to the synthesis of other zinc(II) isoporphyrins. Molecules **24** and **29** were therefore designed, which have one, two or three ester groups; these isoporphyrins could be converted into the corresponding carboxylic acid substituted isoporphyrins so that they could be conjugated with biomolecules. In this way one can compare the differences of the biological properties of isoporphyrins mono-, di- and tri-conjugated with biomolecules. The retrosyntheses of these two molecules are similar to that for zinc(II) isoporphyrin **12**; these involve two dipyrromethanes with two carboxylic acid groups on both ends of one dipyrromethane **25** or **30** and two formyl groups on both ends of the other dipyrromethane **26** or **31**. Of course, the functional groups can be switched between these two dipyrromethanes **27** and **28** or between **32** and **17**. Theoretically, there should be no differences when these two halves approach each other to form macrocycles (Scheme 3.7).

Dipyrromethane **25** was synthesized by condensation of α-free pyrrole with ethyl acetoacetate, catalyzed by $BF_3.OEt_2$ in ethanol; the solution was refluxed overnight and the product was separated by chromatography to give 7-15% yields. Meanwhile, another major fraction was separated and identified to be 5,5-dimethydipyrromethane **14**. A possible mechanism for formation of **14** supposes that the ethyl acetoacetate was

hydrolyzed to carboxylic acid under acidic conditions, which was converted to acetone by acid catalyzed decarboxylation through a six membered ring; the α-free pyrrole then reacted with the generated acetone to form 5,5-dimethyldipyrromethane **14** (Scheme 3.8). The other dipyrromethane half **28** was synthesized with the same strategy as previously used, by bromination of the α-methylpyrrole **20** followed by self-condensation by refluxing it in methanol. The product **28** was crystallized from methanol to give a white solid in 70% yield. Then dipyrromethane **28** was catalytically debenzylated to give the dicarboxylic acid, which was treated with TFA/trimethylorthoformate[23] and then recrystallized from ethanol to give the diformydipyrromethane **26** (Scheme 3.9) in 35% yield. The dipyrrolmethane **25** was debenzylated by hydrogenation catalyzed by Pd/C and the resultant dicarboxylic acid was used as the precursor of the bis-α-free dipyrromethane. The cyclization the corresponding dipyrromethane dicarboxylic acid from **25** with the diformyldipyrromethane **26** was performed under the same conditions as previously reported in three steps (Scheme 3.10). Unfortunately, the desired product was not obtained according to UV/visible absorption spectroscopy, the characteristic peak of zinc(II) isoporphyrin around 800 nm being absent. According to Lash's synthesis[24] of extended indene-fused porphyrins **39** (Scheme 3.11), when the diformyl groups were located on the more strained dipyrromethane **36** instead of **35**, the reaction gave better yields than the other way around. We therefore took the same strategy with the synthesis of our zinc(II) isoporphyrin in this case. Before we switched the carboxylic acid and formyl groups between the two dipyrromethanes; we synthesized dipyrromethane **30** by reacting the α-free pyrrole **15** with ethyl levulinate, catalyzed by $BF_3.OEt_2$ in EtOH, to give a 30% yield compared with dipyrromethane **25** (Scheme 3.12), which had a lower yield of around 10% because of the competition from production of the side product dipyrromethane **23**. The cyclization of dipyrromethane **30** with the same diformydipyrromethane **26** failed to give the corresponding isoporphyrin, the UV/visible

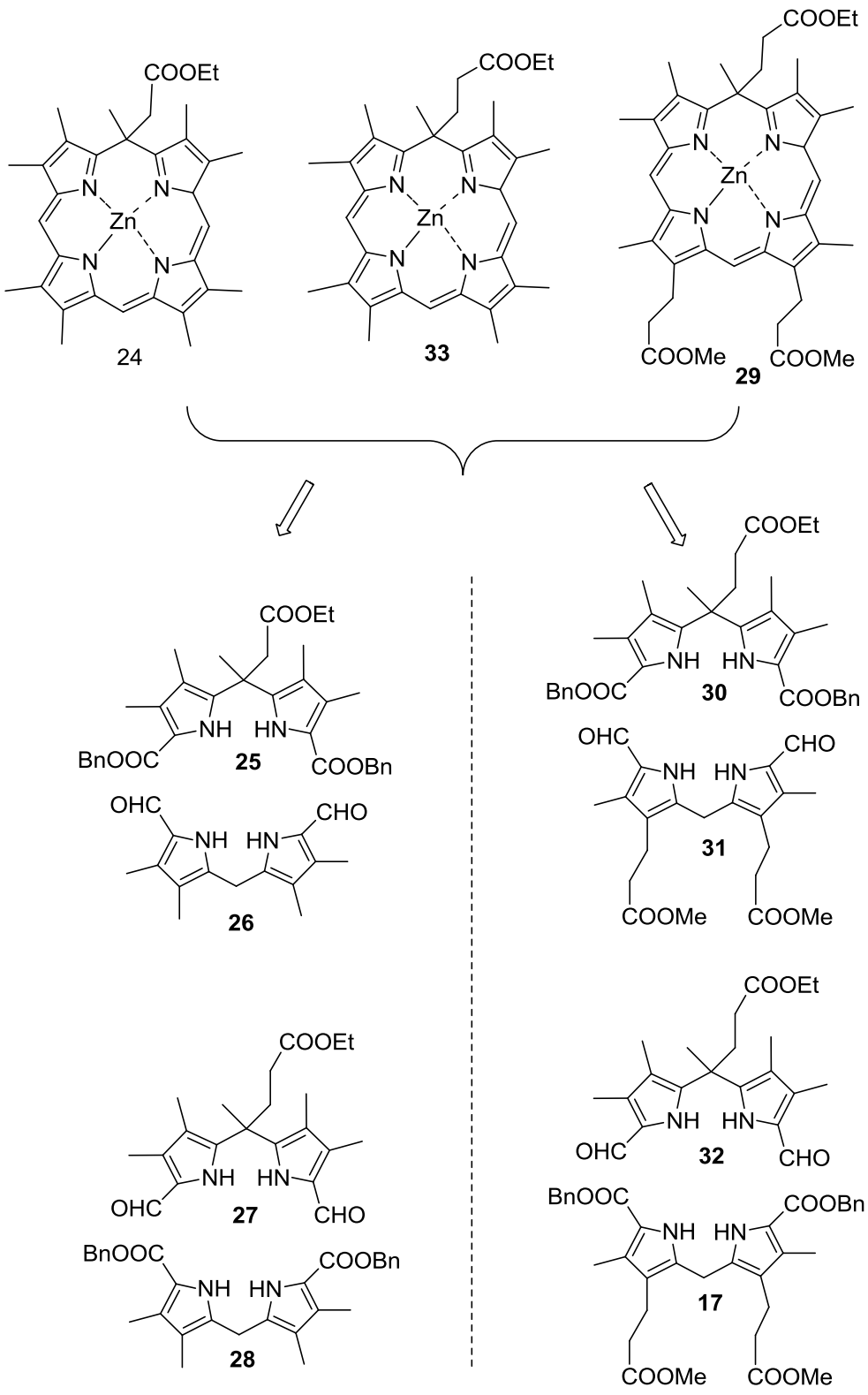

Scheme 3.7: Retrosynthesis of zinc(II) isoporphyrins **24**，**29** and **33** by MacDonald 2+2 condensation.

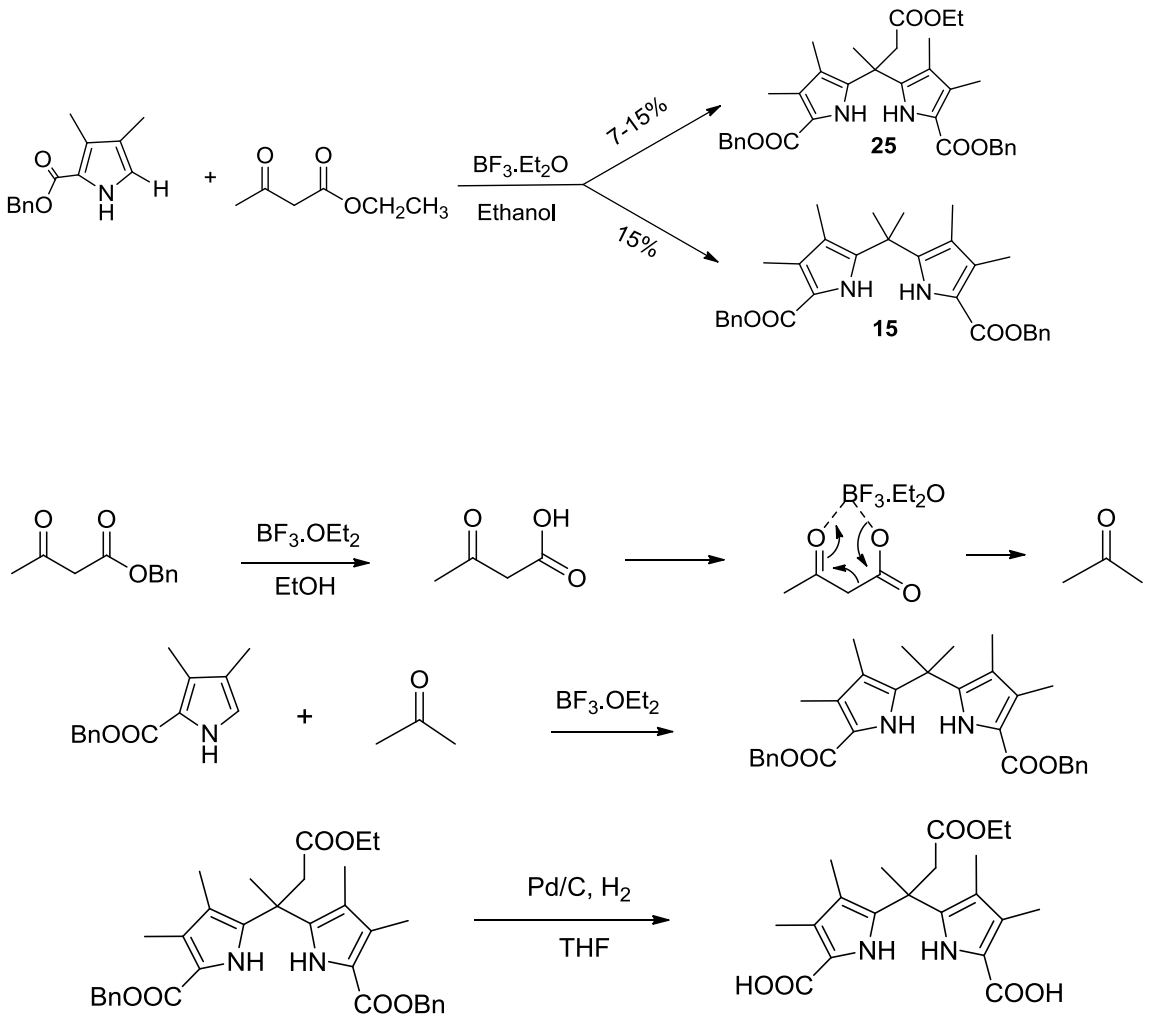

Scheme 3.8: Synthesis of dipyrromethanes and the proposed route for formation of side product **15**.

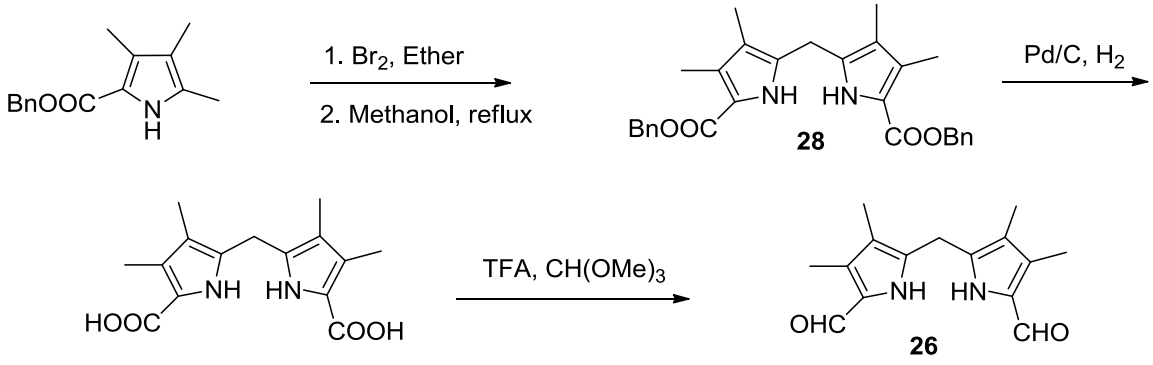

Scheme 3.9: Sythesis of dipyrromethanes **28** and **26**.

absorption around 500 nm indicating only one side was joined together to give an open-chain b-bilene. Therefore, the formyl groups were introduced onto dipyrromethane **30** instead of dipyrromethane **26**, which remained as the dipyrromethane dicarboxylic acid prior to cyclization. These two dipyrromethanes **32** and **28** were used for the cyclization using the identical previous conditions, and finally gave the desired zinc(II) Isoporphyrin product **33**. The reaction was mainly monitored by UV/visible absorption spectroscopy, and the product possessed a Soret band at 423 nm and a Q-band at 813 nm (Scheme 3.13).

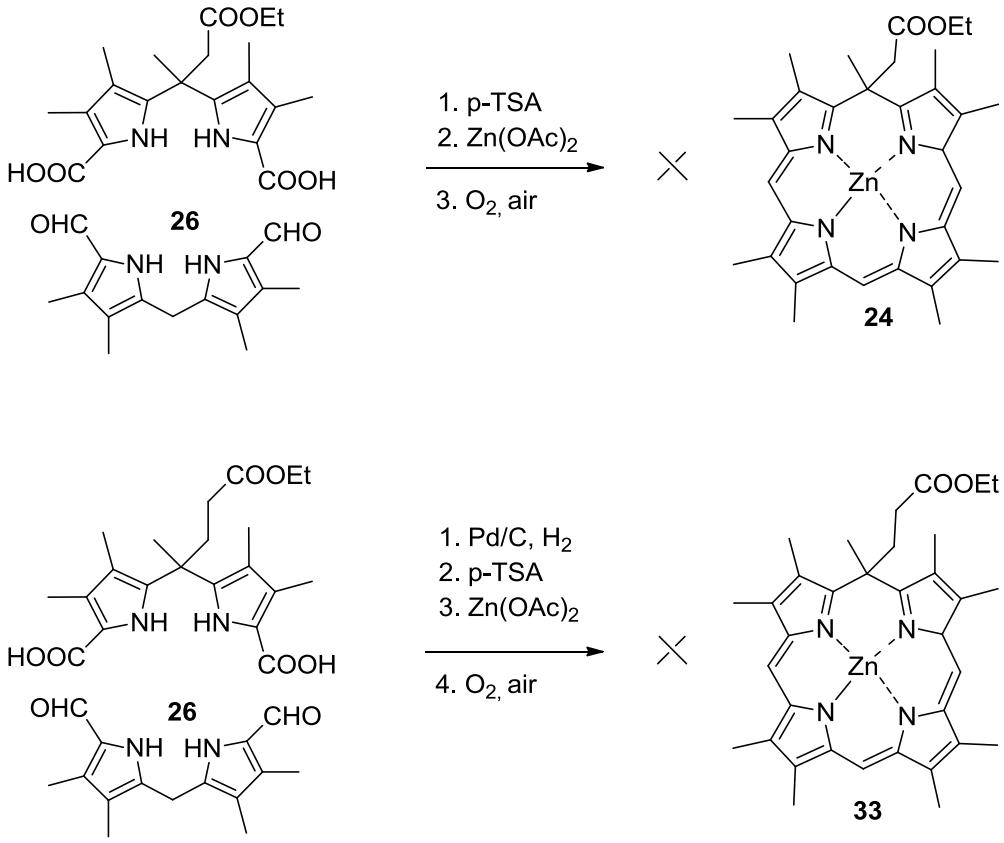

Scheme 3.10: Attempt to synthesize Isoporphyrin **24** and **33** by MacDonald 2+2 condensation.

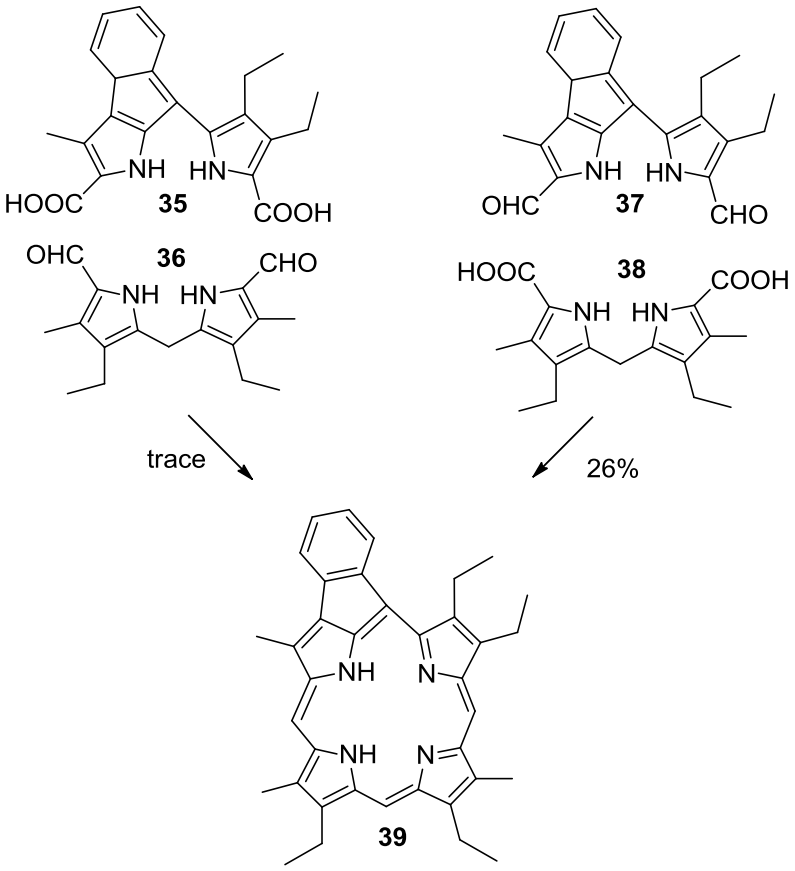

Scheme 3.11: Lash's synthesis of indene-fused porphyrins.[24]

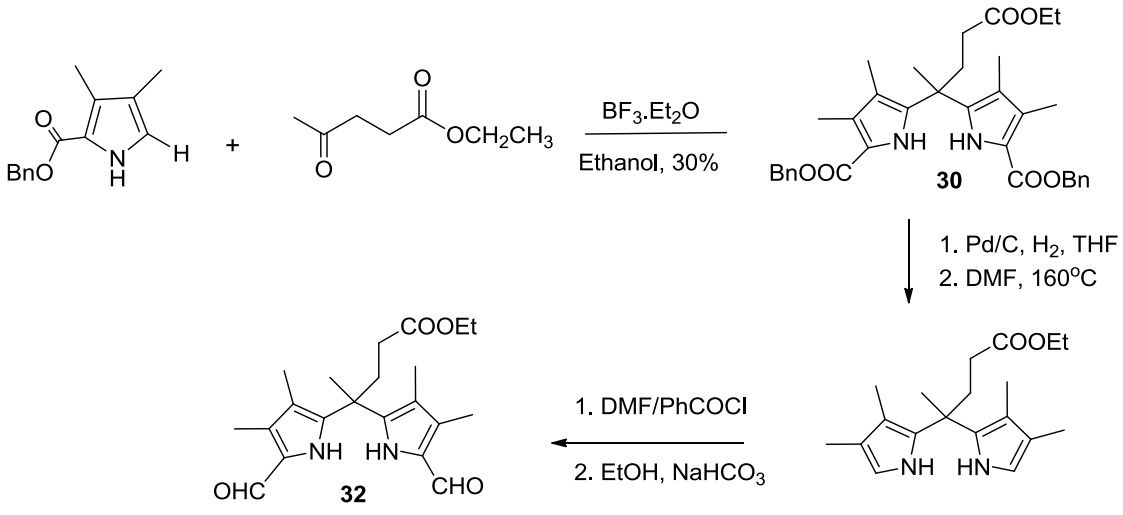

Scheme 3.12: Synthesis of diformydipyrromethane **30** and diformydipyrromethane **32**.

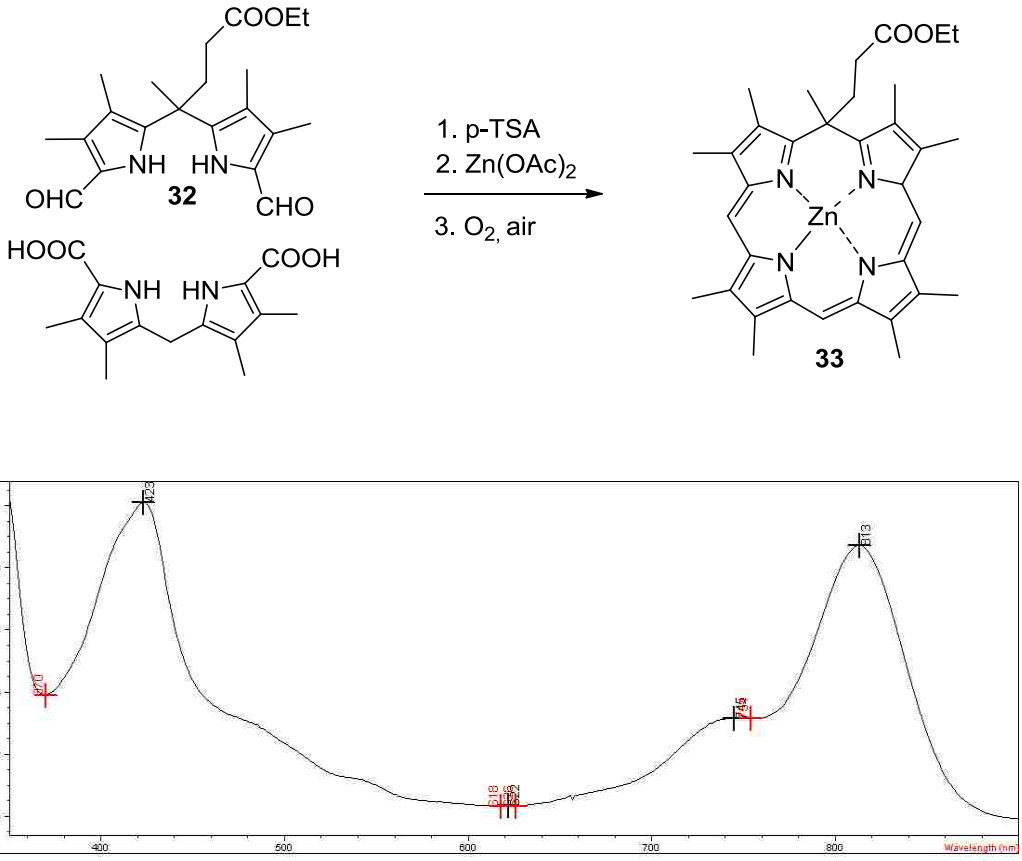

Scheme 3.13: Synthesis of zinc(II) isoporphyrin **34** by MacDonald 2+2 condensation between diformyldipyrromethane **32** and dipyrromethane carboxylate **28**, and UV-visible spectrum of **33** in CH_2Cl_2.

Based on the route used for synthesis of zinc(II) isoporphyrins **12** and **33**, the isoporphyrin **40** was produced by cyclization between the dicarboxylic acid of dipyrromethane **30** and diformydipyrromethane **16** in around 4% yield. This zinc(II) isoporphyrin has a Soret band at 423 nm and a Q-band at 804 nm (Scheme 3.14).

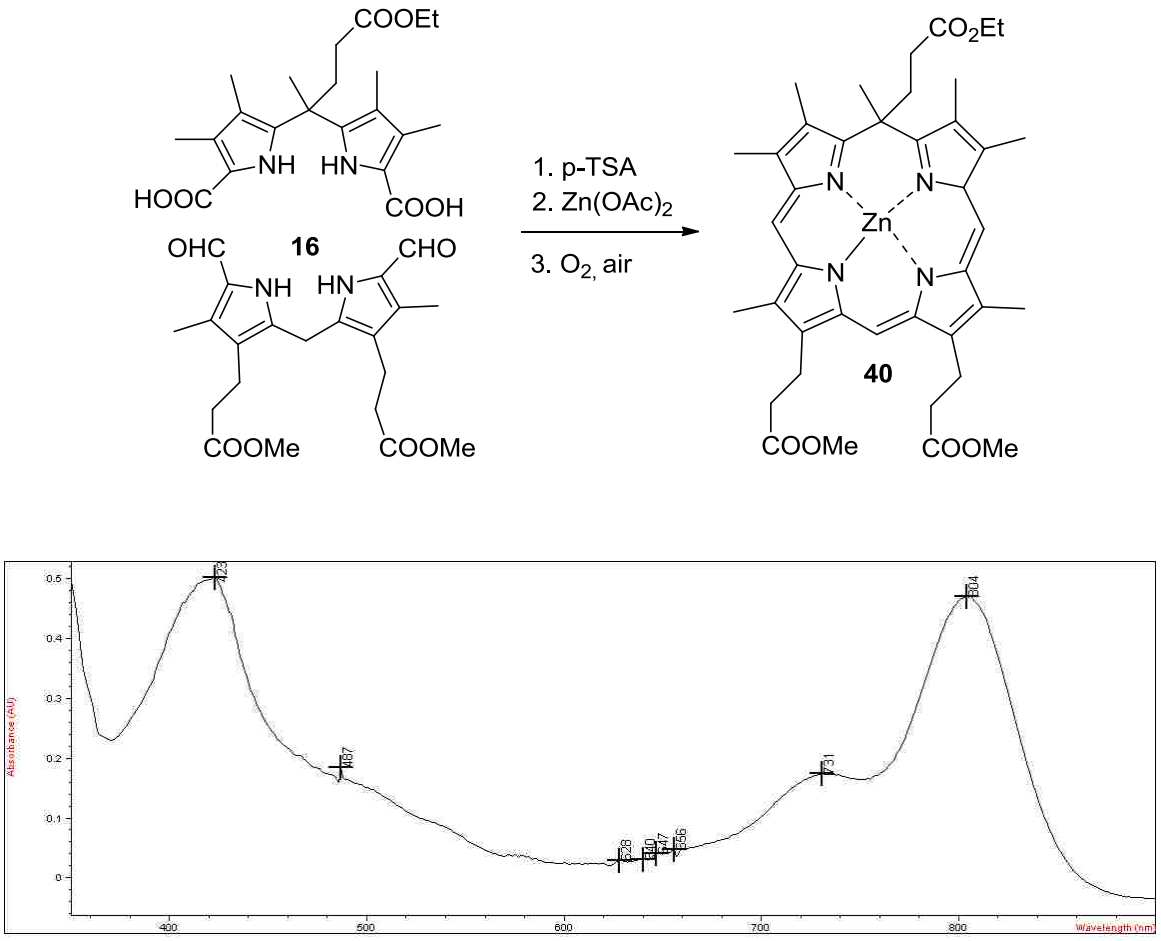

Scheme 3.14: Synthesis of zinc(II) isoporphyrin **40** by 2+2 MacDonald condensation, and the UV/visible spectrum of **40** in CH_2Cl_2.

3.4 Attempts to Hydrolyze Ester Groups on Zinc(II) Isoporphyrins

After success in the synthesis of the zinc(II) isoporphyrins, various methods to convert the meso-methyl ester group into the corresponding carboxylic acid were attempted so that they could subsequently be conjugated with biomolecules. As discussed in Chapter 2, when the ester is directly attached to the 5-position of the zinc(II) isoporphyrin, the isoporphyrin will leave as a zinc(II) porphyrin after hydrolysis and spontaneous decarboxylation. However, with an ester group on the pyrrole unit of zinc(II) isoporphyrin

12, there should be no such problem with the hydrolysis. For the zinc(II) isoporphyrins **33** and **40**, since the ester groups are either distant from the meso-position of the isoporphyrin or attached to the β-positions of the pyrrole subunits of isoporphyrins, there should also be no problem. Therefore, the hydrolysis of zinc(II) isoporphyrins was explored mainly using zinc(II) isoporphyrin **12** since it had the best yield during its synthesis (Table 3.1). Zinc(II) isoporphyrin **12** was therefore subjected to strong basic conditions using NaOH[25] in MeOH at room temperature; the reaction was monitored by UV/visible spectroscopy. With time the peak around 800 nm disappeared and there was a new peak that appeared at 629 nm, which unfortunately belongs to the ring-cleaved open chain system. This was unexpected since it seemed unlikely that this can take place for zinc(II) isoporphyrin **12**. Therefore several neutral hydrolytic conditions were tried on zinc(II) isoporphyrin **12** in the hope that the macrocycle of this isoporphyrin might be preserved under these mild conditions (Scheme 3.15). With iodide-based reagents including LiI,[26] TMSI and TMSCl/LiI,[27] and $CH_3CH_2CH_2SLi$,[28] the macro-ring opened during hydrolysis although ester hydrolysis did take place, especially when LiI was used. A fraction separated by using Sephadex 20, had its major mass peak at *m/z* 629.3317, an ion that belongs to the corresponding zinc(II) isoporphyrin carboxylic acid, was observed from both the ESI and Maldi mass spectra (Figure 3.2). However, the UV/visible absorption of this compound showed no peak around 800 nm; the spectrum showed this compound to be an open-ring system, which proved that the LiI hydrolyzed methyl ester, but also opened the the isoporphyrin ring. With trimethyltin hydroxide[29] and bis(trimethyltin) oxide, the zinc(II) isoporphyrin also decomposed; the UV/visible absorption was similar to that seen when LiI was used. Enzymatic hydrolysis using lipase[30] showed no reactivity in phosphate buffer solution even after one week; the mass spectrum showed the starting material still remained as the only peak. Some acidic conditions such as BCl_3[31] and BBr_3 were also tried on the zinc(II) isoporphyrin but they

did not work either; the spectrophotometry peak around 800 nm became smaller and was completely gone after aqueous work up.

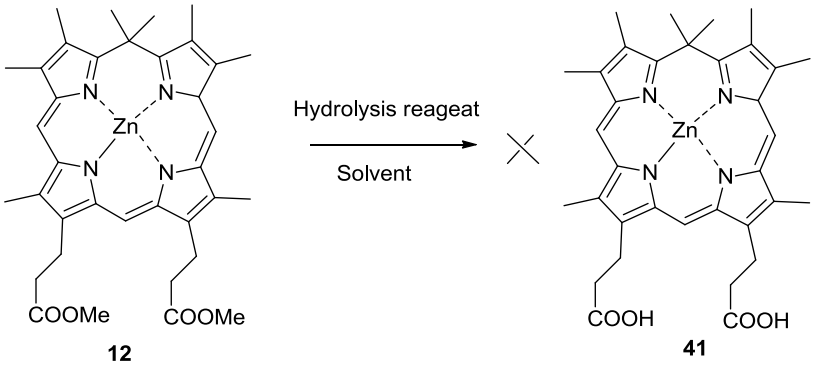

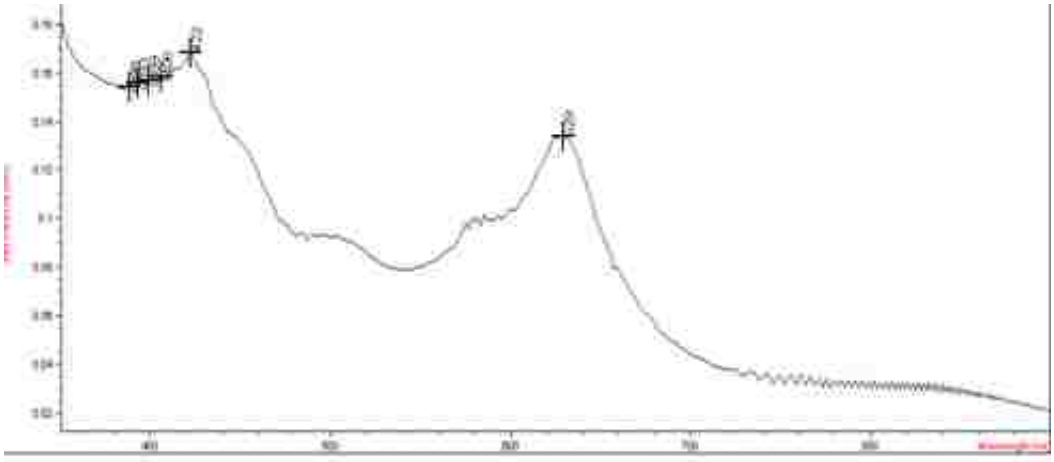

Scheme 3.15: Attempted hydrolysis of zinc(II) isoporphyrin **12** by LiI and the UV/visible spectrum in CH_2Cl_2 of the ring-opened product.

Table 3.1:The Hydrolysis of Zinc(II) Isoporphyrins Under Different Conditions.

Tries	reagents	solvents	temperature	result
1	LiI	Ethyl acetate	reflux	ring-opened
2	TMSI	CHCl3	reflux	ring-opened
3	TMSCl/LiI	Acetonitrile	reflux	ring-opened
4	Li-S-propane	$CH_3CH_2CH_2SH$	R. T	ring-opened
5	$(CH_3)_3SnOH$	1,2-DCE	reflux	ring-opened
6	$(CH_3)_3SnOSn(CH_3)_3$	1,2-DCE	reflux	ring-opened
7	Lipase enzyme	Phosphate buffer	R. T.	no reaction
8	BCl_3 or BBr_3	$CHCl_3$	R. T	ring-opened

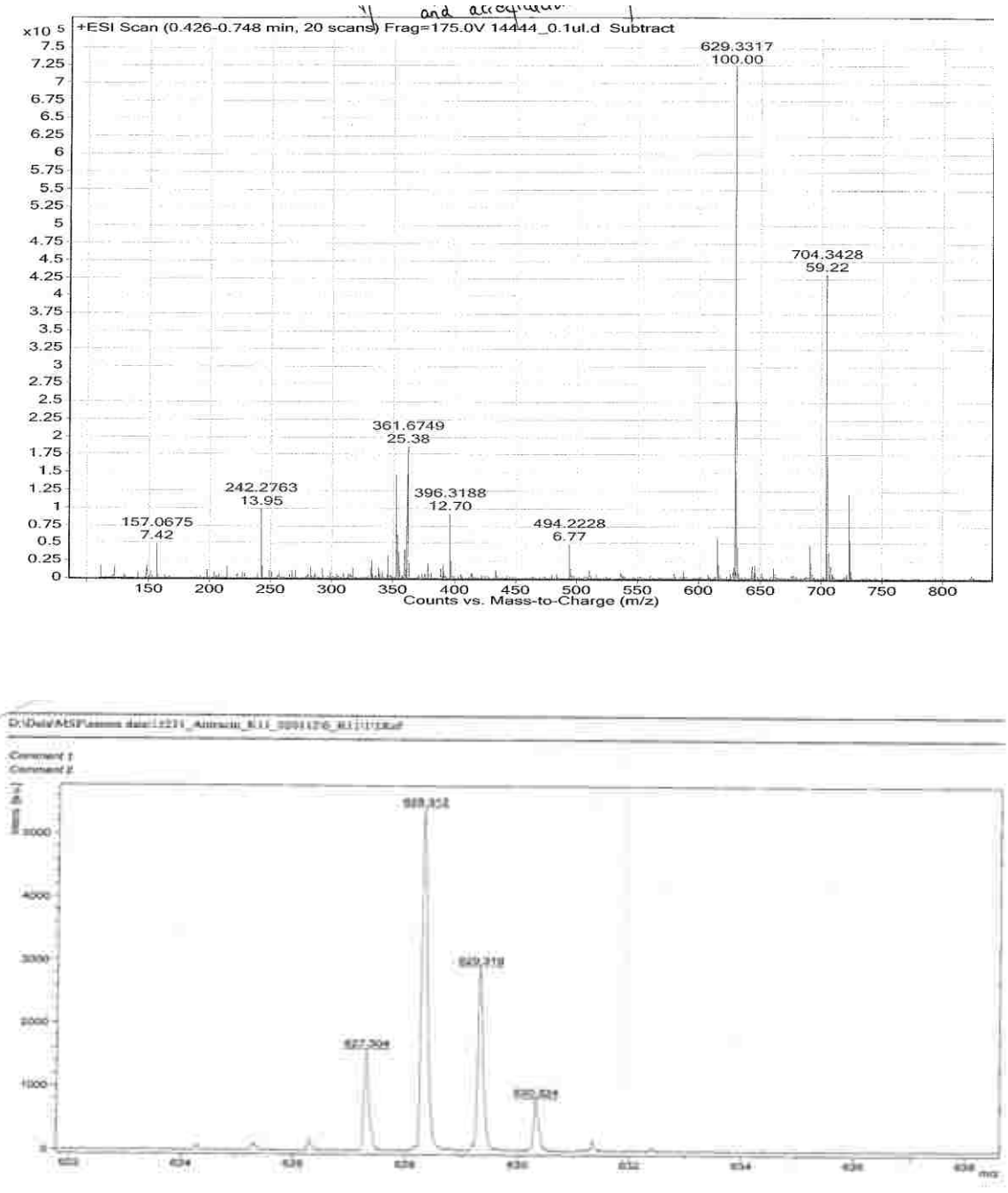

Figure 3.2: Mass spectrum of product of hydrolysis of zinc(II) isoporphyrin **12** by using LiI**.**

3.5 Functionalization of Dipyrromethanes Before Cyclization to Give Zinc(II) Isoporphyrin

From all the hydrolyses attempted using the above conditions, it seemed that zinc(II) isoporphyrins are not very stable to strong acids, bases, or nucleophiles. Under acidic conditions, the zinc ion could be removed from the isoporphyrin, but the metal free isoporphyrins are not very stable and decomposed rapidly. Trimethyltin hydroxide and iodide-based reagents are all strong nucleophiles, which are reactive enough to hydrolyze the ester group but they also open the isoporphyrin ring at the same time. Enzymatic hydrolysis depends on how the molecule fits into the lipase core, and for this case there was no reactivity using zinc(II) isoporphyrins. Since we had no success using methyl esters, we changed our synthetic strategy for isoporphyrins conjugation with biomolecules.

Strategy I: A t-butyl ester was introduced into the zinc(II) isoporphyrin since it is easy to remove compared with a methyl ester. Therefore, the zinc(II) isoporphyrin **42** was designed. The retrosynthetic analysis of this molecule is similar to the previous cases (Scheme 3.16). The dipyrromethane dicarboxylate half remained the same, and it was necessary to convert the methyl esters of the other half into tert-butyl esters. We tried several conditions which could possibly hydrolyze a methyl ester over a benzyl ester on the dipyrromethane **17** (Scheme 3.17). But no selectivity under basic conditions between these two ester groups was observed, so we moved to acidic conditions with H_2SO_4 in DMSO overnight; the solution turned black and the mass spectrum of the product showed only the starting material peak. Then LiI was used in ethyl acetate and THF; both solvents gave a low yield of product after purification. Trimethyltin hydroxide[29] is a very good reagent to hydrolyze methyl esters compared with other esters including ethyl, tert-butyl and other more complicated esters, according to the literature. A solution of dipyrromethane **17** was refluxed in 1,2-DCE with the presence of trimethyltin hydroxide;

with time a white pinkish solid precipitated from the solution and more precipitate came out when the solution was cooled down to room temperature. The precipitate was collected without further purification. ^{1}H NMR spectroscopy showed it to be pure enough to go to next step, and the benzyl esters remained intact. After dipyrromethane dicarboxylic acid **44** was obtained, several attempts at tert-butyl esterification of this dipyrromethane were made (Scheme 3.18). The dipyrromethane dicarboxylic acid **44** was treated with oxalyl chloride in THF with a little DMF as a catalyst, followed by addition of tert-butyl alcohol and TEA (base) in CH_2Cl_2. The mixture was heated to 40 ^{o}C and kept for ten hours under argon. Unfortunately, the tert-butyl ester was not obtained after column chromatography and the mass spectrum did not give any hint of the required product. Then, a typical coupling reaction for making an ester group using EDCI/DMAP in DMF was tried, but unfortunately the reaction did not take place under these conditions. Then $Bu^{t}OAc$[32] was used as an esterification reagent and solvent under acidic conditions, but the product was not detected once again. When neat oxalyl chloride was used as chlorinating reagent and solvent, the acyl chloride was formed. The dipyrromethane dicarboxylic acid **44** is not very soluble in oxalyl chloride; however, when the reaction mixture was heated to 40 ^{o}C, the solid disappeared with time, which indicated that the carboxylic acid was converted into the acyl chloride. The excess oxalyl chloride was removed and the residue was dissolved in CH_2Cl_2 and treated with tert-butyl alcohol in presence of TEA, and then the mixture was kept at 40 ^{o}C for ten hours. As a result, the product was obtained in about 40% yield and its identity was confirmed by mass spectrometry, with a peak at *m/z* 721.3455 (MW+Na).

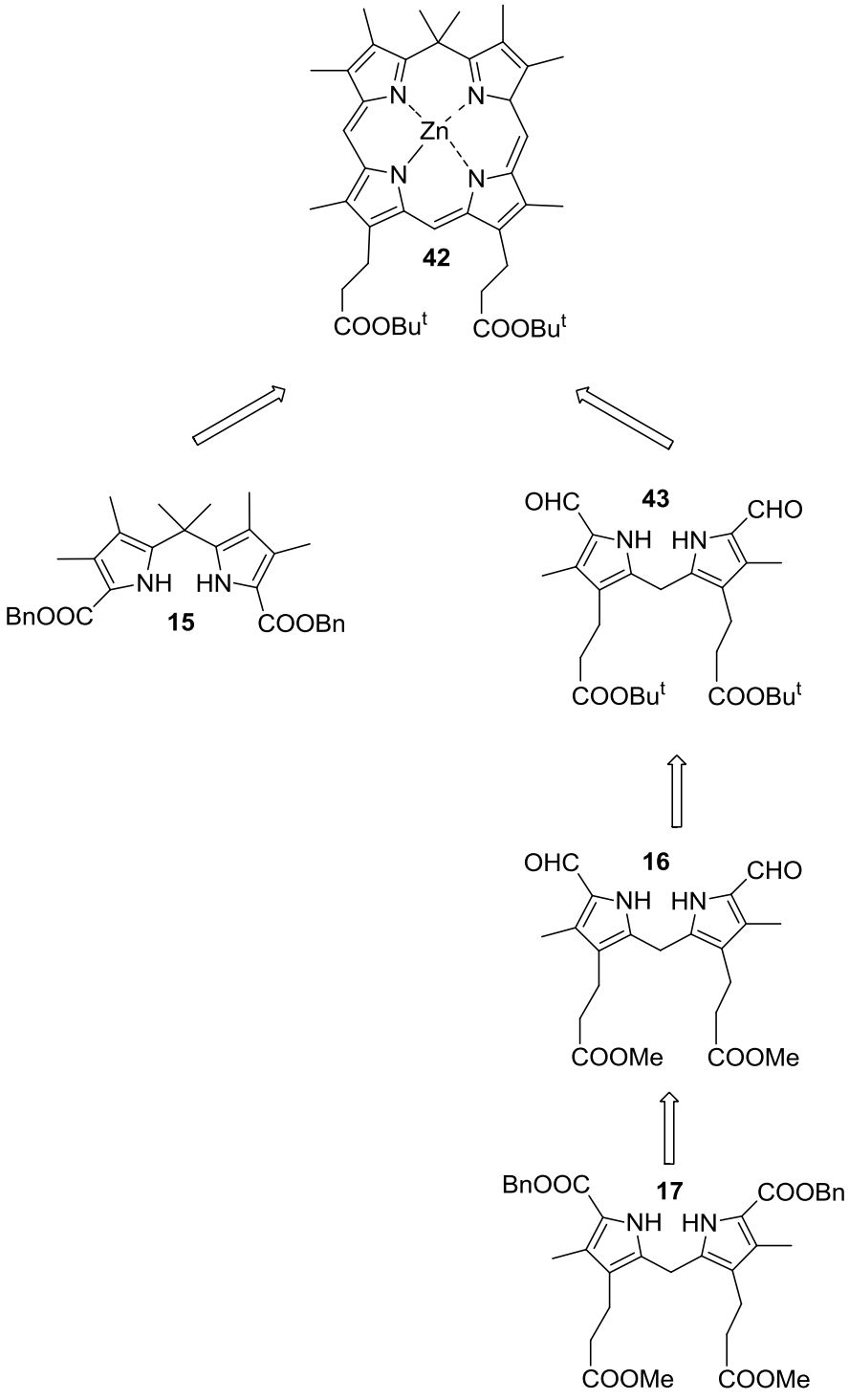

Scheme 3.16: Retrosynthetic analysis of tert-butyl ester substituted zinc(II) isoporphyrin **42**.

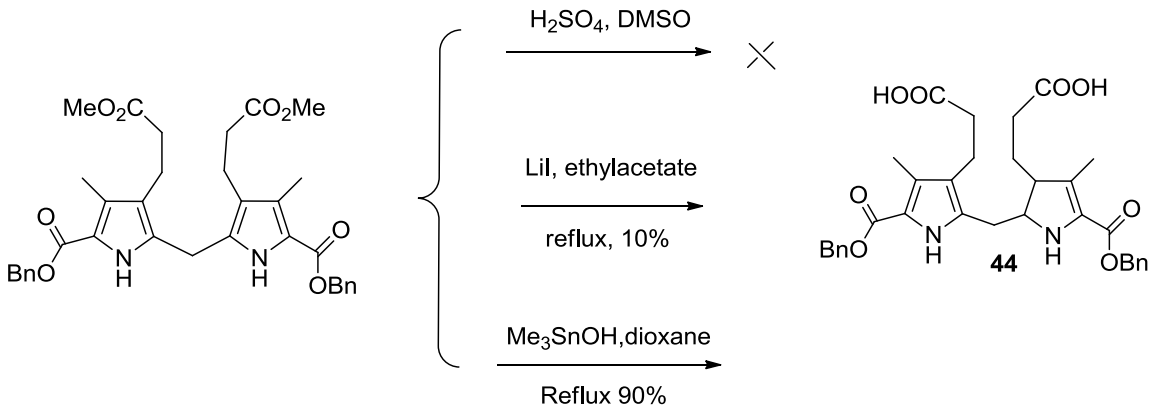

Scheme 3.17: Attempts to preferentially hydrolyze the methyl esters over the benzyl esters of dipyrromethane **17**, to synthesize dipyrromethane **44**.

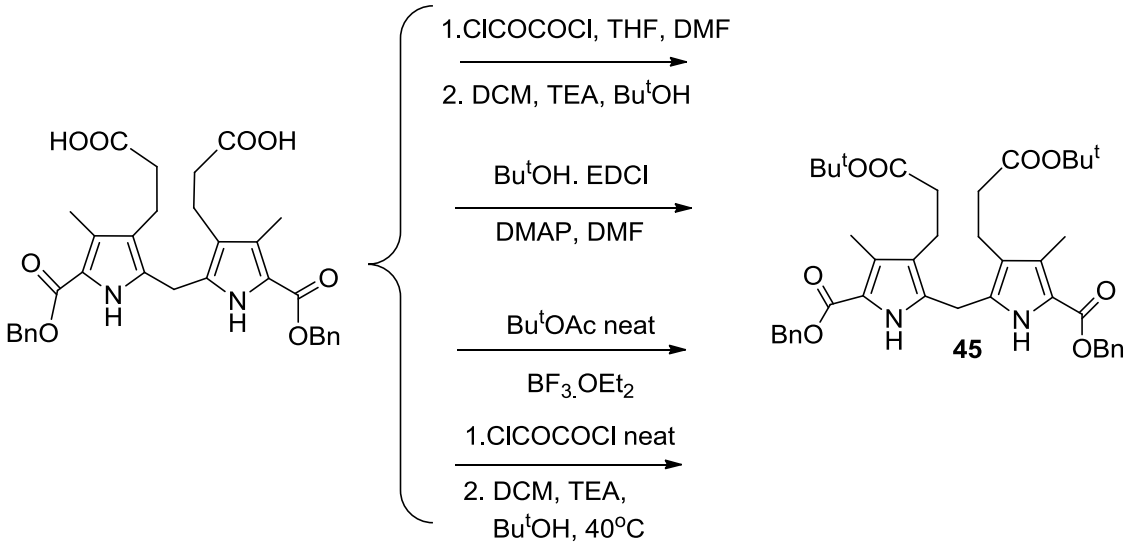

Scheme 3.18: Attempts to transform the carboxylic acid to tert-butyl ester of dipyrromethane **45**.

Then the tert-butyl substituted dipyrromethane **44** was subjected to Pd-catalyzed hydrogenation in THF to remove the benzyl protecting groups, and the resulting dicarboxylic acid was refluxed in DMF at 160 ^oC for one hour and treated the α-free dipyrromethane along with PhCOCl at 0 ^oC; this was followed by hydrolysis using aqueous $NaHCO_3$ in EtOH. A yellow solid was collected and recrystallized from ethanol,

giving the diformyldipyrromethane **43** in about 60% yield (Scheme 3.19). Cyclization of tert-butyl ester-substituted diformyldipyrromethane **43** with 5,5-dimethyldipyrromethane dicarboxylic acid **13** gave the zinc(II) isoporphyrin product **42** smoothly, which has a Soret band and Q-band at 409 and 801 nm, respectively (Scheme 3.20). Then the zinc(II) isoporphyrin **42** was dissolved in $CHCl_3$ and treated with TFA (several drops) under argon; the reaction was again monitored by UV/visible absorption spectroscopy, and the peak at 801 nm disappeared with time, possibly indicating that the TFA had removed the zinc(II) ion from the isoporphyrin. The TFA was removed using a stream of N_2 gas, and then zinc acetate in MeOH was added to the solution of the residue in CH_2Cl_2 [to re-insert the zinc(II) to stabilize the isoporphyrin]. Unfortunately, the UV/visible spectrum did not change at all, (Scheme 3.21). Once the demetalation took place, the isoporphyrin must have decomposed very quickly. An attempt was also made to cleave the tert-butyl ester by using zinc bromide but this was also unsuccessful.

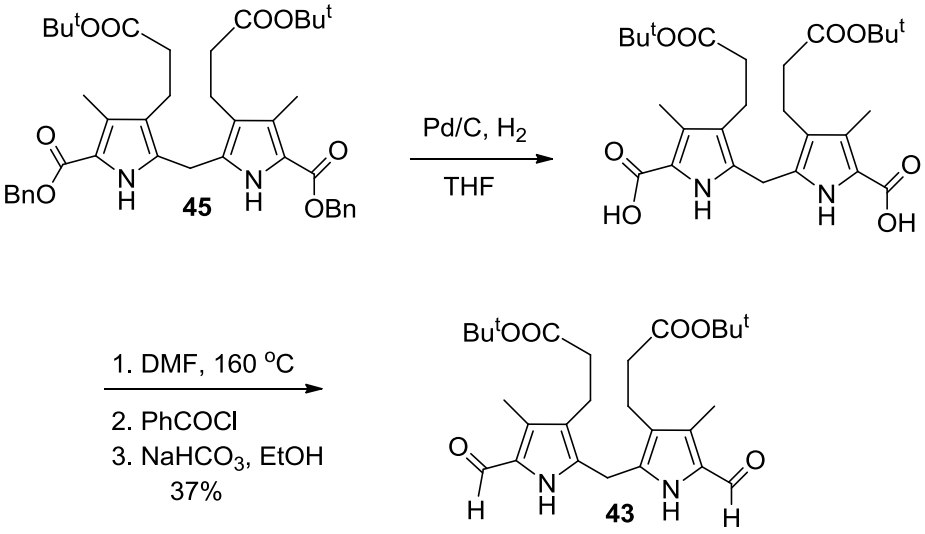

Scheme 3.19: Synthesis of tert-butyl ester-substituted diformydipyrromethane **43**.

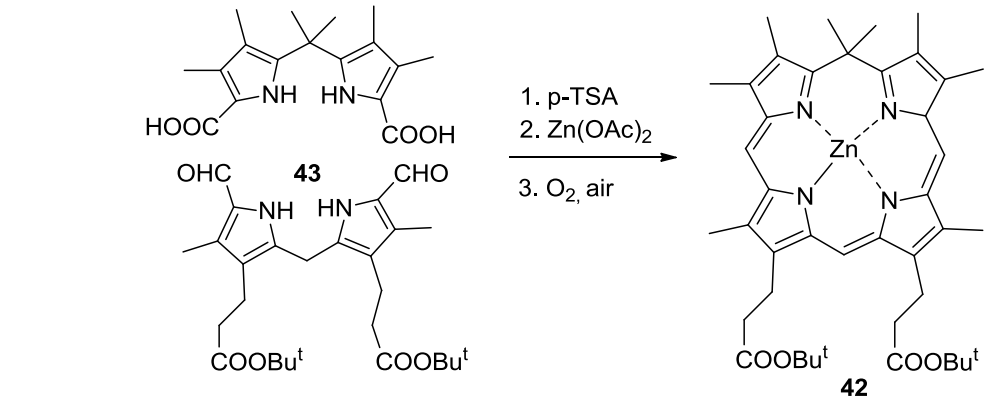

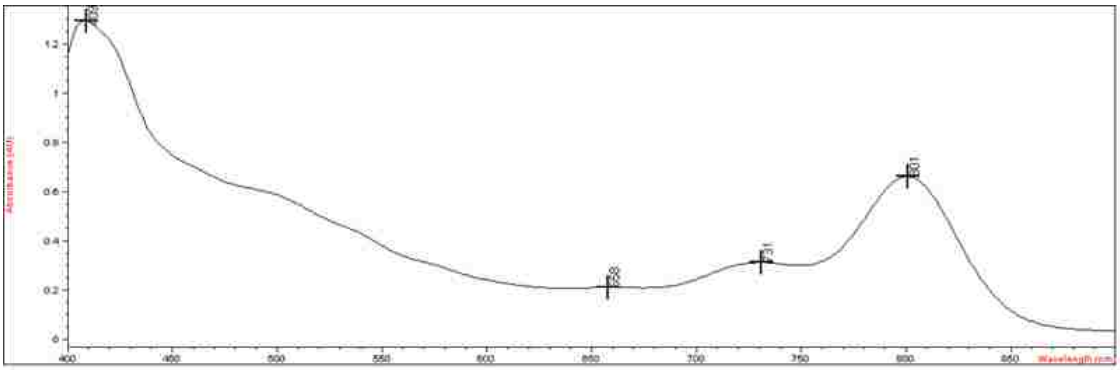

Scheme 3.20: Synthesis of zinc(II) isoporphyrin **42** by MacDonald 2+2 condensation, and UV-visible spectrum of **42** in CH_2Cl_2.

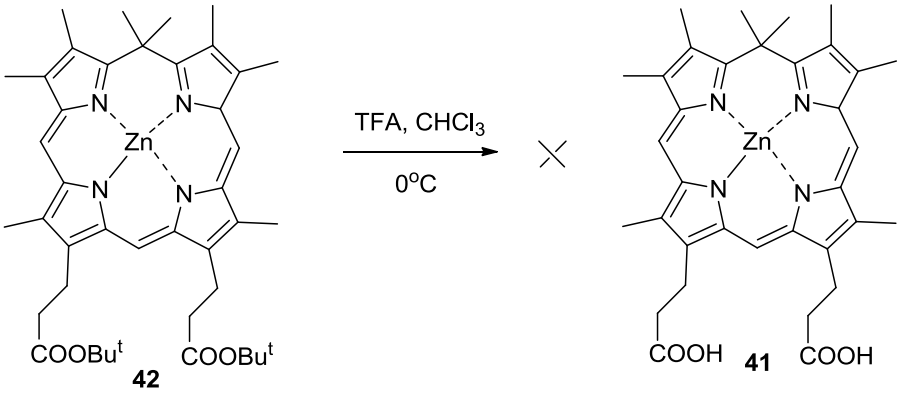

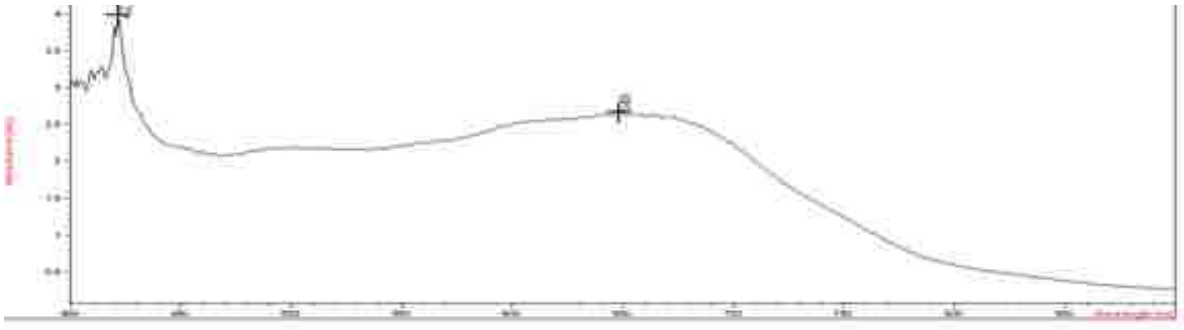

Scheme 3.21: Attempt to hydrolyze tert-butyl ester of zinc(II) isoporphyrin **42** and UV-visible spectrum in CH_2Cl_2 of the reaction product.

Strategy II: Since the transformation of the tert-butyl esters to the corresponding carboxylic acids did not succeed, the strategy was again changed. The new plan was to introduce an imine group into the molecule before cyclization. The mono BOC-protected ethylenediamine was chosen to be introduced into the molecule so that it could be deprotected later. Two methods were tried on dipyrromethane **44;** the first involved chlorination of the dipyrromethane dicarboxylic acid **44** by using oxalyl chloride followed by amination with mono-BOC protected ethylenediamine under basic conditions. This reaction gave about 25% yield. Another method was to use TBTU/HOBt[33] promoted conjugation with DIEA as a base, and this gave a better yield (around 40%); purification was also easier than in the first method. However, the attempt to convert the dipyrromethane **46** in to diformyldipyrromethane **48** failed (Scheme 3.22). The assumption is that in the decarboxylation step, *N*-BOC could be cleaved under high temperature conditions, and the free amine will hinder formylation of α-free dipyrromethane.

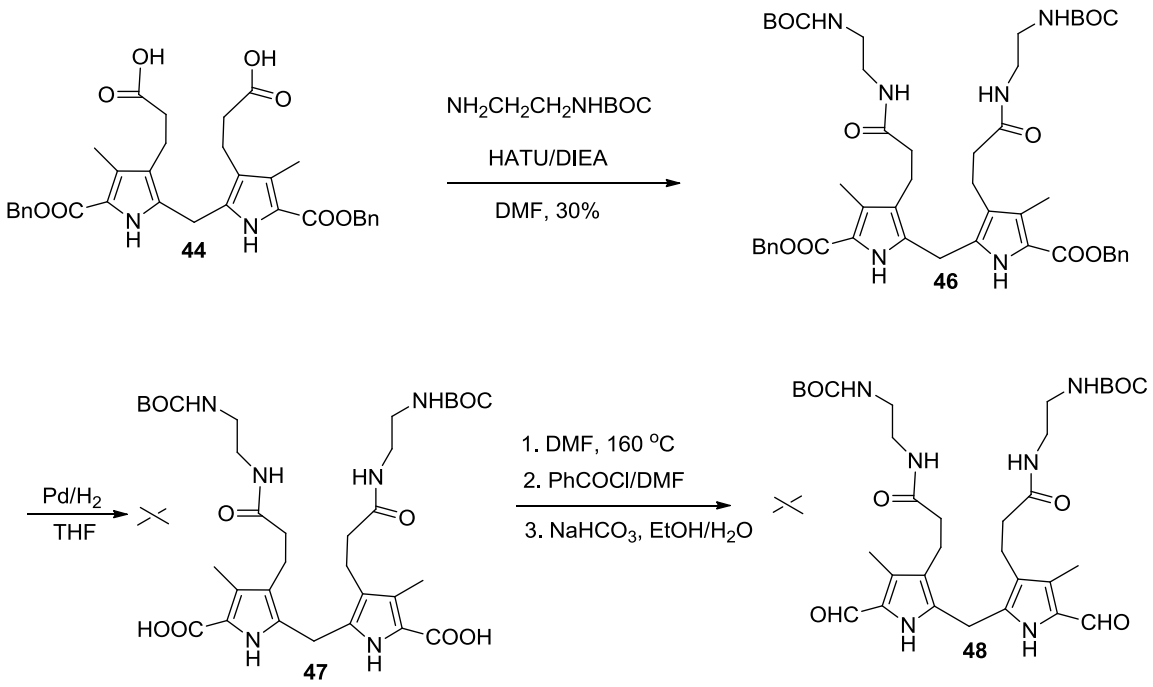

Scheme 3.22: Attempted transformation of dipyrromethane **44** into diformydipyrromethane **48**.

Then we switched the formyl groups and carboxylic acid groups between these two dipyrromethanes in an attempt to avoid the abovementioned problem. Therefore, several attempts were made to synthesize the 5,5-dimethyldipyrromethane **49** (Scheme 3.23). The first attempt was by Vilsmeier-Haack formylation. Dipyrromethane dicarboxylic acid **13** was obtained by debenzylation of the diester and then the dicarboxylic acid was heated to 160 ^{o}C in DMF for one hour before the solution was cooled down to room temperature and the PhCOCl/DMF complex was added. The mixture was stirred for another hour followed finally by hydrolysis with $NaHCO_3$ in ethanol. However the reaction did not give the desired product. Some yellow solid was obtained by filtration after hydrolysis, but it was hard to dissolve it in $CHCl_3$ and it did not move on a TLC plate. The problem is probably because of oxidation or decomposition of α-free dipyrromethane under the high temperature conditions, or the failure of hydrolysis of the Vilsmeier imine intermediate. Then we turned to acidic conditions for decarboxylation, using TFA, followed by addition

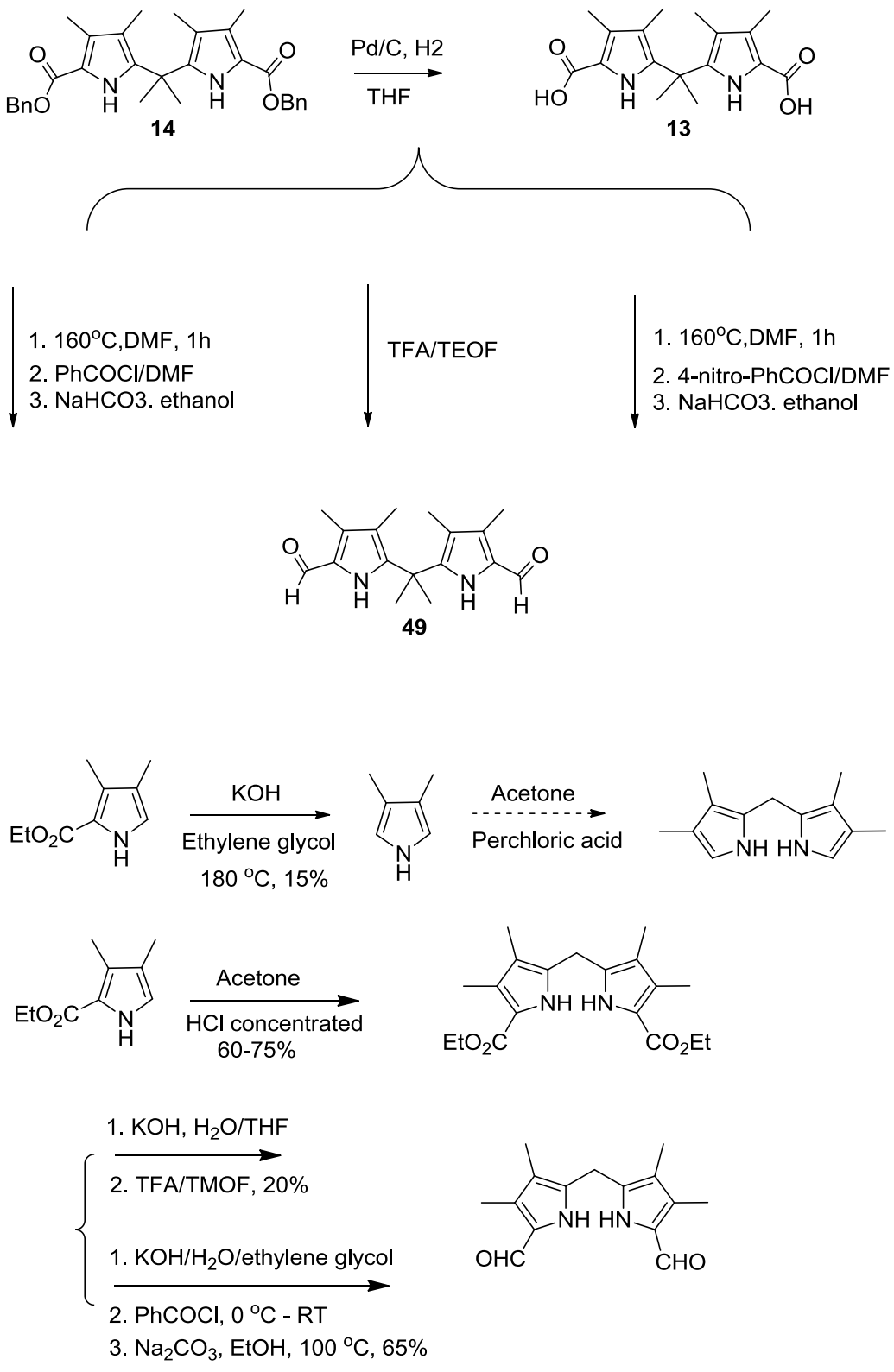

Scheme 3.23: Efforts to synthesize diformydipyrromethane **49** under various conditions.

triethyl orthoformate for the formylation step. The reaction still failed to give the required product. Yet another another formylation complex, 4-nitro-PhCOCl/DMF, was employed since it could generate a better leaving group than PhCOCl/DMF during hydrolysis. However, the reaction still failed.

Since one of the problems was possibly due to incomplete decarboxylation, then we tried to look for a method that can give α-free dipyrromethane **52** directly. According to the literature,[34,35] 3,4-dimethylpyrrole can react with acetone, catalyzed by perchloric acid, to give **52** directly. Therefore, we tried to synthesize 3,4-dimethylpyrrole by hydrolysis of the ethyl pyrrole-2-carboxylate, followed by decarboxylation catalyzed by KOH in ethylene glycol. Unfortunately, this reaction only gave a 15% yield of product **51**. Therefore this route was abandoned. Instead of using the benzyl ester pyrrole, the ethyl ester pyrrole was used to synthesize the corresponding dipyrromethane **53**,[36] which was hydrolyzed to give the corresponding carboxylic acid by using KOH/THF/H_2O, followed TFA/TMOF formylation to give a 20% yield of the product **49**. Another route for formylation was tried by converting the dipyrromethane **53** into the α-free dipyrromethane in one pot by refluxing in ethylene glycol with aqueous KOH. The α-free dipyrromethane **52** was precipitated by adding water and this was used in the next step immediately to make diformydipyrromethane[37] using PhCOCl/DMF at 0 ^{o}C. To avoid the failure of hydrolysis of the imine intermediate, the complex was dissolved in a mixture of EtOH/$NaHCO_3$ and refluxed for about ten minutes; the product diformydipyrromethane **49** was generated in a satisfying 65% yield.

Then the two halves, diformylpyrromethane **49** and dipyrromethane dicarboxylic acid **47** (Scheme 3.24) were subjected to the cyclization conditions once again to see if the macrocycle could be formed; the reaction failed to give the corresponding zinc(II) isoporphyrin , and after one week, there was no peak around 800 nm in the UV/visible

spectrum. The assumption is that the *N*-BOC group was cleaved by p-toluenesulfonic acid, especially when the solution of zinc acetate in methanol was added. The *N*-BOC is easily displaced in polar solvents.[38] Once the *N*-BOC was cleaved, the free amine could react with the formyl group in competition with the α-free dipyrromethane. Based on this assumption, we changed our strategy once again.

The purpose of adding p-TSA was to cleave the carboxylic acid groups and protonate/activate the aldehyde group during cyclization. Therefore, the new plan was to remove the carboxylic acid group (to give free α-positions) before cyclization, and then an acid weaker than p-TSA can be added to protonate the aldehyde during cyclization to avoid the cleavage of the *N*-BOC group. Therefore, the dipyrromethane was obtained by an iodination/de-iodonation procedure. The corresponding dipyrromethane dicarboxylic acid of **47** was treated with I_2/Na_2CO_3 to introduce iodine at both α-positions to give diiododipyrromethane **55**, followed by hydrogenation catalyzed using PtO_2,[39] to give the α-free dipyrromethane **56** for the next step (Scheme 3.25). Then cyclization of dipyrromethanes **49** and **56** was attempted, under the same conditions as earlier, except that acetic acid was used instead of p-TSA. The reaction was kept in air for a week but no product was formed. The UV/visible spectrum was very similar to the previous one. A possible reason could be that acetic acid is not strong enough to promote the reaction (Scheme 3.26). Meanwhile we tried other protecting groups, using mono-FMOC protected ethylenediamine because it is very stable to acid, which is mandatory during cyclization; therefore mono-FMOC protected ethylenediamine was introduced onto dipyrromethane dicarboxylic acid **44** by using two methods. The mono-BOC protected dipyrromethane **46** was cleaved by TFA, and the resultant dipyrromethane was re-protected using FMOC-Cl/$NaHCO_3$ in dioxane/H_2O. The identity of the product was

confirmed by mass spectrometry (*m/z* at 1137.4724), but only a trace amount was separated. Another

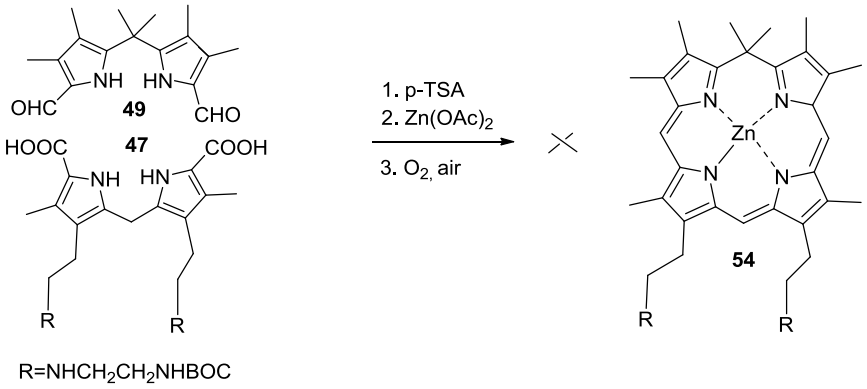

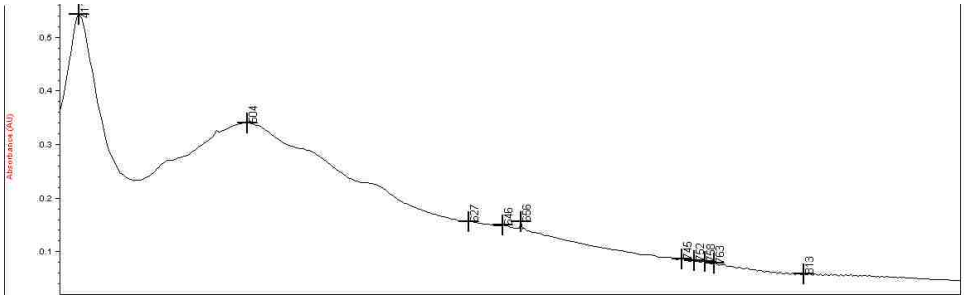

Scheme 3.24: Attempt to synthesize zinc(II) isoporphyrin **54** by MacDonald 2+2 condensation, and the UV-visible spectrum of the product in CH_2Cl_2.

method attempted is the conjugation reaction between dipyrromethane dicarboxylic acid **44** and mono-FMOC protected ethylenediamine using HATU/DIEA. The product **57** was obtained as a redish solid in 30% yield after column chromatography (Scheme 3.27). Then the dipyrromethane **57** needed to be converted into its corresponding carboxylic acid to achieve cyclization later. Usually, the FMOC group is more easily removed than a benzyl ester group under hydrogenolysis conditions. However it has been found that the benzyl group can be cleaved in preference to an FMOC group by using TES/Pd mediated hydrogenation in MeOH. Therefore the solution of dipyrromethane **57** in MeOH was treated with TES/Pd; unfortunately, the benzyl and FMOC were both cleaved. The

assumption is the *N*-FMOC group lessened the difference between benzyl ester compared with *C*-FMOC.

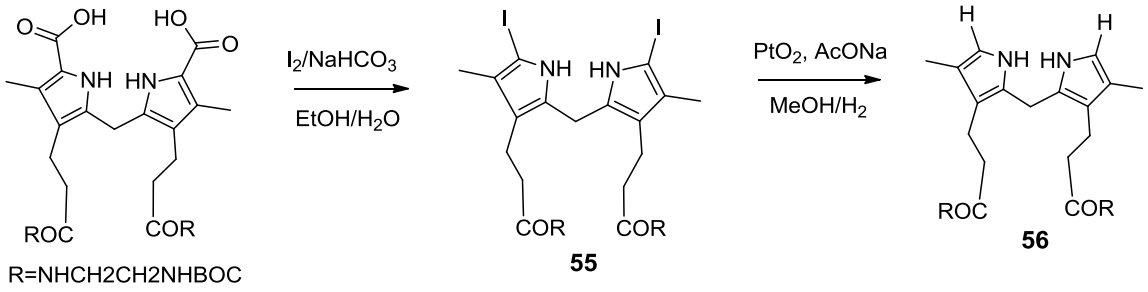

Scheme 3.25: Synthesis of α-free dipyrromethane **56** by iodination to give **55** and de-iodination reactions.

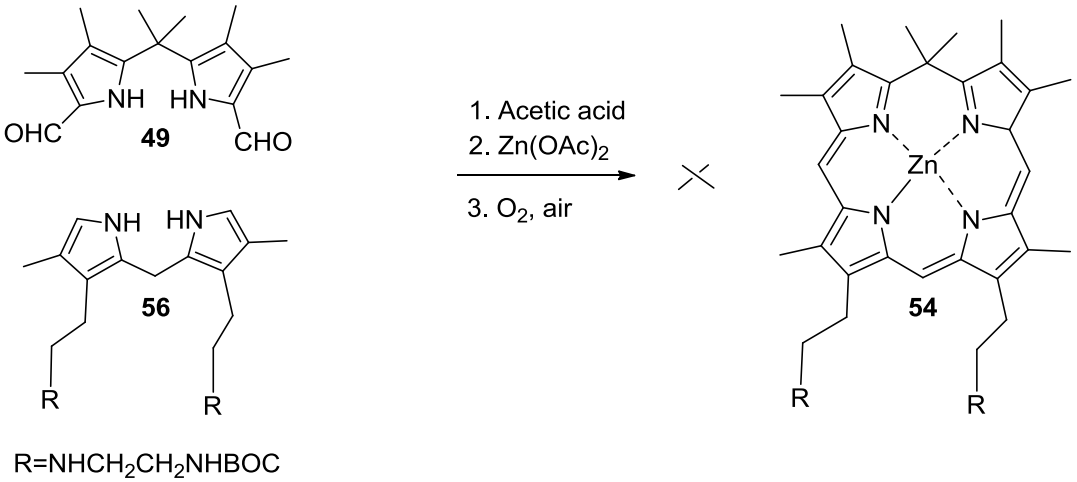

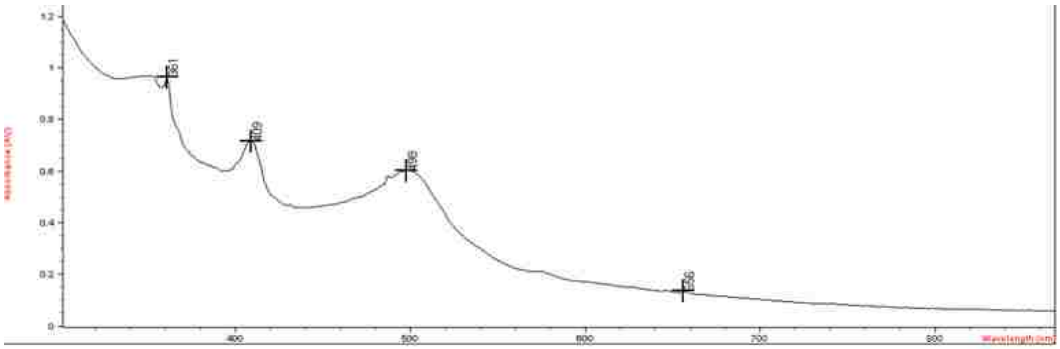

Scheme 3.26**:** Attempt to synthesize zinc(II) isoporphyrin **54** by condensation of dipyrromethanes **49** and **56**, and UV-visible spectrum in CH_2Cl_2 of the product.

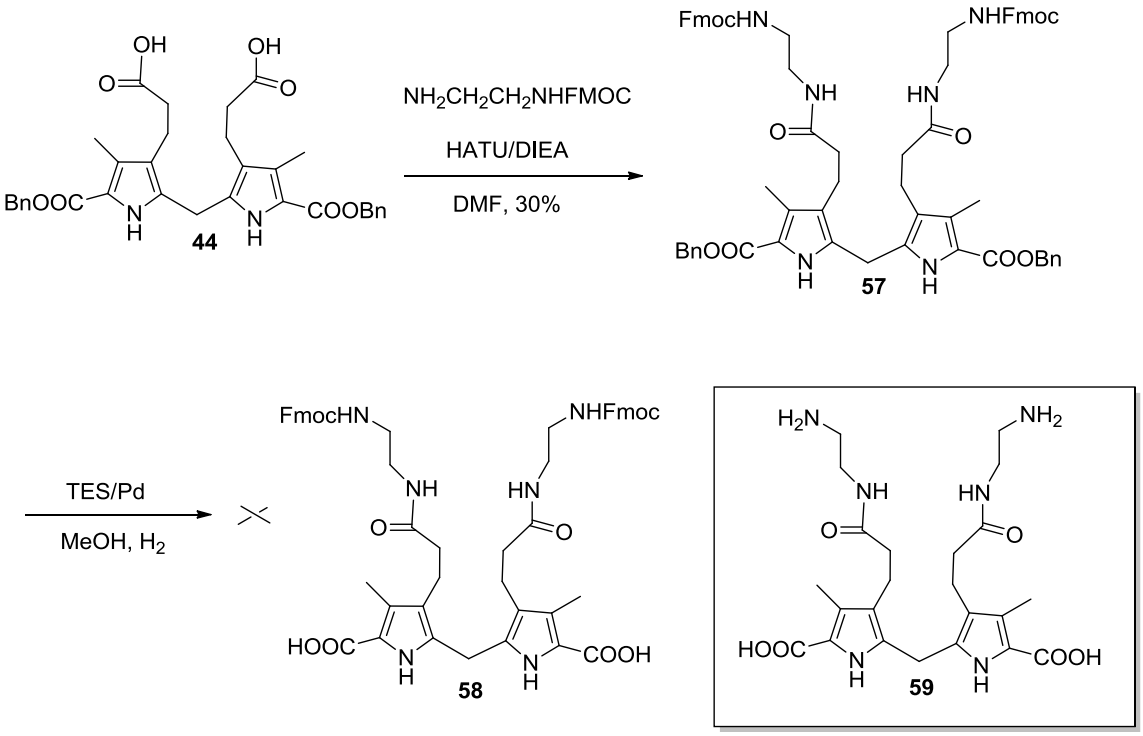

Scheme 3.27: Synthesis of dipyrromethane **59**.

Another way to avoid the deprotection of the benzyl ester in preference to the *N*-FMOC is to introduce a formyl group and then protect the ester groups. Based on this, diformydipyrromethane **16** was hydrolyzed first and protected with benzyl ester groups so that it could be finally cleaved by hydrogenation (Scheme 3.28). Before protection of the carboxylic acids, we used the zinc(II) isoporphyrin **12** as a sample to test the reaction to see if the zinc(II) isoporphyrin is stable to Pd-catalyzed hydrogenation. However, the test showed that the zinc(II) isoporphyrin was reduced to porphyrin according to the UV/visible absorption changes during the reaction. The peak around 800 nm disappeared and a new sharp (Soret) peak appeared at 400 nm along with typical zinc(II) porphyrin Q bands from 531 to 568 nm (Scheme 3.29).

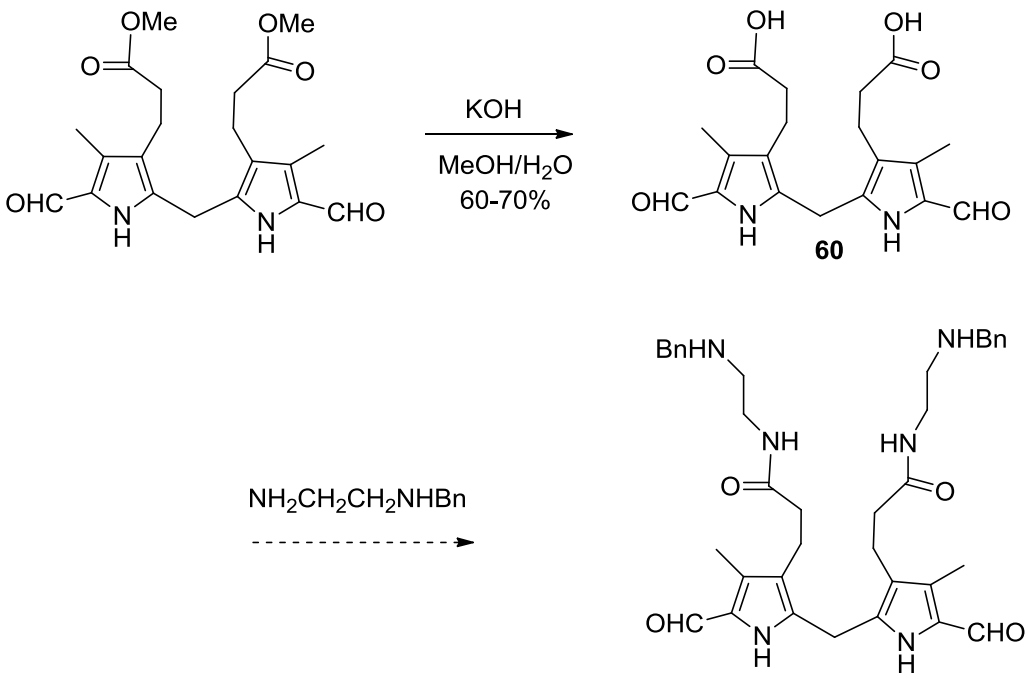

Scheme 3.28: Synthesis of dipyrromethane **60**.

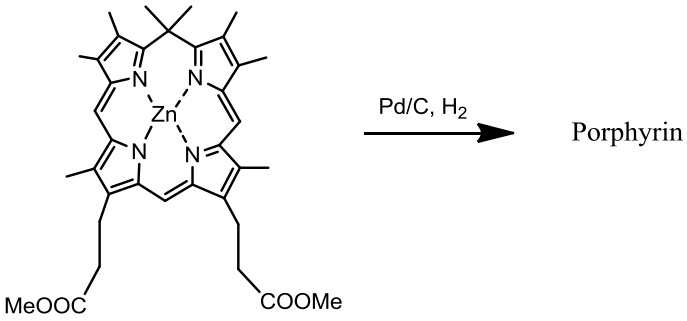

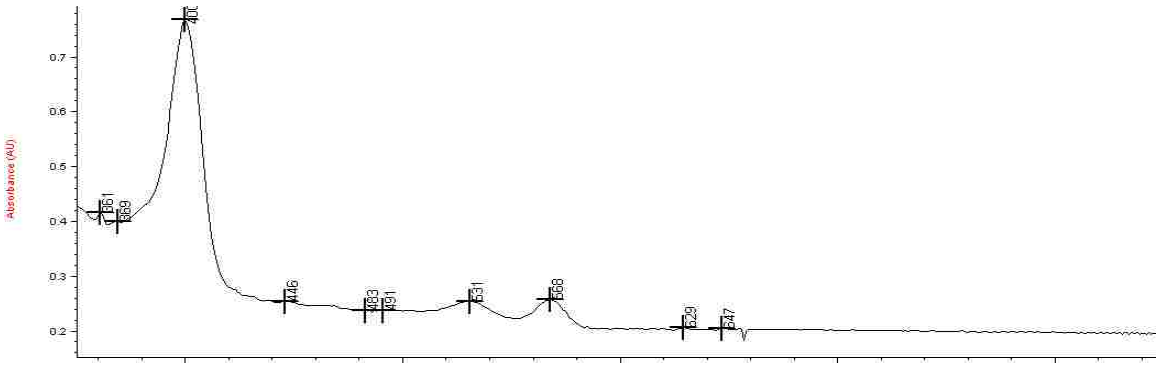

Scheme 3.29: Instability of zinc(II) isoporphyrin under hydrogenation conditions, and the UV-visible spectrum of the zinc(II) porphyrin product in CH_2Cl_2.

3.6 Experiment Part

Compound 19: Sodium nitrite (15.57 g, 0.225 mol) was dissolved in 30 ml of water, and the resulting solution was added to a solution of benzyl acetoacetate (42.05 g, 0.218 mmol) in 60 ml acetic acid in an ice bath; the mixture was well stirred overnight. The solution turned orange and was kept in a refrigerator for use in the next step.

Benzyl 3,4,5-trimethlpyrrole-2-carboxylate 20: To a solution of 2,4-pentanedione (25 g, 0.25 mmol) in acetic acid (100 ml) was added a solution of compound **19** dropwise over 2 h with vigorous magnetic stirring. Simultaneously, a well-mixed powder of 37 g of zinc dust and 37 g of anhydrous sodium acetate was added portion-wise at room temperature. Then the solution was heated to 80 ^{o}C overnight, and the mixture was cooled down to room temperature and poured into ice water with slow stirring. The yellow precipitate was collected by filtration, and the pyrrole was redissolved in CH_2Cl_2 and filtered again to remove residual zinc. The product was recrystallized from ethanol as pale yellow crystals (31.70 g, 60%). Mp 115 ^{o}C, (Lit[19] mp 119-120 ^{o}C). ^{1}H NMR (400 MHz; $CDCl_3$): δ 8.57 (s, 1H), 7.38-7.30 (m, 5H), 5.28 (s, 2H), 2.28 (s, 3H), 2.17 (s, 3H), 1.90 (s, 3H).

Methyl 4-acetyl-5-oxohexanoate 21: 2,4-Pentanedione (100.4 g, 1 mol) and potassium carbonate (3.3 g) were dissolved in 2-butanone (50 ml), and then the temperature was brought to refluxing and a solution of methyl acrylate (83 g, 0.93 mol) in 15 ml of 2-butanone was added slowly to avoid over boiling. After the addition was complete, the mixture was refluxed for 5 h. It was then cooled down to room temperature and filtered to remove potassium carbonate. The filtrate was evaporated under vacuum and further purified by distillation to give a yellow oily liquid (121 g, 70%). ^{1}H NMR (400 MHz; $CDCl_3$): δ 3.72(t, 1H), 3.66(s, 3H), 2.18(s, 6H), 2.1-2.6(m, 4H).

Benzyl 4-(2-methoxycarbonylethyl)-3,5-dimethylpyrrole-2-carboxylate 18: The same amount as above of solution of compound **19** (prepared from the same ratio of chemicals) was added dropwise to a solution of compound **21** (46.56 g, 0.25 mol) in 70 ml glacial acetic acid; at the same time, a mixed powder of 43 g of zinc dust and 43 g of sodium acetate was added portion-wise. After the addition was over, the solution was heated to 80 ^{o}C with stirring for 2-3 h. The mixture was then cooled to room temperature and poured into ice/water with stirring. The pale yellow precipitate was collected by filtration and then the precipitate was dissolved in CH_2Cl_2 (200 ml) and filtered again to remove residual zinc. The residue was crystallized from methanol to give the product as a yellowish solid, (34 g, 50%) M.p 99 ^{o}C, (Lit[19] mp 99-100 ^{o}C). ^{1}H NMR (400 MHz; $CDCl_3$): 8.54 (s, 2H), 7.43-7.32 (m, 5H), 5.28 (s, 2H), 3.66 (s, 6H), 2.70 (t, 2H), 2.42 (t, 2H), 2.29 (s, 3H), 2.20 (s, 3H).

2,2-Bis(5-benzyloxycarbonyl-3,4-dimethylpyrrol-2-yl)propane 14: Pyrrole **15** (2.29 g, 0.01 mol) was dissolved in 30 ml of ethanol and 6 ml of acetone, and the solution was warmed until all the solid was dissolved. Then 0.94 ml (8.55 mmol) $BF_3.OEt_2$ was added and the mixture was refluxed for 1 d, before the solvent was removed and the residue was dissolved in CH_2Cl_2 and washed with Na_2CO_3, brine and then dried over anhydrous Na_2SO_4. After removing the solvent, the product was purified by chromatography using 1:5 ethyl acetate/cyclohexane to give the product (1.5 g, 60% yield). Mp 143 ^{o}C, (Lit[15] Mp 135-136 ^{o}C). ^{1}H NMR (400 MHz; $CDCl_3$): δ 8.79(s, 2H), 746-7.32(m,10H), 5.34(s, 4H), 2.26(s,6H), 1.66(s, 6H), 1.50(s, 6H).

Dibenzy 3,7-bis(2-methoxycarbonylethyl)-2,8-dimethyldipyrromethane-1,9-dicarboxylate 17: Pyrrole **18** (15.7 g, 0.05 mol) was dissolved in 500 ml of anhydrous diethyl ether, and bromine (2.56 ml, 0.05 mol) was added dropwise. The solution turned brown during addition, and the mixture was kept stirring at room temperature overnight,

whereupon a thick precipitate was apparent. Then the diethyl ether was removed to give a pink solid which was dissolved in 100 ml methanol and refluxed overnight. When the solution was cooled down to room temperature, a precipitate appeared, which was filtered and washed with cold methanol to give a white solid (10.70 g, 70%). Mp 102-104 ^{o}C, (Lit[40] mp 96-97 ^{o}C). ^{1}H NMR (400 MHz; $CDCl_3$): δ 9.00(s, 2H), 7.38-7.31(m, 10H), 5.25(s, 4H), 3.97(s, 2H), 3,56 (s, 6H), 2.75(t, 4H), 2.51(t, 4H), 2.28(s, 6H).

1,9-Diformyl-3,7-bis(2-methoxycarbonylethyl)-2,8-dimethyldipyrromethane 16: Dipyrromethane **17** (6.14 g, 0.01 mol) was dissolved in 300 ml THF, and then 5% Pd/C (350 mg) catalyst was added. The suspension was stirred under a H_2 atmosphere overnight. After TLC showed reaction was complete, the reaction was stopped and the solution was passed through a Celite cake to remove the catalyst. A sticky solid on the top of the Celite cake was redissolved in THF and neutralized in water by ammonia and then passed again through the Celite cake. The filtrate was acidified with acetic acid and the product precipitated from aqueous solution. The solid was collected by filtration. The THF part was evaporated and combined with the solid to give a total of 4.0 g (92%) of dpyrromethane dicarboxylic acid. This dipyrromethane dicarboxylic acid (4.00 g, 0.092 mol) was dissolved in 12 ml of DMF and heated to 160 ^{o}C for about 1 h under the protection of an argon atmosphere and then the solution was cooled down to room temperature and the Vilsmeier complex comprising DMF (4.34 ml) and benzoyl chloride (3.25 ml), which had been prepared in advance, was added dropwise at 0 ^{o}C. After the addition was complete, the reaction continued for another 2 h. Some precipitate appeared, so 20 ml of benzene was added and solid was filtered, washed with petroleum ether and then dried in the air. Then the solid was dissolved in ethanol and 3 g of $NaHCO_3$ was added and the mixture was stirred overnight. A yellow precipitate appeared, which was collected and air dried to give product (2.6 g, 70%). Mp 174 ^{o}C

(Lit[41] Mp 180-181°C). ^{1}H NMR (400 MHz; $CDCl_3$): δ 10.03(s, 2H), 9.45(s, 2H), 4.05(s, 2H), 3.71(s, 6H), 2.79(t, 4H), 2.55(t, 4H), 2.29(s, 6H).

Zinc 13,17-bis(2-methoxylcarbonylethyl)-2,3,4,5,7,8,12,18-octamethylisoporphyrin chloride 12: Dipyrromethane **14** (0.249 g, 0.5 mmol) was dissolved in 50 ml THF and then 30 mg 10% Pd/C catalyst was added and the mixture was stirred under a H_2 atmosphere for about 2 h, until TLC showed the reaction was complete. Then the solution was passed thought a Celite cake to remove catalyst, and the filtrate was evaporated to give a yellowish solid. This solid was dissolved in 200 ml of CH_2Cl_2 and p-toluenesulfonic acid (0.375 g,1.97 mmol) in 16 ml MeOH was added and the solution was heated to 40 °C for about 10 min to remove the carboxylic acid groups. After TLC showed the reaction was complete, a solution of diformyldipyrromethane **16** (0.201 mg, 0.005 mmol) in CH_2Cl_2 (30 ml) was added, followed by addition of excess zinc acetate (0.18 g, 0.82 mmol) in MeOH (5 ml). The mixture was stirred at 38 °C for 3 d and then another 4 d at room temperature under air. The solution turned dark with time and finally gave a dark brown mixture. Then the solution was washed with water, sodium bicarbonate solution, and brine, and dried over anhydrous Na_2SO_4. The solvent was removed and the residue was purified by chromatography eluting with 2-4% MeOH/ CH_2Cl_2 and further recrystallized from hexane/ CH_2Cl_2 to give a greenish solid. Mp >260 °C (Lit[43] mp > 250°C). ^{1}H NMR (400 MHz; $CDCl_3$): 7.75 (s, 1H), 7.55 (s, 2H), 3.65 (s, 6H), 3.20 (t, 4H), 2.69 (t, 3H), 2.42 (s, 12H) 2.38 (s, 6H), 1.91 (s, 6H). UV/Vis (CH_2Cl_2): λ_{max} (ε, M^{-1} cm^{-1}): 414 nm (3.0×10^4), 729 (1.6×10^4), 799 (4.7×10^4).

Ethyl 4,4-bis(5-benzyloxycarbonyl-3,4-dimethylpyrrol-2-yl)butanoate 25: α-Free pyrrole **17** (2.29 g, 0.01 mol) and ethyl acetoacetate (0.651 g, 5.0 mmol) were dissolved in 15 ml absolute ethanol and 0.5 ml (4 mmol) of boron trifluoride etherate was added and the mixture was refluxed overnight. Another 2.5 mmol (0.22g, 0.25 ml) of ethyl

acetoacetate was added and the mixture was refluxed for another 1 d. Then the solvent was removed and the residue was taken up in CH_2Cl_2, washed with water, $NaHCO_3$, brine, and dried over anhydrous Na_2SO_4. The solvent was evaporated and the residue was purified by silica gel column chromatography, eluting \with (ethyl acetate/hexane 1:5) to give the product (0.40 g, 7%). ^{1}H NMR (400 MHz; $CDCl_3$): δ 9.34 (s, 2H), 7.46-7.31 (m, 10H), 5.33 (s, 4H), 4.09 (q, 2H), 3.02 (s, 2H), 2.30 (s, 6H), 1.56 (s, 6H), 1.16 (t, 3H).

Dibenzyl 2,3,7,8-tetramethyldipyrromethane-1,9-dicarboxylate 28: Compound **28** was synthesized following the procedure for compound **17** to afford the product (3.20g,70 %). Mp 180 ^{o}C. (Lit[42] mp 178-180 ^{o}C). ^{1}H NMR (400 MHz; $CDCl_3$): δ 8.79 (s, 2H), 7.34-7.30 (m, 10H), 5.25 (s, 4H), 3.79 (s, 2H), 2.25 (s, 6H), 1.93 (s, 6H).

2,2-Bis(5-formyl-3,4-dimethylpyrrol-2-y-l)propane 26: Benzyl 3,4,5-trimethylpyrrole-2-carboxylate (2.35 g, 0.005 mol) was dissolved in THF (100 ml) and 150 mg of 5% Pd/C catalyst was added. The solution was stirred under a H_2 atmosphere overnight, whereupon the TLC showed the reaction was complete. The solution was passed through a Celite cake to remove the catalyst and the sticky part on top of the Celite cake was dissolved in water and neutralized by aqueous ammonia and passed through the Celite cake again. Then the aqueous solution was acidified with acetic acid to afford a white precipitate which was filtered and dried in a vacuum oven. The THF part was evaporated and the solids were combined together to give the product dicarboxylic acid (1.3 g, 90%). Then the acid was added to cold TFA (20 ml) for 10 min and 4 ml of TEOF was added slowly. After addition was complete, the mixture was stirred for about 1 h and then poured into 100 ml of ice/water, and ammonium hydroxide was added to neutralized the solution to pH=7. Then the solution was extracted with CH_2Cl_2 (100 ml x 3). The organic phase was washed with water, brine and then dried over anhydrous Na_2SO_4. The solvent was removed and the brown solid was recrystallized from EtOH to

give the pure product (0.23 g, 20% yield). ^{1}H NMR (400 MHz; $CDCl_3$): δ 9.47(s, 2H), 3.87(s, 2H), 2.24(s, 6H), 1.98(s, 6H).

Ethyl 4,4-bis(5-benzyloxylcarbonyl-3,4-dimethylpyrrol-2-yl)pentanoate 30: The synthesis of compound **30** followed the procedure for compound **25** to afford the product as a transparent oil, (1.7 g, 30% yield). ^{1}H NMR (400 MHz; $CDCl_3$): δ 8.71(s, 2H), 7.45-7.33 (m, 10H), 5.32 (s, 4H), 4.07 (q, 2H), 2.41 (t, 2H), 2.22 (s, 6H), 2.11 (t, 2H), 1.59 (s, 6H).

Ethyl 4,4-bis(5-formyl-3,4-dimethyl-1H-pyrrol-2-yl)pentanoate 32: The synthesis of compound **32** followed the procedure for compound **16** to afford the product (0.29 g, 37%) starting with (1.2 g, 2.0 mmol) of **30** ^{1}H NMR (400 MHz; $CDCl_3$): 9.54 (s, 2H), 9.20 (s, 2H), 4.08 (t, 2H), 2.21 (s, 6H), 2.12 (t, 2H), 1,63 (t, 2H), 1.23 (t, 4H).

3,3'-(2,2'-methylenebis(5-((benzyloxy)carbonyl)-4-methyl-1H-pyrrole-3,2 diyl))dipropanoic acid 44: Dipyrromethane **17** (0.1 g, 0.159 mmol) was dissolved in 1,2-DCE (15 ml) and trimethyltin hydroxide(143 mg, 0.796 mmol) was added. The mixture was refluxed until a large amount of solid was precipitated and the mixture was then refluxed for another 24 h. The mixture was cooled down to room temperature. All of the solid was filtered off and dissolved in ethyl acetate and then neutralized using aqueous HCl. The organic layer was washed with water, brine, and then dried over anhydrous Na_2SO_4. The solvent was removed and a pink solid was obtained (56 mg, 60%). ^{1}H NMR (400 MHz; $CDCl_3$): 11.99 (s, 2H), 11.18 (s, 2H), 7.41-7.28 (m, 10H), 5.25 (s, 4H), 3.85(s, 2H), 2.48 (t, 4H), 2.12 (s, 6H), 2.05 (t, 4H).

Dibenzyl 5,5'-methylenebis[4-(3-(tert-butoxy)-3-oxopropyl]-3-methyl-1H-pyrrole-2-carboxylate) 45: Compound **44** (200 mg, 0.34 mmol) was added to oxalyl chloride (20 ml), and the mixture was warmed to 40 ^{o}C under protection of argon for about 30 min to

1 h, depending on the reaction scale, but in any case until the solid disappeared. The mixture was kept at 40 ^{o}C for another 30 min before the oxalyl chloride was removed and the residue was dissolved in Bu^{t}OH/$CHCl_3$ (10 ml/2 ml) at room temperature and TEA (1 ml) was added The solution was heated to 45-50 ^{o}C and stirred overnight under argon. Then the solvent was removed and the solid was taken up in $CHCl_3$, and washed with water, 3% aqueous HCl, and then $NaHCO_3$, brine and finally dried over anhydrous Na_2SO_4. The solvent was removed and the residue was purified using silica gel column chromatography eluted with 2% MeOH/ CH_2Cl_2 to give the product as a brown sticky oil (95 mg, 40%). ^{1}H NMR (400 MHz; $CDCl_3$): 8.95 (s, 2H), 7.35-7.25) (m, 10H), 5.25 (s, 4H), 3.92 (s, 2H), 2.68 (t, 4H), 2.34 (t, 4H), 2.28 (s, 6H), 1.38 (s, 18H). (

Di-tert-butyl 3,3'-(2,2'-Methylenebis(5-formyl-4-methyl-1H-pyrrole-3,2-diyl))dipropanoate 43: Compound **45** (410 mg, 0.587 mmol) was dissolved in 80 ml THF and 50 mg (10%) Pd/C was added and the solution was stirred under a H_2 atmosphere overnight. After TLC showed the starting material had disappeared, the solution was passed through a Celite cake to remove catalyst, and the resulting carboxylic acid was dissolved in DMF (5 ml) and the solution was heated to 160 ^{o}C with stirring for about I h. The solution was then was cooled down to room temperature and the Vilsmeier complex of PhCOCl/DMF (0.30/0.40 ml) was added dropwise at 0 ^{o}C. The mixture was stirred for about 1 h and then the DMF was removed and the residue was dissolved in EtOH. Aqueous $NaHCO_3$ was added to hydrolyze the intermediate and a yellow precipitate was collected and washed with water, and then air dried. The solid was recrystallized from EtOH to give the product (75 mg, 45%).^{1}H NMR (400 MHz; $CDCl_3$): 10.62 (s, 2H), 9.36 (s, 2H), 3.96 (s, 2H), 2.64 (t, 4H), 2.30 (t, 4H), 2.22 (s, 6H), 1.36 (s, 18H).

Dibenzyl 5,5'-methylenebis{4-[3-(2-(tert-butoxycarbonyl)amino)ethyl)amino)-3-oxopropyl]-3-methyl-1H-pyrrole-2-carboxylate} 46: *Method I*: Dipyrromethane **44** (0.1 g, 0.159 mmol) was dissolved in 15 ml oxalyl chloride and heated at 40 ^{o}C with stirring until all the solid disappeared. The mixture was kept at 40 ^{o}C for another 1 h and then the oxalyl chloride was removed and the residue was dissolved in $CHCl_3$ and a solution of BOC-$NHCH_2CH_2NH_2$ (50 mg, 0.32 mmol) and TEA (32 mg, 0.32 mmol) in $CHCl_3$ (20 ml) was added. The solution was stirred at room temperature overnight before being washed with water, 3% aqueous HCl, aqueous $NaHCO_3$ and brine, and then dried over anhydrous Na_2SO_4. The residue was purified by silica gel column chromatography eluting with 4% MeOH/ CH_2Cl_2 to give the product (27 mg, 20%).

Method II: To a solution of **44** (0.1 g, 0.159 mmol) in DMF (1.5 ml) was sequentially added HATU (110 mg, 0.29 mmol) and DIEA (0.10 ml) and the solution was stirred at room temperature for 1 h before $NH_2CH_2CH_2NHBOC$ (50 mg, 0.32 mmol) was added. The solution was stirred for 1 d, and the solution was then diluted with ethyl acetate (50 ml) and washed with 10% citric acid, saturated $NaHCO_3$ and then brine. The organic phase was dried over anhydrous Na_2SO_4 and the solvent was removed in vacuo and the residue was purified by silica gel column chromatography eluting with 4% MeOH/ CH_2Cl_2 to give the product (55 mg, 41%). ^{1}H NMR (400 MHz; $CDCl_3$): 9.84 (s, 2H), 7.39-7.28 (m, 10H), 6.26 (s, 2H), 5.26 (s, 4H), 3.92 (s, 2H), 3.27 (t, 4H), 3.09 (t, 4H), 2.78 (t, 3H), 2.38 (t, 4H), 2.27 (s, 6H), 1.39 (s, 18H).

1,9-Diformyl-2,3,5,5,7,8-hexamethyldipyrromethane 49: *Method I*: Dipyrromethane **14** (1.245 g, 2.5 mmol) was dissolved in THF (80 ml), and 50 mg (5%) Pd/C catalyst was added. The mixture was stirred under an H_2 atmosphere overnight before the solution was passed through a Celite cake to remove the catalyst. The THF was removed and the solid was dissolved and left in TFA (15 ml) for 5 min, before excess TEOF (2 ml) was

added to the TFA solution and the mixture was stirred at room temperature for 1 h. The solution was poured into ice/water and the aqueous solution was neutralized by aqueous ammonia to pH=7. Then the solution was extracted with $CHCl_3$ three times and washed with water, brine and finally dried over anhydrous Na_2SO_4. The solvent was removed and the solid was recrystallized from EtOH to give the product (140 mg, 20% yield); *Method II*: Dipyrromethane **53** (1.87 g, 5.0 mmol) and KOH (2.0 g) were dissolved in ethylene glycol (15 ml) and a little water was added before the solution was refluxed at 180-200 ^oC for 1 h. After the solution was cooled down to room temperature, it was diluted with water and the mixture was extracted with hexane three times. The organic layer was washed with water, brine and dried over anhydrous Na_2SO_4. The yellowish oily residue was dissolved in DMF (5 ml) and the complex PhCOCl/DMF (2.6/4.2 ml) was added at 0 ^oC dropwise to the solution. After 2 h, 20 ml of toluene was added and the mixture was kept in ice/water for a while until most of the precipitate came out. The imine salt was filtered and washed with toluene and the solid was taken up in 2 g of $NaHCO_3$ in 50/50 ml $EtOH/H_2O$. The solution was heated at reflux for 15 min and after the solution was cooled down to room temperature, 40 ml of water was added and the mixture was allowed to stand overnight. The solid was filtered off, dried and recrystallized from chloroform/petroleum ether to give the desired product aldehyde as pale yellow crystals (0.92 g, 65% yield). ^1H NMR (400 MHz; $CDCl_3$): δ 9.54 (s, 2H), 8.86 (s, 2H), 2.21 (s, 6H), 1.67 (s, 6H), 1.51 (s, 6H).

3,4-Dimethylpyrrole 51: Pyrrole **50** (1.67 g, 0.01 mol) and KOH (1.0 g) were added to 10 ml of ethylene glycol and the solution was refluxed for about 1 h. The solution was cooled down to room temperature and diluted with water to 50 ml and the solution was then extracted with hexane three times. The organic layer was washed with water, brine, and then dried over anhydrous Na_2SO_4. The solvent was removed and the residue was

purified by silica gel column chromatography eluting with hexane/ CH_2Cl_2 (2:1) to give 3,4-dimethylpyrrole as a brown liquid (95 mg, 10% yield). ^{1}H NMR (400 MHz; $CDCl_3$): 7.40 (s, 2H), 6.51 (s, 2H), 2.00 (s, 3H), 1.99 (s, 3H).

Diethyl 5,5'-(propane-2,2-diyl)bis(3,4-dimethyl-1H-pyrrole-2-carboxylate) 53: The synthesis of compound **53** followed the procedure for dipyrromethane **15**, starting with (3.34 g, 0.02 mol) to obtain product (4.8 g, 70%). Mp 131-133^{o}C, (Lit[22] Mp 125-126^{o}C) .^{1}H NMR (400 MHz; $CDCl_3$): δ 8.69 (s, 2H), 4.30 (q, 4H), 2.22 (s, 6H), 1.66 (s, 6H), 1.55 (s, 6H), 1.37 (t, 6H).

Bis(5-iodo-4-(3-((2-((tert-butoxycarbonyl)amino)ethyl)amino)-3-oxopropyl)-3-methylpyrrole)methane 55: Dipyrromethane **46** (1.08 g, 1.25 mmol) was dissolved in THF (80 ml) and 80 mg of (5%) Pd/C catalyst was added before the mixture was stirred under a H_2 atmosphere overnight. Then the solution was passed through a Celite cake and the solvent was removed to give a solid which was added to 90/30 ml (H_2O/MeOH) and then $NaHCO_3$ (0.6 g) was added and the solution was sonicated until a clear pink solution was formed. Then a solution of I_2 (0.5 g) in 60 ml of MeOH was added at room temperature slowly. The mixture was stirred for 2 h before the reaction was stopped. The precipitate was filtered and washed with water, hexane and air dried to give 0.62 g (60%) ^{1}H NMR (400 MHz; $CDCl_3$): 3.20 (t, 4H), 3.18 (t, 4H), 2.93 (t, 4H), 2.35 (t, 4H), 2.0 (t, 6H), 1.42 (t, 9H).

3.7. Supporting information

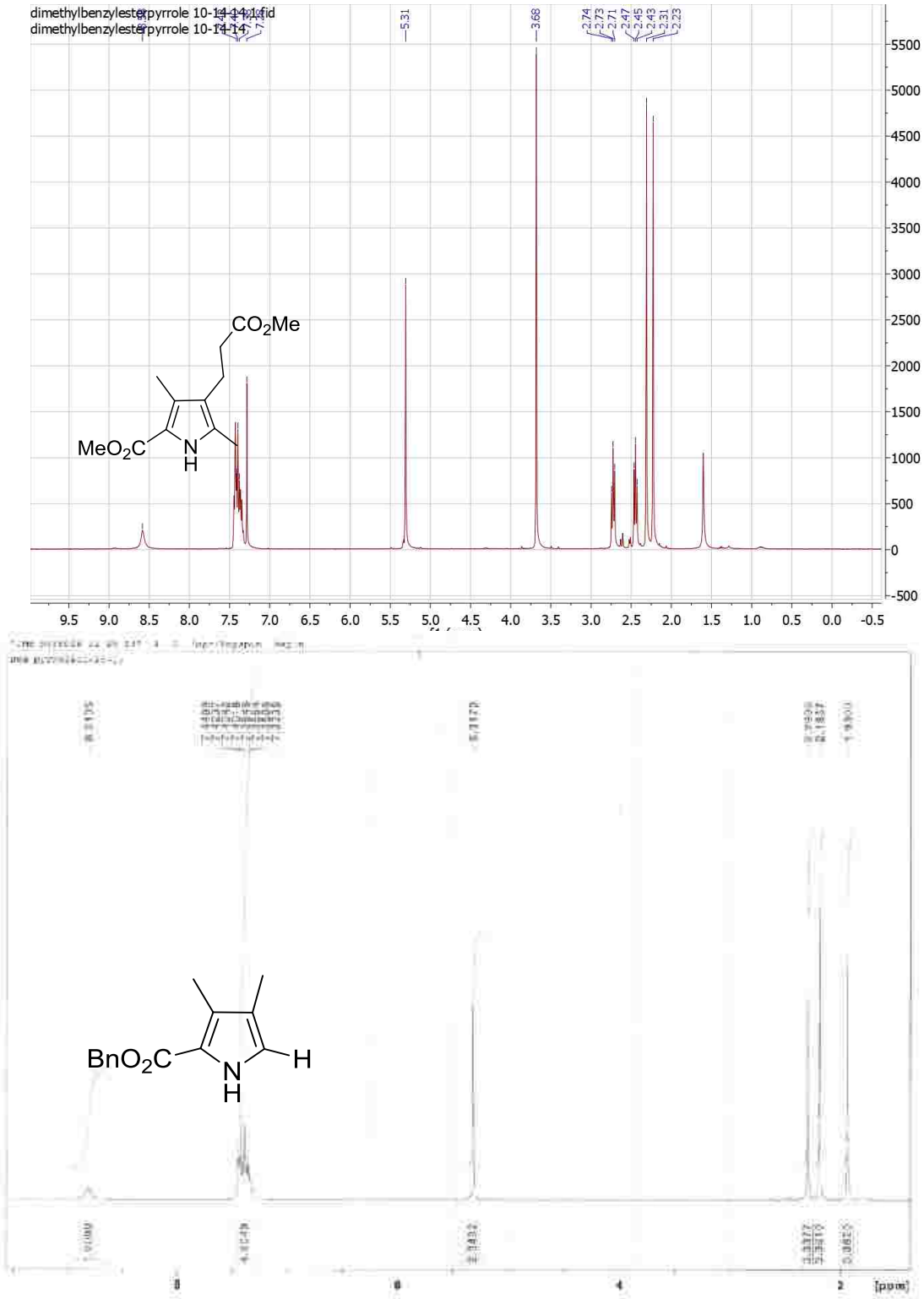

^{1}H NMR spectra of pyrrole **18** and **20** in $CDCl_3$ at 400 MHz

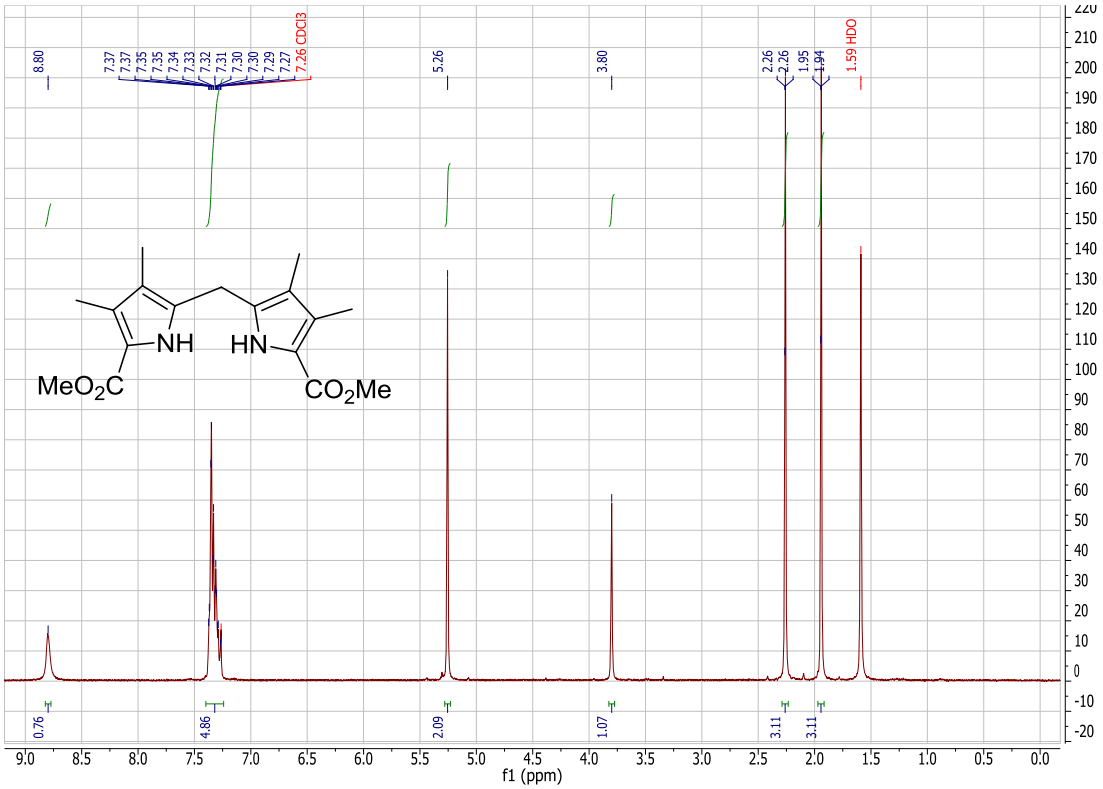

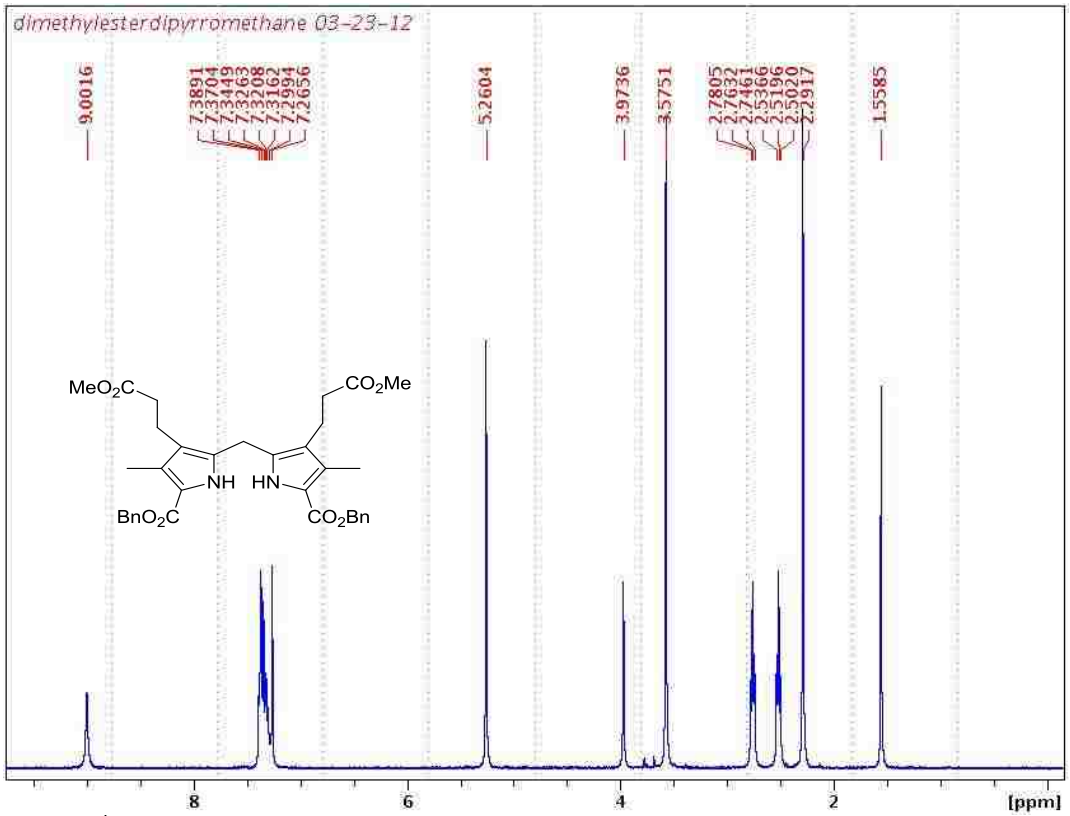

^{1}H NMR spectra of dipyrromethane **17** and **28** in $CDCl_3$ at 400 MHz

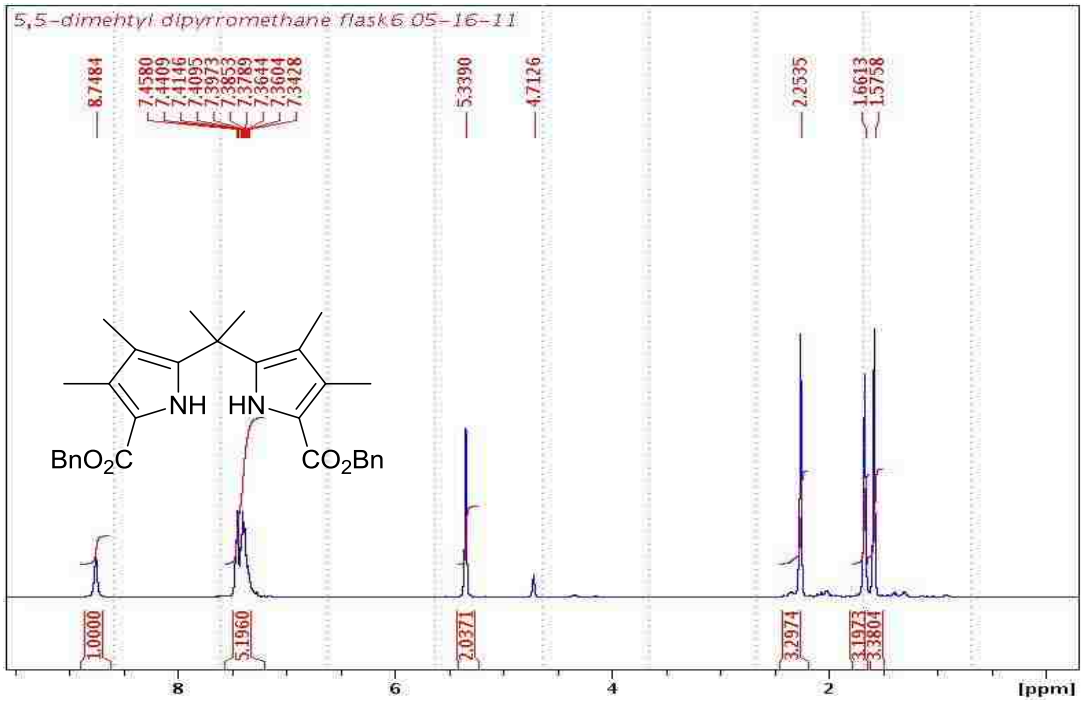

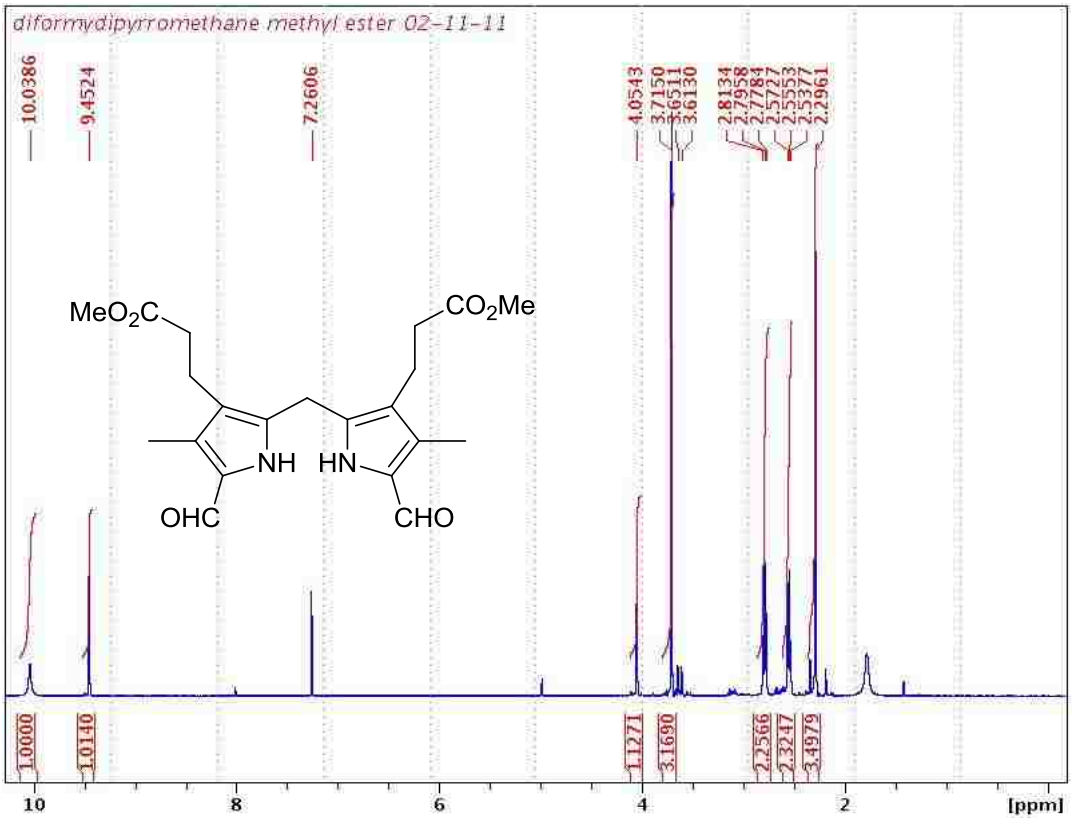

^{1}H NMR spectra of dipyrromethane **14** and **16** in $CDCl_3$ at 400 MHz

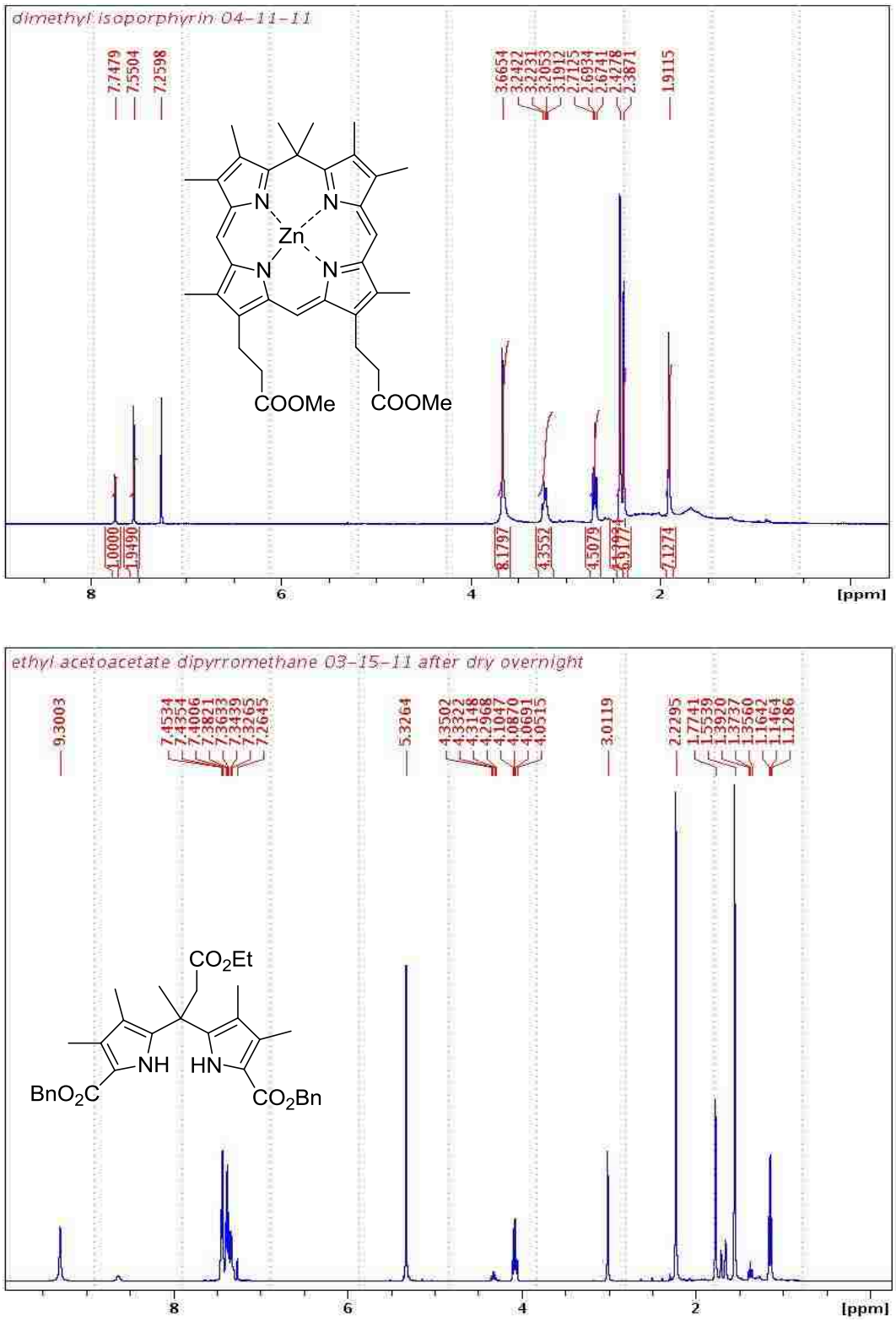

^{1}H NMR spectra of isoporphyrin **12** and dipyrromethane **25** in $CDCl_3$ at 400 MHz

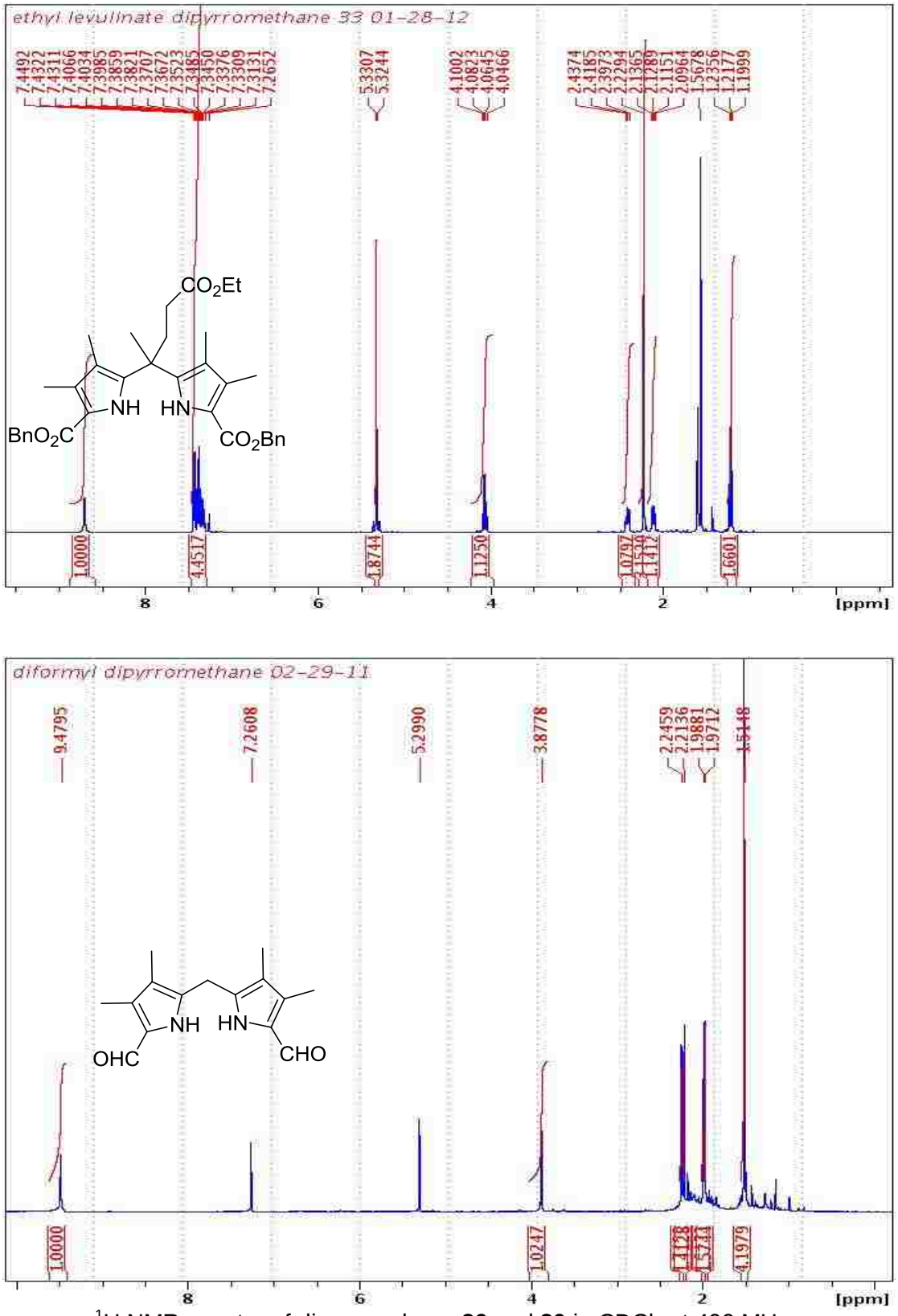

^{1}H NMR spectra of dipyrromehane **26** and **30** in $CDCl_3$ at 400 MHz

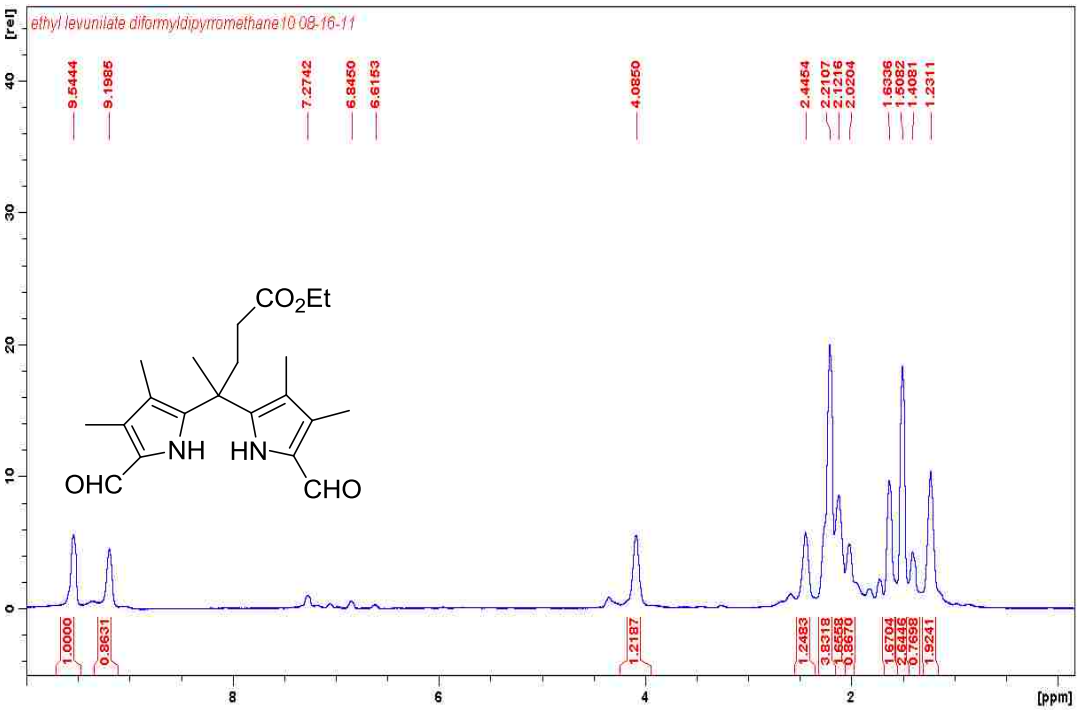

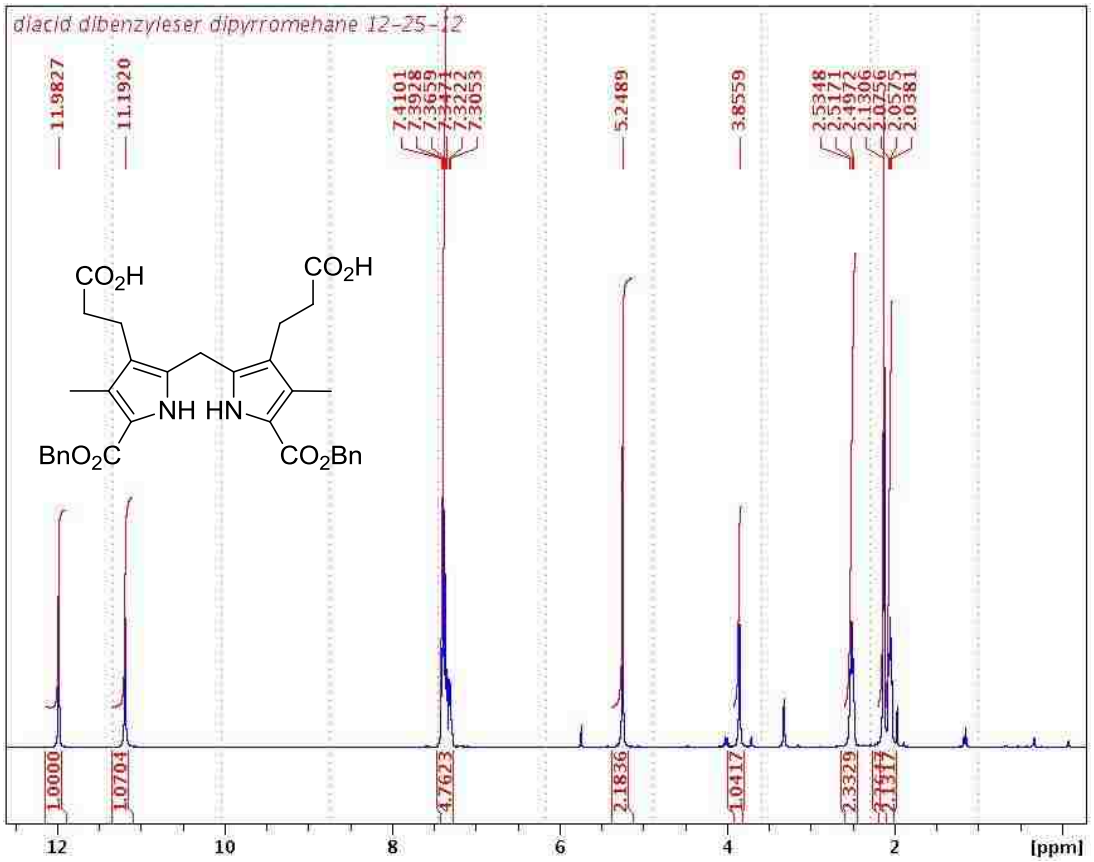

^{1}H NMR spectra of dipyrromehane **32** and **44** in $CDCl_3$ at 400 MHz

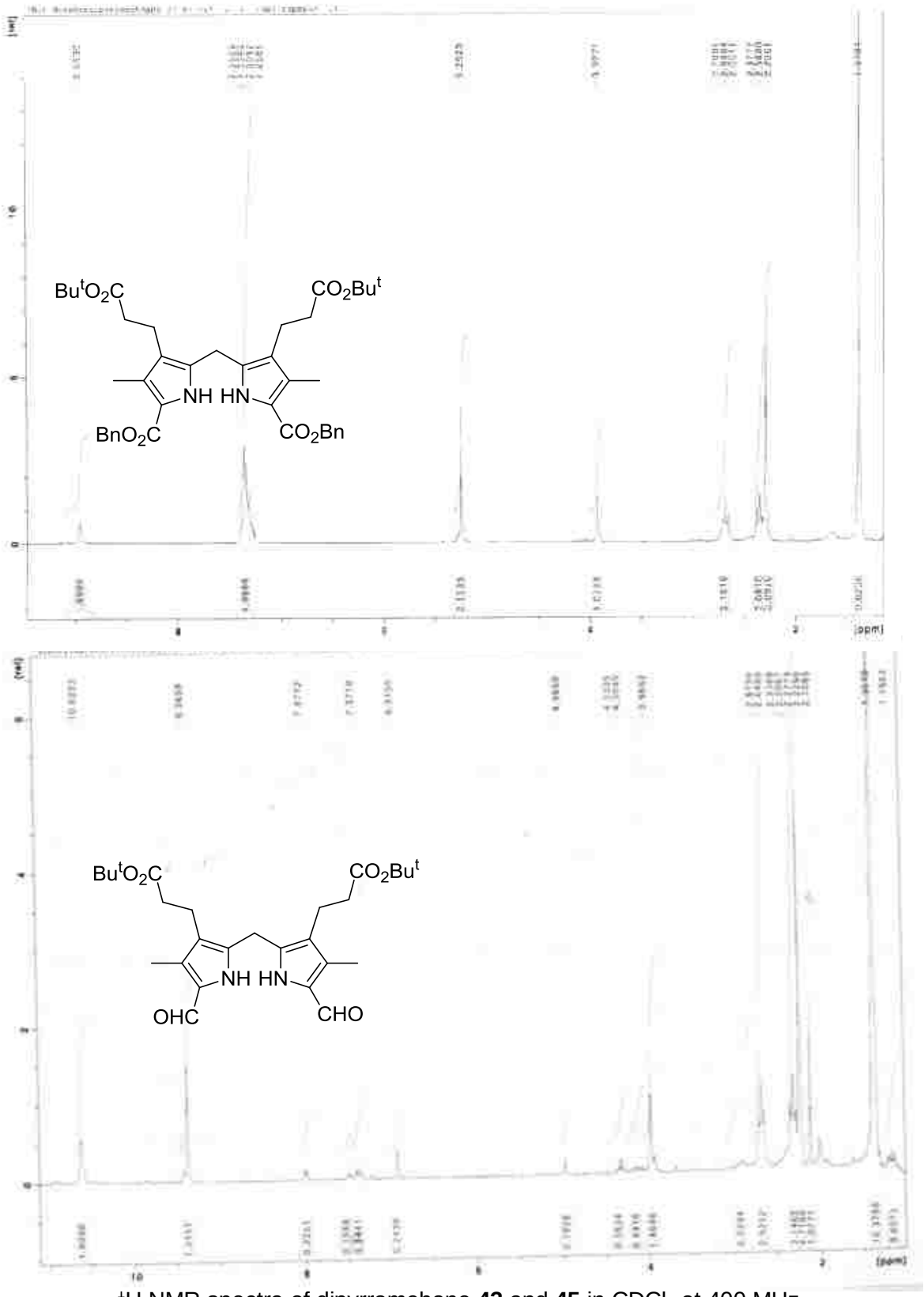

^{1}H NMR spectra of dipyrromehane **43** and **45** in $CDCl_3$ at 400 MHz

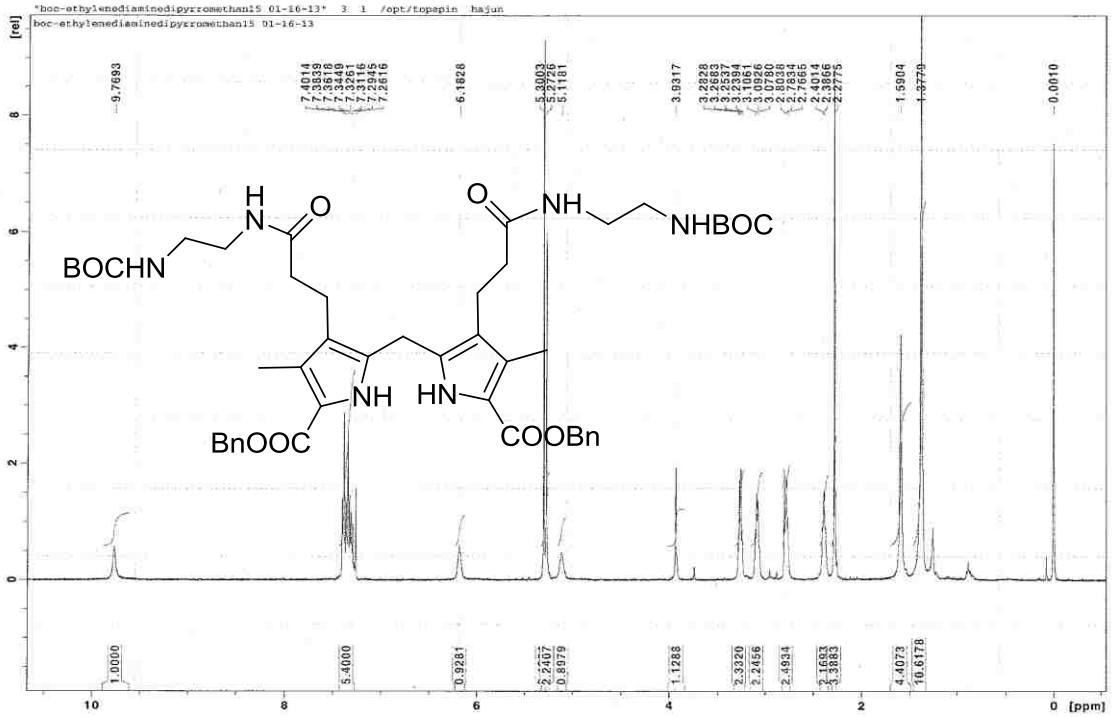

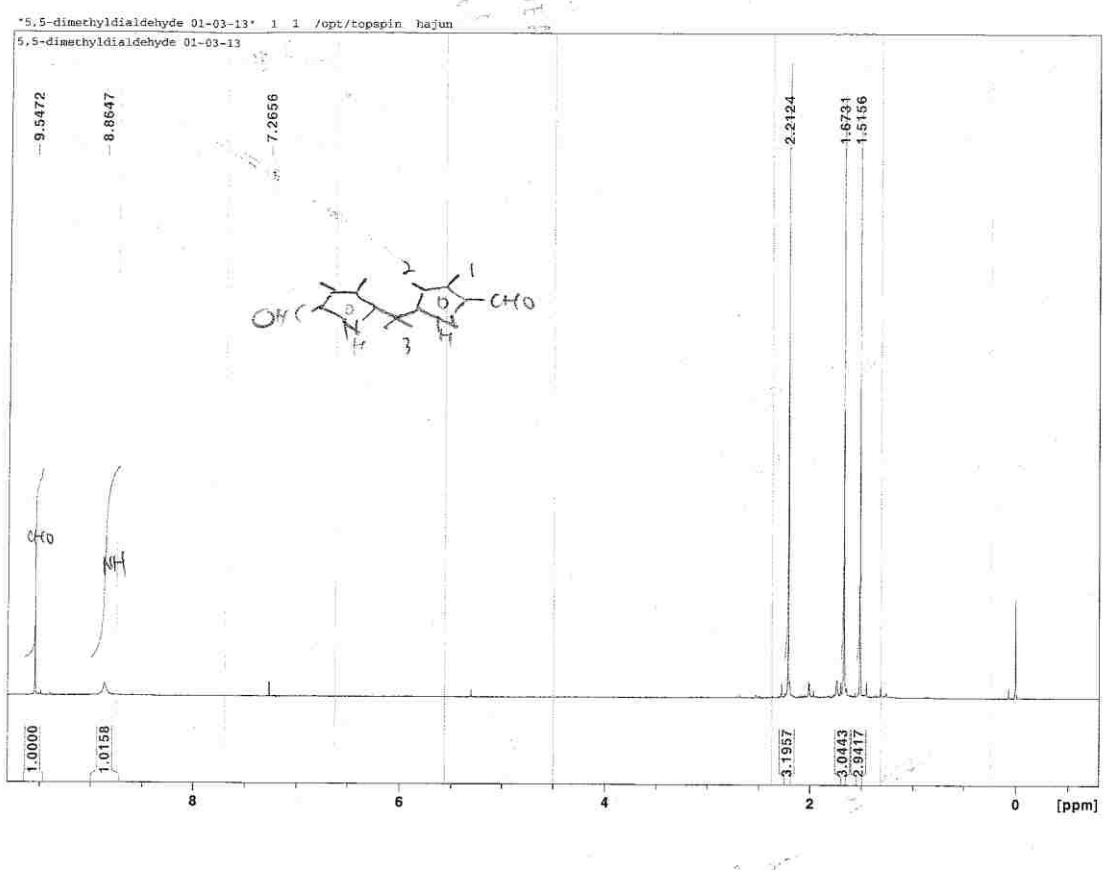

^{1}H NMR spectra of dipyrromehane **46** and **49** in $CDCl_3$ at 400 MHz

3.8. References

1. Fischer, H.; Orth, H. *Die Chemie des Pyrrols*; Akademische VerlagsgeseIlschaft: Leipzig, 1937; Vol. II, part i, p193.

2. Fischer, H.; Orth, H. *Die Chemie des Pyrrols*; Akademische Verlagsgesellschaft: Leipzig, 1937; Vol. II, part i, p165

3. Cavaleiro, J. A. S.; Gonsalves, A. M. d'A. R.; Kenner, G. W.; Smith, K. M. *J. Chem. Soc., Perkin Trans. 1* **1973**, 2471.

4. Tarlton, E. J.; MacDonald, S. F.; Baltazzi, E. *J. Am. Chem. Soc.* **1960**, *82*, 4389.

5. Jackson, A. H.; Pandey, R. K.; Rao, K. R. N.; Roberts, E. *Tetrahedron Lett.* **1985**, *26*, 793.

6. Freeman, B. A.; Smith, K. M. *Syn. Commun.* **1999**, *29*, 1843.

7. Hudson, M. F.; Smith, K. M. *Tetrahedron* **1975**, *31*, 3077.

8. Hudson, M. F.; Smith, K. M. *Chem. Commun.* **1973**, 515.

9. Smith, K. M. *J. Chem. Soc., Perkin Trans. 1* **1972**, 1471.

10. Arsenault, G. P.; Bullock, E.; MacDonald, S. F. *J. Am. Chem. Soc.* **1960**, *82*, 4384.

11. Cavaleiro, J. A. S.; Gonsalves, A. M. d'A. R.; Kenner, G. W.; Smith, K. M. *J. Chem. So.c, Perkin Trans.1* **1974**, 1771.

12. Cavaleiro, J. A. S.; Kenner, G. W.; Smith, K. M. *J. Chem. Soc, Perkin Trans. 1* **1974**, 1188.

13. Woodward, R. B. *Angew. Chem.* **1960**, *72*, 651.

14. Woodward, R. B.; Ayer, W. A.; Beaton, J. M.; Bickelhaupt, F.; Bonnett, R.; Buchschacher, P.; Closs, G. L.; Dutler, H.; Hannah, J.; Hauck, F. P.; Itǒ, S.; Langemann, A.; Le Goff, E.; Leimgruber, W.; Lwowski, W.; Sauer, J.; Valenta, Z.; Volz, H. *Tetrahedron* **1990**, *46*, 7599.

15 Xie, H.; Smith, K. M. *Tetrahedron Lett.* **1992**, *33*, 1197.

16. Barkigia, K. M.; Renner, M. W.; Xie, H.; Smith, K. M.; Fajer, J. *J. Am. Chem. Soc.* **1993**, *115*, 7894.

17. Fawcett, W. R.; **Fedurco**, M.; Smith, K. M.; and Xie, Hong. *J. Electroanal. Chem* **1993**, *354*, 281.

18. Mwakwari, C.; Fronczek, F. R.; Smith, K. M. *Chem. Commun.* **2007**, 2258.

19. Johnson, A. W.; Markham, E.; Price, R.; Shaw, K. B. *J. Chem. Soc.* **1958**, 4254.

20. Bullock, E.; Johnson, A. W.; Markham, E.; Shaw, K. B. *J. Chem. Soc.* **1958**, 1430.

21. Fischer, H. Orth, H. *Die Chemie des Pyrrols*; Akademische Verlagsgesellschaft , Leipzig, 1934; Vol. I.

22. Dolphin, D.; Harris, R. L. N.; Huppatz, J. L.; Johnson, A. W.; Kay, I. T.; Leng, J. *J. Chem. Soc. C.* **1966**, 98.

23. Holmes, R. T.; Jianming, L.; Mwakwari, C.; Smith, K. M. *ARKIVOC* **2010**, 5.

24. Lash, T. D.; Smith, B. E.; Melquist, M. J.; Godfrey, B. A. *J. Org. Chem.* **2011**, *76*, 5335.

25. Martin,P.; Mueller, M., Flubacher, D.; Boudier, A.; Blaser, H. U.; Spielvogel, K. *Org. Process. Res. Dev.* **2010**, *14*, 799.

26. Mattsson, S.; Dahlström, M.; Karlsson, S. *Tetrahedron Lett.* **2007**, *48*, 2497.

27. David E Seitza, L. F. *Syn. Commun.* **1979**, *9*, 931.

28. D. L. Boger, D. Y. *J. Org. Chem.* **1989**, *54*, 2498.

29. Nicolaou, K. C.; Estrada, A. A.; Zak, M.; Lee, S. H.; Safina, B. S. *Angew. Chem. Int. Ed.* **2005**, *44*, 1378.

30. Graffner-Nordberg, M.; Sjodin, K.; Tunek, A.; Hallberg, A. *Chem. Pharm. Bull.* **1998**, *46*, 591.

31. Manchand, P. S. *Chem. Commun.* **1971**, 667.

32. Adamczyk, M.; Fishpaugh, J. R.; Heuser, K. J.; Ramp, J. M.; Reddy, R. E.; Wong, M. *Tetrahedron* **1998**, *54*, 3093.

33. Rolf Dobler, M. R.; Parker, D. T.;Peng, Y.; Piizzi, G.; Wattanasin, S. ; . WO2010031750 A1**. 2010.**

34. Robben, U.; Lindner, I.; Gartner, W. *J. Am. Chem. Soc.* **2008**, *130*, 11303.

35. Nogales, D. F.; Anstine, D. T.; Lightner, D. A. *Tetrahedron* **1994**, *50*, 8579.

36. Lash, T. D. *Tetrahedron* **2005**, *61*, 11577.

37. Sessler, **J. L**; Hugdahl, **J**.; **Johnson**, M. R. *J. Org. Chem.* **1986**, *51*, 2838.

38. Yu, W.; Williams, L.; M. Camp, V. M.; Malveaux, E. J.; Zhang, Z.; Olson, J. J.; Goodman, M. M. *J. Med. Chem.* **2010**, *53*, 876.

39. Beckmann, S.; Wessel, T.; Franck, B.; Hönle, W.; Borrmann, H.; von Schnering, H. G. *Angew. Chem.* **1990**, *102*, 1439.

40. Jonson, A. H; Kay, I. T.; Markham, E.; Price, R.; Shaw, K. B. *J. Chem. Soc*. **1959**, 3416.

41. Chong, R.; Clezy, P. S.; Liepa, A. J.; Nichol, A. W. *Aust. J. Chem*. **1969**, *22*, 229.

42.Szulbinski, W.; Strojeck, J. W. *J. Electroanal. Chem. Interfac. Electrochem*. **1988**, 252, 323.

43. Xie.Hong. In *PhD Dissertation*; University of California,: Davis, **1992**

Chapter 4: Synthesis of BODIPY Dyes from Dipyrrolyketones and Their Transformations

4.1. Introduction

4,4-Difluoro-4-bora-3a,4a-diaza-*s*-indacene[1,2](Figure 4.1), known well as BODIPY have been recognized as one of the most versatile fluorophore dyes in last three decades since their potential use as photo labels was discovered. Because of their sharp fluorescence emissions, high quantum yields, large molar absorption coefficients and relative chemical and thermal stabilities,[3,4] BODIPY dyes have been intensively employed as biological labeling reagents[5,6] in protein and DNA research. Moreover, the electrochemical activity of BODIPYs makes these dyes promising candidates as dopants in light emitting devices and polymer-based electroactive films.[7]

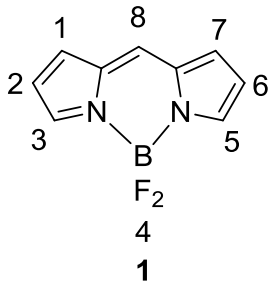

1

Figure 4.1: The structure of BODIPY.

Synthetic approaches to BODIPY dyes have not changed much since they were discovered. The first synthesis of BODIPY was reported by Treibs and Kreuzer in 1968;[1] however, this molecule was ignored until the potential uses of this this dye in biological labeling was discovered at the end of the 1980s. Since then numerous syntheses of these molecules were documented. All kinds of functionalization of these molecules have also been well-explored. After 30 years, achieving long wavelength absorbing and emitting BODIPYs with amphiphilic properties is still the target of chemists.

There are several strategies used to synthesize BODIPY dyes. The first synthetic method involved condensation of two identical pyrrole and a carbonyl source such as an aldehyde,[8] acyl chloride[9] or anhydride[10] catalyzed by acid; then oxidation of the resulting dipyrromethane into a dipyrromethene followed by complexation with $BF_3.OEt_2$ will lead to BODIPYs (Scheme 4.1**A**). This method was usually employed to build symmetrical BODIPYs. Another method involves acid catalyzed condensation of two different pyrrolic units where one of them bears a carbonyl group and the other one is an α-free pyrrole[11] (Scheme 4.1**B**). This method can directly give dipyrrins, which can be converted into BODIPYs by complexation with $BF_3.OEt_2$ in one step. This method is generally used to construct unsymmetrical BODIPYs. The third approach is derived from method one, which involves condensation of two identical α-formylpyrroles catalyzed by $POCl_3$[12] (Scheme 4.1**C**). The mechanism is believed to be analogous to the Vilsmeyer-Haack reaction to form a vinylogous intermediate between one α-formylpyrrole and $POCl_3$, followed by attack of another α-formylpyrrole. This method is only suitable to

(A)

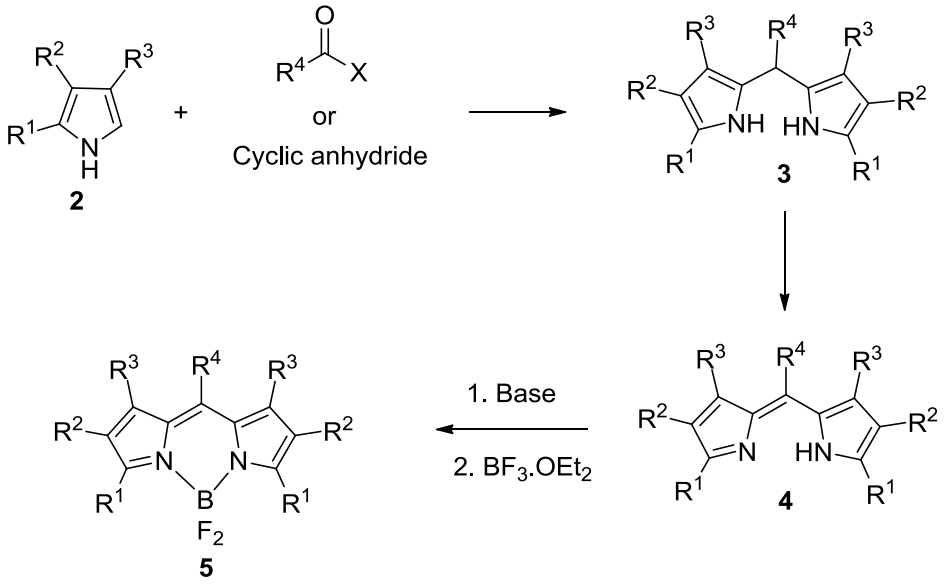

(B)

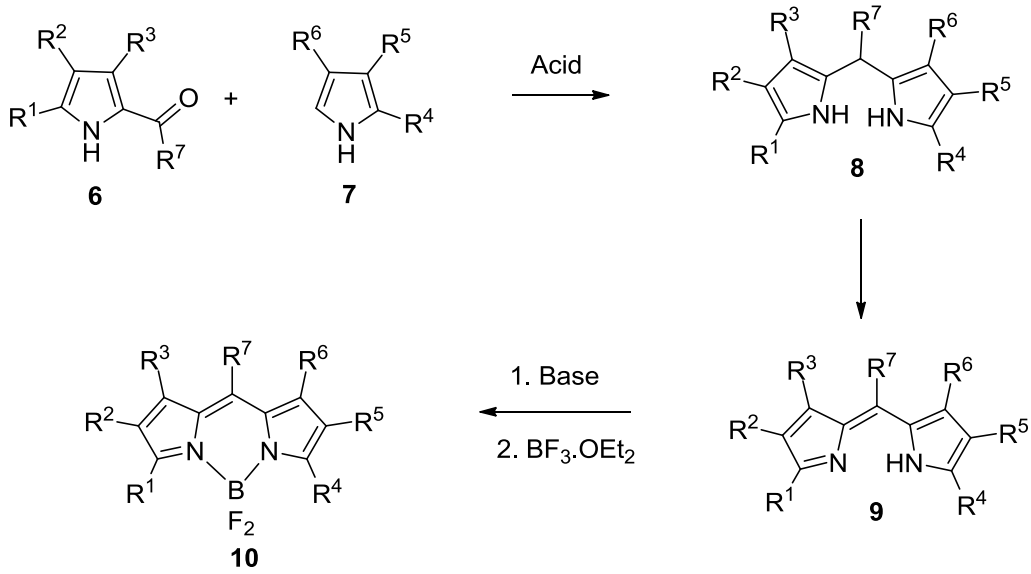

(C)

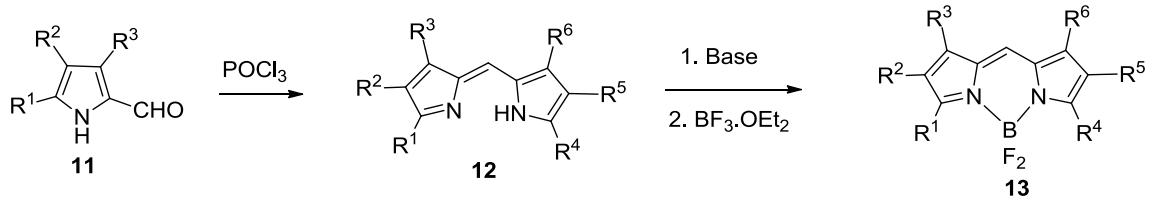

Scheme 4.1: Various routes to synthesize BODIPYs.

synthesize meso-unsubstituted BODIPYs. So far, the meso-aryl BODIPYs account for most synthesis of these molecules in the literatures and in patents.

Depending on which substitutuents are required to be introduced on the meso-carbon, the methods in Scheme 4.1 can be applied accordingly. For example, for method **A**, para-iodobenzaldehyde or a para-esterified benzaldehyde were used during BODIPY synthesis so that BODIPYs could be functionalized later by coupling reactions or by conjugation. Carboxylic acids can be introduced into BODIPYs directly when a cyclic anhydride was used as the carbonyl source, which can be further conjugated with

proteins and used for protein labeling. Method **B** allows more versatile functionalization of BODIPYs since it is easier to modulate the photophysical properties and hydrophobic and hydrophilic properties by various functionalizations of different position on BODIPYs. Many BODIPY-based labeling dyes are made using this particular method. Method **C** is useful to make highly symmetrical BODIPYs; this reaction gives excellent yields compared with method **A.**

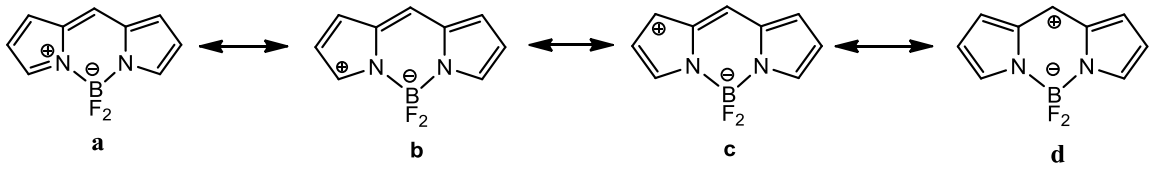

Scheme 4.2: Some resonance structures of BODIPY.

According to the resonance structure of BODIPYs (Scheme 4.2), carbons 1, 3, 5, and 7 are electrophilic positions on BODIPYs, and carbons 2 and 6 are nucleophilic positions. So the functionalization of BODIPYs actually follows these fundamental principles. Knoevenagel condensation can be performed on the active methyl groups on all electrophilic carbons at 1, 3, 5, and 7 with benzaldehyde to extend the π-electron conjugation, thereby increasing the wavelength of absorption of BODIPYs since these methyl groups are very nucleophilic,[13-17](Scheme 4.3**A**). Another electrophilic point is carbon 8, for the meso-free BODIPYs. Nucleophilic attack on carbon 8 usually needs to be accomplished with oxidation to remove a hydrogen. So far, there is only one example of this case, which is use of NaCN as a nucleophile.[1,18,19] *Meso*-cyanoBODIPYs have a significant red shift compared with *meso*-free BODIPYs. Introduction of sulfur[20] and halogens[21] at the meso-position allows more versatility for modification of carbon 8.. Replacement and coupling reactions can introduce many groups at the meso-carbon. Even some natural products have been introduced. Substitution reactions were also well explored at the boron to introduce aryl,[22] alkynyl[23], alkyl,[24] alkyloxy,[25] etc. From the

resonance structure of BODIPYs we can see that the 2, 6 positions are the most electron rich sites and therefore most susceptible to nucleophiles. Formylation,[26] nitration,[27] sulfonation,[28] and halogenation[29] were already reported. Palladium catalyzed oxidative coupling reactions[30] to extend the π-conjugation was also reported (Scheme 4.3**B**).

(A)

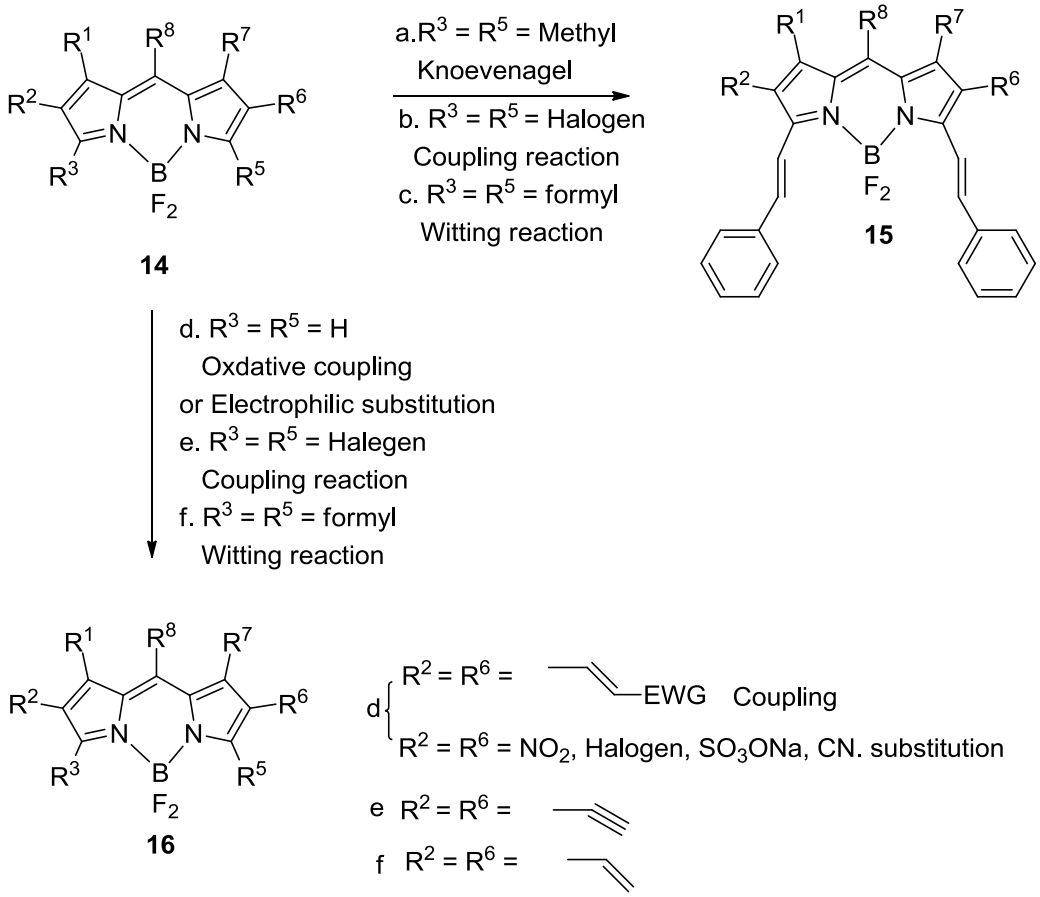

(B)

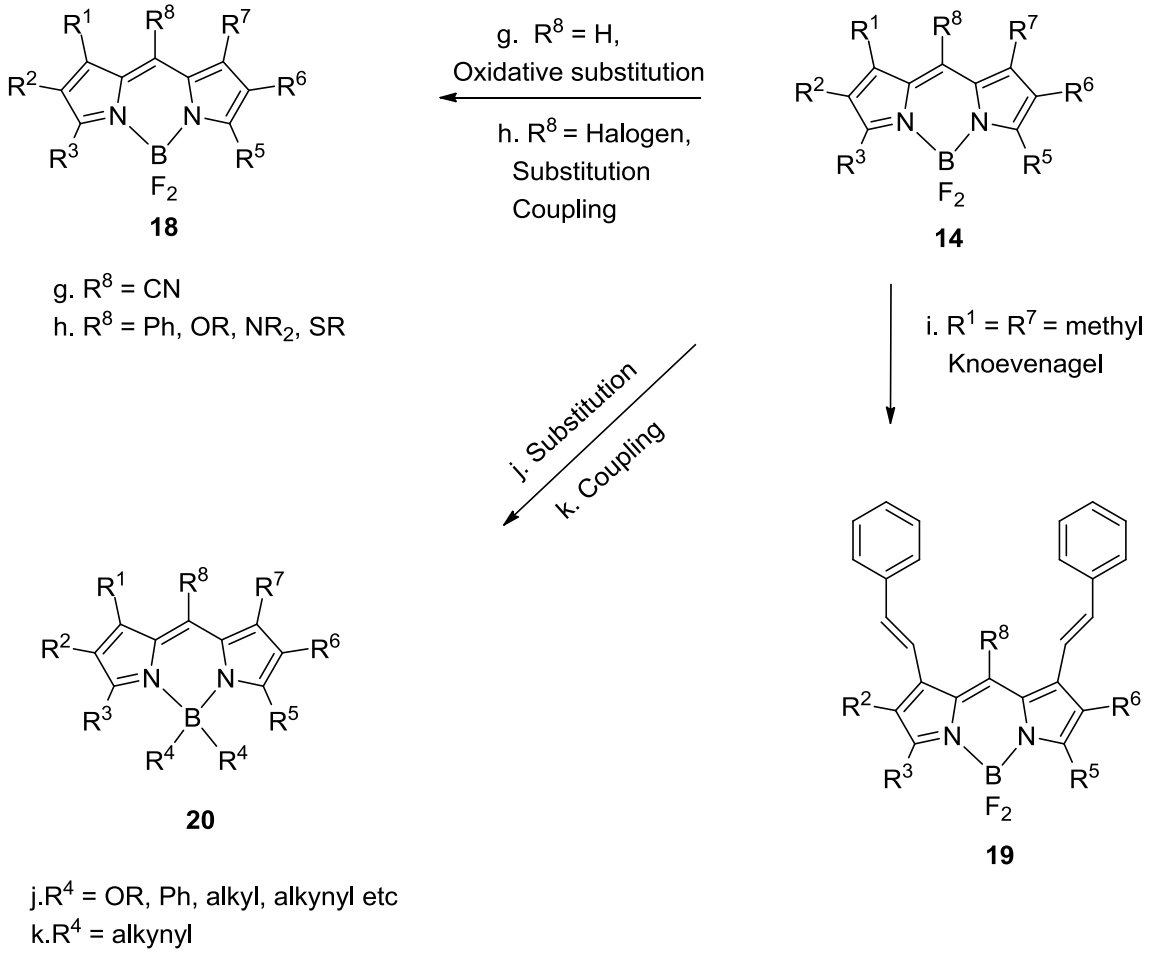

Scheme 4.3: Functionalization of BODIPYs by various methods.

Dipyrrolyketone (pyrroketones) have not been used much in polypyrrole chemistry. From their structure (Scheme 4.4), pyrroketones are actually bis-vinylogous amides and therefore do not react as normal ketones. For instance, pyrroketones can not be reduced by borohydride[31] to dipyrromethane or dipyrromethene.[32] Various syntheses of dipyrroketones are well documented. The symmetrical dipyrromethanes can be synthesized by treatment of pyrrole Grignard reagents with phosgene in one step (Scheme 4.5).

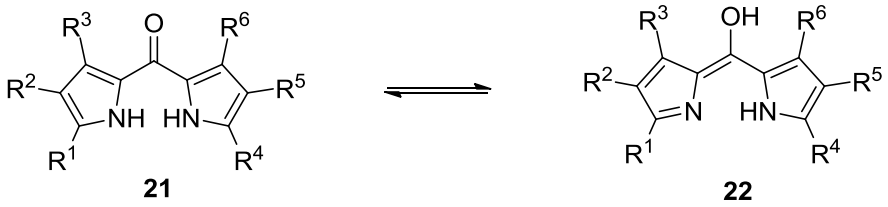

Scheme 4.4: Keto-enol tautomers of pyrroketone.

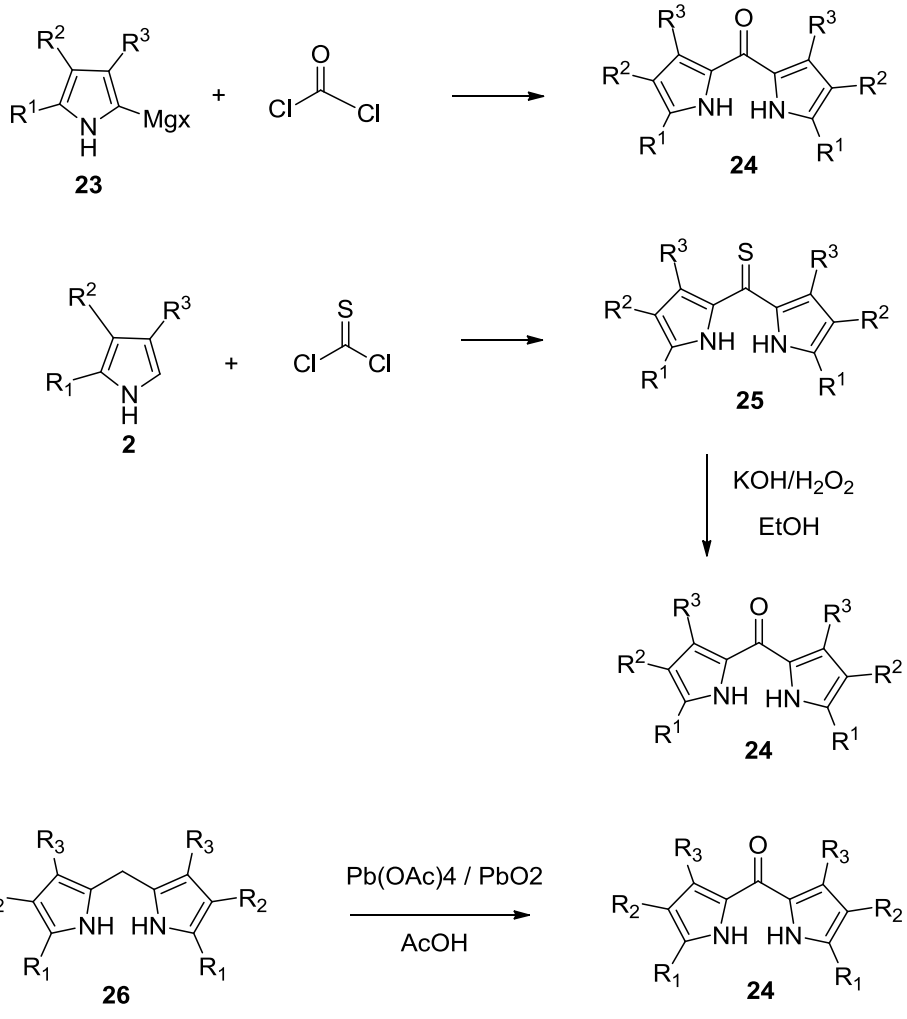

Scheme 4.5: Syntheses of symmetrical pyrroketones.

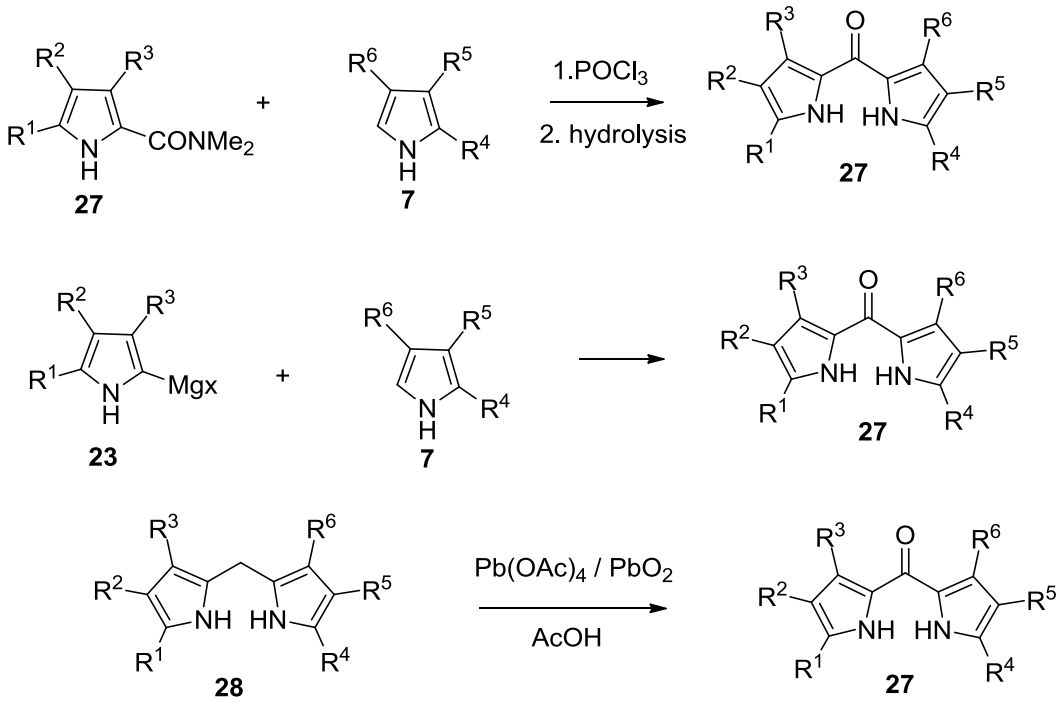

Scheme 4.6: Synthesis of unsymmetrical pyrroketones.

with phosgene in one step, or treatment α-free pyrroles with thiophosgene followed by oxidative hydrolysis of the corresponding symmetrical thioketone products.[20] An alternative approach for synthesis of symmetrical pyrroketones is to oxidize the corresponding symmetrical dipyrromethane with $PbO_2/Pb(OAc)_4$ or $Br_2/SOCl_2$[33] (Scheme 4.5). For the unsymmetrical pyrroketones, the most efficient method involves a modified Vilsmeier-Haack reaction between a pyrrole *N,N*-dimethylcarboxamide complex with another different α-free pyrrole using phosphoryl chloride.[32]

Some of the methods used to synthesize symmetrical pyrroketone can also be applied to unsymmetrical pyrroketone. For example, treatment of a pyrrole acyl chloride with another pyrrole Grignard derivative or oxidation of unsymmetrical dipyrromethane with $PbO_2/Pb(OAc)_4$ or $Br_2/SOCl_2$ gives the corresponding unsymmetrical pyrroketones (Scheme 4.6). A very important related analogue is a reaction of dipyrromethane *N,N*-

dimethylcarboxamide with phosphoryl chloride and another α-free dipyrromethane followed by hydrolysis of corresponding tetrapyrrole to give

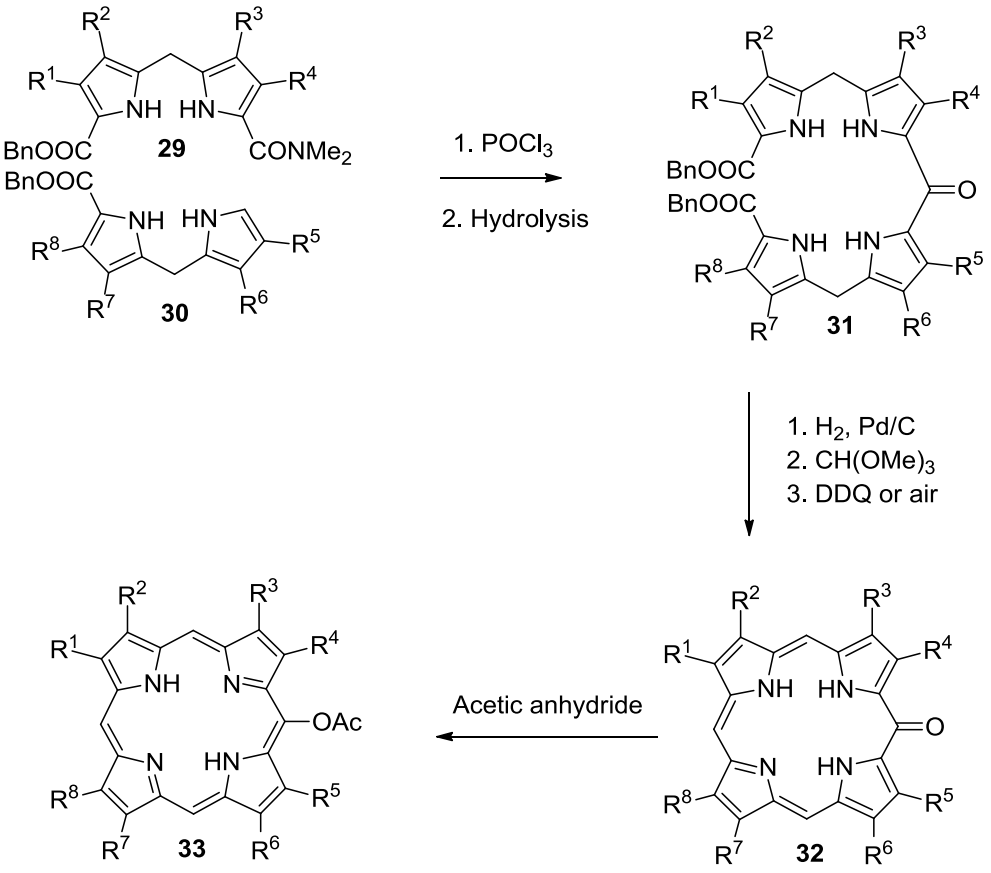

Scheme 4.7: Synthesis of meso-acetoxyporphyrin from oxophlorin.

b-oxobilanes, which are stable to acid catalyzed distribution of pyrrole rings because of the oxo-function, and therefore can be cyclized into oxophlorin and eventually transformed into porphyrin. Acetylation of the oxophlorin with acetic anhydride gives meso-acetoxyporphyrin[31,34,35] (Scheme 4.7).

From the above brief introduction to BODIPYs and pyrroketones and to their chemical transformation into porphyrins, one can see that BODIPYs and pyrrokeotnes are structurally related. Based on the reactivity of pyrroktones in the synthesis of porphyrins, it is possible that pyrroketones can be converted into their fully conjugated

dipyrromethene by use of reagents such as acetic anhydride, which can lead to BODIPYs directly after complexation with $BF_3.OEt_2$. The objective of this project is to expore a new synthetic method to BODIPYs from pyrroketones and to further functionalization of the new BODIPYs such as nucleophilic addition/elimination and coupling reactions. We also wanted to look at various pyrroketones to investigate the substituent applicability of any new methods.

4.2. Synthesis of Pyrroketones and Their Trasformation

Pyrroketones are actually bis-vinylogous amides; therefore the proposed transformations of pyrroketone are shown in Scheme 4.8. Protonation takes place on the oxygen atom, and depending on the electrophiles, substituents can be introduced either on nitrogen or on oxygen atoms. Pyrroketones can also be converted into their imidoyl halides through substitution of the oxygen atom. It was also planned to examine reactions including protonation,[36] O-alkylation,[37] and halogenation[38] (highlighted by green arrows) to convert

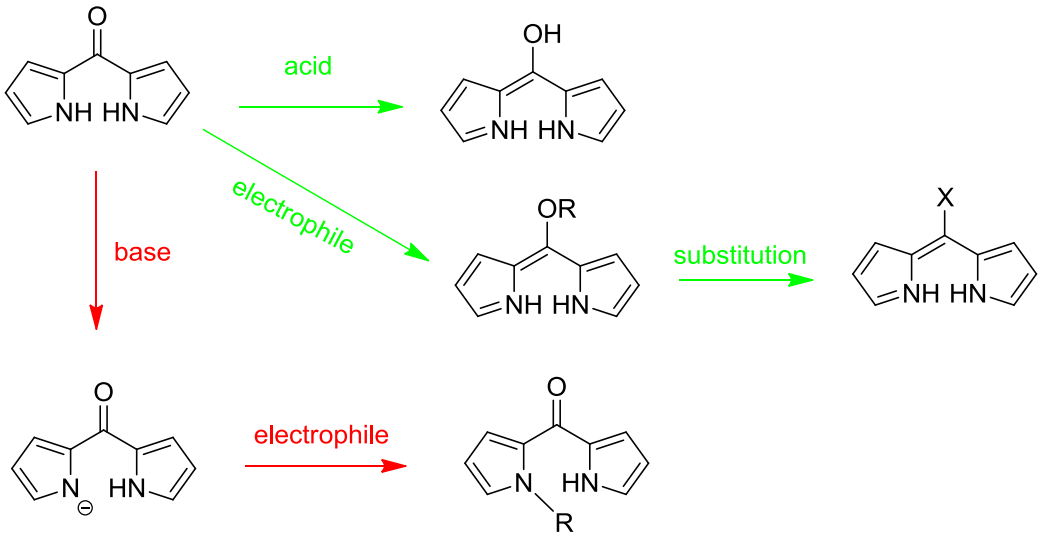

Scheme 4.8: Transformations of pyrroketones.

pyrroketones into their dipyrrins (dipyrromethenes) which can then be used later in BODIPY synthesis.

Firstly, some pyrroketones were synthesized by the methods mentioned above. Two major dipyrromethanes bearing ester groups on the α-positions were synthesized according to the procedure in Chapter 3. These two dipyrromethane **34** and **35** were then oxidized into the corresponding pyrroketones **36** and **37**[33] with $PbO_2/Pb(OAc)_4$ in acetic acid in about 50% yield (Scheme 4.9). From the ^1H NMR spectrum, protons at 3.97 and 3.79 ppm, which belong to meso carbon of dipyrromethane **34** and **35** disappeared, and the identity of these two product **36** and **37** was confirmed by mass spectroscopy, with *m/z* at 651.231(MW + Na) and 484.21, respectively.

Attempts were made to protonate these two pyrroketones with all kinds of acids such as HCl, TFA and BF3.OEt2; all acids partially converted pyrroketones into their dipyrrins salts; according to UV-visible absorptions around 430 nm, the most pronounced peak still belonged to starting material pyrroketones at 360 nm. Protonated pyrroketones are deprotonated during aqueous workup or treatment with bases. Then activation of the pyrroketones with acetic anhydride to convert them into their fully conjugated molecules was tried. Acetic anhydride and triflic anhydride[39] (Scheme 4.10) were therefore tried on the pyrroketones **36** and **37**. The pyrroketones did not react upon treatment with acetic anhydride according their UV-visible absorption. However, the stronger triflic anhydride/pyridine mixture formed a red solution and peaks at 432 and 534 nm in the UV-visible spectrs indicated the formation of a fully conjugated dipyrrin-type system. However, this intermediate can not withstand an aqueous workup and the peak around 430 nm disappeared. $DIEA/BF_3.OEt_2$ was added to if the intermediate could be converted into a BODIPY and characterized. However, the intermediate could not withstand organic bases either. Another strategy tried was to introduce a bromine atom

at the meso carbon by adding LiBr to a solution of activated pyrroketone after Tf_2O/pyridine treatment;[37,40] this did not work either.

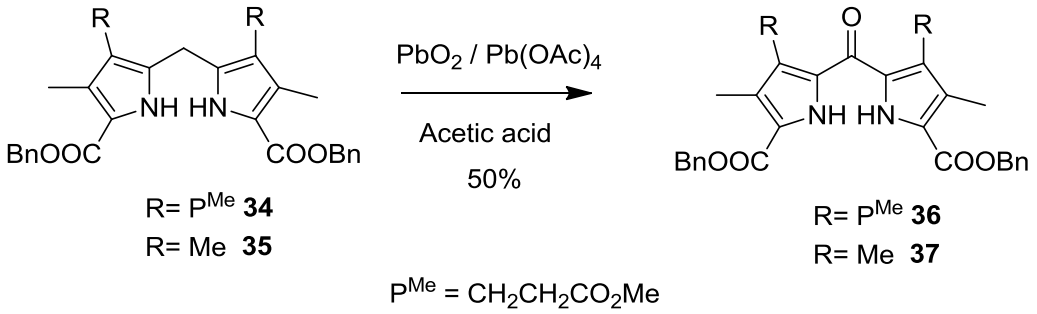

Scheme 4.9: Synthesis of pyrroketone through oxidation.

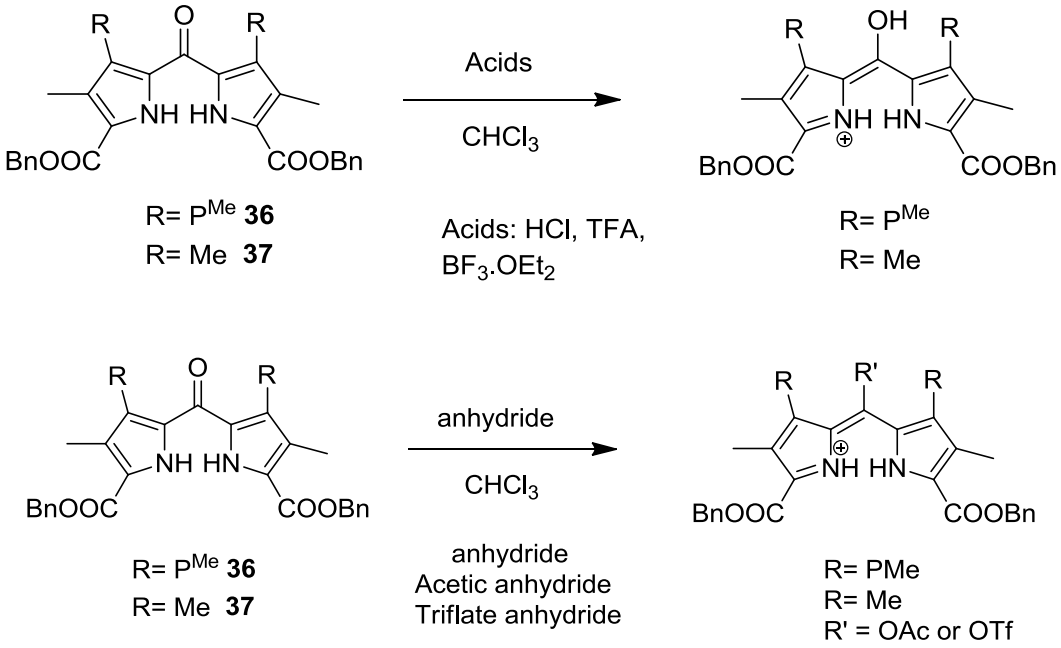

Scheme 4.10: Activation of pyrroketones by acids and anhydrides.

Eletrophiles such as methyl trifluoromethansulfonate[41] and Meerwein's salts[42] (Et_3OBF_4 and Me_3OBF_4) were reacted with pyrroketones **36** and **37** (Scheme 4.11). Methyl trifluoromethanesulfonate slightly changed the reaction solution from colorless to red. With Meerwein's reagents, the pyrroketones were converted completely into their

dipyrrin analogues based on the orange red color of the reaction solution and their UV-visible absorption at 446 nm. Unfortunately, upon aqueous workup, this intermediate reversed to the starting material according to the UV-visible spectral change (Figure 4.2), DIEA/ $BF_3.OEt_2$ was added to make corresponding the BODIPY but this did not work. However, from ^1H NMR spectra (Figure 4.3), extra peaks at 4.20 (q, 2H) and 1.22 (t, 3H)

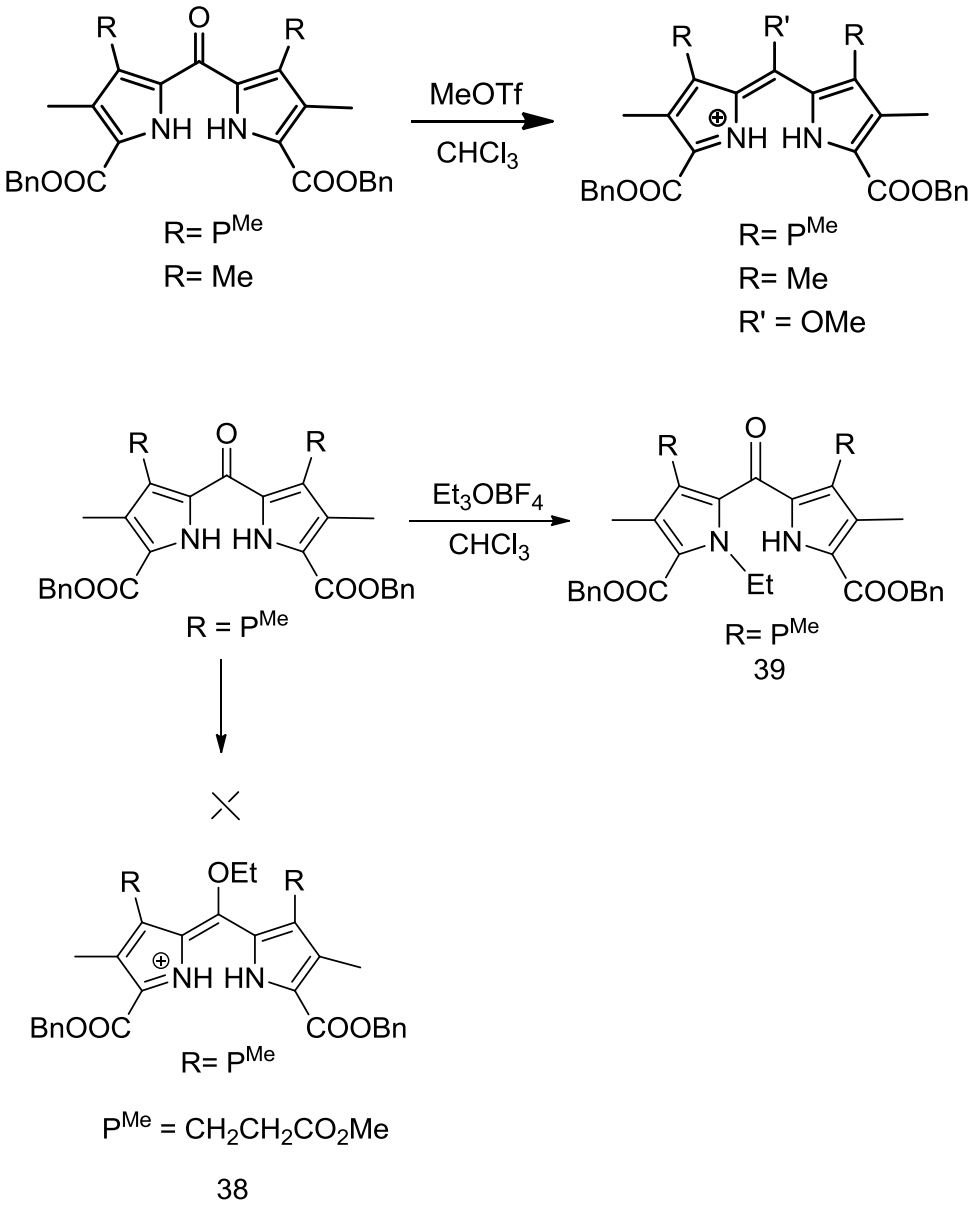

Scheme 4.11: Alkylation of pyrroketone using Et_3OBF_4 in $CHCl_3$.

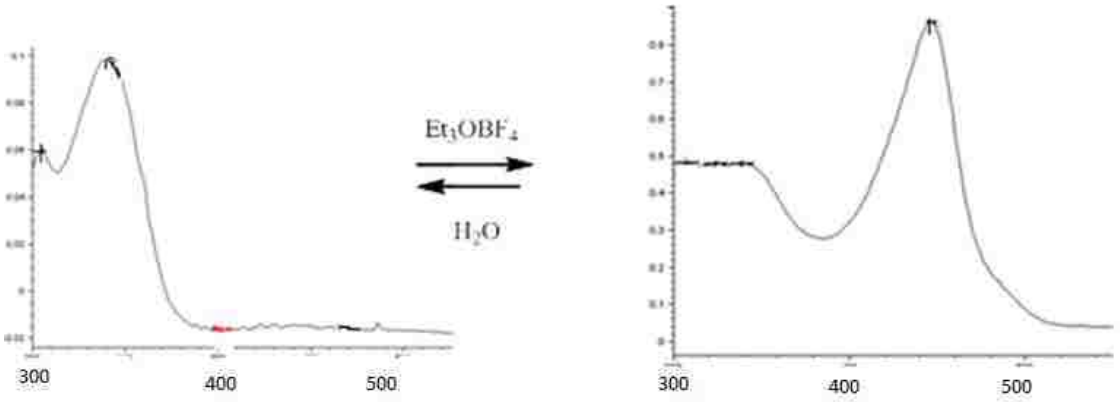

Figure 4.2: UV/Vis absorption spectrum of Alkylation of pyrroketone using Et_3OBF_4 in CH_2Cl_2

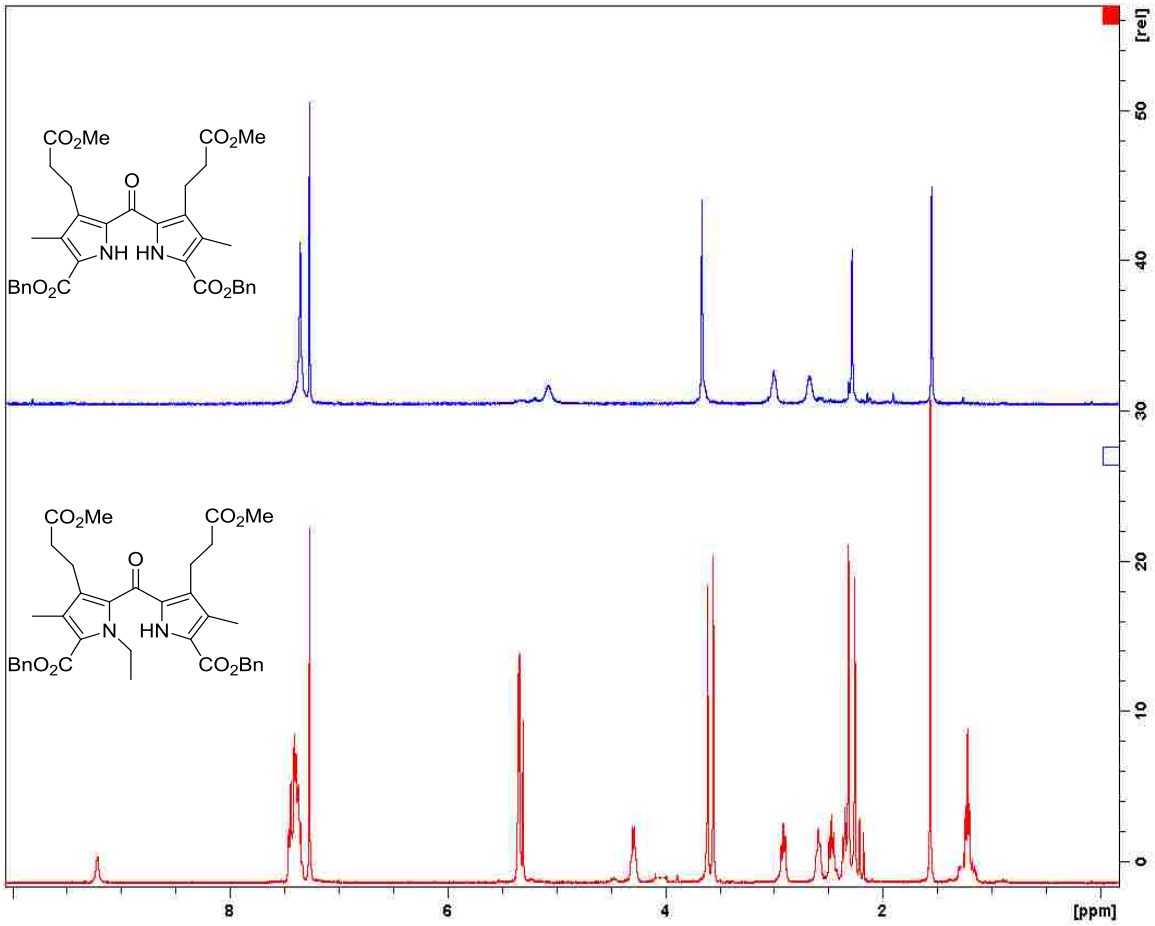

Figure 4.3: ^1H NMR spectra of pyrroketone **36** and product **39** in $CDCl_3$

attributed to ethyl group on the heteroatom nitrogen proved the ethyl group actually went to the nitrogen of the pyrrole instead of the oxygen on the meso carbon, and this result was further confirmed by the mass spectrum with *m/z* at 656.27

From all the protonation and nucleophilic substitution reactions tried on the pyrroketones, one can see that even strong acids do not react with pyrroketones, and strong nucleophiles can convert pyrroketones partially or completely into their fully conjugated dipyrrin intermediates. The problem is that these intermediates are not stable enough to withstand water or nucleophiles during work-up. Halogenation reactions were also attempted on the two pyrroketones. Typical chlorinating reagents such as $POCl_3$,[43] PCl_5,[37] oxalyl chloridel[44] and phosgene[45] were tried under different conditions at room temperature or at reflux. All these reagents gave a red solution which indicated the formation of the fully conjugated dipyrrin system, and UV-visible absorption spectroscopy showed a sharp peak around 500-530 nm. However, the stability of these compounds or intermediates was was a serious problem which made them hard to separate and they easily decomposed upon aqueous work-up or interaction with nucleophiles. Specifically, when $POCl_3$/DMF was used to chlorinate the pyrroketone, the fully conjugated system was formed according to UV-visible absorptions at 528 (pyrroketone **36**) and 534 nm (pyrroketone **37**), which are most likely the intermediates or products (Scheme 4.12). Especially for pyrroketone **36**, a peak at *m/z* 645.17 in the mass spectrum showed that the product **40** was actually formed (Figure 4.4), along with some other side products, such as a dimer or trimer. However, it was not possible to separate the product by chromatography or by crystallization. When $POCl_3$/PCl_5[46] was used as the chlorinating reagent，the UV-visible absorptions at 505 and 529 nm (pyrroketone **37**) indicated the fully conjugated dipyrrin system had been formed and aqueous workup did not destroy it since the UV-visible absorptions almost had no

change. Mass spectrometry showed *m/z* peaks at 1279.4662 (MW+K) for pyrroketone **36**, which indicated the formation of dimer of dipyrromethene (Scheme 4.13).

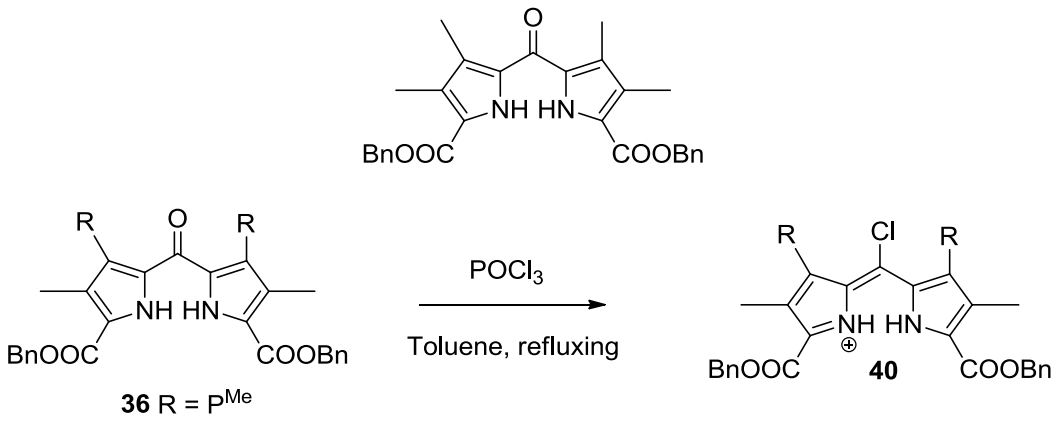

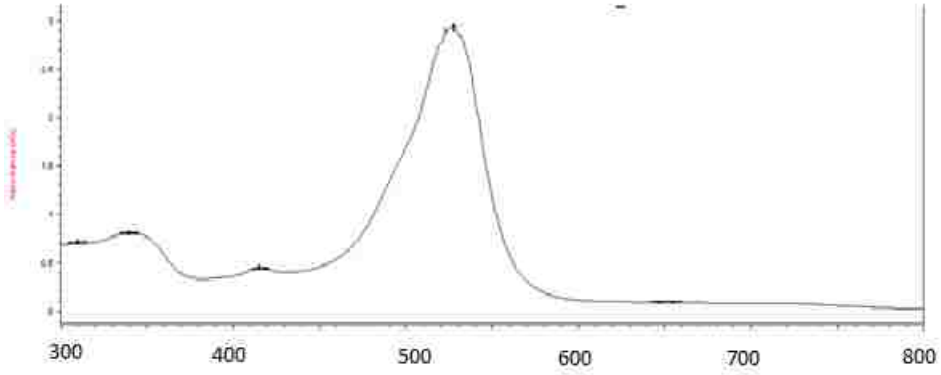

Scheme 4.12: Chlorination of pyrroketone **36** using $POCl_3$ and the UV-Visible absorption spectrum in CH_2Cl_2.

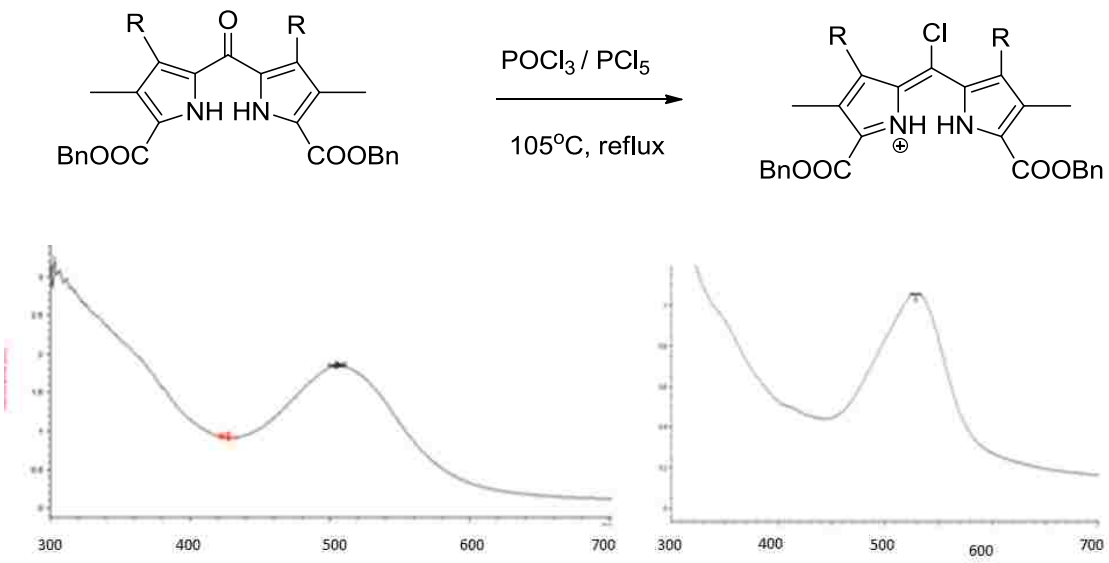

Scheme 4.13: Chlorination of pyrroketone **36** using POCl/PCl_5 and the UV-visible absorption spectrum in CH_2Cl_2.

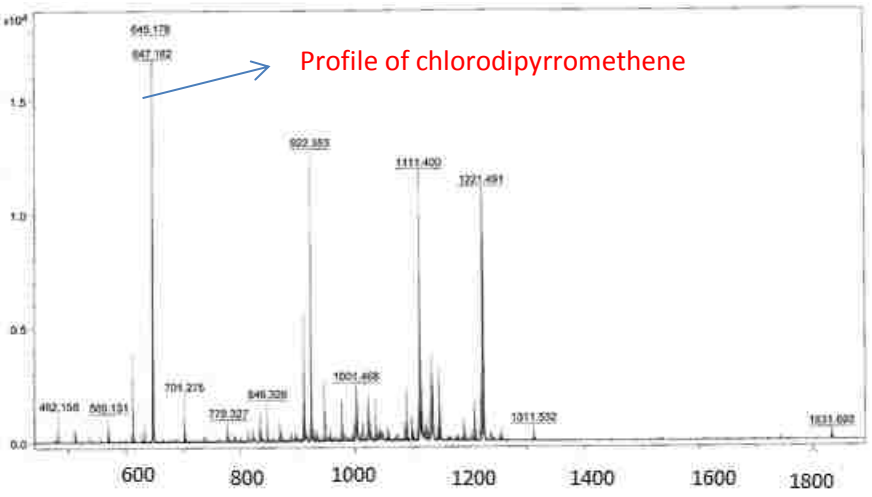

Figure 4.4: Mass spectrum of the product from chlorination of pyrroketone **36** with $POCl_3/PCl_5$.

The reactivity of various activiting reagents such acids, anhydrides and halogenating reagents on pyrroketones were investigated. Specifically, triflic anhydride can only partially convert pyrroketones into their dipyrryl system; soft halogenating reagents such as $SOCl_2$ have no reactivity. For strong chloronating reagents such as $POCl_3$ or PCl_5, the pyrroketones are completely converted into the fully conjugated dipyrrin intermediates or

products. However, these intermediates or products are not stable enough to survive aqueous workup, base treatment, or other nucleophiles. The combination of $POCl_3$ and PCl_5 transformed the pyrroketones into their dipyrrin, but this deduction is based only on its mass spectrum. From the chemistry of pyrroketones used in porphyrin synthesis, it is assumed that the electron-withdrawing benzyl ester groups on the pyrroketone destablize the conjugated intermediates which revert to starting material very easily upon attack of water or other nucleophiles (Scheme 4.14). Therefore, It was planned to eliminate the electron withdrawing group from pyrroles on the pyrroketones and use alkyl substituted pyrroketone to explore all these reactions. Extremely successful reactions with the dipyrroketone dibenzyl esters **36** and **37** are reported in Chapter 5 of this Dissertation.

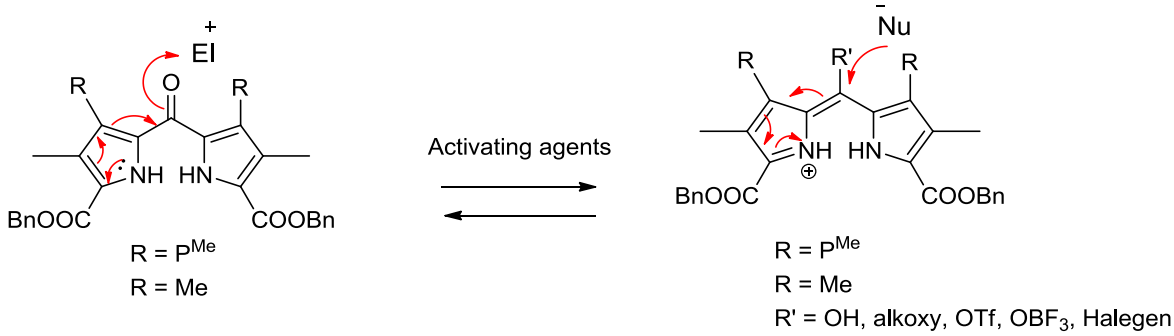

Scheme 4.14: The reversible process of pyrroketone and its dipyrromethene.

Before synthesis of the new alkylpyrroketones, several α-free pyrroles were made by the following methods depending on the structure of pyrroles (Scheme 4.15). (1) The 2-ethoxyl carbonyl pyrroles were converted into corresponding α-free pyrroles **44**, **45** and **46** by de-esterification under basic conditions.[47] (2) The 5-tert-butoxylcarbonylpyrrole **47** was transformed into α-free pyrrole **48** by de-esterification under acetic conditions.[48] (3) 5-Benzyl ester pyrroles **50** and **51** were debenzylated, followed by decarboxylation of all resultant carboxylic acids to make α-free pyrroles **48** and **52**. (4) 2-Ethoxylpyrrole **49** was

reduced to give the α-free pyrrole **48** using $LiAlH_4$ directly.[49] Specifically, α-free pyrroles **44**, **45** and **46** were made by refluxing pyrroles **41**, **42** and **43** using NaOH as base in ethylene glycol solvent at 180 ^oC, all with a yield around 30%. Pyrrole **48** was made by treatment of pyrrole **47** with TFA in 10% yield. Pyrroles **48** and **52** were made by debenzylation of pyrroles **50** and **51,** respectively**,** followed by decarboxylation with TFA. These reacxtions gave a yield around 30%. α-Free pyrrole **48** can also be obtained directly by reducing the ester group of α-free pyrrole to alkyl using $LiAlH_4$ in THF. Some α-free pyrroles were made in 2 or 3 steps by a combination of these methods. For example, pyrrole **44** was also made by de-esterification of pyrrole **53** followed by reduction of the acetyl group at the 3-position of pyrrole **54.** This two-step reaction actually gave a higher yield than the one step reaction using Method (1). Overall, de-esterification under basic conditions gave better yields than under acidic conditions, and reduction gave the best yield among all these condtions. All these compounds were characterized by ^1H NMR, ^{13}C NMR and HRMS (ESI). Usually the de-esterification causes the peaks of the ester to disappear from the ^1HNMR spectrum and the resultant α-free pyrrole shows a new 2-H peak around 6.30-6.50 ppm. These α-free pyrroles are not very stable in light or air; therefore, once synthesized, they were stored in the freezer or immediately used in the next step for syntheses of thioketones.

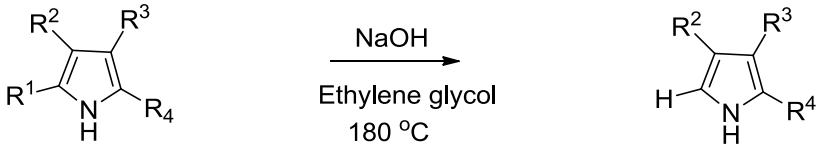

R^1 = COOEt, R^2 = R^4 = Me, R^3 = Et **41**
R^1 = COOEt, R^2 = R^4 = Me, R^3 = H **42**
R^1 = COOEt, R^2 = R^4 = Me, R^3 = n-Butyl **43**

R^2 = R^4 = Me, R^3 = Et 30% **44**
R^2 = R^4 = Me, R^3 = H 27% **45**
R^2 = R^4 = Me, R^3 = n-Butyl 43% **46**

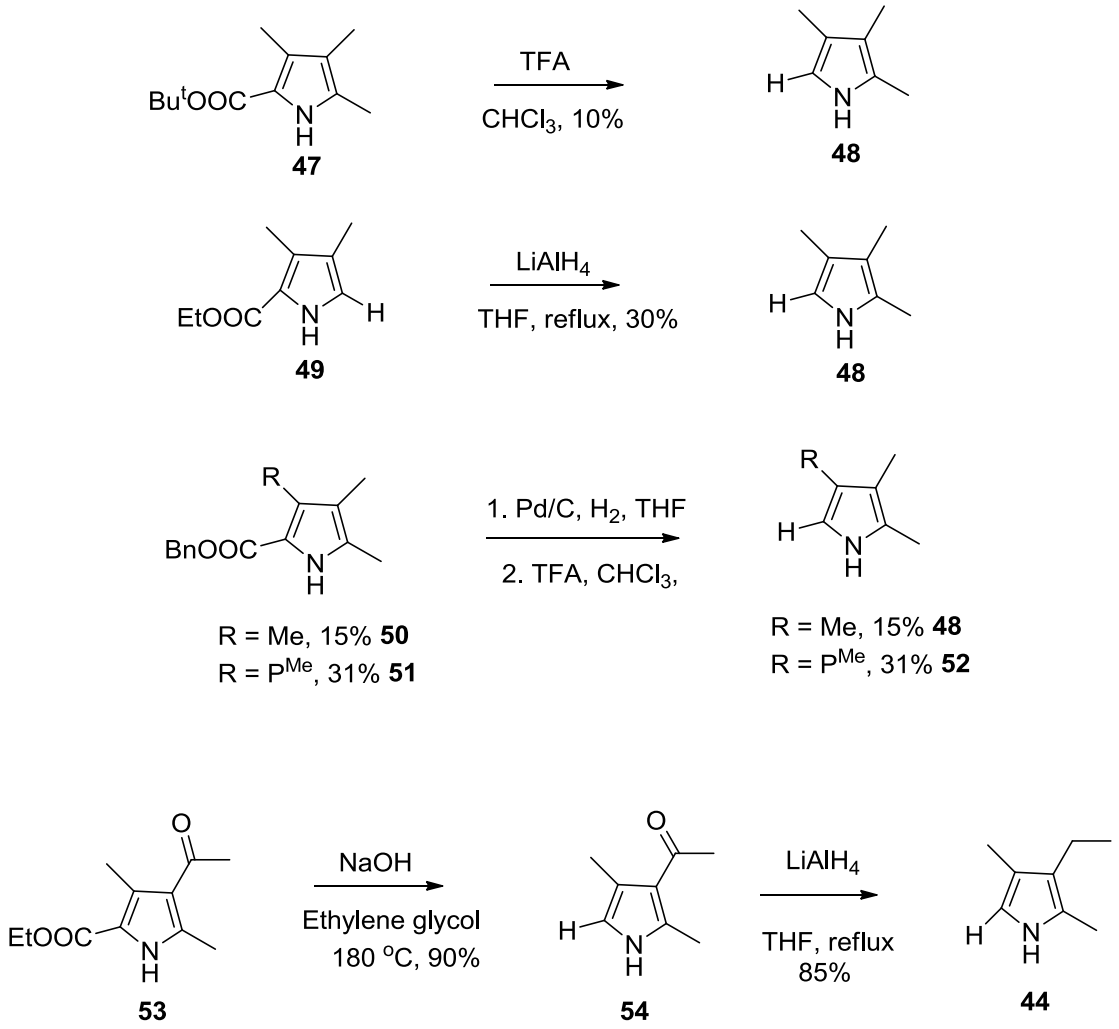

Scheme 4.15: Syntheses of α-free pyrroles from their precursors under various conditions.

Some of the α-free pyrroles **44-46** and **48** were used to synthesize dipyrrothiones (Scheme 4.16). Pyrroles **44**, **45**, **46** and **48** were treated with thiophosgene[20,50,51] in THF or ether at 0 °C; the reaction was monitored by TLC until starting material had disappeared. Then methanol was added to destroy excess thiophosgene. The residue was purified by silica gel column chromatography, eluting with toluene/chloroform (4/1) or hexane/ethyl acetate (4/1) to give an organge solid in about 40% yield. From ^{1}H NMR, the pyrrole α-H around 6.40 ppm disappeared, and the NH group of the product pyrrothiones exibited a huge downshift from 7.4 to 9.0 ppm compared with the α-free

pyrroles. The structures of the pyrrothiones **55** and **58** were comfired by their mass spectra, with peaks at *m/z* 289.1739 (MW+H) and 233.1106 (MW+H), respectively.

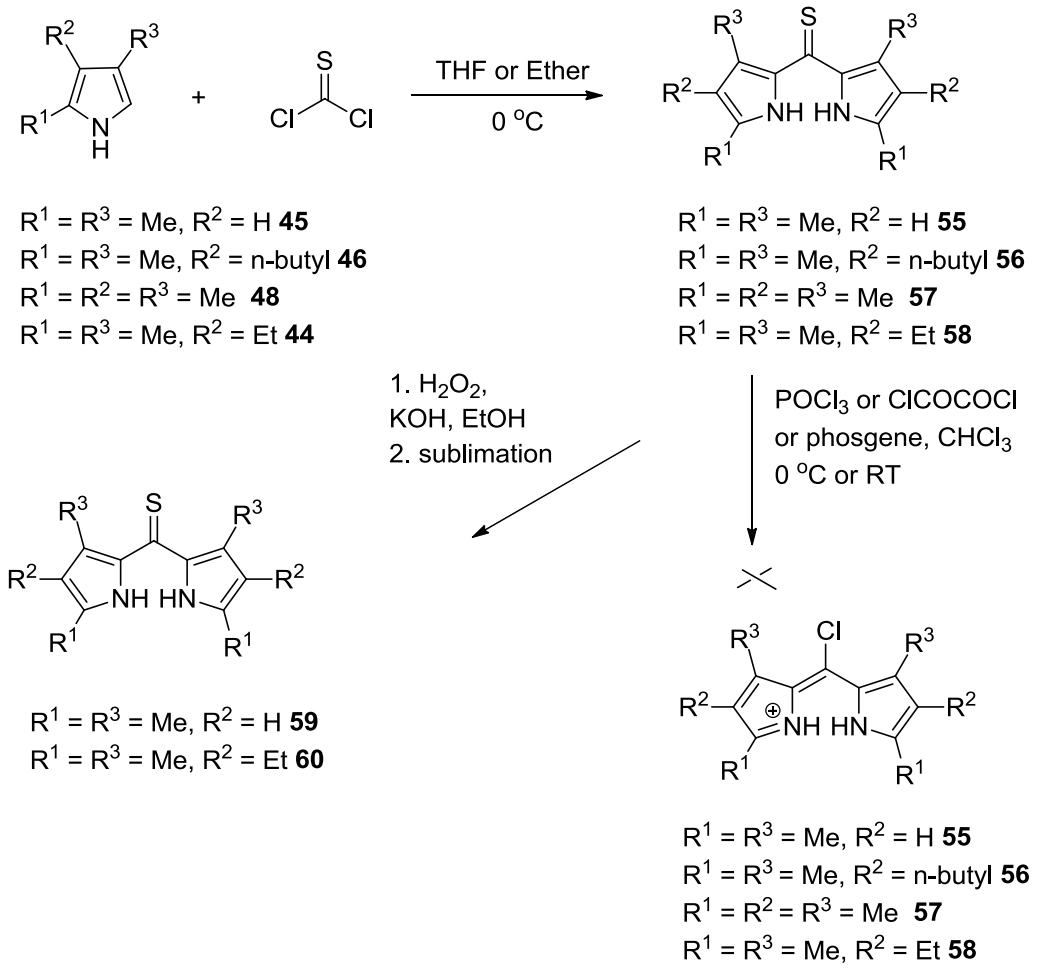

$R^1 = R^3 = Me, R^2 = H$ **45**
$R^1 = R^3 = Me, R^2 = n\text{-butyl}$ **46**
$R^1 = R^2 = R^3 = Me$ **48**
$R^1 = R^3 = Me, R^2 = Et$ **44**

$R^1 = R^3 = Me, R^2 = H$ **55**
$R^1 = R^3 = Me, R^2 = n\text{-butyl}$ **56**
$R^1 = R^2 = R^3 = Me$ **57**
$R^1 = R^3 = Me, R^2 = Et$ **58**

$R^1 = R^3 = Me, R^2 = H$ **59**
$R^1 = R^3 = Me, R^2 = Et$ **60**

$R^1 = R^3 = Me, R^2 = H$ **55**
$R^1 = R^3 = Me, R^2 = n\text{-butyl}$ **56**
$R^1 = R^2 = R^3 = Me$ **57**
$R^1 = R^3 = Me, R^2 = Et$ **58**

Scheme 4.16: Synthesis of pyrrothiones and pyrroketones.

During chlorination of thioketones with various chlorinating reagent such as $POCl_3$, oxalyl chloridfe or phosgene at room temperature, the solutions of these intermediates turned red upon addition of the chlorinating reagent but turned brown with time. Then the reaction was tried at 0 ^oC this also happened; low temperature can not prevent the color change. The reaction was monitored by UV-visible spectroscopy; the thiokeone **55** has an absorption at 421 nm, and the fully conjugated intermediate shifted to 500 nm after chlorination with phosgene in CH_2Cl_2. Similarly, thioketone **58** has an absorption at 437 nm and the intermediate shifted to 518 nm after chlorination with oxalyl chloride in

CH_2Cl_2. All these peaks disappeared with time, probably because the strong chlorinating reagents decomposed the thioketones. Since chlorination of thioketones failed to give chlorodipyrromethene, the thioketones were transformed into pyrroketones by using hydrogen peroxide under basic conditions. Analytically pure samples were purified by sublimition using a strong vaccum pump. The product sublimed around 220 ^{o}C. Compared with thioketones, the NH group is slightly shifted from about 9.00 to 8.50 ppm; the alkyl groups on thioketones have nearly same shift as do those of pyrroketones. These structures of the two pyrroketones were confirmed by mass spectra, with peaks at *m/z* 233.1334 and 273.2013, respectively.

From the previous experiments and discussion, pyrroketone with electron withdrawing group do not have significant reactivity toward acid and eletrophiles; therefore, It was dedided to try the same reactions on electron rich alky substituted pyrroketones. Therefore pyrroketone **59** was protonated by HCl gas in CH_2Cl_2. The solution turned yellow from colorless, and UV-visible spectroscopy showed a sharp peak at 428 nm compared with pyrroketone **59** which has an absorption around 341 nm (Figure 4.5). An attempt was made to convert the meso-hydroxydipyrromethene system into a BODIPY using DIEA/BF3.OEt2 (Scheme 4.17). Unfortunately, the intermediates were not stable upon treatment with the organic base, DIEA, and they reverted to the starting material pyrroketone by deprotanation. Then pyrroketones **59** and **60** were subjected to treatrment with DIEA/BF_3.OEt_2 directly, and sharp peaks at 466 and 476 nm (Figure 4.6), respectively,were observed in the UV-visible spectra (Figure 4.5). Purification was still problematic using a chromatography column. But isolation of product **62** was confirmed by its mass spectrum with *m/z* at 338.3426. Since pyrroketones can be protonated into their meso-hydroxydipyrromethene salt, it is very likely they can also be converted into similar intermediates by electrophiles.

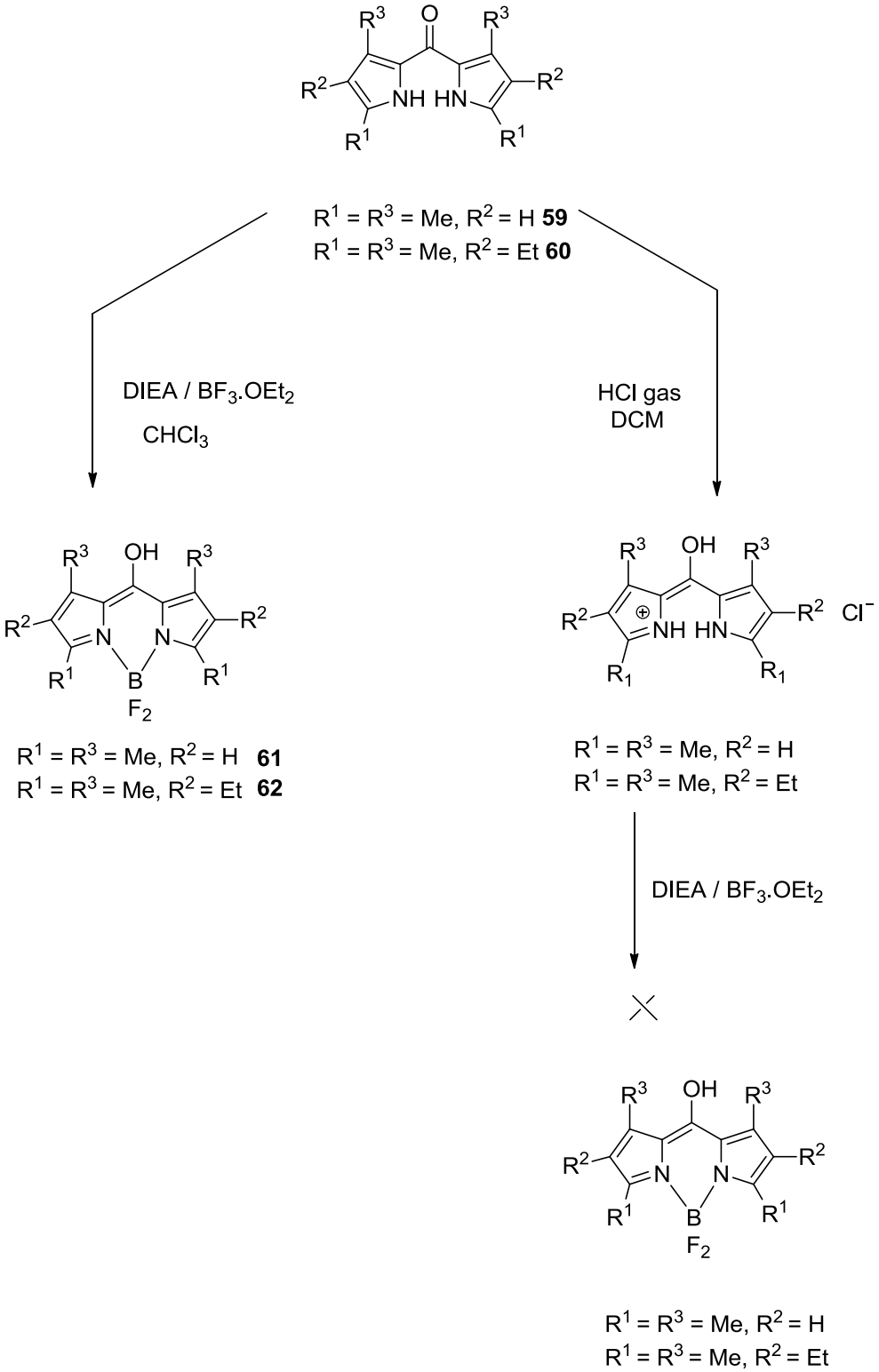

Scheme 4.17: Attempts to synthesize meso-hydroxy BODIPY.

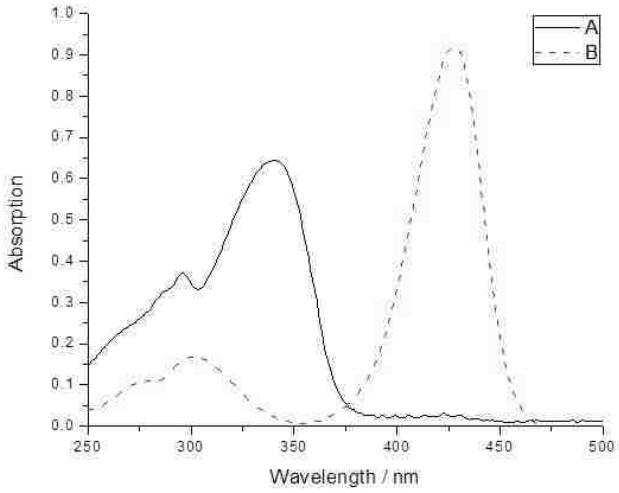

Figure 4.5: Optical spectra in CH_2Cl_2 of dipyrrylketone (A) and salt (B) after treatment with HCl(g).

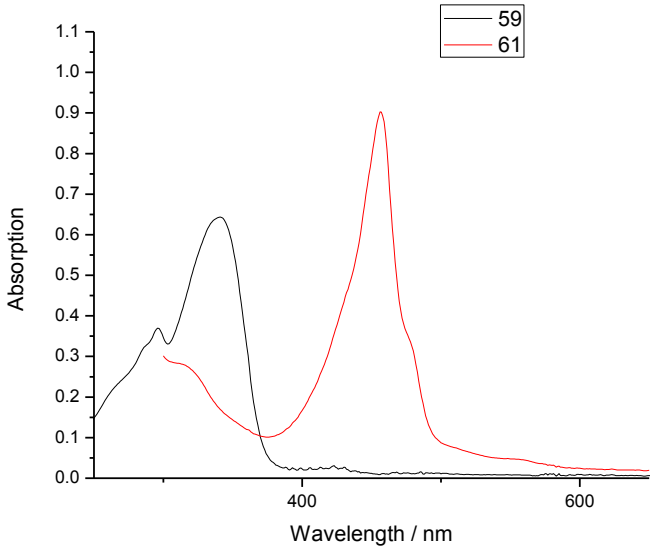

Figure 4.6: The Abosorption spectra of pyrroketone **59** and its corresponding BODIPY **61** in CH_2Cl_2.

Therefore reactions with Meerwein's reagent Et_3OBF_4 were attempted (Scheme 4.18). Pyrroketones **59** and **60** were treated with Et_3OBF_4[52] in $CHCl_3$. and a red solution resulted, indicating the presence of fully conjugated dipyrrin system; this was confirmed

by UV-visible spectroscopy, showing peaks at 438 and 451 nm, repectively. The solution was washed with water and saturated $NaHCO_3$ and the intermediates were not destroyed or decolorized according to their UV-visible spectra.

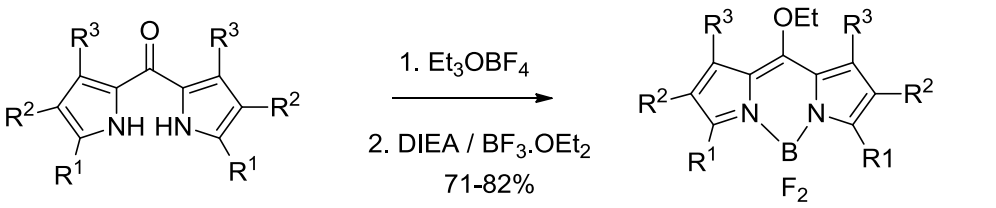

$R^1 = R^3 = Me$, $R^2 = H$ **59**
$R^1 = R^3 = Me$, $R^2 = Et$ **60**

$R^1 = R^3 = Me$, $R^2 = H$ **63**
$R^1 = R^3 = Me$, $R^2 = Et$ **64**

Scheme 4.18: Reaction of pyrroketones with Meerwein's salt in $CHCl_3$.

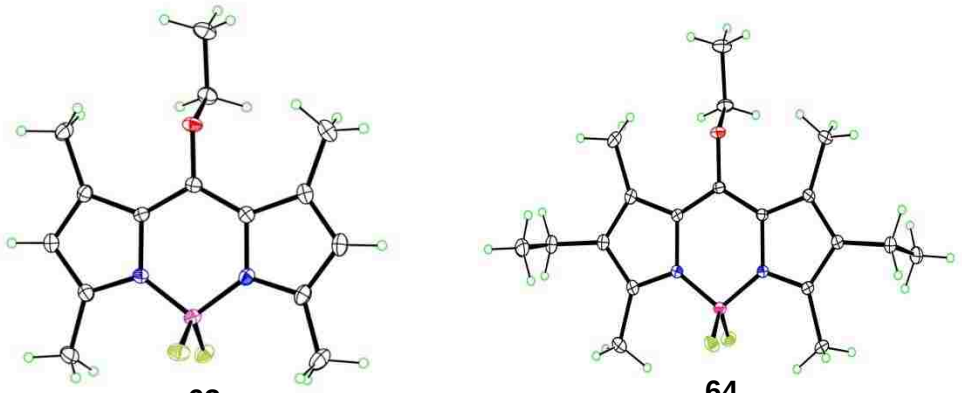

63 **64**

Figure 4.7: Crystal structures of BODIPY **63** and **64**.

These new intermediates were treated with DIEA/BF_3OEt_2 in $CHCl_3$ to give the corresponding BODIPYs. BODIPY **63** has an absorption maximum at 487 nm and BODIPY **64** has its absorption at 508 nm. Characteristic resonances for the ethoxy group in their ^1H NMR spectra appeared at 4.12 (q) and and 1.52 (t) ppm The X-ray structures for both BODIPYs **63** and **64** were also obtained (Figure 4.7). The molecule **63** has very nearly C_s symmetry, with the BF_2 plane and dipyrryl plane forming a dihedral angle of 89.37(4)^o, with the atoms of the OEt group lying a mean of 0.012 Å from the BF_2

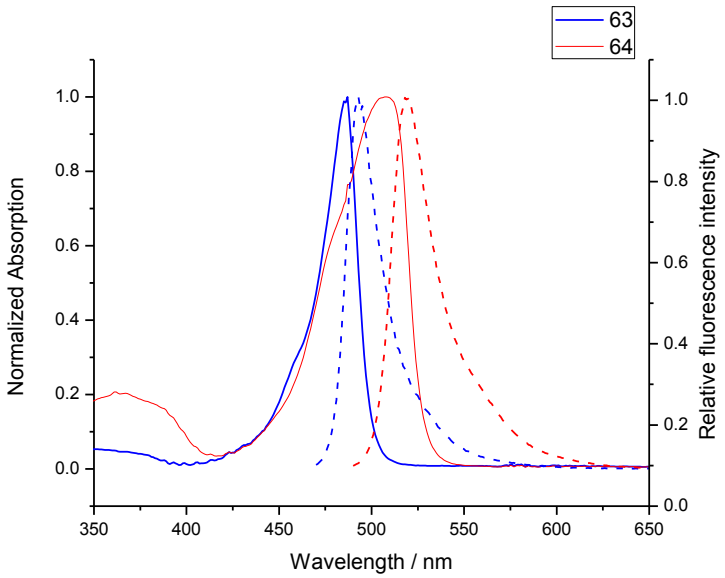

Figure 4.8: Normalized aborption and fluorescence spectra of BODIPYs **63** and **64** in CH_2Cl_2.

plane; BODIPY **64** has a similar structure, with dihedral angle 88.68(1)^o, but the dipyrryl ethyl groups are *anti* related to each other. Their nomalized absorption and fluorescence were also studied and showed in Figure 4.8. The spectra of these two BODIPYs are of comparable shape to those already described in the literature with a narrow absorption band around 500 nm (which belongs to S^0-S^1 transition) plus a weak broad absorption around 460 nm. The two BODIPYs also have a slightly shifted sharp emission bands at 493 and 518 nm, respectively, with a mirror image shape compared to the absorption spectra.

Next, chlorination of pyrroketones **59** and **60** was attempted using phosgene in CH_2Cl_2 (Scheme 4.19). Pyrroketone **59** and **60** were dissolved in $CHCl_3$ and treated with phosgene solution in toluene. The solution turned red with time and the UV-visible spectra showed peaks at 485 and 505 nm (Figure 4.9). Then nitrogen gas was passed

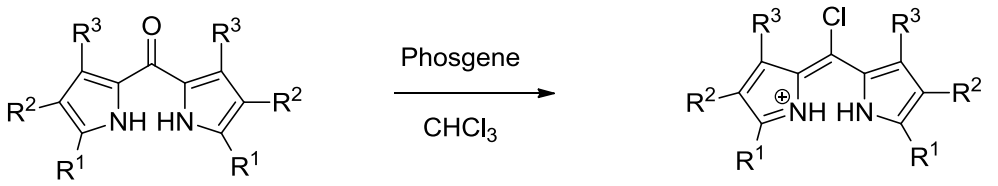

$R^1 = R^3 = Me, R^2 = H$ **59**
$R^1 = R^3 = Me, R^2 = Et$ **60**

$R^1 = R^3 = Me, R^2 = H$ **65**
$R^1 = R^3 = Me, R^2 = Et$ **66**

Scheme 4.19: Chlorination of pyrroketone using phosgene.

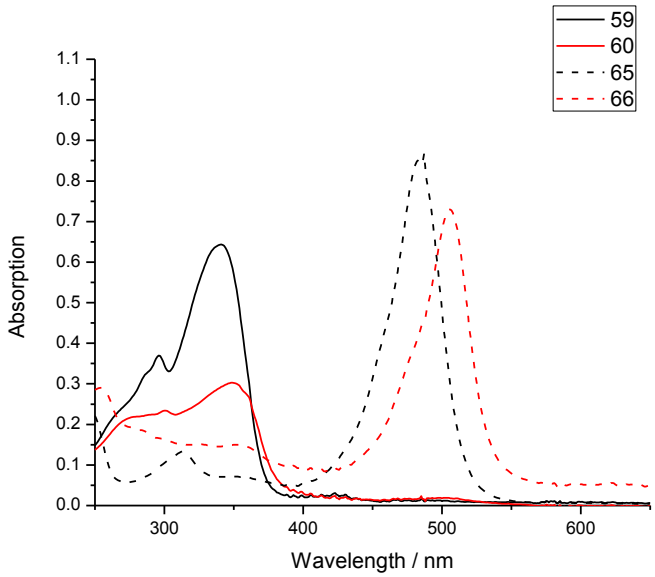

Figure 4.9: Absorption spectra of pyrroketones and their meso-chlorodipyrrins in CH_2Cl_2.

through solution to purge excess phosgene into a $NaHCO_3$ solution. The products **65** and **66** were crystallized from CH_2Cl_2/petroleum ether system as red solids in about 90% yield. The most noticeable change in the ^1H NMR spectrs is the downfield shift of the NH group, which is shifted from around 8.60 ppm to 12.50 and 12.93 ppm for dipyrromethenes **65** and **66**. The identity of the products was also comfirmed by mass spectroscopy, with *m/z* at 235.0992 and 291.1623, respectively. Figure 4.8 shows the UV-visible changes during chlorination.

The chlorination of pyrroketone was explored first by Fisher[53] in 1933. However, very little work has been done with chlorodipyrromethene. Therefore, we explored several electrophilic substitution reactions and some coupling reactions using chloro-dipyrromethene to investigate their reactivities.

Chlorodipyrromethene **65** was used as the substrate and several replacement (addition-elimination) reactions were explored (Scheme 4.20). The first one attempted was with the Grignard reagent EtMgBr. From the resulting mass spectra, both meso-ethyl dipyromethene **67** and meso-free dipyrromethene **68** were obtained when **65** was treated with EtMgBr. However, It was difficult to separate these two products using silica gel column chromatography. Therefore, they were converted into the corresponding BODIPYs by complexation with $BF_3.OEt_2$ using DIEA as base. The two resulting BODIPYs **69** and **70** were easily separated with CH_2Cl_2/hexane as eluting system on a silica gel column. Meso-free BODIPY was found to be the major product in 47% yield, and the expected ethyl-substituted product was obtained as the minor product in only 17% yield. From the ^1H NMR spectra, the meso-ethyl group of BODIPY **69** appeared at 3.02 ppm (q) and the meso-H of BODIPY **70** appeared at 7.02 ppm. The structures of these two BODIPYs were also comfirmed by mass spectroscopy with *m/z* at 276.1713 and 248.1404, respectively.

Addition/elimination reactions using sodium methoxide were also tried on chlorodipyrromethene **65**; instead of giving the meso-methoxy dipyrromethene **71**, the product was found to be α-methyl ester pyrrole **72**. Sodium ethoxide was also used to test if the reaction was reproducible, and once again α-ethyl ester pyrrole **73** was the product; the structures of these two unexpected pyrroles were also confirmed by their crystal structures. A possible mechanism for their formation is proposed in Scheme 4.21. This involves the addition of the the meso-chloro of the meso-dipyrromethene to give a methoxy intermediate, which re-aromatized into meso-alkoxy dipyrromethene through

elimination of chloride (the better leaving group), followed by attack of alkoxide to form 5,5-dimethoxydipyrromehtane intermediate. This then undergoes a base-catalyzed version of the already known pyrrole and very facile deacylation reaction to give the unexpected pyrroles **72** or **73**; the overall mechanism involves a dipyrrole cleavage reaction.

Replacement reactions by weak nucleophiles such TBAF and KCN were attempted but did not work. For coupling reactions, Suzuki and stille coupling reactions were attempted on chlorodipyrromethene but they failed to give the expected products.

Since chlorodipyrromethenes seemed unstable and products from them were difficult to separate, they were converted into their BODIPYs which are more stable and more easy to isolate. Chlorodipyrromethene **74** and **75** were treated with DIEA/BF_3.OEt_2 and their BODIPYs (Scheme 4.22) showed about a 20 nm red-shifted UV-visible absorption at 503 and 527 nm (Figure 4.10) compared with the starting materials at 485 and 505 nm, respectively. Both showed a small shoulder at 460 nm in their UV/visible absorption spectra. The structures of the products were confirmed by mass spectroscopy, with peaks at *m/z* 282.1010 and 319.1550 (MW – F) for BODIPYs **74** and **75**, respectively. Single crystals suitable for X-ray structure analysis were obtained for both 8-chloro-BODIPYs **74** and **75** (Figure 4.11). The non-hydrogen atoms. except for fluorine in **74**, are fairly coplanar, with mean deviation 0.052 Å, and the BF_2 plane is nearly orthogonal to it, with dihedral angle 89.88(2)^o. Compound **75** has three molecules in the asymmetric unit, two of which have the ethyl groups related *syn*, and one with *anti* ethyls, Analogous dihedral angles in the three molecules are in the range 88.45(2)-89.37(2)°.

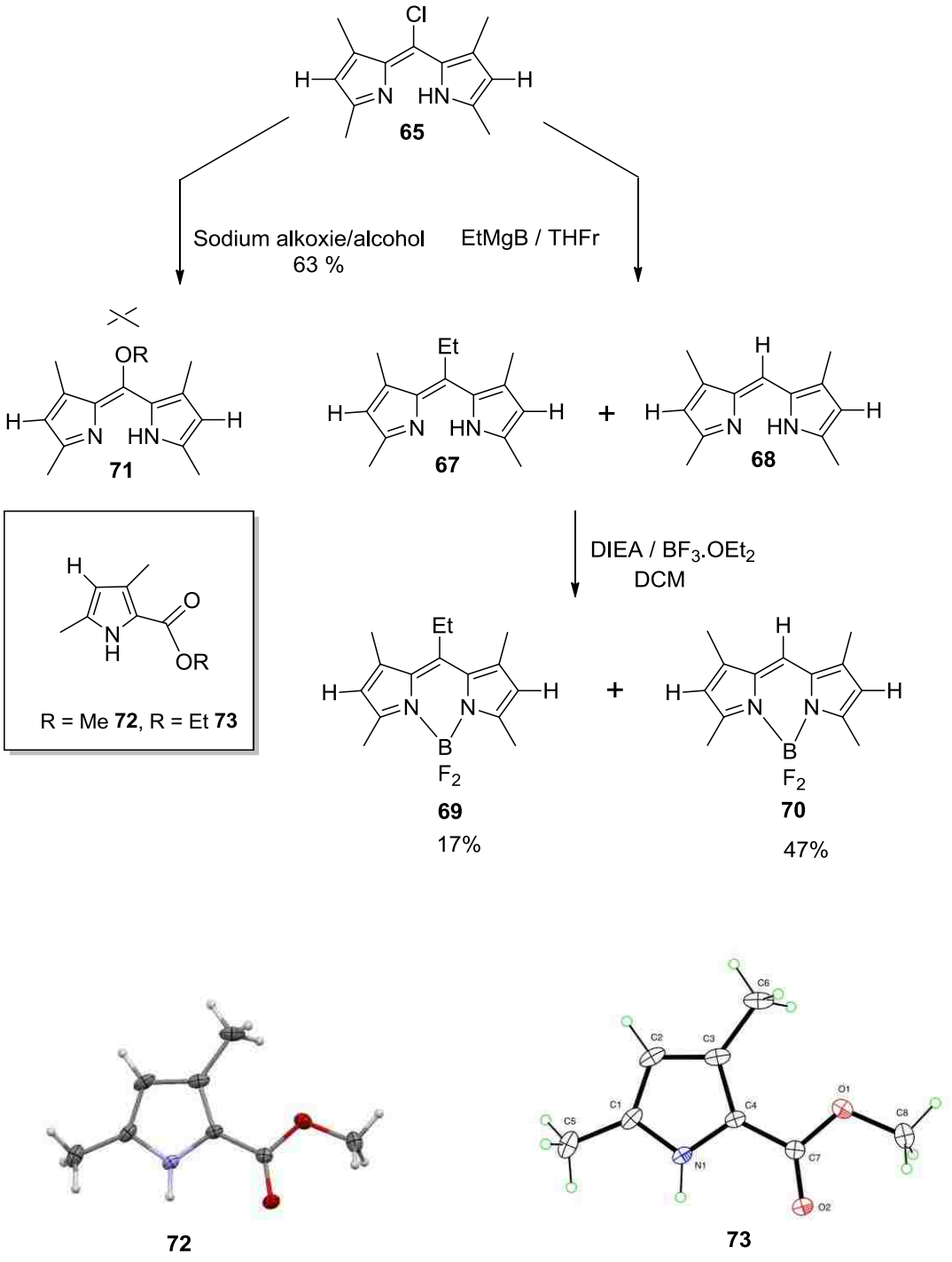

Scheme 4.20: Investigation of reactivity of meso-chloro dipyrromethene and X-ray Crystal structure of unexpected pyrroles **72** and **73**.

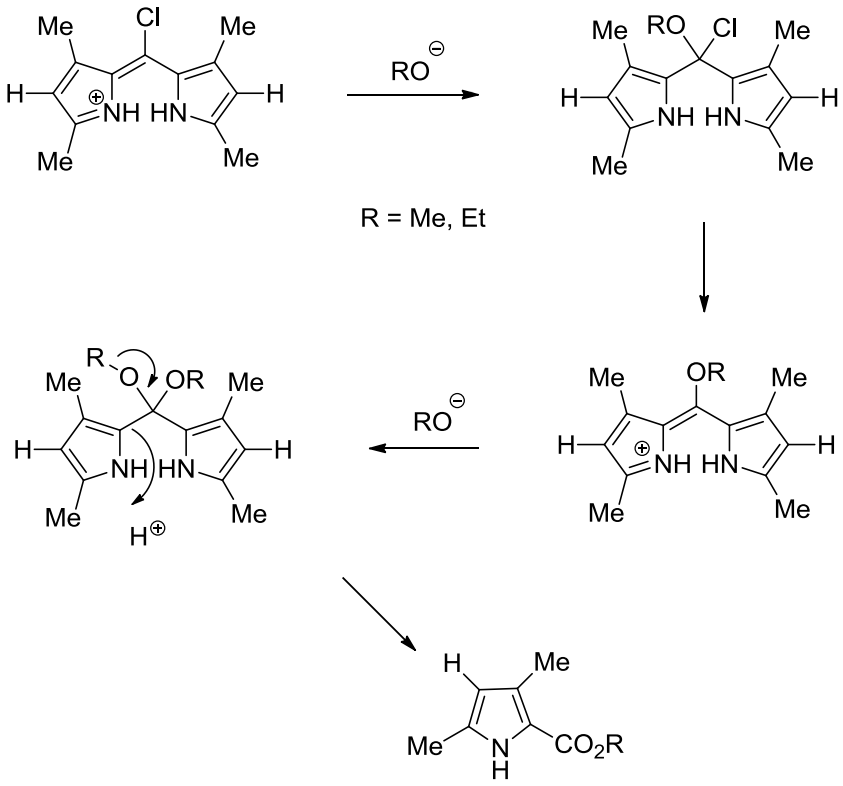

Scheme 4.21: Proposed mechanism for cleavage of meso-chlorodipyrromethene by alkoxide.

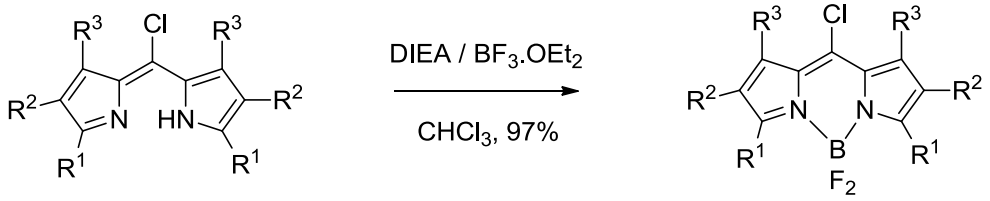

$R^1 = R^3 = Me$, $R^2 = H$ **65**
$R^1 = R^3 = Me$, $R^2 = Et$ **66**

$R^1 = R^3 = Me$, $R^2 = H$ **74**
$R^1 = R^3 = Me$, $R^2 = Et$ **75**

Scheme 4.22: Synthesis of meso-chloro BODIPYs.

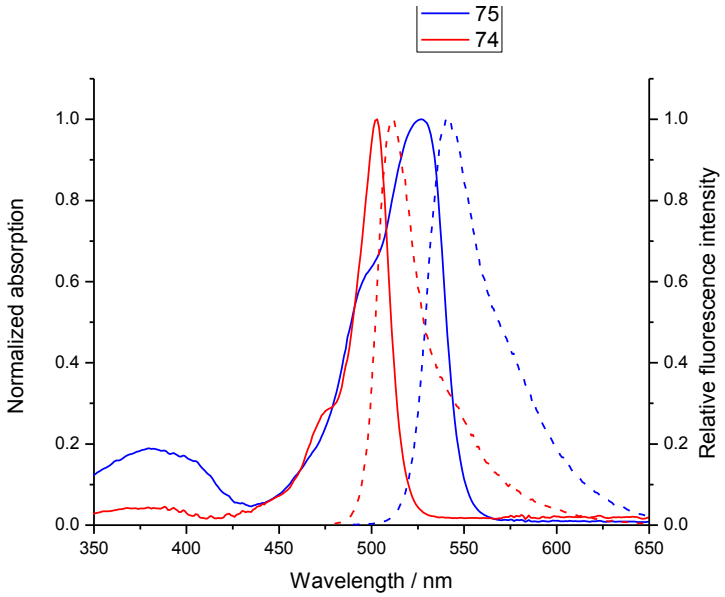

Figure 4.10: Normalized absorption and relative fluorescence spectra, in CH_2Cl_2 of chloro-BODIPYs.

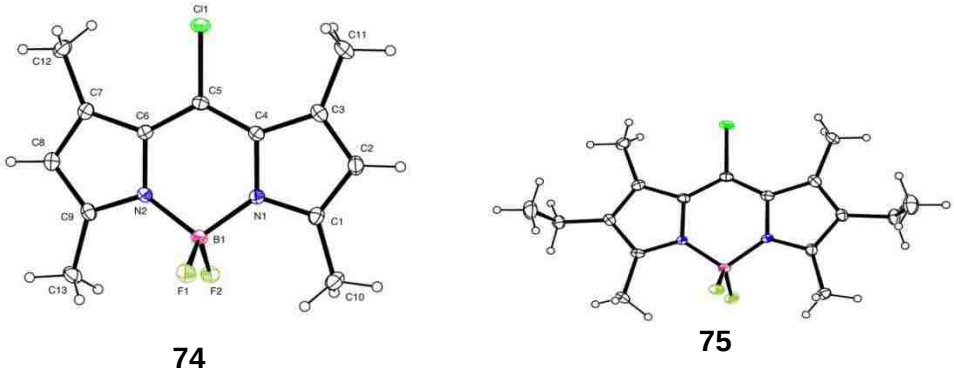

74 **75**

Figure 4.11: Chrystal structures of meso-chloro BODIPYs **74** and **75**.

The same addition/elimination reactions were tried on BODIPY **74** (Scheme 4.23). A solution of EtMgBr[24] in THF was added at -78 ^{o}C and also at room temperature and the two reactions gave different products. The replacement reaction only took place at the meso-position without effecting the fluorides on the boron to give product **69** in a 75% yield at low temperature. However, at room temperature,[7,22] all the halogens, including the two B-F groups were replaced by EtMgBr to give the fully substituted product **76** in

83% yield. Both BODIPYs **69** and **76** have characteristic UV-visible absorptions at 499 nm and *m/z* at 276.1713 and 296.2507, respectively. The ^{1}H NMR spectra of BODIPYs **69** and **76** showed the characteristic 8-ethyl protons at 3.02 (q) and 1.32 (t) ppm, respectively; the B-ethyl protons of BODIPY **76** appeared at 0.79 and 0.30 ppm.

The replacement reaction with the oxygen-centered nucleophile[25] sodium methoxide was performed both at room temperature and under reflux at 80 ^{o}C (Scheme 4.23); both conditions gave mixtures of meso-substituted and boron-substituted products but in different percentages. At room temperature, displacement of meso-chlorine ocurred rapidly to give the major product **77**, and one of the boron florines was also displaced with extended reaction times to give the minor product **78**. If the same reaction was performed at reflux with exess sodium methoxide, the fully substituted product **79** was obtained as the major product. The B-monomethoxy product **78** was found to be the minor product. The ^{1}H NMR spectra of BODIPYs **77**, **78** and **79** showed the 8-OMe protons as a singlet around 3.97 ppm, while the B-OMe protons of **78** and **79** appeared at around 2.89 ppm. All three methoxy substituted products were structurally confirmed by mass spectroscopy with *m/z* at 278.1504 for **77**, 259.1392(MW-F) for **78**, and 324.1719 (MW-OMe) for BODIPY **79**.

The same reaction was carried out with sodium ethoxide to compare with the yield of alkylation of pyrroketones with Meerweit's reagents. The replacement reaction gave a slightly lower yield (46-52%) compared with when Meerwein's reagent was used. Another oxygen-centered nucleophile, sodium phenoxide, was also tried using BODIPY **74**, and the reaction gave the expected product **80** in 81% yield. The aromatic phenoxy group has resonances around 6.99-7.33 ppm in the ^{1}HNMR spectrum, and mass spectroscopy showed a *m/z* at 340.1662. The normalized absorption and fluorescence spectra are shown in Figure 12. All these BODIPYs absorption/emission spectra have a similar shape to the BODIPYs described in the literature with a sharp absorption peak

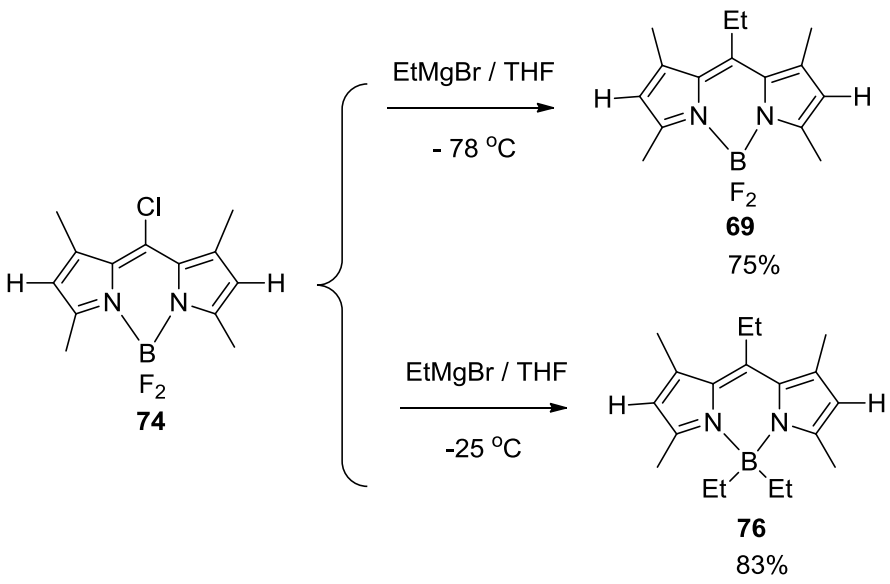
EtMgBr / THF
- 78 °C
EtMgBr / THF
-25 °C
Et
Cl
H
N
B
F2
74
69
75%
76
83%

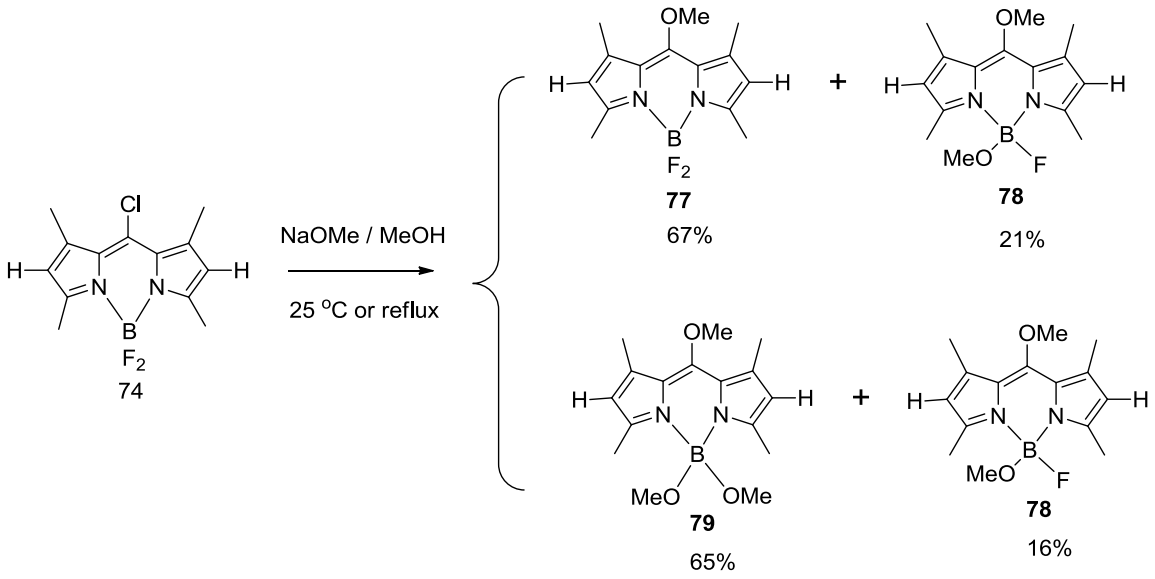
NaOMe / MeOH
25 °C or reflux
OMe
MeO
F
OMe
77
67%
78
21%
79
65%
78
16%
74

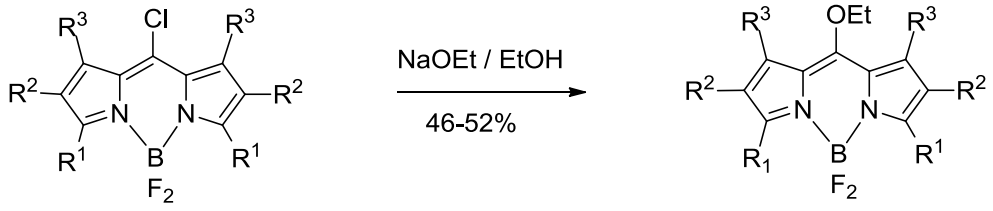
NaOEt / EtOH
46-52%
R1 = R3 = Me, R2 = H 74
R1 = R3 = Me, R2 = Et 75
R1 = R3 = Me, R2 = H 63
R1 = R3 = Me, R2 = Et 64

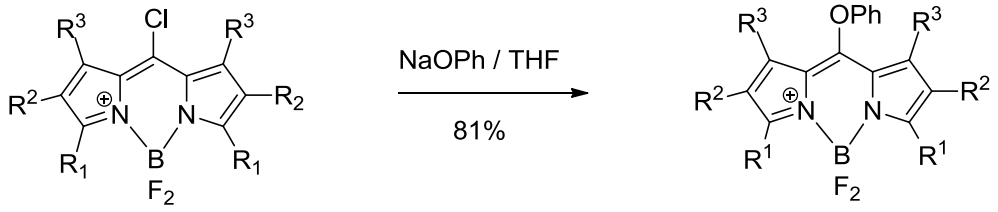

$R^1 = R^3 = Me$, $R^2 = H$ **74**

$R^1 = R^3 = Me$, $R^2 = H$ **80**

Scheme 4.23: Replacement reactions of meso-chloroBODIPY by various nucleophiles.

around 500 nm and a small shoulder around 460 nm, (Figure 4.12). Compared with the starting material, meso-chloroBODIPY, substitution by an alkoxy group caused a blue shift of 12-16 nm, and alkyl substitution gave the BODIPY a mirror blue shift of 4 nm. Their emission bands are slightly shifted to long wavelength as a mirror image with around a 10 nm Stokes shift.

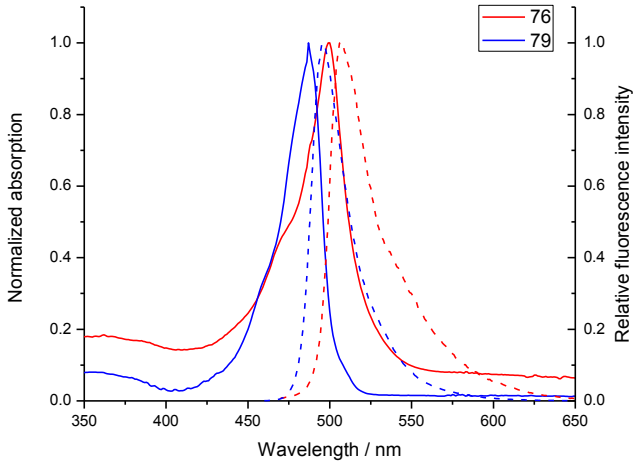

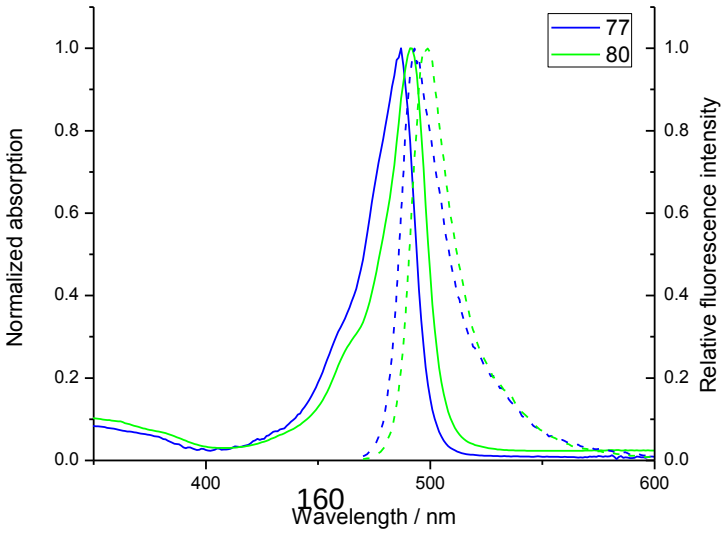

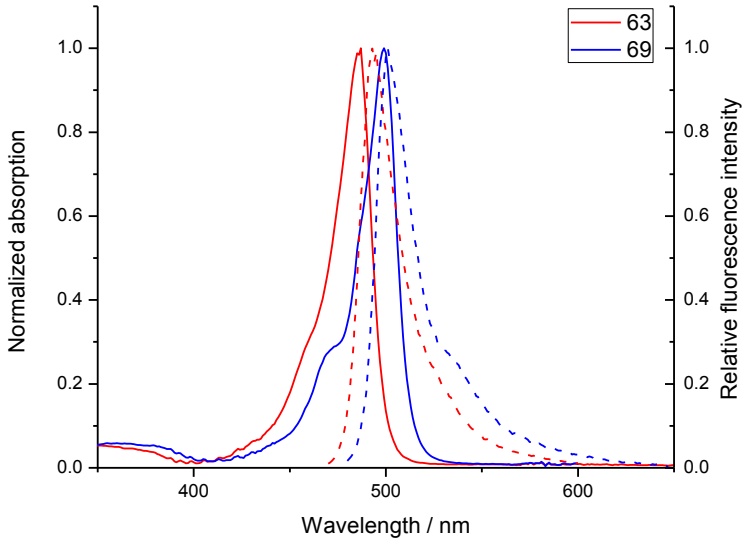

Figure 4.12: Normalized absorption and relative fluorescence spectra of BODIPYs **63**, **69**, **76**, **77**, **79** and **80** in CH_2Cl_2.

Three sulfur nucleophiles[54] (Scheme 4.24) were also reacted with BODIPY **74**. Typically a solution of chloroBODIPY **74** and sulfur nucleophile in THF was stirred in the presence of K_2CO_3 as base at room temperature and gave a very good yield of products. With 2-mercaptobenzothiozole, the reaction gave BODIPY **81** in 56% yield, while 1-mercaptomethyl-*p*-carborane gave **82** in 92% yield and SH-1,2-carborane gave BODIPY **83** in 90% yield. One nitrogen-centered nucleophile, propargyl amine, was investigated using chloroBODIPY **74**. The reaction gave BODIPY **83** in 92% yield with excess propargyl amine as base.

BODIPYs **81, 82** and **83** showed red-shifted UV-visible absorptions at 539 and 529 and 554 nm, respectively, (Figure 4.13). Amine-substituted BODIPY **83** showed a blue shift from 503 to 458 nm compared with the starting material **74**. In the ^{1}H NMR spectrum of BODIPY **81**, the aromatic protons appear at 7.28-7.98 ppm and BODIPY **82** has the SC*H*$_2$ protons at 2.95 ppm; BODIPY **84** has chemical shift at 5.25 for the amine group

and 2.47 for the ethynyl group. Mass spectroscopy confirmed the structure of BODIPYs **81**, **82** and **83** with *m/z* at 394.1019 (MW-F), 437.3033 and 423.2571, respectively. BODIPYs **81**, **82** and **83** were characterized by X-ray crystallography (Figure 4.14). In BODIPY **81**, the dipyrryl and BF_2 planes form a dihedral angle of 88.03(7)^o, while the mercaptobenzothiazole plane forms a dihedral angle of 77.03(2)^o with the dipyrryl unit. In BODIPY **82**, the dipyrryl and BF_2 planes form a dihedral angle of 88.8 (1)°, the linkage between dipyrryl and p-carborane is extended, with a C-S-CH_2-C torsion angle of

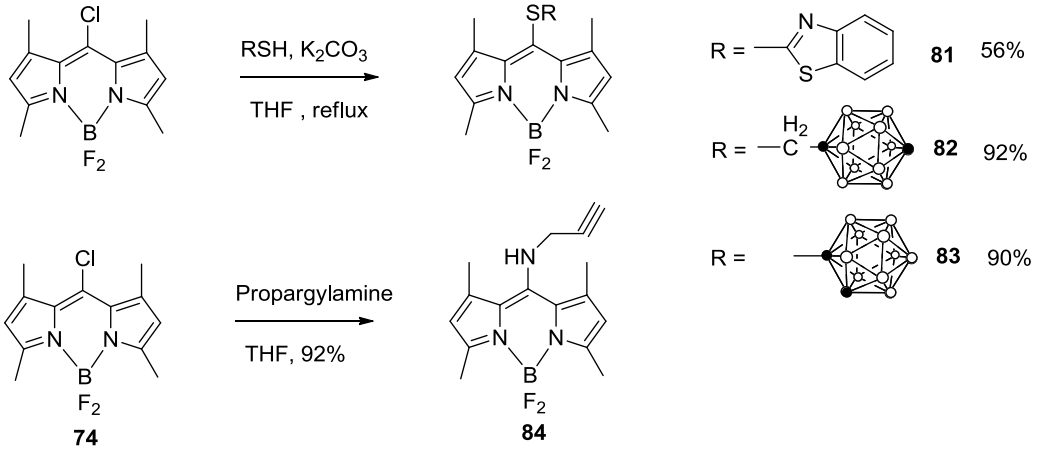

Scheme 4.24: The replacement reactons of meso-chloroBODIPY by sulfur and nitrogen centered nucleophiles.

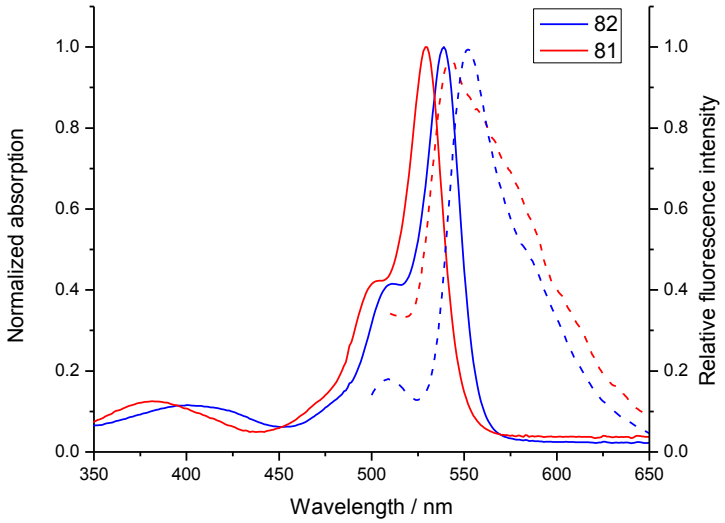

Figure 4.13: Normalized absorption and relative fluorescence intensity of BODIPYs **81** and **82** in CH_2Cl_2.

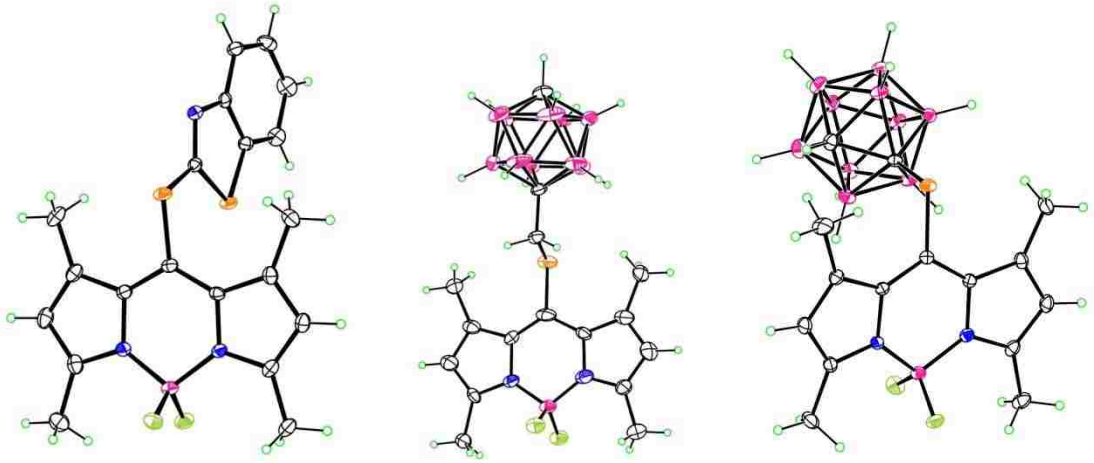

81 **82** **83**

Figure 4.14: The crystal structures of BODIPYs **81-83**.

175.3(6)^o. The best plane of the CSCC linkage forms a dihedral angle of 83.8(2)^o with the dipyrryl plane.

Replacement reactions with Grignard reagents[7,55] such as phenyl magnesium bromide, vinyl magnesium bromide and phenyethynyl magnesium bromide were attempted in order to introduce meso-phenyl, vinyl or phenylenthynyl substitutents into the BODIPYs. However, all these reagents were unreactive toward meso-chloroBODIPY with used with only one equivalent. Excess of these reagents quenched the fluorescence of chloroBODIPY. Once heated, the BODIPY would precipitate immediately and there were some TLC spots appearing under short wavelength UV light. Some weak nucleophiles such as TBAF and KCN were also investigated using chloroBODIPY, but they did not react either.

Pd(0)-catalyzed cross-coupling procedures with BODIPYs have been well explored, including use of the Suzuki,[56] Stille,[57] Heck[58] and Sonogoshira[59] reactions. These transformations have been performed either directly on the BODIPY core[30,60,61] or on a substituent,[26] and have largely facilitated the functionalization of BODIPYs. In particular coupling reactions of 3,5-dichloro-BODIPYs afforded many sophisticated products.[60] Compared with the 3,5-positions, the *meso*-carbon is more electrophilic based on their vibration structures and Mulliken-charge analysis on the core carbon atoms of tetramethyl-BODIPY.[13] Recently, various Pd(0)-catalyzed cross-coupling reactions were performed on 8-halo-BODIPYs.[21] We also attempted numerous coupling reactions of BODIPYs with intention to provide more a versatile functionalization access to new BODIPYs.

The Suzuki coupling reaction[56,62-65] was attempted first. ChloroBODIPY **74** was coupled with phenylboronic acid using $Pd(PPh_3)_4$ as catalyst and K_2CO_3 as base (Scheme 4.25). The mixture was heated under refux in DME or THF for 24 hours and monitored using UV-visible spectroscopy and TLC. The starting material disappeared with time and several new peaks appeared in the UV-visible spectra around 500 nm in CH_2Cl_2, indicating a mixture of products. The expected product, meso-phenyl BODIPY **85** was separated as the major fraction in 46% yield. ^{1}H NMR spectroscopy showed the expected aromatic area at 7.27-7.49 nm, which is consistent with literature reports and the structure of the product was also confirmed by its mass spectrum with *m/z* at 324.1717. Another two fractions were also separated upon chromatography, which were found to be meso-phenoxy-BODIPY **80** and the meso-free BODIPY **70**. The mechanism of formation of the meso-phenoxy BODIPY is still under investigation, and all data are identical with those from the replacement reaction with sodium phenoxide. The ^{1}H NMR spectrum of meso-free BODIPY is also identical with that from the replacement reaction when a Grignard reagent is used. Some alkyl boronic acids such as methyl, ethyl,

isopropyl, and vinyl boronic acid were also used. However, only meso-free BODIPY was separated and the starting material was still the major fraction. The reaction was also tried under microwave conditions but again did not work. This is probably due to the fact that these boronic acids have a small organic part compared with phenyl boronic acid.

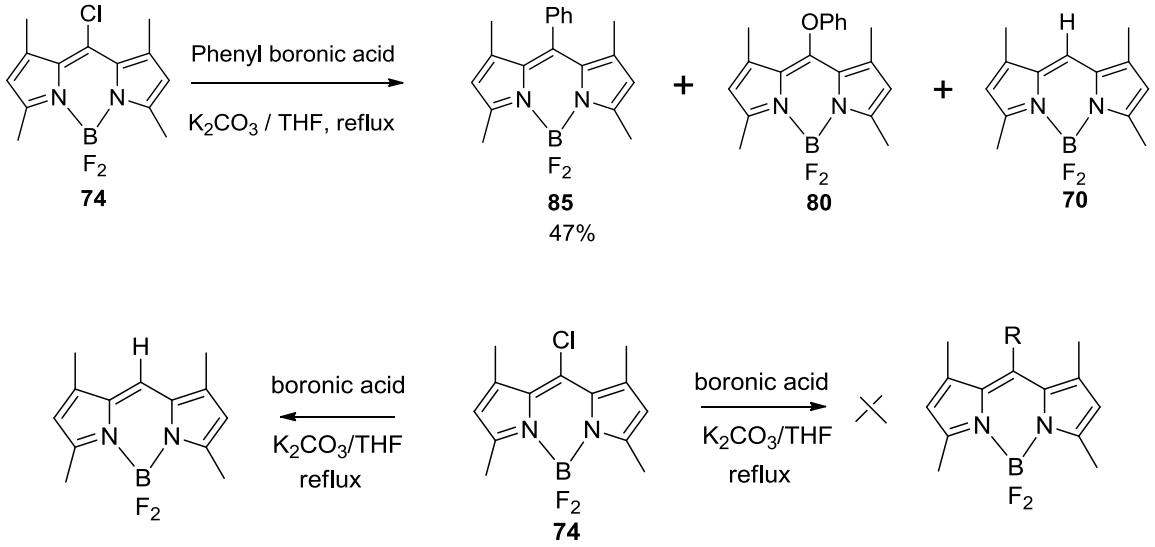

Boronic acid: $CH_3B(OH)_2$, $CH_3CH_2B(OH)_2$, $CH_2=CHB(OH)_2$

Scheme 4.25: Suzuki coupling reactions of BODIPY **74** with boronic acids.

The Sonogashira coupling reacton[66-68] of ethylnyltrimethylsilane with chloroBODIPY **74** catalyzed by $PdCl_2(PPh_3)_2$ was performed under standard conditions with TEA as base (Scheme 4.26). The mixture was refluxed in THF for about 24 hours and the reaction was monitored by TLC and UV-visible spectroscopy. The reaction resulted a very obvious color change caused by the product which has about a 40 nm red shift compared with the starting material. The separation of product was problematic using silica gel column chromatography. Separation was achieved later using a peptic TLC plate to give about a 35% yield of product **86** with UV/visible absorption at 544 nm in CH_2Cl_2. A similar compound was also recently synthesized by conventional methods using an alkynyl aldehyde as electrophile.[69] In the replacement reaction, Grignard

reagents did not work on chloroBODIPYs, so a coupling reaction of Grignard reagent with BODIPYs was attempted. The chloroBODIPY was treated with phenylethynyl magnesium bromide in the presence of the catalyst $Pd(PPh_3)_4$ in THF and the mixture was refluxed for five minutes. The reaction resulted in a red solution and the UV/visible absorption spectrum showed a sharp peak at 554 nm. The structure of the product was confirmed by ^1H NMR spectroscopy to be the fully substituted BODIPY **87**. The assumption is that the strong Grignard reagents diminished the difference between chloride and fluoride under palladium catalysis.

Finally, Stille coupling reactions[57,70,71] were performed on chloroBODIPY with tributylphenylstannane catalyzed by $Pd(PPh_3)_4$ without any base. The mixture was refluxed in toluene and TLC showed the reaction was not only completed within five hours, but also the product was the only spot on a TLC plate. The product **85** was separated with a flash column on silica gel to remove very minor reaction impurities to give the product in 93% yield. This yield is far better than those from the Suzuki reaction.

Heck coupling reactions were attempted with styrene using $Pd(II)(PPh_3)_2Cl_2$ as catalyst and TEA as base, but the reaction did not yield any useful product. There was no UV/visible absorption change during this reaction.

From the above coupling reactions performed on cloroBODIPY **74**, one can see that Suzuki, Stille and Sonogashira coupling reactions all worked, but the Heck coupling reaction did not. The products from these reactions were obtained in 36-93% yields, with the lowest yield obtained for the 8-chloro-BODIPY under Suzuki conditions and highest yield with organotin reagent.

Since we observed the Stille coupling reaction to be the most efficient and economic reaction among all these coupling reactions, we therefore further investigated the Stille coupling reaction with other reagents to see if we could expand this method to more substrates and make it a more versatile approach for functionalization of BODIPYs.

Various organotin reagents bearing alkyl, alkenyl, alkynyl and heterocyclic aromatic groups were used in coupling reactions to investigate the sp_2-sp_3, sp_2-sp_2 and sp_2-sp coupling reactions with BODIPYs (Table 4.1). All the coupling reactions produced the corresponding 8-functionalized BODIPYs in nearly quantitative yields, except for the reaction with tributylethynyltin, which gave BODIPY **91** in only 31% yield. When TMS-protected ethynyl organotin was used, the yield improved to 71% yield for product **86**, presumably because the TMS-protected ethynyl product is more stable. Aromatic Stille reagents such as 2-(tributylstannyl)pyrrole, 2-(tributylstannyl)thiophene and 2-(tributylstannyl)pyridine were also employed since these compounds can also be synthesized by traditional methods. For the first two electron-rich stannane reagents, the products **92** and **93** were obtained in excellent yields around 95-99%, However, for the electron deficient pyridyl tin reagent, only meso-free BODIPY was generated. The structures of the BODIPY products were confirmed by ^{1}H and ^{13}C NMR, HRMS (ESI-TOF) mass spectrometry and UV-visible spectroscopy. The ^{1}H NMR spectrum of 8-phenyl-BODIPY **85** showed aromatic protons between 7.49-7.27 ppm, consistent with literature reports,[40,41] and the structure of the product was confirmed by mass spectroscopy (*m/z* 324.1717). The *meso*-methyl group of BODIPY **88** appeared at 2.40 ppm in its ^{1}H NMR spectrum and the product showed *m/z* at 262.1556. For BODIPYs **89** and **90**, the ^{1}H NMR spectra showed the alkene group as two doublets at 6.74 (dd),5.69 (dd) and 5.56 (dd) ppm for BODIPY **89** and 4.46 (dd), 4.37 (dd) ppm for BODIPY **90**. The ethoxy group of **90** absorbed at 3.90 (q) and 1.38 (t) ppm. The mass spectra confirmed the identity of the two product with *m/z* at 274.1557 and 318.1817, respectively. BODIPY **91** has a typical peak at 3.92 ppm for the alkynyl group in its ^{1}H NMR spectrum, and *m/z* at 272.1380. BODIPY **86** showed the TMS protecting group at 0.29 ppm in its ^{1}H NMR spectrum and *m/z* 325.1708 (MW-F) in its mass spectrum; the aromatic ring of BODIPYs **92 and 93** showed peaks between 6.77-6.06 ppm and 7.51-

6.98 ppm, and the *N*-CH_3 of BODIPY **92** showed a peak at 3.40 ppm in its ^{1}H NMR spectrum. These two BODIPYs were also characterized by *m/z* at 327.1799 and 352.1094, respectively. The X-ray crystal structures of BODIPYs **85**, **88**, **89**, **92** and **93** were also obtained by slow diffusion of hexane into a CH_2Cl_2 solution of each, and they are shown in Figure 4.15.

In the X-ray structures, BODIPY **85** deviates from its potential C_s symmetry by the BF_2 and phenyl planes being twisted in opposite directions from orthogonality with the dipyrryl plane, the BF_2 forming a dihedral angle of 88.13(5)° and the phenyl a dihedral angle of 82.40(3)° with it. BODIPY **88** is unusual in that its dipyrryl group lies in a crystallographic mirror and its BF_2 across it; thus they are exactly orthogonal.The X-ray structure for BODIPY **89** was also obtained. Its dipyrryl and BF_2 planes form a dihedral angle of 88.82(2)^o. The ethene substitutent is not quite orthogonal to the dipyrryl nor coplanar with the BF_2, a C-C-C=C tortion angle about the bond to it being 65(10)°. BODIPY **92** deviates only slightly form C_s symmetry, with the BF_2 plane forming a dihedral angle of 89.51(9)^o with the dipyrryl plane and the methylpyrrole plane forming an angle of 85.77(4)^o with it, only one of the major orientations of the disordered thiophene is shown for BODIPY **93**; it forms a dihedral angle of 84.31(8)° with dipyrryl, and the BF_2 plane forms a dihedral angle of 88.56(4)° with the dipyrryl plane.

The spectroscopic properties of these compounds were studied and their UV/visible absorption and steady-state fluorescence emission spectra in CH_2Cl_2 were recorded. As an example, Figures 4.10, 4.12, 4.13 and 4.16 show the normalized absorption and fluorescence spectra of some BODIPYs. Specifically, literature compounds **85** and **88** have absorption and emission values similar to those previously reported.[42] The newly synthesized BODIPYs **74**, **63 75** and **64** show spectra of comparable shape to those BODIPYs described in the literature, with a narrow absorption band (λ_{max} *ca*. 500 nm),

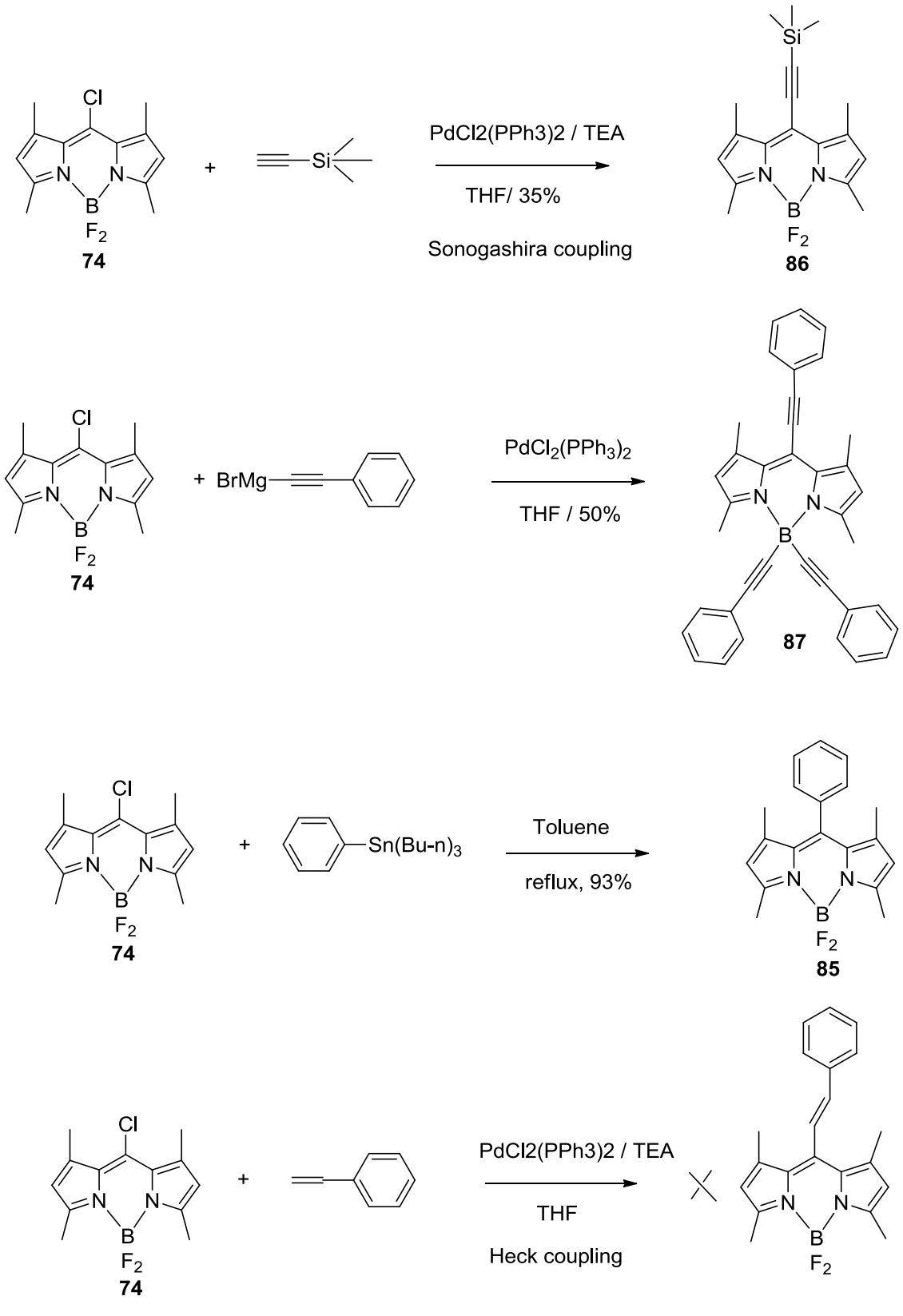

Scheme 4.26: Coupling reactions of BODIPY **74** with different reagents.

Table 4.1: Stille coupling reactions of 8-chloro-BODIPY **74**

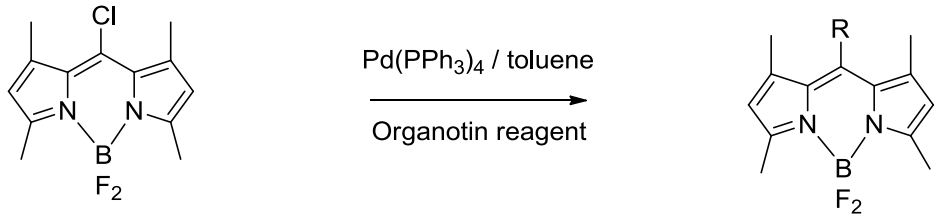

BODIPYS	Organotin	R	Yield (%)
85	Bu3SnPh	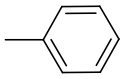	93
86	Bu_3Sn—≡—TMS	—≡—TMS	71
88	Me4Sn	—CH_3	97
89	Bu3Sn(CH=CH2)	—═	97
90	Bu3Sn(EtOC=CH2)	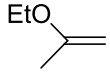	93
91	Bu3Sn(C≡CH)	—≡	31
92	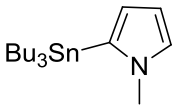	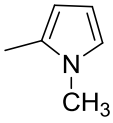	95
93	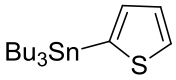	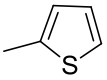	99

Note: The reaction was performed using 0.2 mmol for all the organotin reagents except for **86** which started with (25 mg, 0.088 mmol).

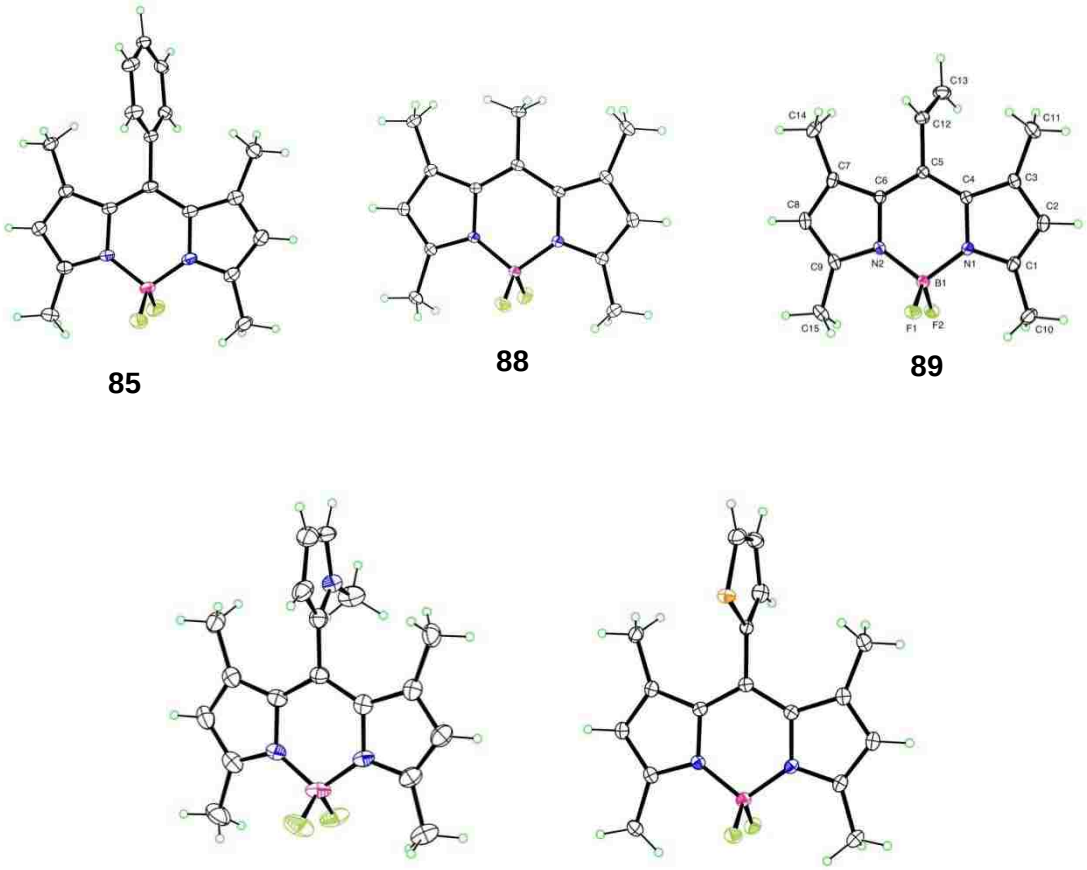

85 **88** **89**

92 **93**

Figure 4.15: X-Ray structures of BODIPYs synthesized from Stille coupling reactions.

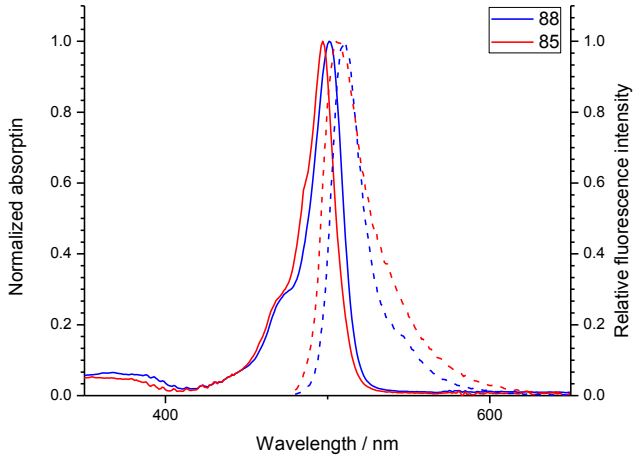

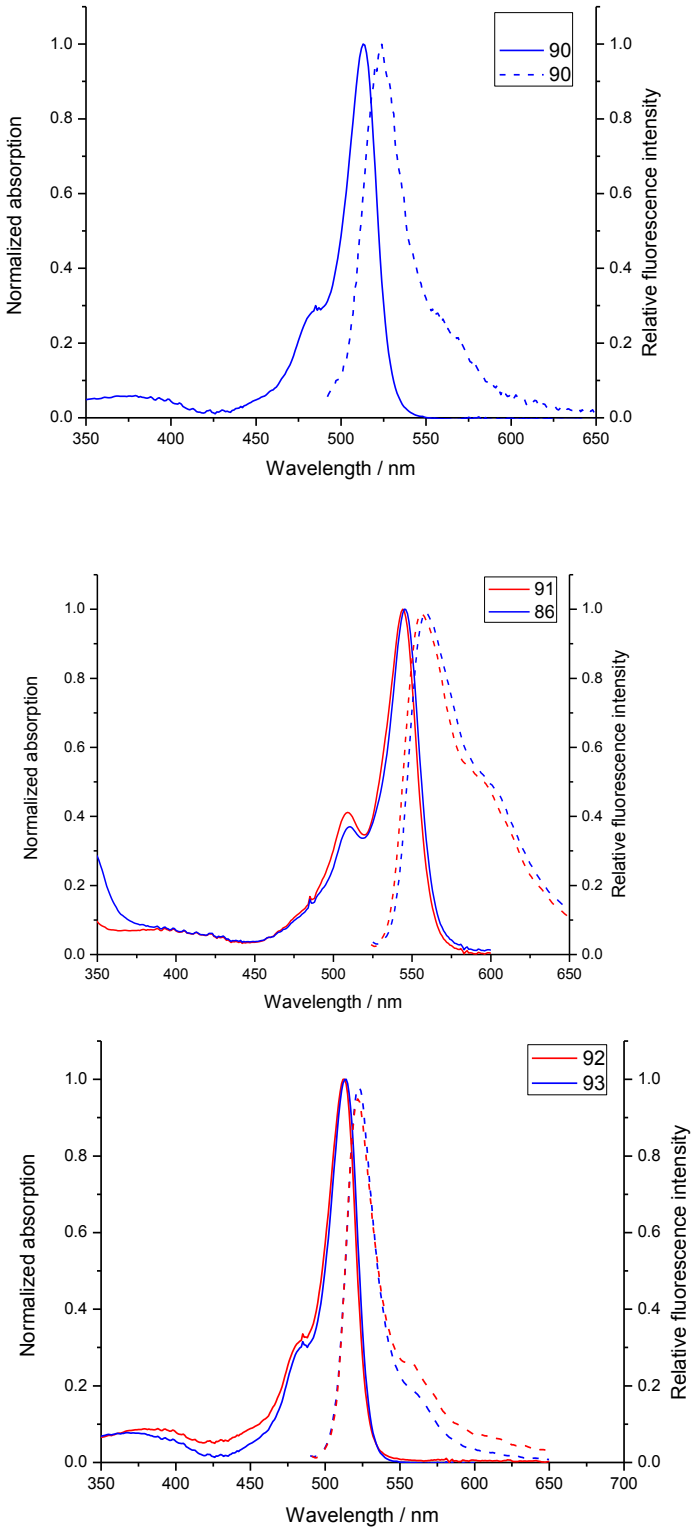

Figure 4.16: Normalized absorption and relative fluorescence intensity spectra, in CH_2Cl_2, of BODIPYs **85**, **86**, **90**, **91**, **92** and **93**.

which belongs to the s_0-s_1 transition, plus a weak broad absorption around 460 nm assigned to s_0-s_2 transition. All the BODIPYs have a slightly shifted sharp emission band with a mirror image shape. Table 4.1 presents the photophysical data of these BODIPYs, including the maximum absorption and fluorescence wavelengths, molar extinction coefficients and fluorescence quantum yields in CH_2Cl_2. *Meso*-chloro-BODIPY **74** has an absorption at 503 nm and a 9 nm Stokes-shifted fluorescence. The replacement of the chloro- by methoxy- (BODIPY **77**), ethoxy- (BODIPYs **63** and **64**), or phenoxy- (BODIPY **80**) causes a 12-16 nm blue-shift of the BODIPYs. On the other hand, substitution with alkenyl- (BODIPYs **89** and **90**), ethynyl- (BODIPYs **86** and **91**), thio- (BODIPYs **81**, **82** and **83**) or an aromatic heterocyclic ring (BODIPYs **92** and **93**) causes a red-shift (within 40 nm) in the corresponding BODIPYs. Carbon nucleophiles induce a very small blue shift The fluorescence quantum yields of **74** and **75** are around 0.51 and 0.33; replacement of the *meso*-chloro by an oxygen-centered nucleophile causes the quantum yields to increase significantly. In particular, for **63** and **64,** they increased about 0.30 compared with their meso-chloro-BODIPY counterparts **74** and **75**; in particular, the quantum yield of BODIPY **63** is close to 1.00. Substitution of the chloro- by alkyl- (e.g. methyl and ethyl as in BODIPY **69** and **88**) or aromatic (phenyl) groups (BODIPY **85**) also causes the quantum yields to increase significantly compared with the precursor chloro-BODIPY. However, sulfur-centered nucleophiles (BODIPY **81**-**83**) caused the quantum yield to decrease; for example, the corresponding compounds **81** and **82** have very low quantum yields (0.04 and 0.09, respectively). *Meso*-alkenyl-, ethynyl- and heteroaromatic ring-substituted BODIPYs **89**-**93** have relatively low quantum yields, especially so for BODIPY **89** which is almost non-fluorescent. Substitution on the boron has no significant impact on absorption, but does have a large effect on the quantum yield. For example, the substitution by a methoxy group on boron causes the quantum

yield to increase by 0.42 (BODIPY **79**). However, alkyl substitution on the boron reduces the quantum yield of BODIPY **69** from 0.83 to the 0.32 value of BODIPY **76** .

Steady-state Absorption and Fluorescence Spectroscopy

The absorption measurements were carried out on an Agilent 8453 spectrophotometer and the steady-state fluorescence spectroscopic studies were performed in CH_2Cl_2 on a PTI QuantaMaster4 / 2006SE spectrofluorometer. The slit width was 3 nm for both the excitation and emission measurements. The fluorescence quantum yields of BODIPYs was obtained by comparing the area under the corrected emission spectrum of the test sample with that of Rhodamine 6G in ethanol.

The fluorescent quantum yields (Φ_{exp}) were calculated using the following equation

$$\Phi_{\mathrm{exp}} = \Phi_{\mathrm{ref}} \frac{\mathrm{F_x}[\mathrm{A_{std}}]\mathrm{n}^2}{\mathrm{F_{std}}[\mathrm{A_x}]\mathrm{n}_{\mathrm{std}}^2}$$

Φ_{ref} is the standard fluorescent quantum yield, F_x is the area under the sample emission peak, F_{std} is the area under the standard's emission peak, A_{std} is the optical density at which the standard was excited, A_x is the optical density at which the sample was excited, n represents the refractive index of the solvent of sample solution, and n_{std} is the refractive index of the standard's solvent.

Table 4.2. Spectral properties of BODIPYS in CH_2Cl_2 at room temperature. The fluorescence quantum yields (λ_{exc} = 490 nm) were calculated using, rhodamine 6G (0.80 in ethanol) as the reference[32] and a PTI Quantum Master4/2006SE spectrofluorimeter was used

BODIPY	Abs λ_{max} (nm)	Emission λ_{max} (nm)	ϕ_f	Log ε ($M^{-1}.cm^{-1}$)
63	487	493	0.99	4.77
64	508	518	0.67	4.44
69	499	505	0.83	4.75
74	503	512	0.51	4.79
75	527	542	0.33	4.50
76	499	507	0.32	4.20
77	487	493	0.57	4.95
79	487	496	1.00	4.67
80	491	499	0.99	4.71
81	539	553	0.04	4.69
82	529	542	0.09	4.23
85	501	511	0.62	4.76
86	545	556	0.13	4.63
88	497	508	0.77	4.82
89	505	511	0.00	4.67
90	513	522	0.14	4.61
91	544	556	0.29	4.57
92	513	521	0.10	4.73
93	514	521	0.05	4.87

4.3 Conclusion

Symmetrical pyrroketones were made via thioketones by treatment with PbO_2/$Pb(OAc)_2$ The chemistry of pyrroketones was investigated by electrophilic alkylation with Meerwein's salt, chlorination by phosgene and protonation by acids. Reactivity of their derivatives, 8-chloro-dipyrromethenes and 8-chloroBODIPYs, were compared using nucleophilic substitution (addition/elimination) with, for example, oxygen-centered nucleophiles, sulfur-centered nucleophiles and carbon-centered nucleophiles and coupling reactions including Sonogashira, Heck, Suzuki and Stille coupling were also investigated. The resuls show that BODIPYs are more stable than dipyrromethenes (dipyrrins) in most of the reactions, and they are easy to handle during purification. The advantage of dipyrrins over BODIPYs is that there are no competitive reactions involving the B-F bonds during substutition reactions. Some BODIPYs were obtained by substitution (addition/elimination) or coupling reactions of 8-chloroBODIPYs, which are hard to synthesize by conventional methods. The photophysical properties of these new BODIPYs were studied including absorption, fluorescence and determination of their quantum yields.

4.4 Experimental Part

General information:

All the solvents and chemicals were purchased from Aldrich, Fisher and TCI. Silica gel 60 (230 x 400 mesh) and TLC plates (0.2 mm thickness) were purchased from Sorbent Technologies. All conmertial reagents were used without further purification. Water and air sensitive reactions were performed under argon protection and in dry solvents. Melting points were measured on an electrothermal Mel-Temp instrument, UV/visible absorption spectra was measured on an Agilent 8453 spectrophotometer and the steady state fluorescence spectroscopic studies were performed on a PTI

QuantaMaster4/2006SE spectrofluorometer with the slit width set at 3 nm. High and low resolution mass spectra were performed on Bruker ProFlex III MALDI-TOF and Hitachi M8000 ESI mass spectrometers. FT-IR data were obtained on a Bruker Tensor 27 system (2004), ^{1}H NMR and ^{13}C NMR spectra were obtained with a Bruker AV-400 MHZ spectrometer, and chemical shifts are expressed in ppm.

Dibenzyl 5,5'-carbonylbis(4-(3-methoxy-3-oxopropyl)-3-methyl-1*H*-pyrrole-2-carboxylate) 36: A solution of dipyrromethane **34** (2.0 g, 3.25 mmol) in acetic acid (80 ml) was treated with $Pb(OAc)_4$ (3.12 g, 7.0 mmol) and stirred at room temperature for 4 d under argon. Then PbO_2 (2.4 g, 9.3 mmol) was added and the solution was stirred for another two d. The solution was centrifuged and the supernatant was poured into ice water. The precipitate was collected and dissolved in diethyl ether, before being washed with water, 5% $NaHCO_3$ and brine and then dried over anhydrous Na_2SO_4. Then the solution was concentrated to a minimum volume and crystallized in a refrigerator to give product as a yellowish white solid (1.2 g, 60%). ^{1}H NMR (400 MHz; $CDCl_3$): 7.38-7.31 (m, 10H), 5.00 (s, 4H), 3,67 (s, 6H), 3.01 (t, 3H), 2.71 (t, 3H), 2.27 (s, 6H). ^{1}H-NMR (400 MHz; $CDCl_3$): 176.73, 173.56, 161.74, 135.02, 132.23, 130.16, 128.66, 128.36, 127.73, 126.97, 121.68, 66.77, 51.58, 35.19, 20.28, 10.37.

Dibenzyl 5,5'-carbonylbis(3,4-dimethyl-1H-pyrrole-2-carboxylate) 37 was synthesized using the same procedure as used for **36**: (0.79g, 50%)^{1}H NMR (400 MHz; $CDCl_3$): 7.37 (m, 10H), 5.14 (s, 4H), 2,25 (s,3H), 2.23 (s, 3H).

Benzyl 5-(5-((benzyloxy)carbonyl)-3-(3-methoxy-3-oxopropyl)-4-methyl-1H-pyrrole-2-carbonyl)-1-ethyl-4-(3-methoxy-3-oxopropyl)-3-methyl-1H-pyrrole-2-carboxylate 39: ^{1}H NMR (400 MHz, $CDCl_3$): 9.22 (s, 2H), 7.46-7.27 (m, 10H), 5.34 (s, 2H), 5.35 (s, 2H), 4.30 (q, *J* = 4.29 Hz, 2H), 3.56 (s, 3H), 3.62 (s, 3H) 2.89 (t, 2H) 2.59 (t, 2H), 2.47 (t, 2H)2.35 (t, 2H) 2.31 (s, 3H), 2.25 (s, 3H), 1.22 (t, *J* = 4.29 Hz, 3H); ^{13}C NMR

($CDCl_3$):179.40, 173.06, 172.82, 161,28, 160.71, 135.99, 135.53, 133.26, 131.03, 130.87, 128.67, 128.62, 128.47, 128.42, 128.33, 128.29, 128.26, 127.82,124.37, 122.94, 122.05, 66.67, 51.56, ,42.16, 34.89, 34.26, 29..69, 19.96, 19.87, 17.35, 14.15, 14.11, 11.50, 10.07.

Preparation of α-Free Pyrroles

General procedure for hydrolysis under basic conditions: α-Ester pyrrole (5.0 mmol) was dissolved in 10-15 ml of ethylene glycol. Then potassium hydroxide (10.0 mmol) was added under an argon atmosphere and the mixture was refluxed for 2 h. After the reaction had cooled down to room temperature, the mixture was diluted with water and extracted with hexane and then washed with water, brine and finally dried over anhydrous Na_2SO_4. After removal of the solvent, the residue was purified by chromatography on a silica gel column eluted with hexane/ CH_2Cl_2 (2/1) to give the pure product.

General procedure for hydrolysis under acidic conditions: tert-Butyl ester pyrrole or pyrrole carboxylic acid (2.0 mmol) was dissolved in TFA at 0 ^oC, the mixture was stirred for 1 h and then poured into ice water and neutralized with ammonia to pH = 7. The solution was extracted with hexane or CH_2Cl_2 and washed with water, brine, and dried over anhydrous Na_2SO_4. After removal of the solvent, the residue was purified by chromatography on a silica gel column eluted with hexane/ CH_2Cl_2 (2/1) to give the pure product

General procedure for reduction of ester pyrrole to alkyl pyrrole: 2-Unsubstituted 5-ester pyrrole (2.0 mmol) was dissolved in dry THF (50 ml) and the solution was added to a suspension of $LiAlH_4$ (2.4 mmol). The mixture was refluxed for 5 h and then it was cooled to room temperature and the excess $LiAlH_4$ was destroyed by addition of

aqueous saturated Na_2SO_4. The solution was extracted with hexane or $CHCl_3$ and then washed with water, brine and dried over anhydrous Na_2SO_4 and the residue was purified by chromatography on a silica gel column eluted with hexane/ CH_2Cl_2 or hexane/ethyl acetate.

2,4-Dimethyl-3-ethylpyrrole 44: ^{1}H NMR (400 MHz; $CDCl_3$): 7.48 (s, 1H), 6.40 (s, 1H), 2.42 (q, 2H), 2.10 (s, 3H), 2.00 (s, 3H), 1.09 (t, 3H).

2,4-Dimethylpyrrole 45: ^{1}H-NMR (400 MHz; $CDCl_3$): 7.64 (s, 1H), 6.50 (s, 1H), 5.89 (s,1H), 2.34 (s, 3H), 2.22 (s, 3H).

2,4-Dimethyl-3-butylpyrrole 46: ^{1}H NMR (400 MHz; $CDCl_3$): 7.51 (s, 1H), 6.45 (s, 1H), 2.45 (t, 2H), 2.24 (s, 3H), 2.12 (s, 3H), 1.48 (m, 4H), 1.04 (t, 3H).

2,3,4-Trimethylpyrrole 48: ^{1}H NMR (400 MHz; $CDCl_3$): 7.45 (s, 1H), 6.40 (s, 1H), 2.16 (s, 3H), 2.12 (s, 3H), 1.94 (s, 3H)

2,4-Dimethyl-3-acetylpyrrole 54: ^{1}H NMR (400 MHz; $CDCl_3$): 8.45 (s, 1H), 6.35 (s, 1H), 2.50 (s, 3H)， 2.42 (s, 3H), 2.27 (s, 3H)

2,4,7,9-Tetramethyldipyrryl-5-thioketone 55 *:* A solution of thiophosgene (1.15 g, 10.0 mmol) in toluene (10 ml) was added dropwise to a solution of 2,4-dimethylpyrrole **45** (2.0 g, 21.0 mmol) in dry ether (30 ml) at 0 °C. The mixture was stirred for about 1 h (until TLC showed the starting material had disappeared). Then methanol (30 ml) was added and the mixture was stirred for another 30 min. The solvents were removed in vacuo and the residue was purified on a silica gel column eluted with toluene/chloroform (4:1). The thioketone product was obtained as an orange solid (980 mg, 40%), with Mp 180-181°C.^{1}H NMR (400 MHz; $CDCl_3$): 8.96 (s, 2H), 5.91 (s, 2H), 2.27 (s, 6H), 2.07 (s, 6H); ^{13}C NMR ($CDCl_3$): δ 175.30, 133.30, 127.98, 127.56, 111.74, 13.09, 12.65; HRMS (ESI): Calcd *m/z* for $C_{13}H_{16}N_2S$: 233.1107; found: 233.1106.

The synthesis of **3,5-dibutyl-2,4,7,9-tetramethyldipyrryl-5-thioketone 56** followed the procedure reported above for **55**: (Yield: 1.23g, 34%). ^{1}H NMR (400 MHz; $CDCl_3$): 8.95 (s, 2H), 2.36 (t, 4H), 2.23 (s, 6H), 1.99 (s, 6H), 1,40-1.31(m, 8H), 0.92(t, 6H). HRMS (ESI): Calcd *m/z* for $C_{17}H_{25}N_2S$: 344.5572; found: 344.5576.

The synthesis of **3,8-diethyl-2,4,7,9-tetramethyl-5-dipyrryl-5-thioketone 58** followed the procedure reported above for **55**. Yield 1.30 g, (43%). Mp 205-207 ^{o}C ^{1}H NMR (400 MHz; $CDCl_3$): 8.95 (s, 2H), 2.40-2.35 (q, *J* = 7.5 Hz, 4H), 2.23 (s, 6H), 2.00 (s, 6H), 1.07-1.03 (t, *J* = 7.5 Hz, 6H); ^{13}C-NMR ($CDCl_3$): 189.39, 136.19, 134.67, 126.67, 125.56, 17.47, 14.99, 11.73, 10.88. HRMS (ESI): Calcd *m/z* for $C_{17}H_{25}N_2S$: 289.1733; found: 289.1739.

2,4,7,9-Tetramethyldipyrryl-5-dipyrroketone 59: To the thioketone **55** (232 mg, 1.0 mmol) in EtOH (95%, 100 ml) was added KOH (1.0 g) and to the mixture was added aqueous H_2O_2 (5%, 10 ml) dropwise in an ice bath. Then the solution was heated on a steam bath for about 5 min. The solution was cooled to room temperature and water (300 ml) was added and it was then extracted with chloroform three times. The organic layers were collected and washed with water, brine and then dried over anhydrous Na_2SO_4. The solvent was evaporated and the residue was purified by sublimation to give the product dipyrrylketone as a pale yellow solid. (170 mg, 78%). Mp 232-233 °C. ^{1}H NMR (400 MHz; $CDCl_3$): 8.63 (s, 2H), 5.85(s, 2H), 2.28 (s, 6H), 2.19 (s, 6H); ^{13}C-NMR ($CDCl_3$): 175.30, 133.30, 127.98, 127.56, 111.74, 13.09, 12.65; HRMS (ESI): Calcd *m/z* for $C_{13}H_{16}N_2O$: 217.1335; found: 217.1334. UV/vis (CH_2Cl_2) λ_{max} (ε) 295 nm (8600), 341 nm (14600). IR ν_{max} (C=O) (Nujol) 1573 cm^{-1}.

3,5-Diethyl-2,4,7,9-tetramethyl-5-dipyrroketone *60*: Yield, 224 mg, (82%). Mp 205-207 °C . ^{1}H NMR (400 MHz; $CDCl_3$): 8.61 (s, 2H), 2.43-2.37 (q, *J* = 7.5 Hz, 4H), 2.23 (s,

6H), 2.14 (s, 6H), 1.07 (t, *J* = 7.5 Hz, 3H) ^{13}C-NMR ($CDCl_3$): 175.23, 129.65, 127.24, 125.27, 124.25, 17.37, 15.20, 11.41, 10.70. HRMS (ESI): Calcd *m/z* for $C_{17}H_{25}N_2O$: 273.1967; found: 273.2013. UV/vis λ_{max} ($CHCl_3$) 288 nm (11700), 357 (25000). IR ν_{max} (C=O) ($CHCl_3$ or Nujol) 1575 cm^{-1}.

BODIPY 63*: Method A*: Dipyrrylketone **59** (60 mg, 0.27 mmol) was dissolved in dry $CHCl_3$ (20 mL) and triethyloxonium tetrafluoroborate (105.1 mg, 0.54 mmol) was added. The solution turned red with time and UV-visible spectroscopy showed a sharp peak at 438 nm. The mixture was stirred overnight and then washed with water, brine and finally dried over anhydrous Na_2SO_4. After evaporation, the residue was dissolved in $CHCl_3$ (30.0 ml) and DIEA (1.62 mmol, 6 equiv) was added and the solution was stirred for about 30 min before addition of $BF_3.OEt_2$ (2.7 mmol, 10 equiv); the reaction solution was then stirred overnight. UV-visible spectroscopy showed a sharp peak at 487 nm. Then the mixture was washed with aqueous $NaHCO_3$, brine and then dried over anhydrous Na_2SO_4. The residue was purified by chromatography (eluted with CH_2Cl_2/hexane) to give BODIPY **63** as an orange red solid. (64 mg, 82%).

Method B: BODIPY **74** (56.4 mg, 0.20 mmol) was dissolved in MeOH (20 ml) in an ice bath and NaOEt (20.4 mg, 0.3 mmol) was added. The mixture was stirred for 45 min while being monitored by TLC and UV-visible spectroscopy. The solvent was removed in vacuo and the residue was taken up in $CHCl_3$ and washed with water, brine and then dried over anhydrous Na_2SO_4. The product was purified by chromatography (eluted with CH_2Cl_2/hexane) to give an orange solid (26.8 mg, 46%). Mp. 126-128 °C; ^{1}H NMR (400 MHz; $CDCl_3$): 6.02 (s, 2H), 4.12 (q, *J* = 7.1 Hz, 2H), 2.51 (s, 6H), 2.38 (s, 6H), 1.53 (t, *J* = 7.1 Hz, 3H); ^{13}C NMR (100 MHz; $CDCl_3$): 159.12, 154.13, 139.13, 127.94, 119.57, 74.14,

15.31, 14.45, 13.75; HRMS (ESI): *m/z* Calcd for $C_{15}H_{19}BF_2N_2O$: 292.1668; found: 292.1654; UV/vis (CH_2Cl_2) λ_{max} (ε) 487 nm (58900).

BODIPY 64*: Method A*: Yield: (66 mg, 71%); *Method B*: Yield: (36.2 mg, 52%); Mp. 135-137 °C; ^{1}H NMR (400 MHz; $CDCl_3$): 4.09 (q, *J* = 7.1 Hz, 2H), 2.48 (s, 6H), 2.48 (q, *J* = 7.5 Hz, 4H), 2.32 (s, 6H), 1.55 (t, *J* = 7.1 Hz, 3H), 1.06 (t, *J* = 7.5 Hz, 6H); ^{13}C NMR (100 MHz; $CDCl_3$): 158.04, 152.19, 134.73, 131.53, 73.88, 17.04, 15.29, 14.68, 12.41, 11.22; HRMS (ESI): *m/z* Calcd for $C_{19}H_{27}BFN_2O$ (M^+-F): 329.2200; found: 329.2167.; UV/vis (CH_2Cl_2) λ_{max} (ε) 508 nm (27500).

5-Chloro-2,4,7,9-tetramethyldipyrromethene hydrochloride 65: Dipyrrylketone **59** (314 mg, 1.45 mmol) was dissolved in $CHCl_3$ (100 ml) and excess phosgene in toluene solution was added and stirred at room temperature for 1 h. When the reaction was complete according to UV-visible spectra and TLC, nitrogen gas was passed through solution to purge it of excess phosgene that was directed into an aqueous $NaHCO_3$ solution trap. Solvent was then removed in vacco and the red solid was recrystallized from $CHCl_3$/petroleum ether to give **65** as a red solid (306 mg, 90%). Mp > 260 °C. ^{1}H NMR (400 MHz; $CDCl_3$): 12.93 (s, 2H), 6.23 (s, 2H), 2.59 (s, 6H), 2.34 (s, 6H); ^{13}C NMR ($CDCl_3$): 153.70, 144.35, 139.63, 128.18, 120.71, 16.27, 14.38; HRMS (ESI): Calcd *m/z* for $C_{13}H_{16}ClN_2$: 235.0997, found: 235.0992. UV/vis (CH_2Cl_2) λ_{max}(ε) 485 nm (23500).

5-Chloro-3,8-diethyl-2,4,7,9-tetramethyldipyrromethene hydrochloride 66. Yield: 392 mg, (93%). Mp >300 °C. ^{1}H NMR (400 MHz; $CDCl_3$): 12.50 (s, 2H), 2.35 (s, 6H), 2.15 (s, 6H), 2.40 (q, 4H), 1.05 (t, 6H). ^{13}C NMR ($CDCl_3$): 152.41, 138.81, 137.68, 133.13, 128.08, 17.44, 14.28, 12.72, 12.63 HRMS (ESI): Calcd *m/z* for $C_{17}H_{24}ClN_2$ 291.1623, found: 291.1635. Anal. Calcd for $C_{17}H_{24}Cl_2N_2$: C, 62.4; H, 7.3; N, 8.6; found: C, 62.7; H, 7.5; N, 8.8%. UV/vis ($CHCl_3$) λ_{max}(ε) 509 nm (57500).

BODIPY 69: *Method A*: 5-Chloro-dipyrrin **65** (100 mg, 0.37 mmol) was dissolved in $CHCl_3$ (40 mL) and 1.0 M EtMgBr in THF (1.30 mL, 1.30 mmol) was added dropwise at 0 °C; the mixture was left stirring for 1 h at 0 °C and then for another 2 h at room temperature. Then the solution was poured into ice/water to destroy excess EtMgBr and it was extracted with $CHCl_3$. The organic layers were combined and washed with water, brine and then dried over anhydrous Na_2SO_4. After evaporation, the residue in $CHCl_3$ (30 mL) and DIEA (0.45 ml, 7 equiv, 2.58 mmol) in an ice bath was treated with $BF_3.OEt_2$ (0.53 ml, 12.0 equiv, 4.3 mmol) and the mixture was stirred overnight. The solvent was removed and the residue was purified on a silica gel column (eluted with CH_2Cl_2/hexane) to give BODIPY **69**. Yield: 20.1 mg, 19.6%.

Method B: ChloroBODIPY **74** (56.4 mg, 0.2 mmol) was dissolved in anhydrous THF (30 ml) and 1.0 M EtMgBr in THF (0.5 mL, 0.5 mmol) was added dropwise to the solution at - 70 °C with vigorous stirring. When the reaction was complete according to TLC and spectrophotometry, the solution was poured into ice/water to destroy the exess Grignard reagent. Then the mixture was extracted 3 times with $CHCl_3$ and the organic phases were combined and washed with water, brine and then dried over anhydrous Na_2SO_4. The solvent was evaporated and the residue was purified by silica gel column chromatography (eluted with CH_2Cl_2/hexane) to give the product **69** as an orange-red solid (40 mg, 75%); Mp. 214-216 °C; ^{1}H NMR (400 MHz; $CDCl_3$): 6.05 (s, 2H), 3.01 (q, *J* = 7.5 Hz, 2H), 2.52 (s, 6H), 2.44 (s, 6H), 1.32 (t, *J* = 7.5 Hz, 3H); ^{13}C NMR (100 MHz; $CDCl_3$): 153.87, 147.87, 140.30, 131.20, 121.55, 21.29, 16.30, 15.45, 14.45; HRMS (ESI): *m/z* calcd for $C_{15}H_{19}BF_2N_2$: 276.1718; found: 276.1713; UV/vis (CH_2Cl_2) λ_{max} (ε) 499 nm (56200). The *meso*-unsubstituted BODIPY was also eluted from the column (6.0 mg, 10%); Mp. 185-187 °C; ^{1}H NMR (400 MHz; $CDCl_3$): 7.04 (s, 1H), 6.05 (s, 2H), 2.53 (s, 6H), 2.25 (s, 6H); ^{13}C NMR (100 MHz; $CDCl_3$): 156.75, 141.20, 133.41, 120.07,

119.02, 14.67, 11.28; HRMS (ESI): *m/z* Calcd for $C_{13}H_{15}BF_2N_2$: 248.1405; found: 248.1404; UV/vis (CH_2Cl_2) λ_{max} (ε) 507 nm (19600).

Methyl 3,5-dimethylpyrrole-2-carboxylate 72: Chlorodipyrrin hydrochloride **65** (47.0 mg, 0.17 mmol) was dissolved in $CHCl_3$ and 0.5 M NaOMe in MeOH (1.0 mL, 0.5 mmol) was added at room temperature; the mixture was stirred overnight and the reaction was monitored by TLC and spectrophotometry. The solution was washed with water, brine and then dried over anhydrous Na_2SO_4. The solvent was removed and the product was purified by silica gel column chromatography (eluted with MeOH/CH_2Cl_2); Yield: 21 mg, 80.8%; Mp 93-95 °C (lit.[44] 98-99 °C); ^{1}H NMR (400 MHz; $CDCl_3$): 9.27 (s, 1H), 5.79 (s, 1H), 3.83 (s, 3H), 2.30 (s, 3H), 2.25 (s, 3H); ^{13}C NMR (100 MHz; $CDCl_3$): 163.43, 132.97, 129.14, 117.53, 111.34, 50.92, 12.96, 12.82. HRMS (ESI): *m/z* Calcd for $C_8H_{12}NO_2$ ($M+H^+$): 154.0868; found: 154.0870.

Ethyl 3,5-dimethylpyrrole-2-carboxylate 73: This compound was prepared as described for pyrrole **72** (above) except that sodium ethoxide was used as the base in ethanol. Yield: 19.0 mg, 66.2%. Mp. 118-119 °C (lit.[45] 125 °C); ^{1}H NMR (400 MHz, $CDCl_3$): 8.68 (s, 1H), 5.79 (s, 1H), 4.31 (q, *J* = 7.1 Hz, 2H), 2.30 (s, 3H), 2.24 (s, 3H), 1.34 (t, *J* = 7.1 Hz, 3H); ^{13}C NMR (100 MHz; $CDCl_3$): 161.69, 132.28, 129.02, 117.78, 111.35, 59.68, 14.57, 13.07, 12.77; HRMS (ESI): *m/z* Calcd for $C_9H_{14}NO_2$ ($M+H^+$): 168.1019; found: 168.1016

BODIPY 74*:* Chloro-dipyrrin hydrochloride **65** (235 mg, 0.87 mmol) was dissolved in $CHCl_3$ and DIEA (8 mmol, 9.0 equiv) was added before the mixture was stirred for 30 min. Then $BF_3.OEt_2$ (14 mmol, 16 equiv) was added. The resulting mixture was stirred overnight at room temperature. The solution was washed with saturated aq $NaHCO_3$,

brine and then dried over anhydrous Na_2SO_4. The solvent was evaporated and the residue was purified by chromatography on a silica gel column (eluted with CH_2Cl_2/hexane) to give the BODIPY **74** (230 mg, 94%); Mp. 235-237 °C; ^{1}H NMR (400 MHz; $CDCl_3$): 6.09 (s, 2H), 2.52 (s, 6H), 2.45 (s, 6H); ^{13}C NMR (100 MHz; $CDCl_3$): 155.26, 142.84, 136.54, 129.72, 121.36, 16.68, 14.54; HRMS (ESI): *m/z* Calcd for C13H15BClF2N2: 282.1016; found: 282.1010; UV/vis (CH_2Cl_2) λ_{max} (ε) 503 nm (61700).

BODIPY 75: This BODIPY was prepared using the same procedure, from 5-chloro-dipyrrin hydrochloride **66** (yield: 325 mg, 96%). Mp. 173-175 °C; ^{1}H NMR (400 MHz; $CDCl_3$): 2.50 (s, 6H), 2.41 (m, 10H), 1.05 (t, *J* = 7.6 Hz, 6H); ^{13}C NMR (100 MHz; $CDCl_3$): 153.36, 138.10, 135.16, 133.20, 129.16, 17.11, 14.75, 13.82, 12.49; HRMS (ESI): *m/z* Calcd for $C_{17}H_{22}BClFN_2$ (M^+-F): 319.1549; found: 319.1550; UV/vis (CH_2Cl_2) λ_{max} (ε) 527 nm (31600).

BODIPY 76: 1.0 M Ethyl magnesium bromide (1.0 ml, 1.0 mmol) in THF was added to chloro-BODIPY **65** (56.4 mg, 0.2 mmol) in THF (20 ml) at room temperature and stirred for 1 h; the reaction was quenched by addition of aqueous NH_4Cl and then extracted with $CHCl_3$. The organic extract was washed with water, brine and then dried over anhydrous Na_2SO_4. The BODIPY **76** was isolated as the sole product using silica gel column chromatography (eluted with CH_2Cl_2/hexane). Yield: 49 mg, 83%; Mp. 135-137 °C; ^{1}H NMR (400 MHz; $CDCl_3$): 6.08 (s, 2H), 3.07 (q, J = 7.5 Hz, 2H), 2.46 (s, 6H), 2.44 (s, 6H), 1.31 (t, *J* = 7.5 Hz, 3H), 0.79 (m, 4H), 0.30 (m, 6H); ^{13}C NMR (100 MHz; $CDCl_3$): 150.08, 135.52, 131.77, 122.06, 21.34 16.97, 16.39, 15.93, 9.00, 1.02; ^{11}B-NMR (128 MHz; $CDCl_3$): δ = 1.37; HRMS (ESI): *m/z* Calcd for $C_{19}H_{30}BN_2$: 296.2533; found: 296.2507; UV/vis (CH_2Cl_2) λ_{max} (ε) 499 nm (15800).

BODIPYs 77 and **78**: 8-Chloro-BODIPY **65** (56.4 mg, 0.2 mmol) was dissolved in MeOH (30 ml) in an ice bath and NaOMe (16.5 mg, 0.3 mmol) was added; the mixture was stirred for 45 min and the reaction was monitored by TLC and spectrophotometry. The solvent was removed in vacuo and the residue was taken up in $CHCl_3$ and washed with water, brine and then dried over anhydrous Na_2SO_4. The product was purified by silica gel column chromatography (eluted with CH_2Cl_2/hexane). The major fraction was the desired BODIPY product **77**. Yield: 37.1 mg, 67%; Mp. 160-161 °C; ^{1}H NMR (400 HMz; $CDCl_3$): 6.03 (s, 2H), 3.98 (s, 3H), 2.51 (s, 6H), 2.40 (s, 6H); ^{13}C NMR (100 MHz; $CDCl_3$): 159.95, 154.76, 138.33, 128.30, 119.56, 64.32, 49.12, 14.47, 13.76; HRMS (ESI): *m/z* Calcd for $C_{14}H_{18}BF_2N_2O$: 278.1511; found: 278.1504; UV/vis (CH_2Cl_2) λ_{max} (ε) 487 nm (89100). The monomethoxy-boron substituted BODIPY **78** was also separated as a minor fraction from the column (Yield: 12.0 mg, 21%); ^{1}H NMR (400 MHz; $CDCl_3$): 6.02 (s, 2H), 3.97 (s, 3H), 2.89 (s, 3H), 2.51 (s, 6H), 2.37 (s, 6H); ^{13}C NMR (100 MHz; $CDCl_3$): 159.95, 154.76, 138.33, 128.30, 119.56, 64.24, 49.12, 14.47, 13.76; ^{11}B NMR (128 MHz; $CDCl_3$): δ = 1.58; HRMS (ESI): *m/z* Calcd for $C_{14}H_{17}BFN_2O$ (M^+-OMe): 259.1418; found: 259.1392. A small amount of the dimethoxyboron-BODIPY **79** was also isolated from the column, but in insufficient quantity to characterizeit from this reaction.

BODIPY 79: 8-Chloro-BODIPY **74** (56.4 mg, 0.2 mmol) was dissolved in MeOH (30 ml) and NaOMe (54.0 mg, 0.75 mmol) was added before the solution was refluxed under argon for 12 h. The solvent was removed and the residue was taken up in $CHCl_3$ and washed with water, brine and then dried over anhydrous Na_2SO_4. The product was separated by silica gel column chromatography (eluted with MeOH/CH_2Cl_2). Yield: 38 mg, 65%; Mp. 93-95 °C; ^{1}H NMR (400 HMz; $CDCl_3$): 6.01 (s, 2H), 3.97 (s, 3H), 2.86 (s, 6H), 2.48 (s, 6H), 2.41 (s, 6H); ^{13}C NMR (100 MHz; $CDCl_3$): 159.92, 154.87, 137.38, 129.02, 119.33, 64.13, 49.04, 14.41, 13.81; ^{11}B NMR (128 MHz; $CDCl_3$): 2.39; HRMS

(ESI): *m/z* Calcd for $C_{16}H_{23}BN_2NaO_3$ (M^++Na): 324.173; found: 324.1719; UV/vis (CH_2Cl_2) λ_{max} (ε) 487 nm (46800). The monomethoxy-boron substituted BODIPY (see earlier) was also separated as a minor fraction from the column (Yield: 9.3 mg, 16%).

BODIPY 80*:* 8-ChloroBODIPY **74** (56.4 mg, 0.2 mmol) was dissolved in THF (30 ml) in an ice bath and sodium phenoxide (34.8 mg, 0.3 mmol) was added; the mixture was stirred for 2 h at room temperature and monitored by TLC and spectrophotometry. The solvent was removed in vacuo and the residue was taken up in $CHCl_3$ and washed with water, brine and then dried over anhydrous Na_2SO_4. The product was purified by column chromatography (eluted with CH_2Cl_2/hexane). Yield: 55 mg, (81%). Mp. 188-190 °C ^{1}H NMR (400 HMz; $CDCl_3$): 7.33-7.29 (m, 2H), 7.08-7.06 (m, 1H), 7.01-6.99 (m, 2H), 5.99 (s, 2H), 2.55 (s, 6H), 2.04 (s, 6H); ^{13}C NMR ($CDCl_3$): 157.52, 155.78, 151.59, 140.42, 130.08, 127.62, 122.84, 119.99, 114.70, 14.60, 14.14; HRMS (ESI): Calcd *m/z* for $C_{19}H_{20}BF_2N_2O$: 340.1668, found: 340.1662. λ_{max} (CH_2Cl_2) 491 nm (ε 51286).

BODIPY 81: A solution of 8-chloro-BODIPY **74** (56.4 mg, 0.2 mmol), 2-mercaptobenzothiozole (40.0 mg, 0.24 mmol) and K_2CO_3 (41.5 mg, 0.3 mmol) in THF (30 ml) was stirred at room temperature for 12 h or until the starting material was completely consumed. The solvent was removed in vacuo and the residue was taken up in $CHCl_3$ and washed with water, brine and then dried over anhydrous Na_2SO_4. The product was purified by silica gel column chromatography (eluted with CH_2Cl_2/hexane). Yield: 46.1 mg, 56%; Mp. 208-210 °C. ^{1}H NMR (400 HMz; $CDCl_3$): 7.90 (dt, *J* = 8.4, 0.9 Hz, 1H), 7.68 (m, 1H), 7.44 (ddd, *J* = 8.4, 7.3, 1.3 Hz, 1H), 7.31 (ddd, *J* = 8.3, 7.3, 1.2 Hz, 1H), 6.10 (s, 2H), 2.58 (s, 6H), 2.46 (s, 6H); ^{13}C NMR (100 MHz; $CDCl_3$): 166.56, 158.25, 153.59, 144.75, 135.37, 134.42, 128.70, 126.46, 124.76, 123.07, 122.00, 121.08, 17.26,

14.97; HRMS (ESI): *m/z* Calcd for $C_{20}H_{18}BFN_3S$(MW -F): 394.1019; found: 394.1010; UV/vis (CH_2Cl_2) λ_{max} (ε) 539 nm (49000).

BODIPY 82: A solution of chloroBODIPY **4a** (56.4 mg, 0.2 mmol), *p*-carborane thiol (45.6 mg, 0.24 mmol) and K_2CO_3 (41.5mg, 3.0 mmol) in THF (30 ml) was stirred at room temperature for 12 h or until the starting material was consumed, The solvent was removed in vacuo and the residue was taken up in $CHCl_3$ and washed with water, brine and then dried over anhydrous Na_2SO_4. The product was purified by silica gel column chromatography (eluted with CH_2Cl_2/hexane) and was obtained as a red solid. Yield: 80 mg, (92%). Mp 150-152 °C. ^{1}H NMR (400 MHz; $CDCl_3$): 6.06 (s, 2H), 2.95 (s, 2H), 2.51 (s, 3H), 2.49 (s, 3H), 2.17-1.68 (m, 11H); ^{13}C NMR ($CDCl_3$): 156.14, 143.51, 136.84, 134.23, 122.50, 59.04, 46.04, 31.91, 16.91, 14.68. HRMS (ESI): Calcd *m/z* for $C_{16}H_{26}B_{11}F_2N_2S$: 437.2808, found: 437.3033. . λ_{max} (ε)(CH_2Cl_2) 529 nm (17000).

BODIPY 83: yield :94%^{1}H NMR (400 MHz; $CDCl_3$): 6.15 (s, 2H), 2.57 (s, 6H),2.49 (s,6H), 2.20-1.70 (m, 11H); ^{13}C NMR ($CDCl_3$): 158.91, 143.66, 129.61, 123.83, 135.66, 60.07, 17.15, 15.10; HRMS (ESI): *m/z* Calcd for $C_{19}H_{20}BF_2N_2$: 423.2882; found: 423.2871.

BODIPY 84: yield 92% ^{1}H NMR (400 MHz; $CDCl_3$): δ 6.05 (s, 2H), 5.25 (s, 1H), 4.19 (q, 2H), 2.51 (s, 3H), 2.47 (t, 1H), 2.42 (s, 3H).

***BODIPY 85*:** *Method A*: In a Suzuki coupling reaction, 8-chloro-BODIPY **74** (56.4 mg, 0.2 mmol), $Pd(PPh_3)_4$ (10.0 mg, 5% mmol), phenylboronic acid (24.4 mg, 0.2 mmol) and K_2CO_3 (41.5mg, 0.3 mmol) were added to THF or DME (30 ml). The reaction flask was evacuated and filled with argon several times. Then the solution was refluxed overnight under argon. The solvent was removed and the residue was taken up in $CHCl_3$ and washed with water, brine, and dried over anhydrous Na_2SO_4. The solvent was removed

and the product was purified by chromatography on a silica gel column (eluting with CH_2Cl_2/hexane), The product is the major fraction from the column. (yield: 30.3 mg, 46%).

Method B: In a Stille coupling reaction, 8-chloro-BODIPY **74** (56.4 mg, 0.2 mmol), $Pd(PPh_3)_4$ (10.0 mg, 5% mmol) and tributylphenyl tin (80.0 mg, 0.24 mmol) were added to a round-bottomed flask. The flask was flushed with argon and then anhydrous toluene (20 ml) was added. The mixture was refluxed for 5 h after which the reaction was completed; the toluene was then removed and the residue was taken up in CH_2Cl_2 and washed with water, brine and then dried over anhydrous Na_2SO_4. The crude product was purified by silica gel column chromatography (eluting with CH_2Cl_2/hexane). Yield: 60.1 mg, 93%; Mp. 165-166 °C. ^{1}H NMR (400 MHz; $CDCl_3$): 7.49-7.47 (m, 3H), 7.29-7.27(m, 2H), 5.98 (s, 2H), 2.56 (s, 6H), 1.37 (s, 6H); ^{13}C NMR (100 MHz; $CDCl_3$): 154.90, 142.19, 140.52, 131.14, 123.79, 121.11, 17.24, 14.55; HRMS (ESI): *m/z* Calcd for $C_{19}H_{20}BF_2N_2$: 324.1718; found: 324.1717. UV/vis (CH_2Cl_2) λ_{max} (ε) 501 nm (57500).

***BODIPY 86*:** *Method A*: In a Sonogashira coupling reaction, 8-chloro-BODIPY **74** (56.4 mg, 0.2 mmol), $Pd(PPh_3)_2Cl_2$ (7.0 mg, 5% mmol), ethynyltrimethylsilane (21.6 mg, 0.22 mmol), TEA (10.0 ml) and THF (10.0 ml) were mixed together and the reaction flask was flushed with argon several times. Then the solution was refluxed overnight under argon. Before the solvent was removed, the residue was taken up in $CHCl_3$ and washed with water, aqueous 1 M HCl, water and brine, and then the organic layer was dried over anhydrous Na_2SO_4. The solvent was removed and the product was purified by silica gel column chromatography (eluting with CH_2Cl_2/hexane), and the product was isolated as a deep red solid (22.6 mg, 35%).

Method B: In a Stille coupling reaction,8-chloro-BODIPY **74** (25.0, 0.088 mmol), $Pd(PPh_3)_4$ (4.6 mg, 5% mmol) and TMS-ethynyltin (41.0 mg, 0.11 mmol) were added to a round-bottomed flask. The flask was flushed with argon and then anhydrous toluene (20 ml) was added and the mixture was refluxed for 5 h, after which the reaction was completed; the toluene was then removed and the residue was taken up in CH_2Cl_2 and washed with water, brine and then dried over anhydrous Na_2SO_4. The crude product was purified by silica gel column chromatography (eluting with CH_2Cl_2/hexane).Yield: (21.7 mg, 71%); Mp. dec. ~250 °C; ^{1}H NMR (400 MHz; $CDCl_3$): 6.06 (s, 2H), 2.52 (s, 6H), 2.46 (s, 6H), 0.29 (s, 9H); ^{13}C NMR (100 MHz; $CDCl_3$): 154.40, 142.23, 133.05, 120.78, 120.05, 115.01, 110.44, 15.54, 14.61, 0.68; HRMS (ESI): *m/z* Calcd for $C_{18}H_{23}BFN_2Si$: 325.1708 (M^+-F); found: 325.1699; UV/vis (CH_2Cl_2) λ_{max} (ε) 545 nm (42500).

BODIPY 87: 8-Chloro-BODIPY **74** (25 mg, 0.088 mmol) and $Pd(PPh_3)_4$ (5.0 mg, 5% mmol) was dissolved in anhydrous THF (20 ml). Then the mixture was cooled to 0 ^{o}C and 1 M phenylethynyl magnesium bromide (0.264 mmol, 0.26 ml) was added and the reaction was refluxed for 5 min and the entire solution turned red. The mixture was cooled to room temperature and quenched with aqueous NH_4Cl solution and then extracted with CH_2Cl_2 or $CHCl_3$ (three times) and the combined organic layers were washed with water, brine and dried over anhydrous Na_2SO_4, The solvent was removed and the product was purified by silica gel column chromatography (eluting with CH_2Cl_2/hexane) to give the product. ^{1}H NMR (400 MHz; $CDCl_3$): 7.39-7.19 (m, 15H), 6.18 (s, 2H), 2.88 (s, 6H), 2.62(s, 6H).

General procedure for Stille coupling reactions

8-Chloro-BODIPY **74** (56.4 mg, 0.2 mmol), $Pd(PPh_3)_4$ (10.0 mg, 5% mmol) and organotin reagent (2.4-3.0 mmol) were added to a round bottom flask. The flask was

flushed with argon and then anhydrous toluene was added, followed by injection of the Stille reagents. The mixture was refluxed for 5 h after which the reaction was completed; the toluene was then removed and the residue was taken up in CH_2Cl_2 and washed with water, brine and then dried over anhydrous Na_2SO_4. The crude product was purified by column chromatography on silica gel (eluting with CH_2Cl_2/hexane).

BODIPY 88: Yield: 50.7 mg, 97%; Mp 245-247 °C; ^{1}H NMR (400 MHz; $CDCl_3$): δ = 6.05 (s, 2H), 2.56 (s, 6H), 2.51 (s, 6H), 2.40 (s, 3H); ^{13}C NMR (100 MHz; $CDCl_3$): δ = 153.59, 141.43, 141.01, 132.06, 121.25, 17.31, 16.37, 14.43; HRMS (ESI): *m/z* Calcd for $C_{14}H_{18}BF_2N_2$: 262.1562; found: 262.1556; UV/vis (CH_2Cl_2) λ_{max} (ε) 487 nm (66000).

BODIPY 89: Yield: 50.7 mg, 97%; Mp 245-247 °C; ^{1}H NMR (400 MHz; $CDCl_3$): δ = 6.05 (s, 2H), 2.56 (s, 6H), 2.51 (s, 6H), 2.40 (s, 3H); ^{13}C NMR (100 MHz; $CDCl_3$): δ = 153.59, 141.43, 141.01, 132.06, 121.25, 17.31, 16.37, 14.43; HRMS (ESI): *m/z* Calcd for $C_{14}H_{18}BF_2N_2$: 262.1562; found: 262.1556; UV/vis (CH_2Cl_2) λ_{max} (ε) 487 nm (66000).

BODIPY 90: Yield: 59.1 mg, 93%; Mp. 105-107 °C; ^{1}H NMR (400 MHz; $CDCl_3$): δ = 6.03 (s, 2H), 4.46 (d, *J* = 2.9 Hz, 1H), 4.37 (d, *J* = 2.8 Hz, 1H), 3.89 (q, *J* = 7.0 Hz, 2H), 2.52 (s, 6H), 2.23 (s, 6H), 1.39 (t, *J* = 7.0 Hz, 3H); ^{13}C NMR (100 MHz; $CDCl_3$): δ = 155.97, 153.56, 142.50, 134.98, 131.29, 88.11, 63.67, 14.65, 14.34; HRMS (ESI): *m/z* Calcd for $C_{17}H_{22}BF_2N_2O$: 318.1824; found: 318.1817; UV/vis (CH_2Cl_2) λ_{max} (ε) 513 nm (40700).

BODIPY 91: Yield: 16.8 mg, 31%; Mp. > 260 °C; ^{1}H NMR (400 MHz; $CDCl_3$): δ = 6.07 (s, 2H), 3.92 (s, 1H), 2.53 (s, 6H), 2.45 (s, 6H); ^{13}C NMR (100 MHz; $CDCl_3$): δ = 155.07, 142.61, 133.28, 121.06, 118.92, 94.42, 79.19, 15.47, 14.63; HRMS (ESI): *m/z* Calcd for $C_{15}H_{16}BF_2N_2$: 272.1405; found: 272.1380; UV/vis (CH_2Cl_2) λ_{max} (ε) 544 nm (37200).

BODIPY 92: Yield: 62.1 mg, 95%; Mp 179-181 °C; ^{1}H NMR (400 MHz; $CDCl_3$): δ = 6.77 (dd, *J* = 2.7, 1.7 Hz, 1H), 6.21 (dd, *J* = 3.6, 2.7 Hz, 1H), 6.07 (dd, *J* = 3.6, 1.7 Hz,1H), 6.01 (s, 2H), 3.40 (s, 3H), 2.55 (s, 6H), 1.50 (s, 6H); ^{13}C NMR (100 MHz; $CDCl_3$): δ 156.14, 143.34, 133.13, 131.73, 124.64, 122.47, 121.01, 109.34, 108.84, 33.84, 14.67, 12.68; HRMS (ESI): *m/z* calcd for $C_{18}H_{21}BF_2N_2$: 327.1827; UV/vis (CH_2Cl_2) λ_{max} (ε) 513 nm (53700).

BODIPY 93: Yield: 69.8 mg, 99%; Mp 197-199 °C; ^{1}H NMR (400 MHz; $CDCl_3$): δ = 7.50 (dd, *J* = 5.0, 1.3 Hz, 1H), 7.13 (dd, *J* =5.1, 3.5 Hz, 1H), 6.99 (dd, *J* = 3.5, 1.3 Hz, 1H), 6.00 (s, 2H), 2.55 (s, 6H), 1.58 (s, 6H); ^{13}C NMR (100 MHz; $CDCl_3$): δ = 156.07, 143.50, 134.64, 133.99, 132.41, 127.81, 127.61, 127.41, 121.50, 14.64, 13.55; HRMS (ESI): *m/z* Calcd for $C_{17}H_{17}BF_2N_{2Na}S$ (M^++Na): 352.1102; found: 352.1094; UV/vis (CH_2Cl_2) λ_{max} (ε) 514 nm (74100).

4.5 Supporting Information

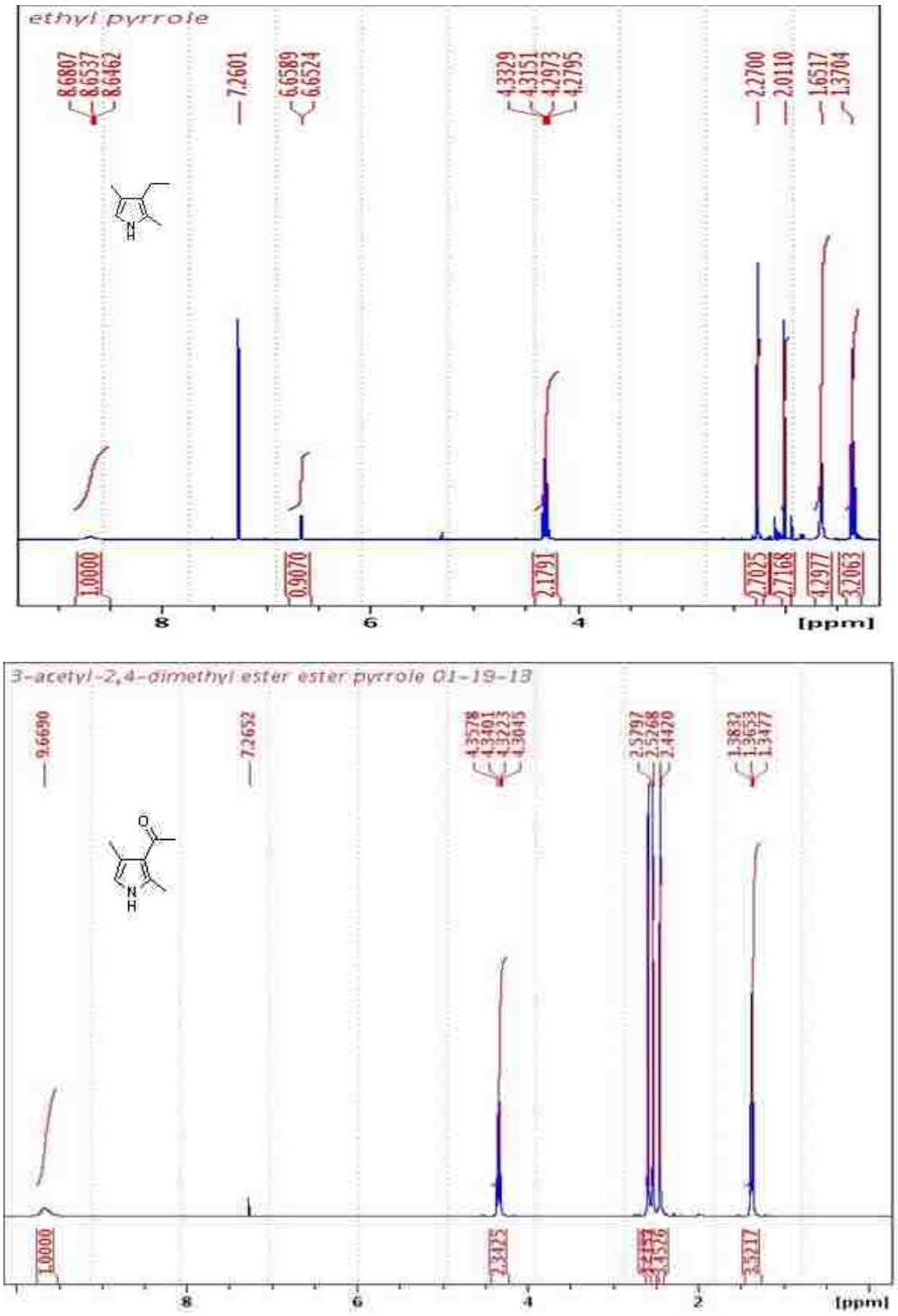

^{1}H-NMR spectra of pyrroles **44** and **54** in $CDCl_3$ at 400 MHz

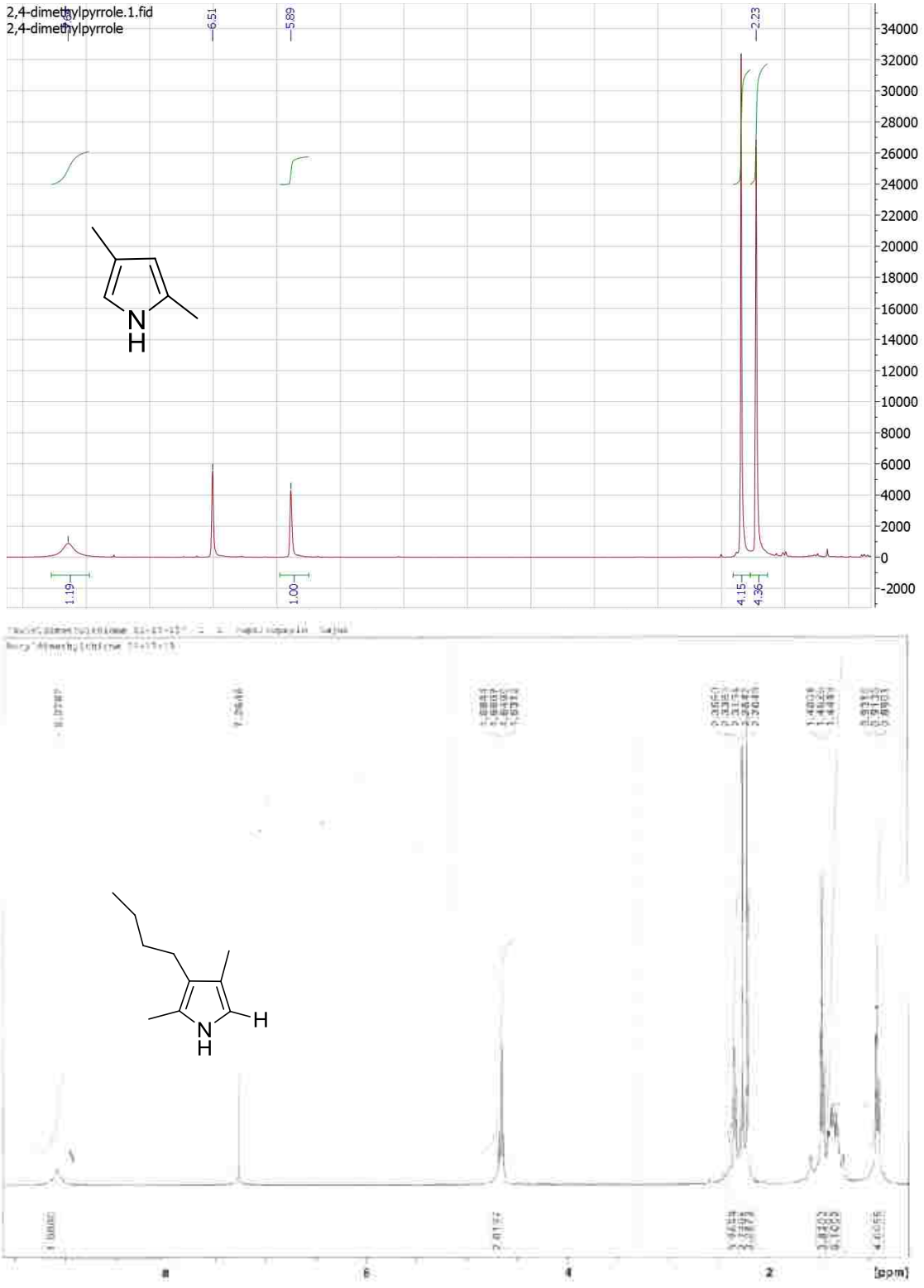

^{1}H-NMR spectra of pyrroles **41** and **43** in $CDCl_3$ at 400 MHz

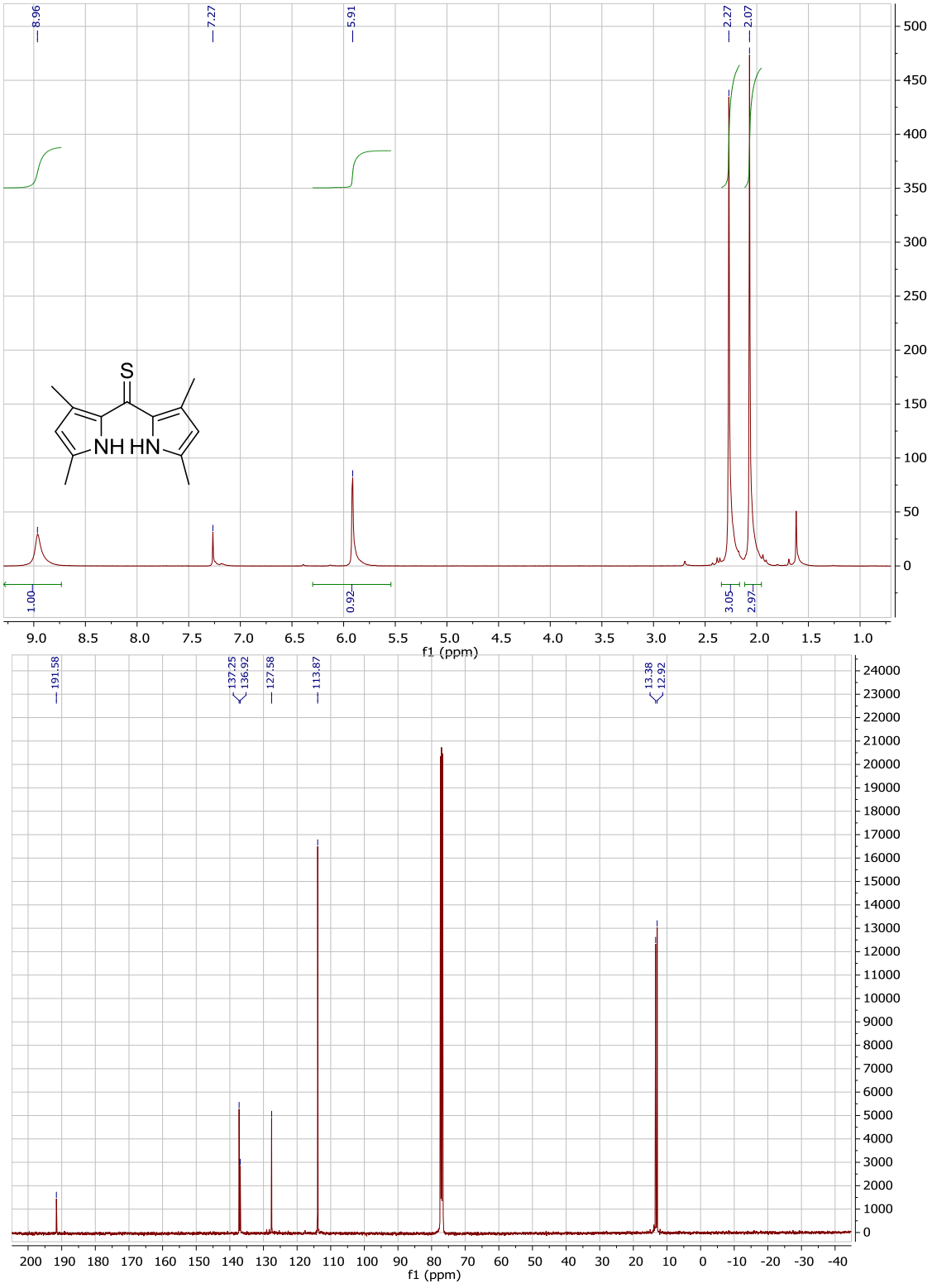

^{1}H- and ^{13}C-NMR spectra of dipyrrothione **55** in $CDCl_3$

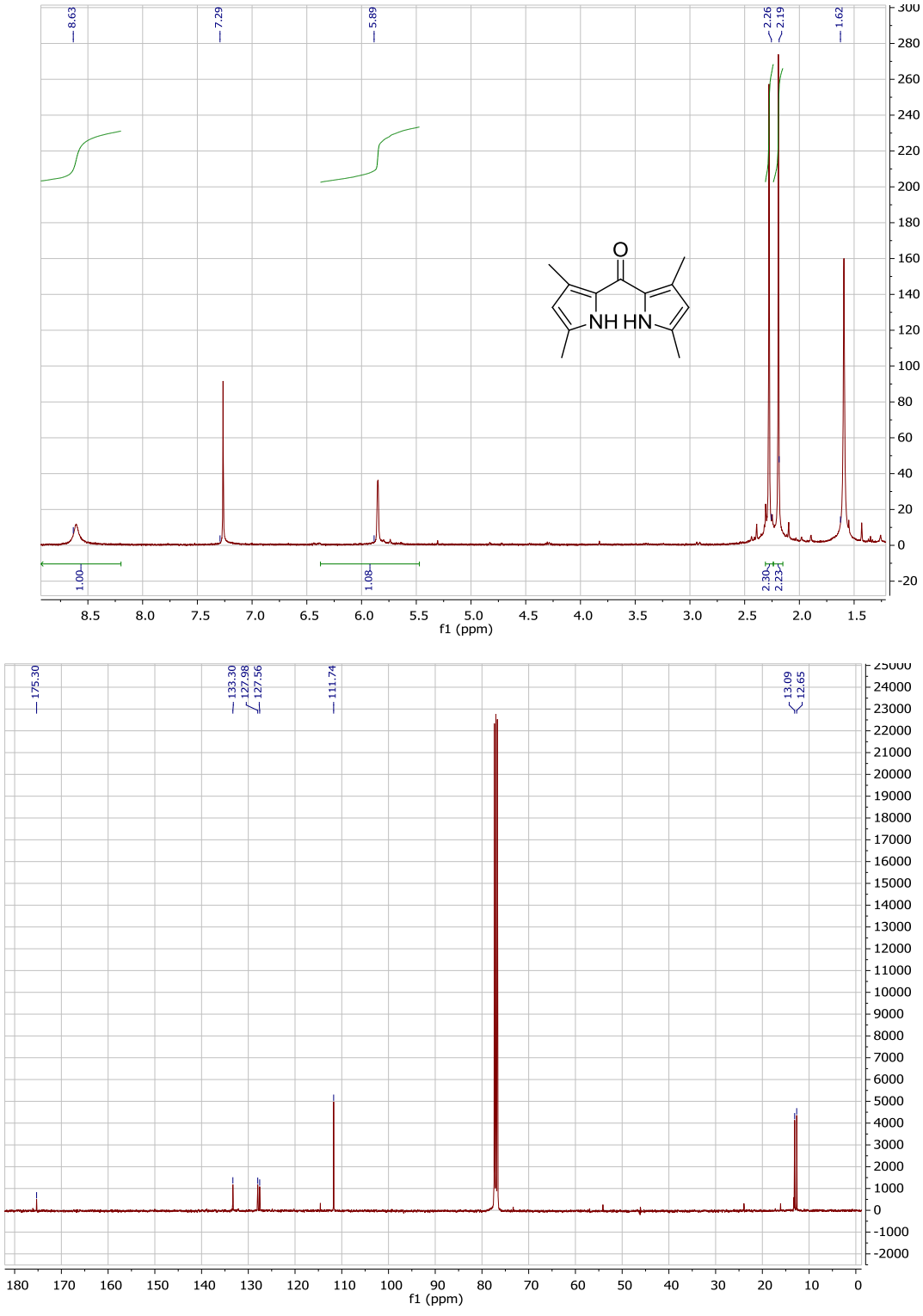

^{1}H- and ^{13}C-NMR spectra of dipyrroketone **59** in $CDCl_3$

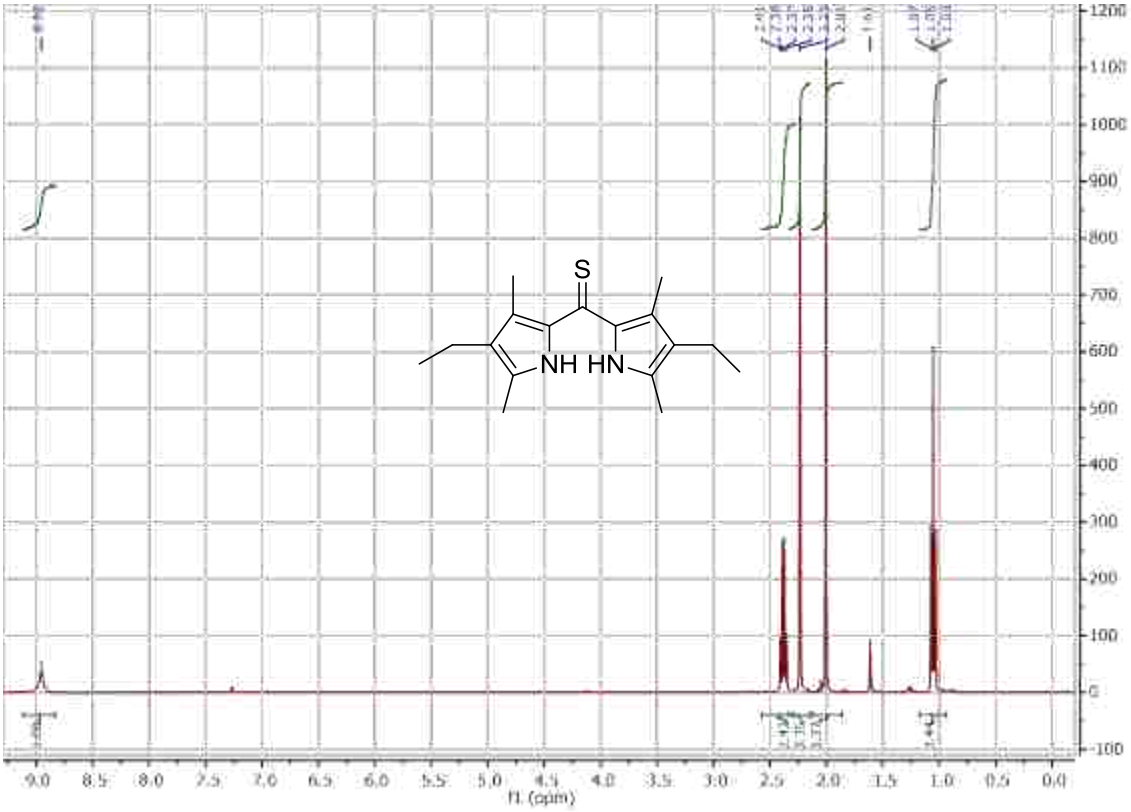

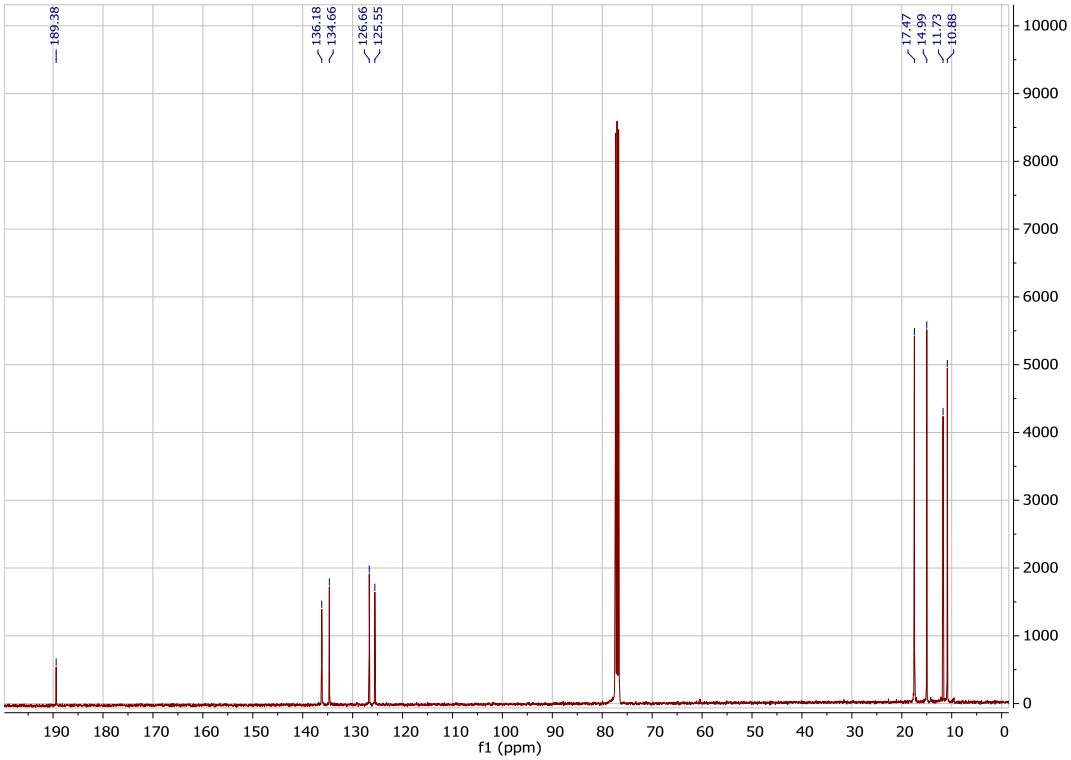

^{1}H- and ^{13}C-NMR spectra of dipyrrothione **58** in $CDCl_3$

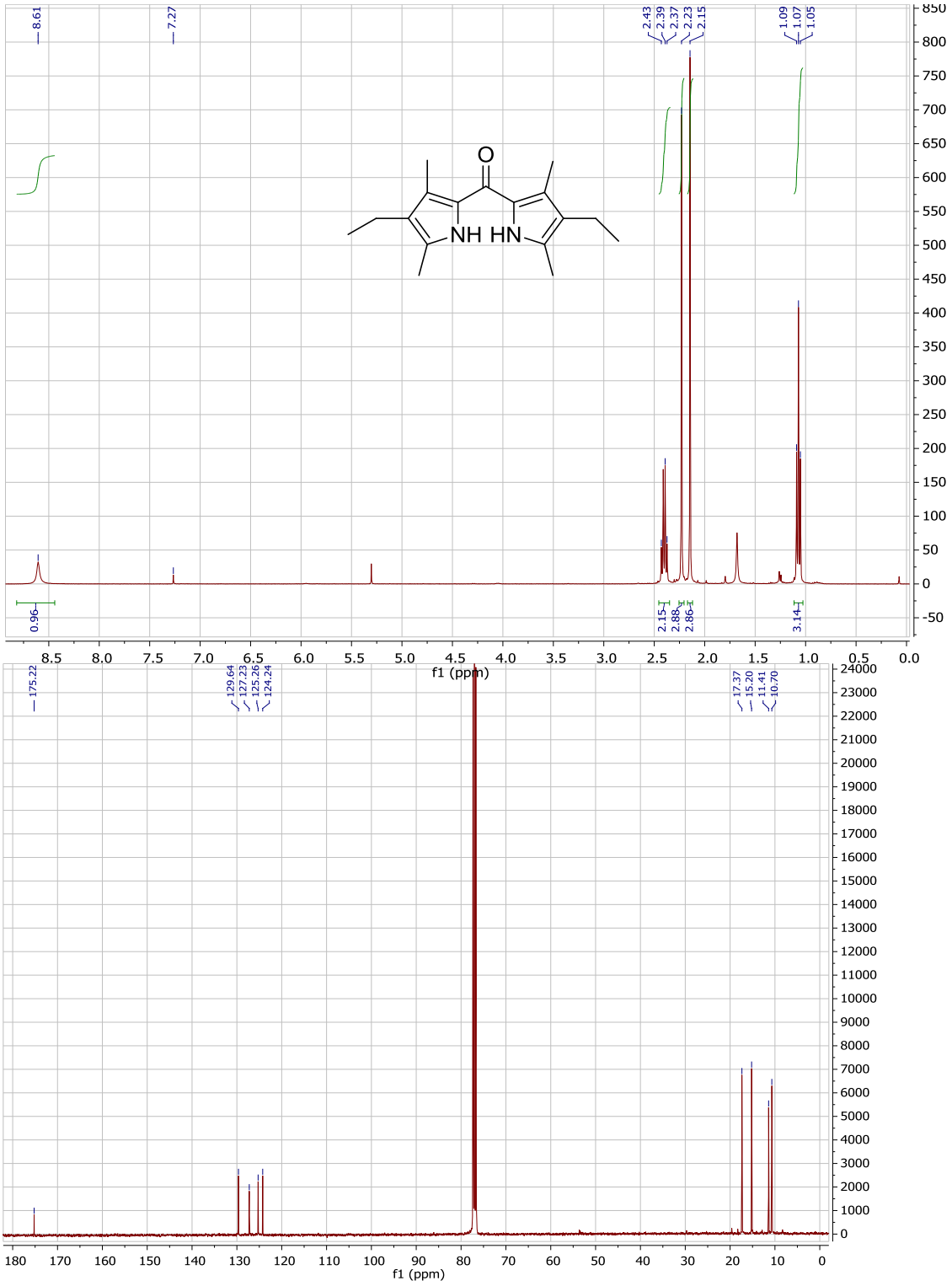

^{1}H- and ^{13}C-NMR spectra of dipyrroketone **60** in $CDCl_3$

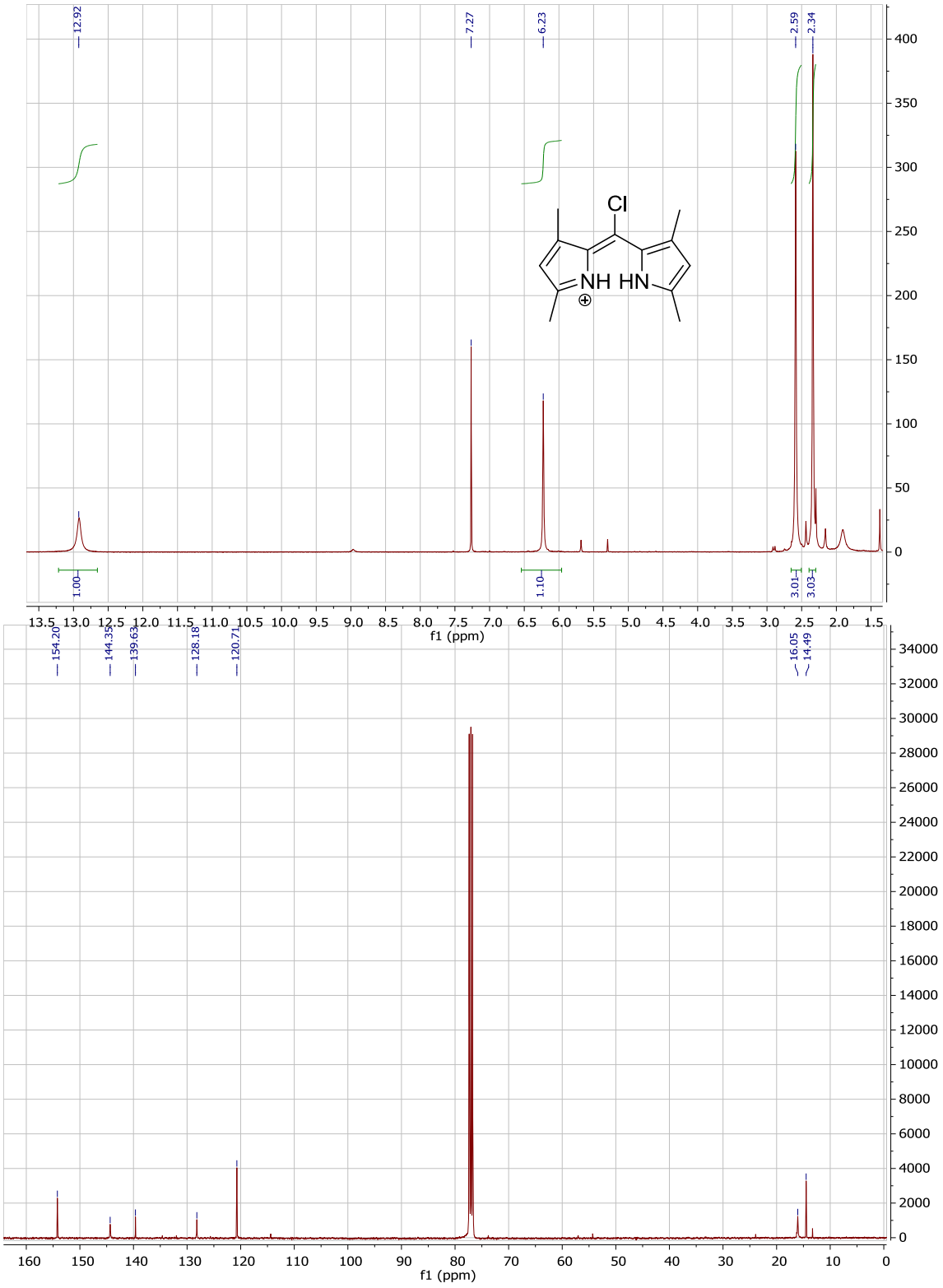

^{1}H- and ^{13}C-NMR spectra of meso-chloro-dipyrrin **65** in $CDCl_3$

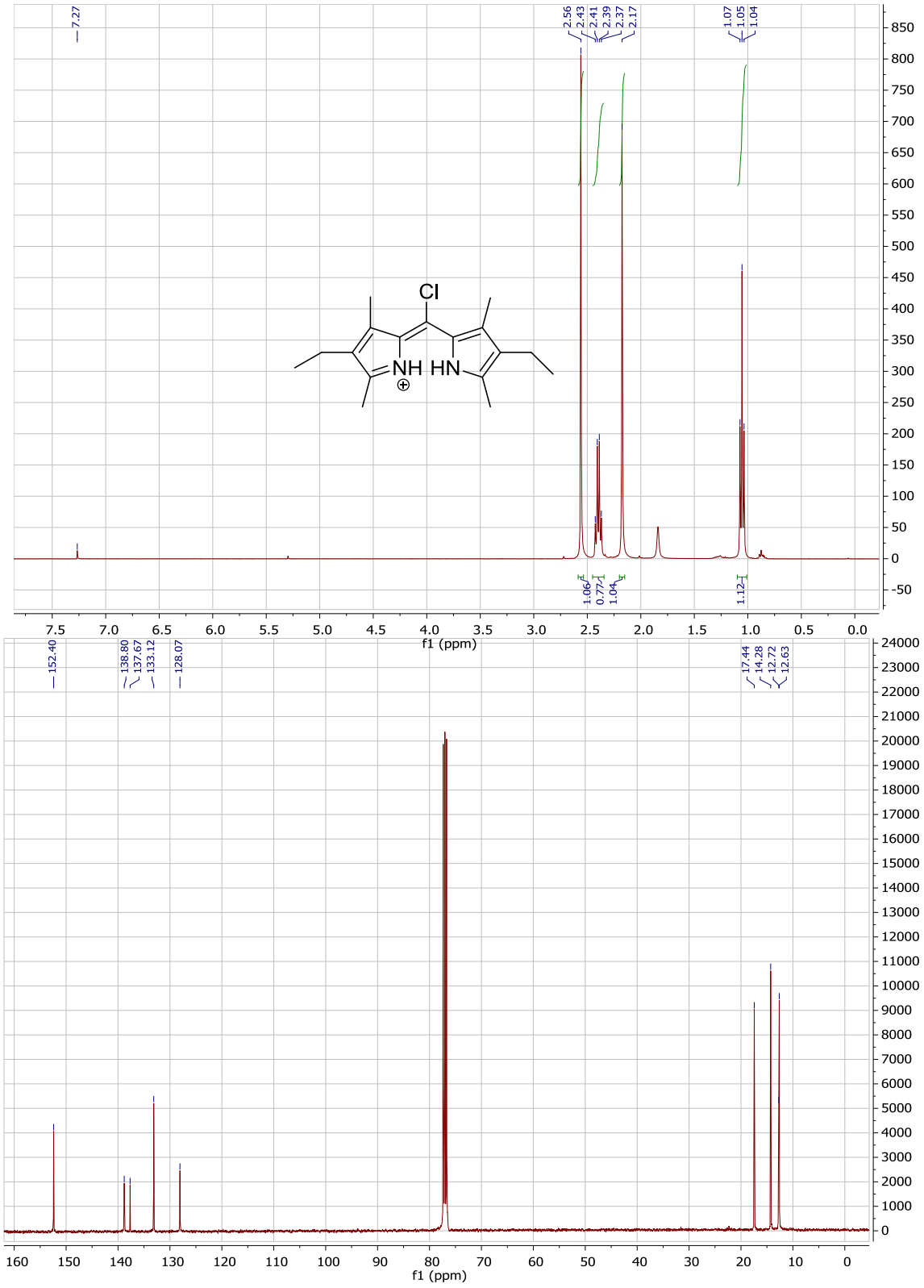

^{1}H- and ^{13}C NMR spectra of dipyrrothione **66** in $CDCl_3$

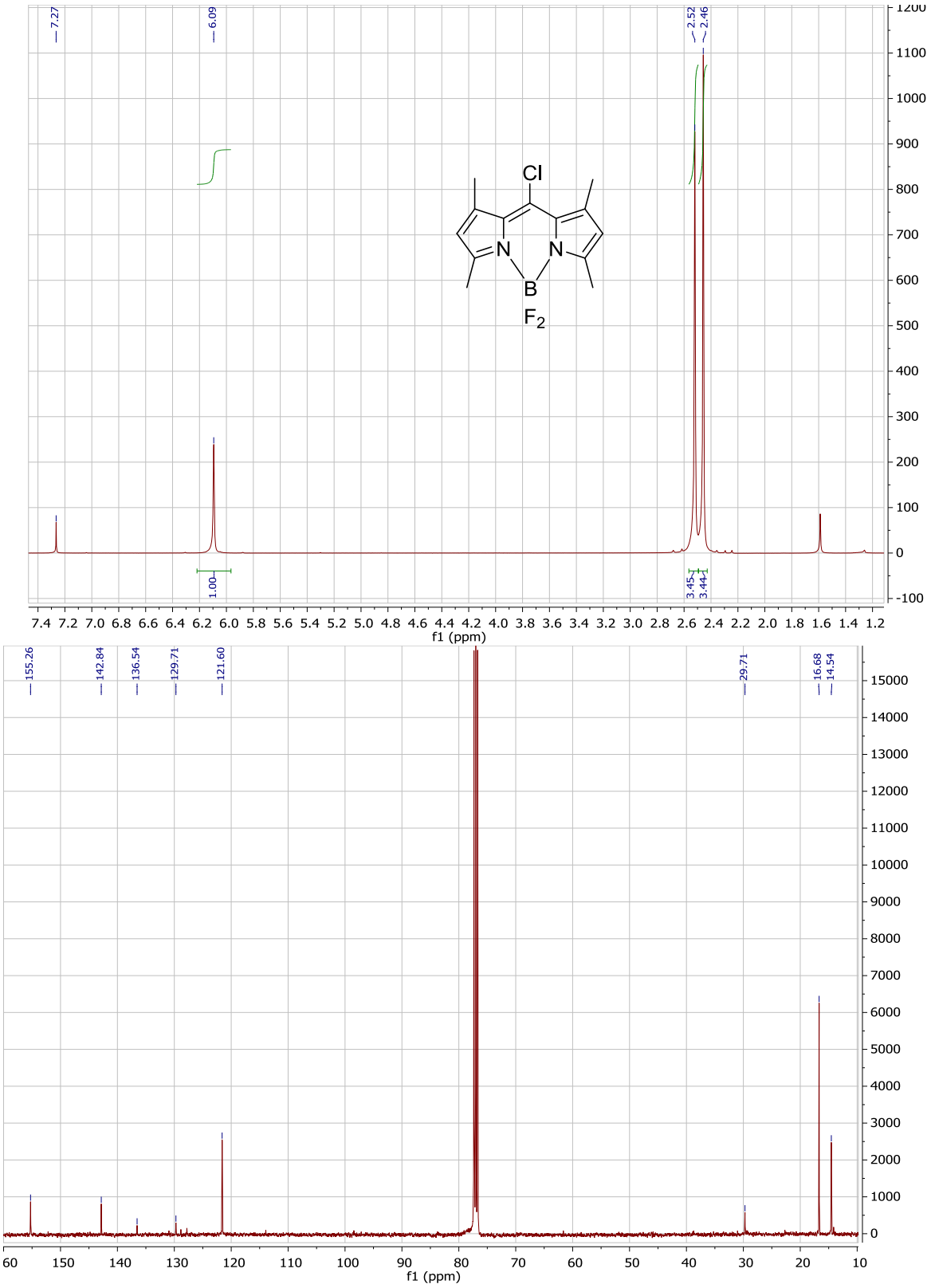

^{1}H- and ^{13}C-NMR spectra of BODIPY **74** in $CDCl_3$

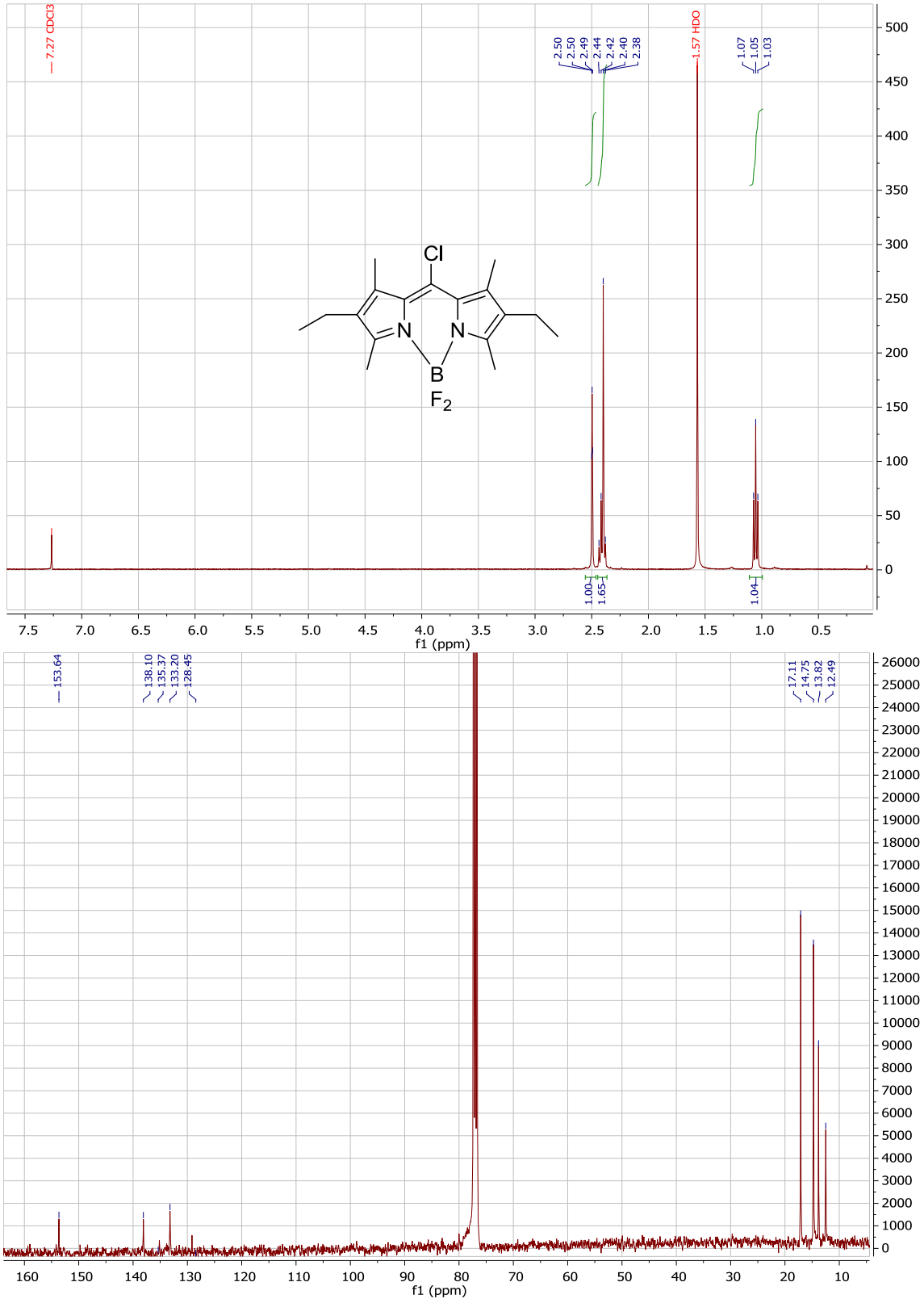

^{1}H- and ^{13}C-NMR spectra of BODIPY **75** in $CDCl_3$

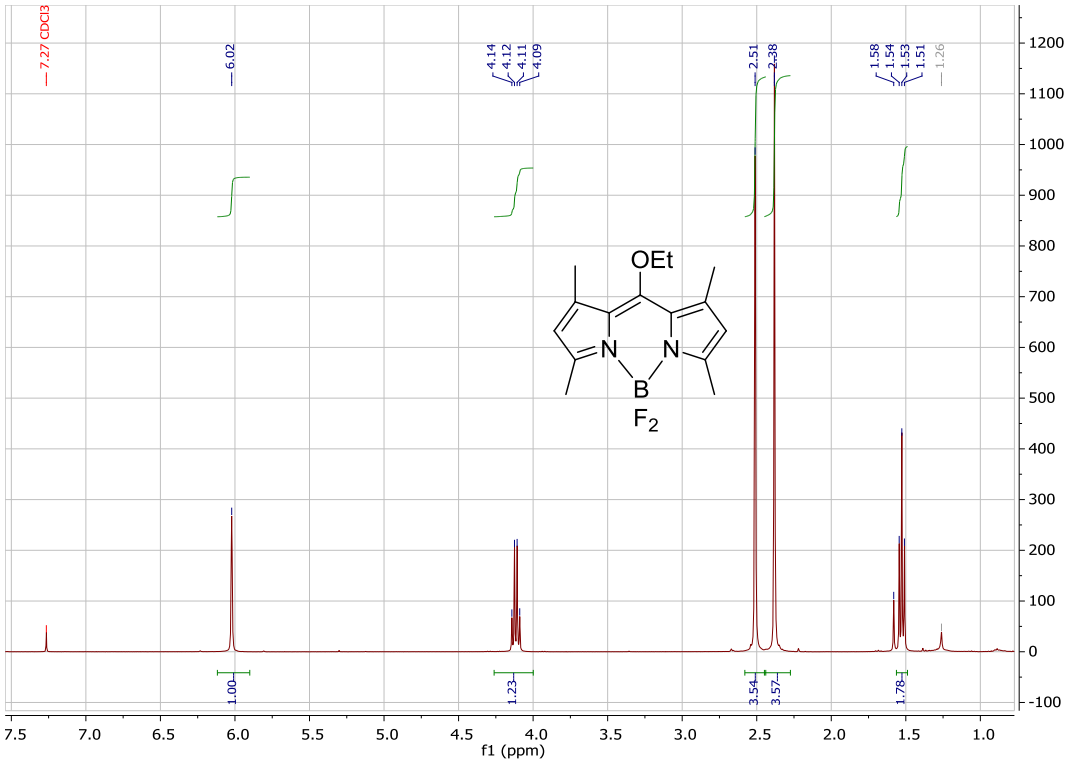

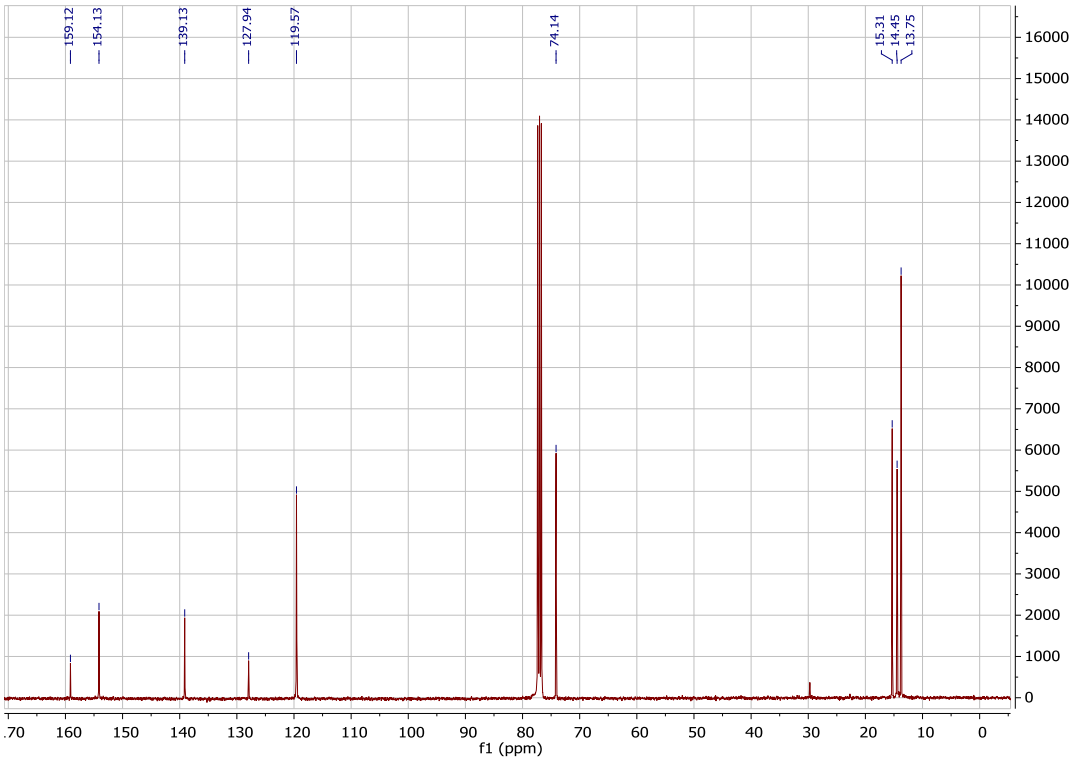

^{1}H- and ^{13}C-NMR spectra of BODIPY **63** in $CDCl_3$

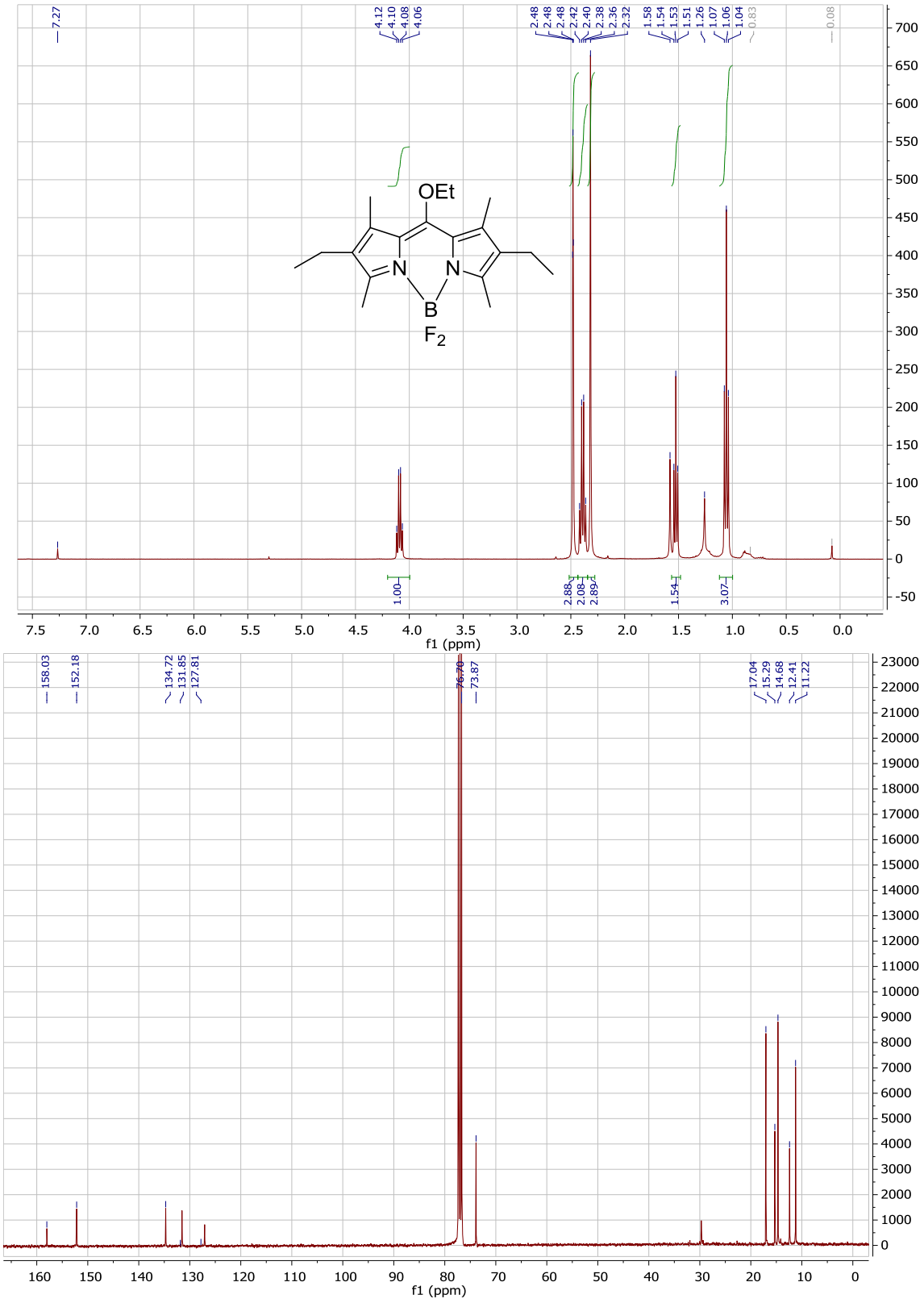

^{1}H- and ^{13}C-NMR spectra of BODIPY **64** in $CDCl_3$

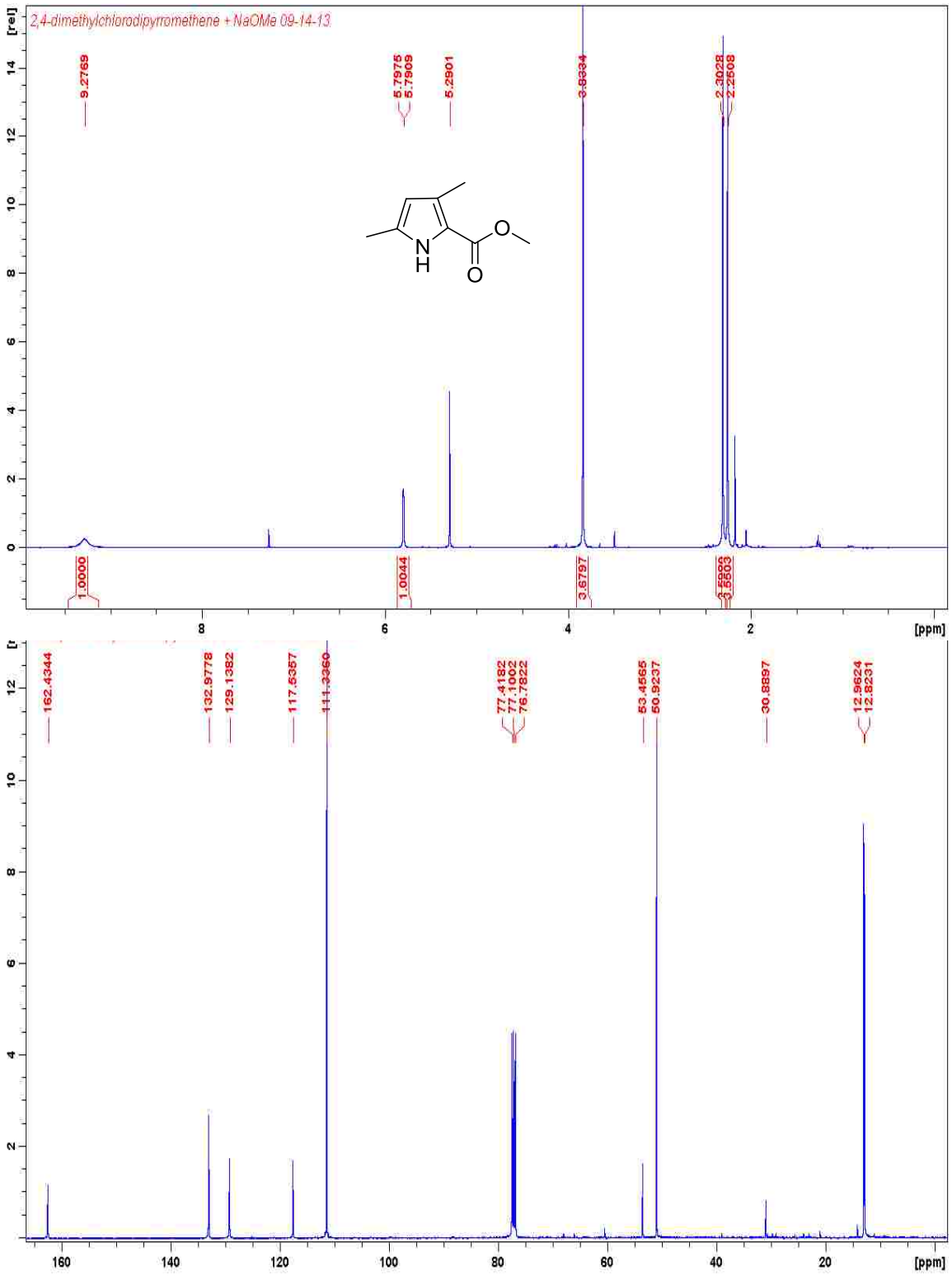

^{1}H- and ^{13}C-NMR spectra of unexpected pyrrole **72** in $CDCl_3$

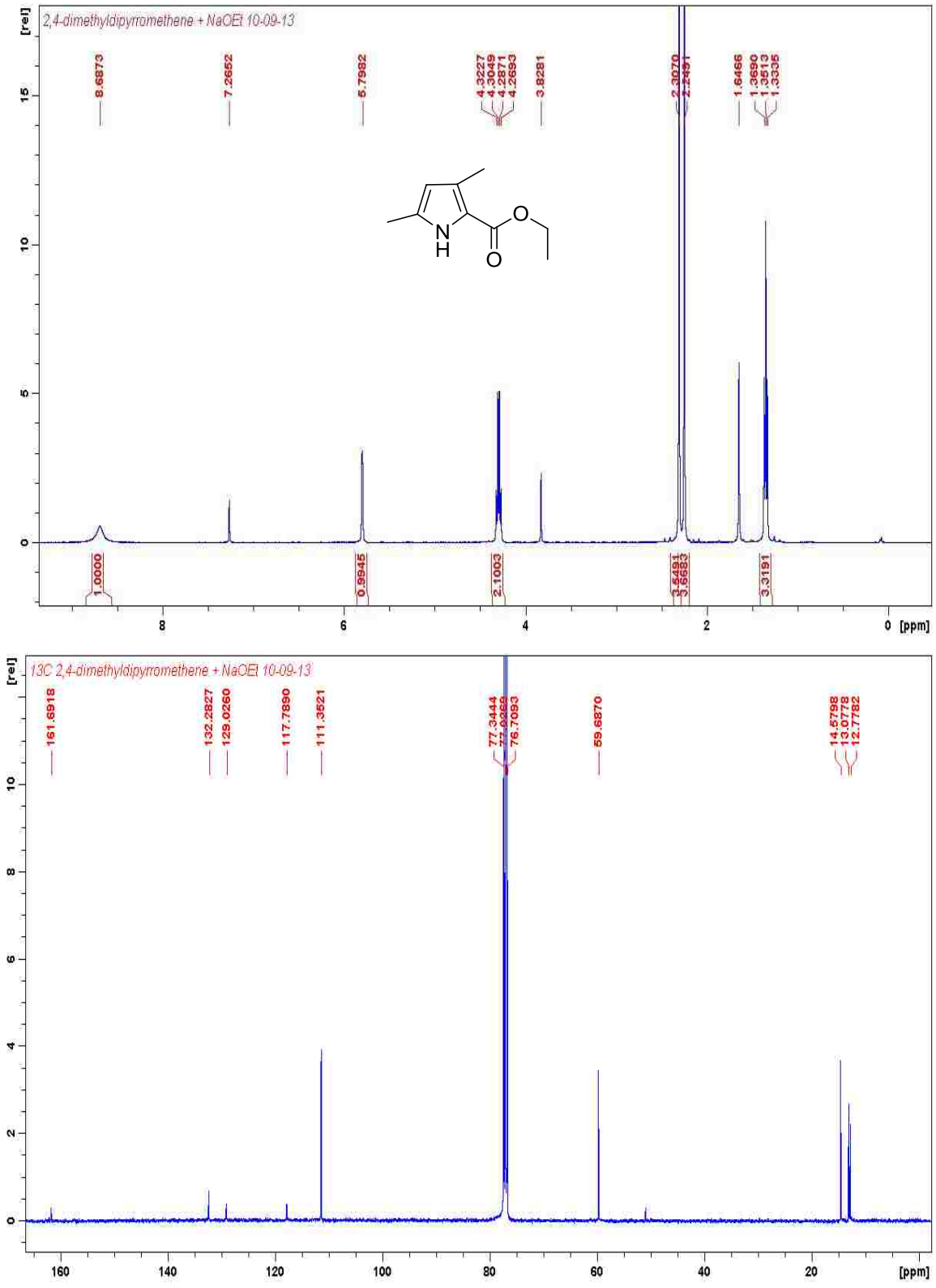

^{1}H- and ^{13}C-NMR spectra of unexpected pyrrole **73** in $CDCl_3$

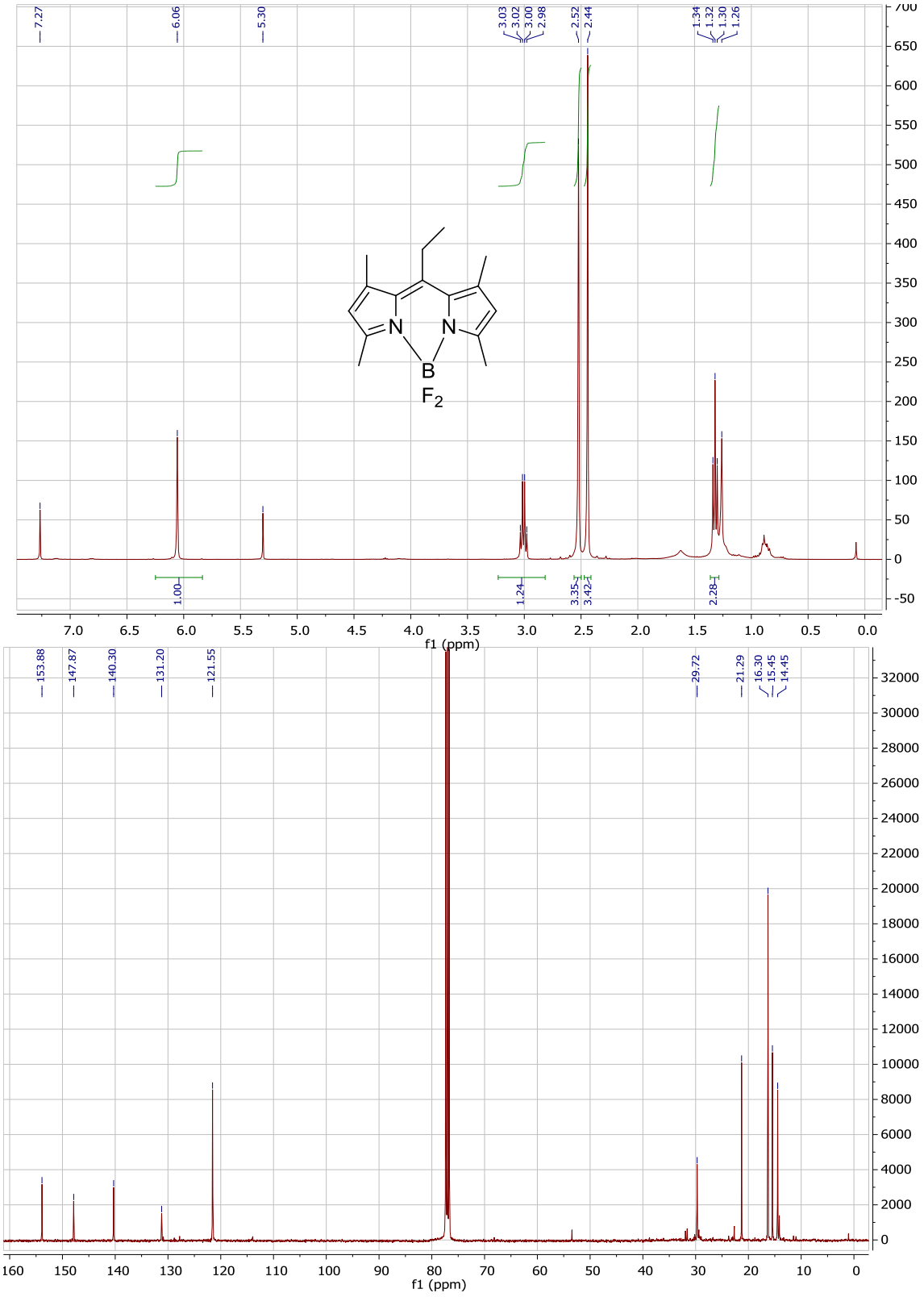

^{1}H- and ^{13}C-NMR spectra of BODIPY **69** in $CDCl_3$

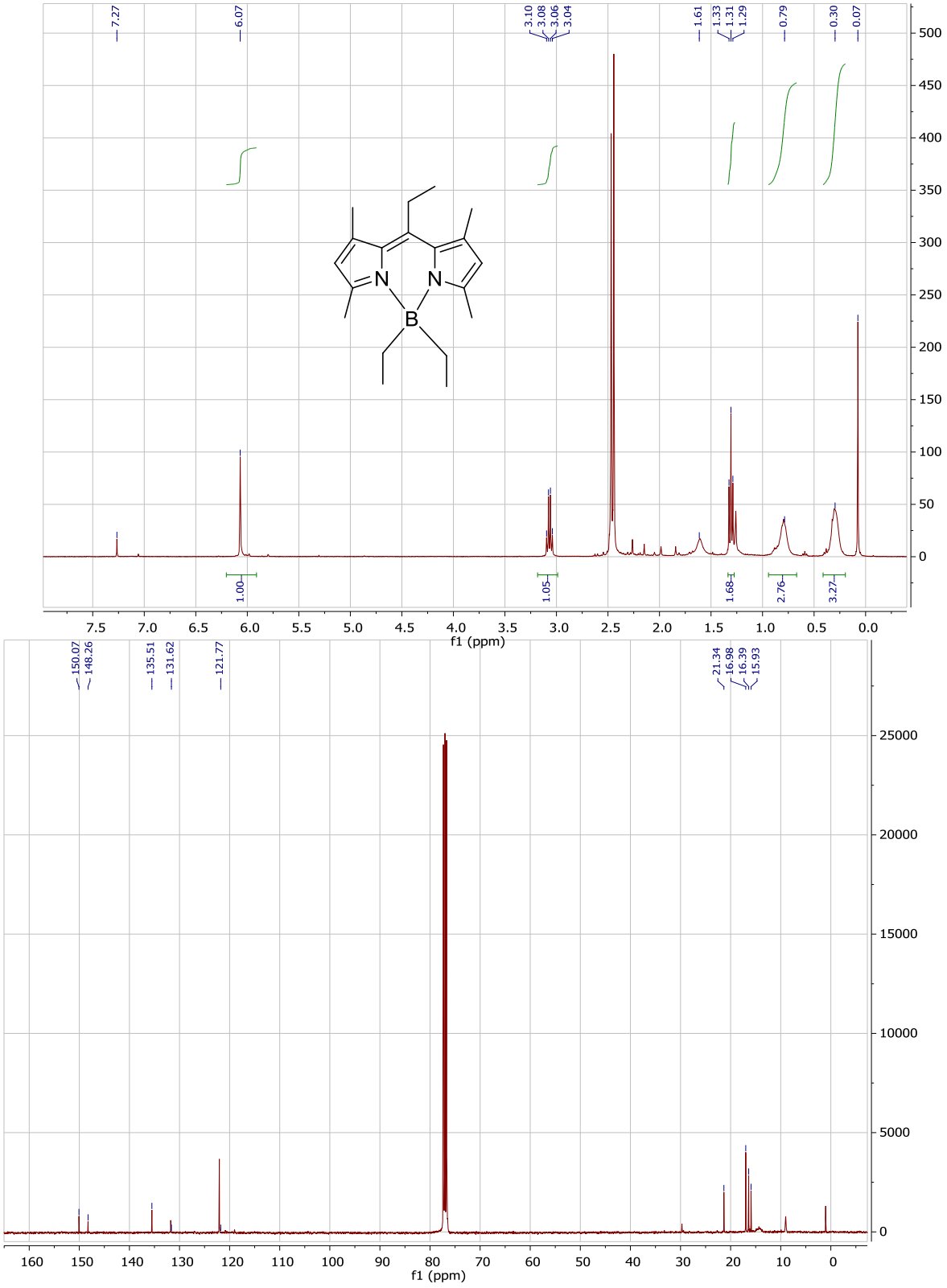

^{1}H- and ^{13}C-NMR spectra of BODIPY **76** in $CDCl_3$

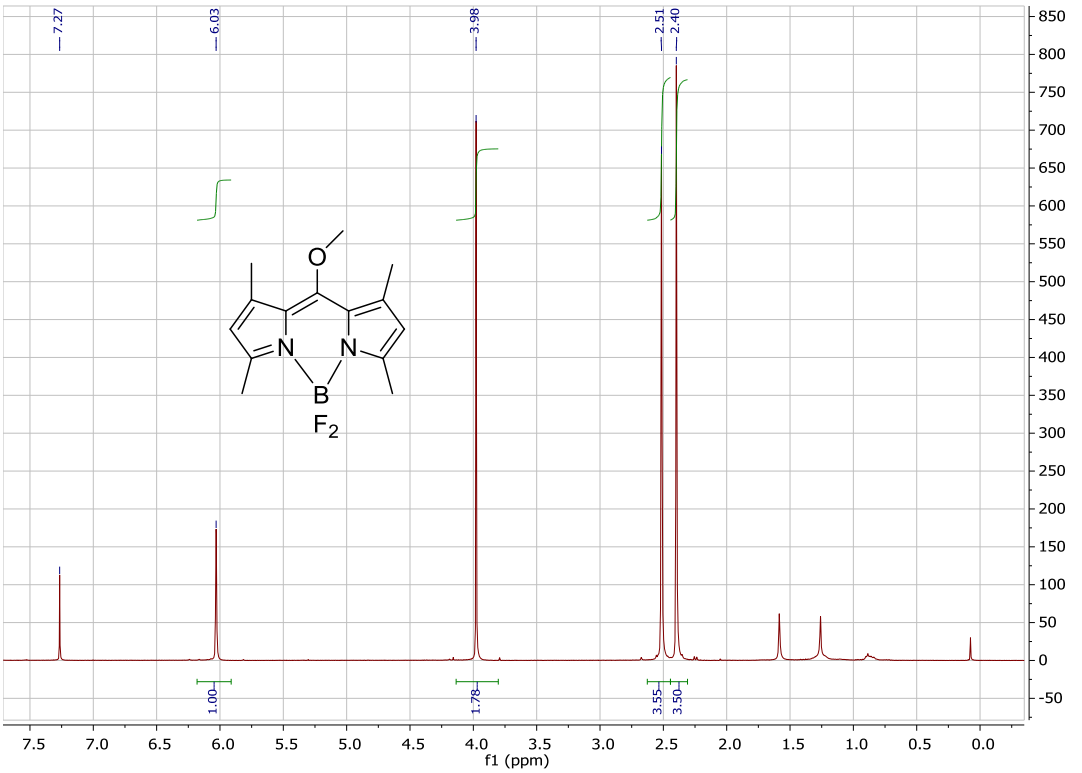

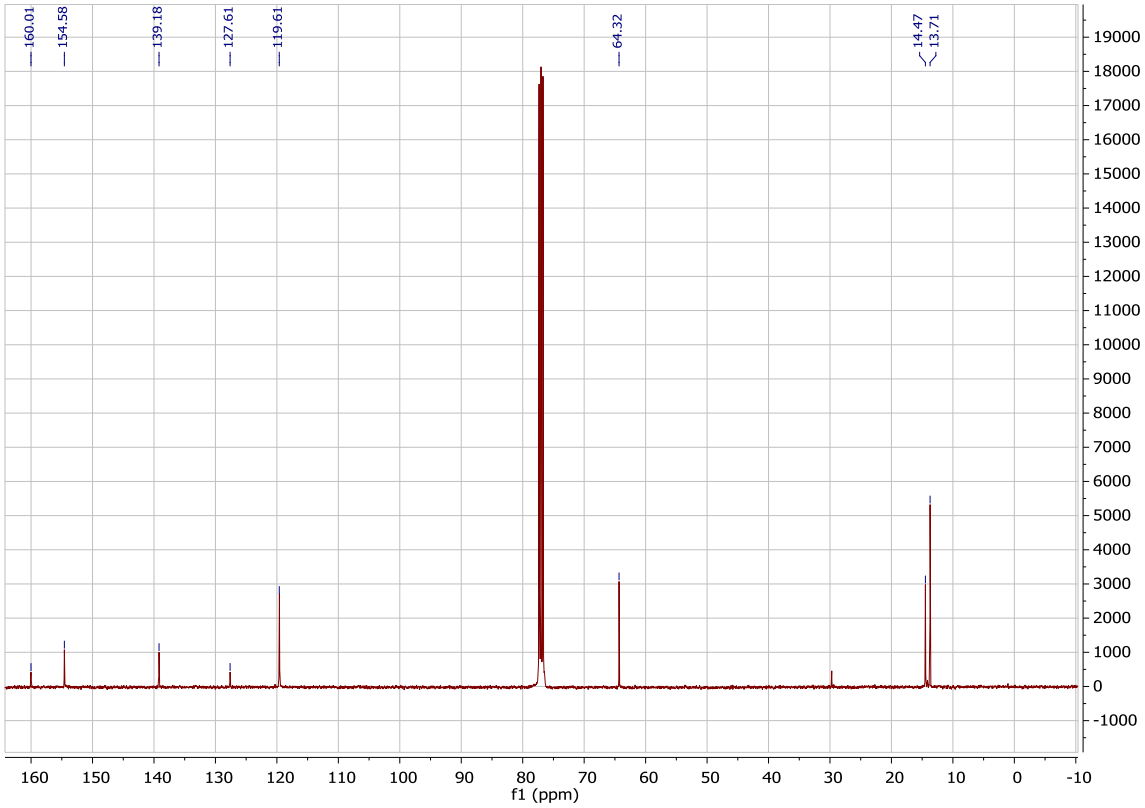

^{1}H- and ^{13}C-NMR spectra of BODIPY **77** in $CDCl_3$

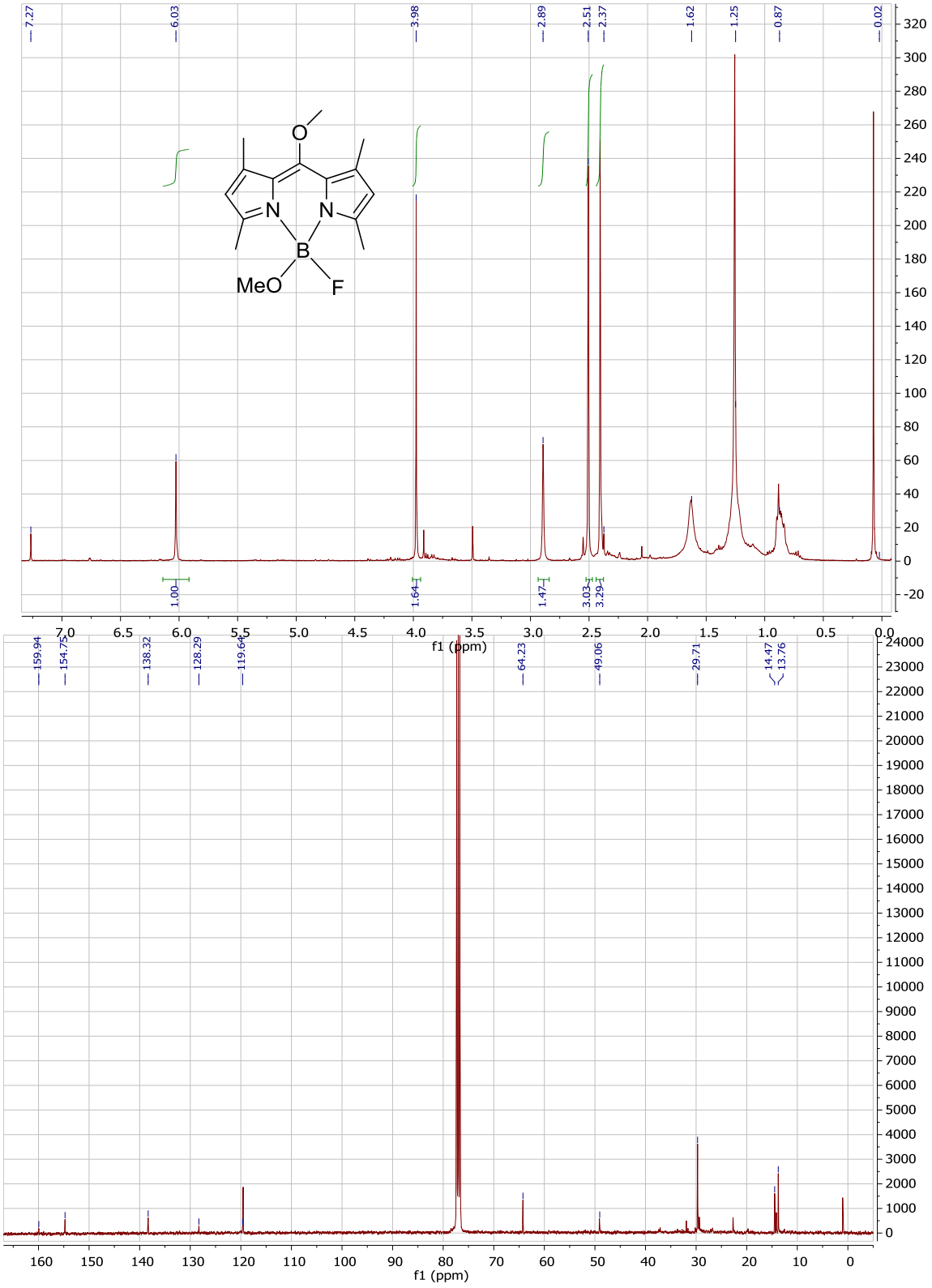

^{1}H- and ^{13}C-NMR spectra of BODIPY **78** in $CDCl_3$

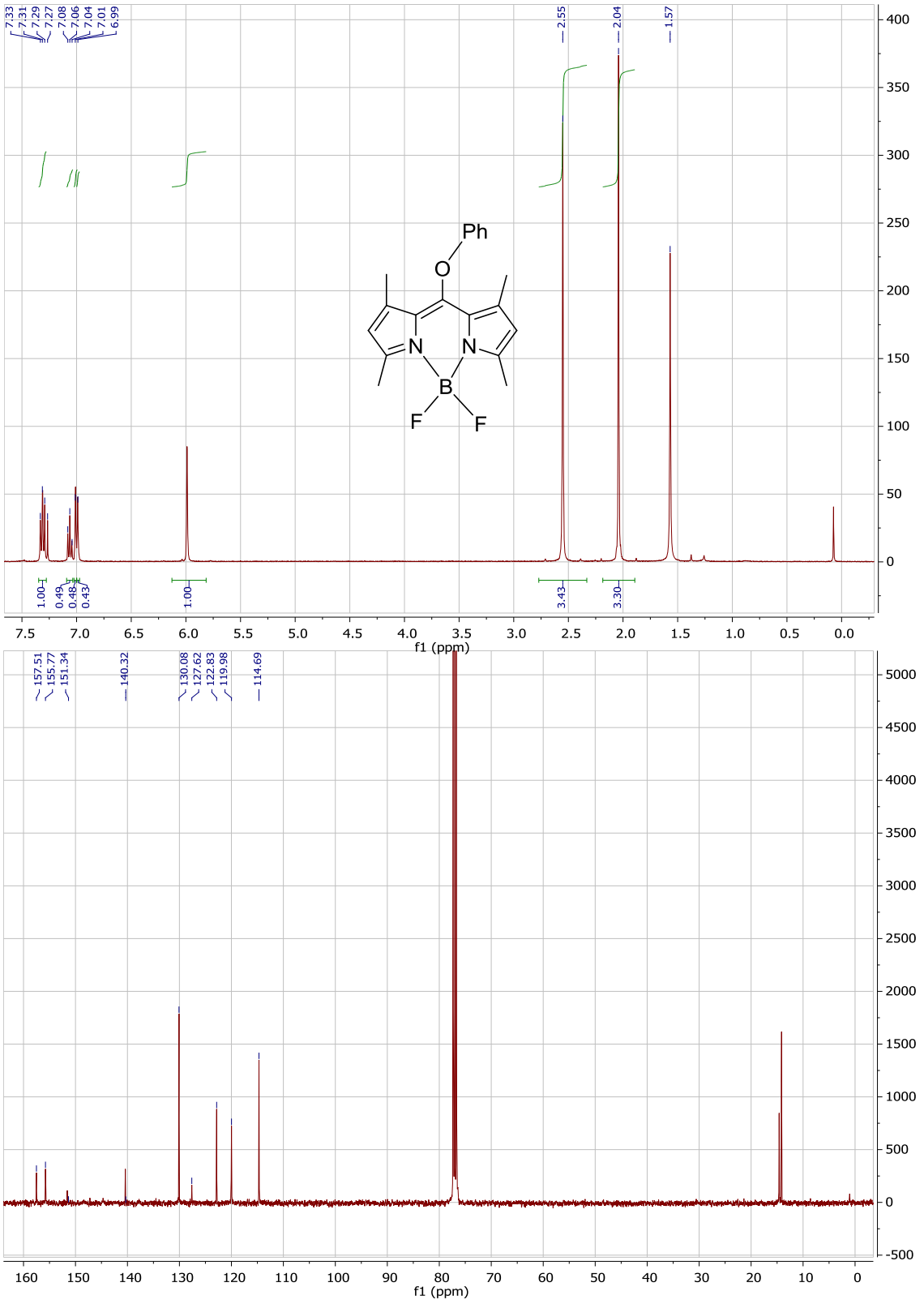

^{1}H- and ^{13}C-NMR spectra of BODIPY **80** in $CDCl_3$

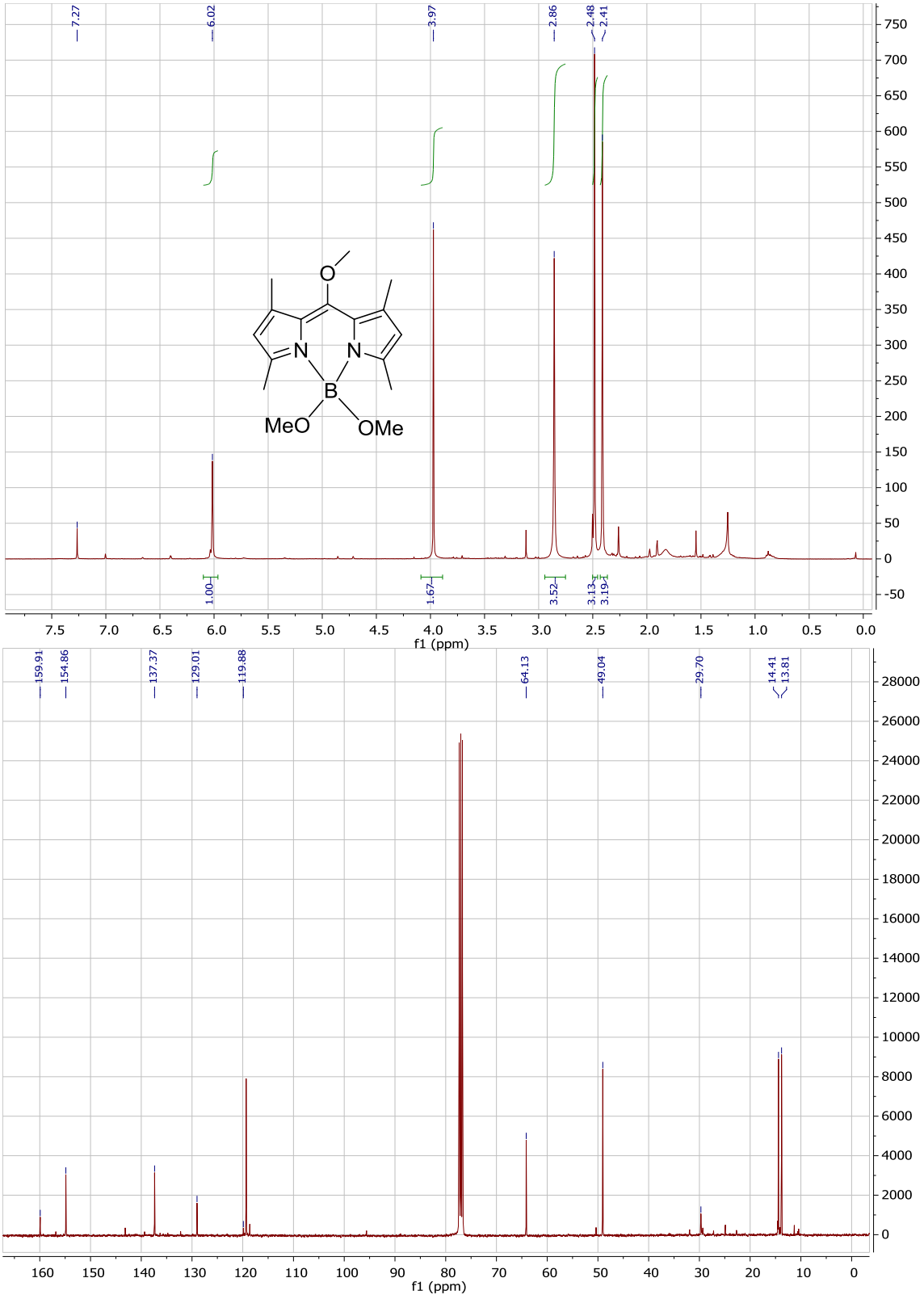

^{1}H- and ^{13}C-NMR spectra of BODIPY **79** in $CDCl_3$

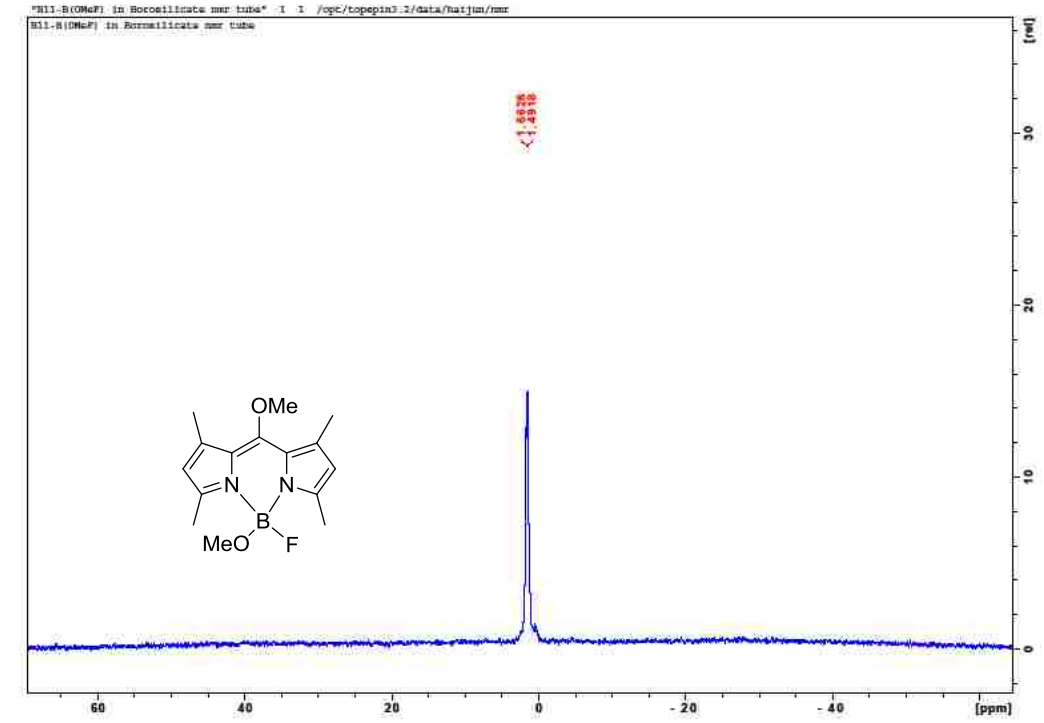

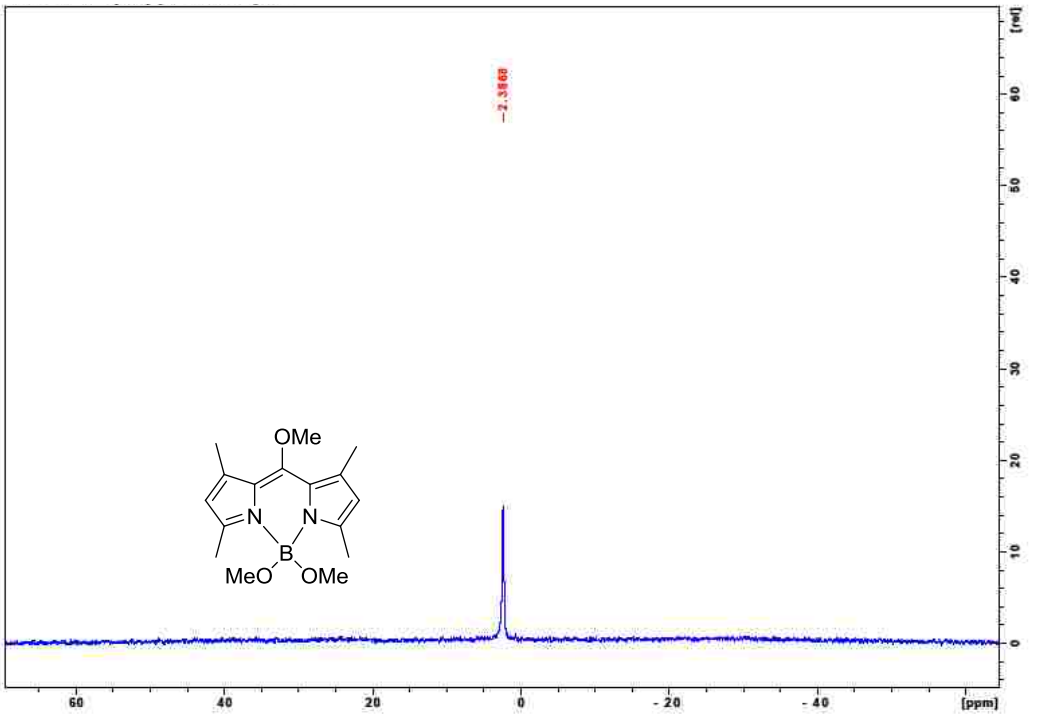

^{11}B-NMR spectra of BODIPYs **78** and **79** in $CDCl_3$

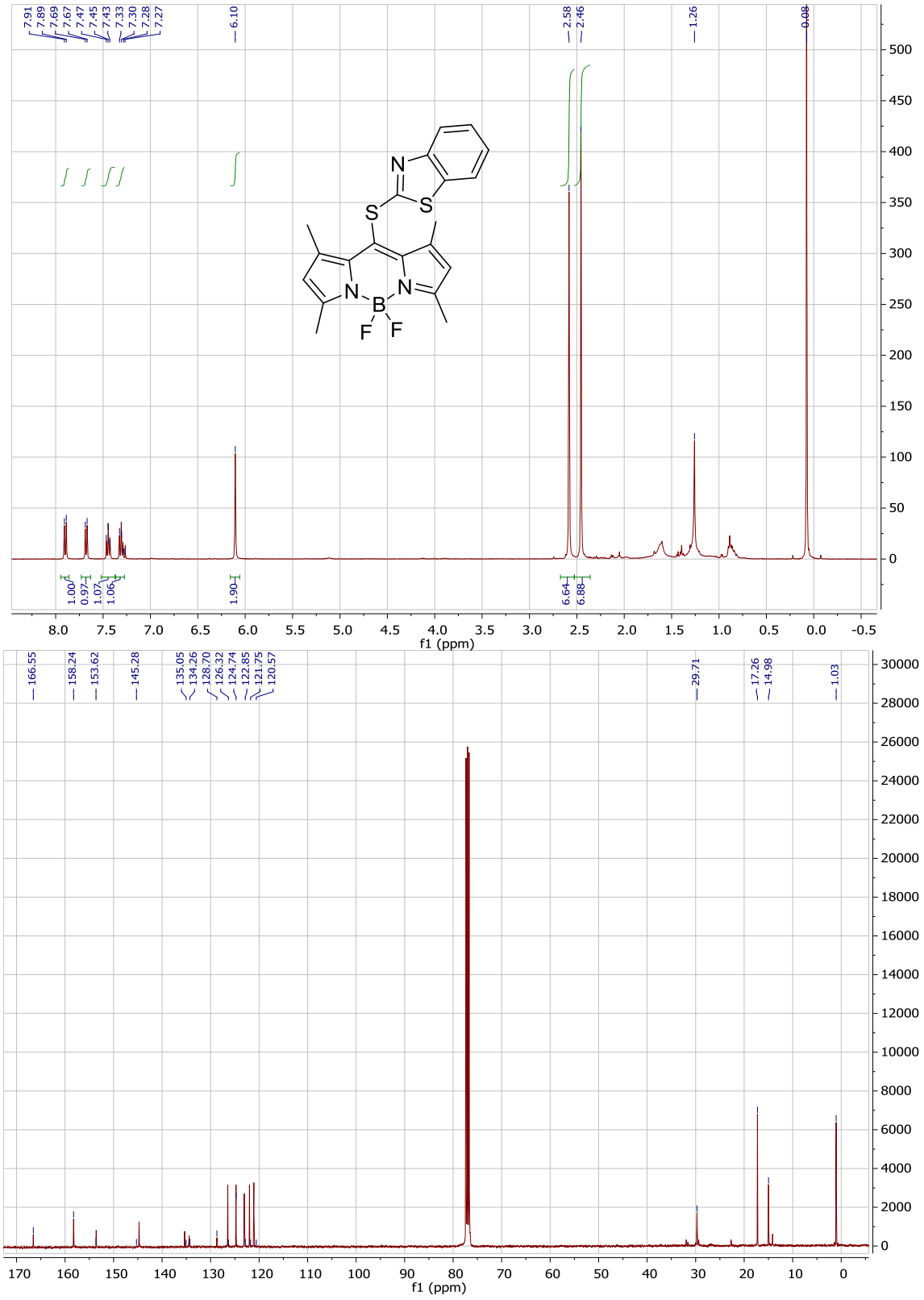

^{1}H- and ^{13}C-NMR of BODIPY **81** in $CDCl_3$

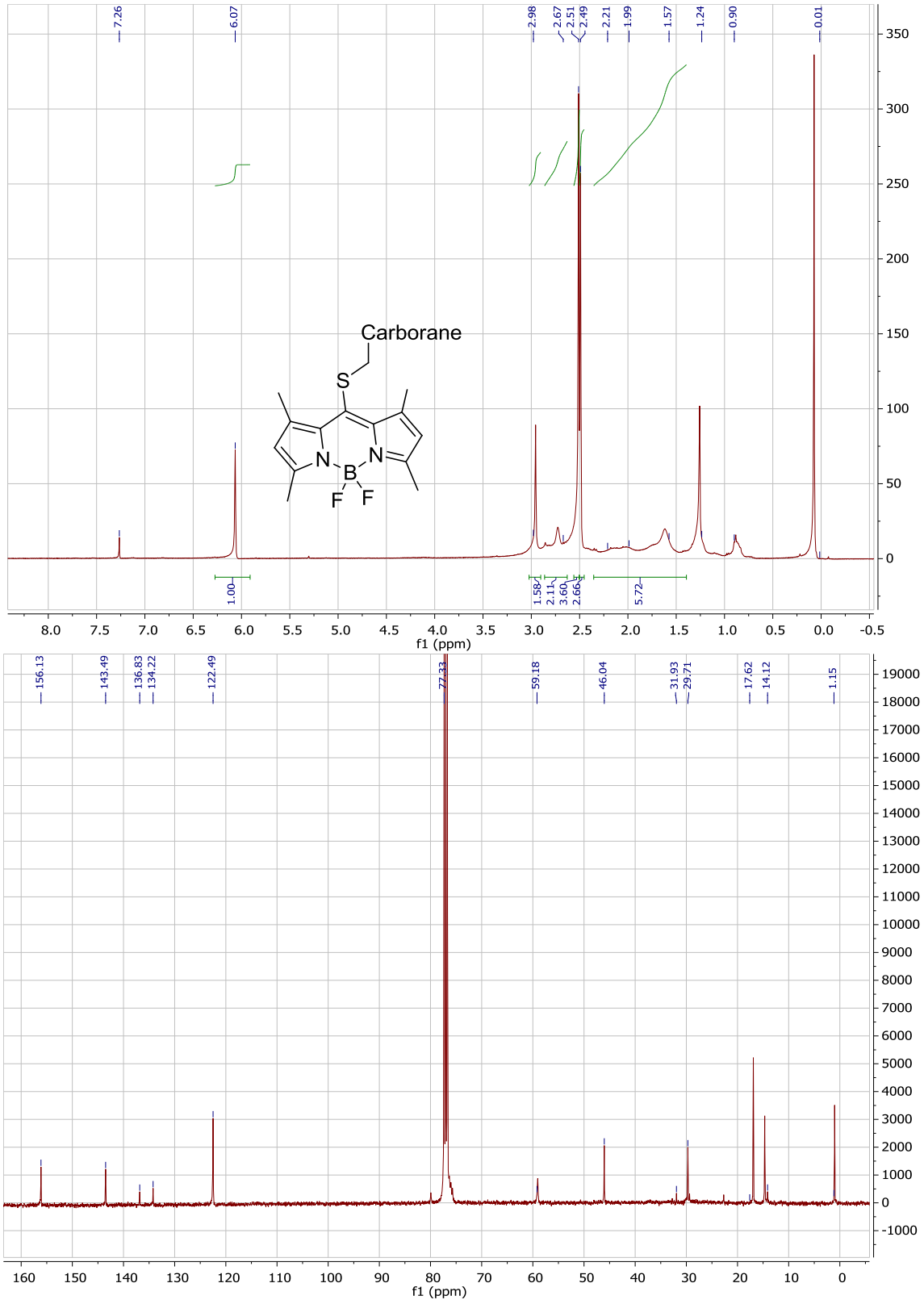

^{1}H- and ^{13}C-NMR of BODIPY **82** in $CDCl_3$

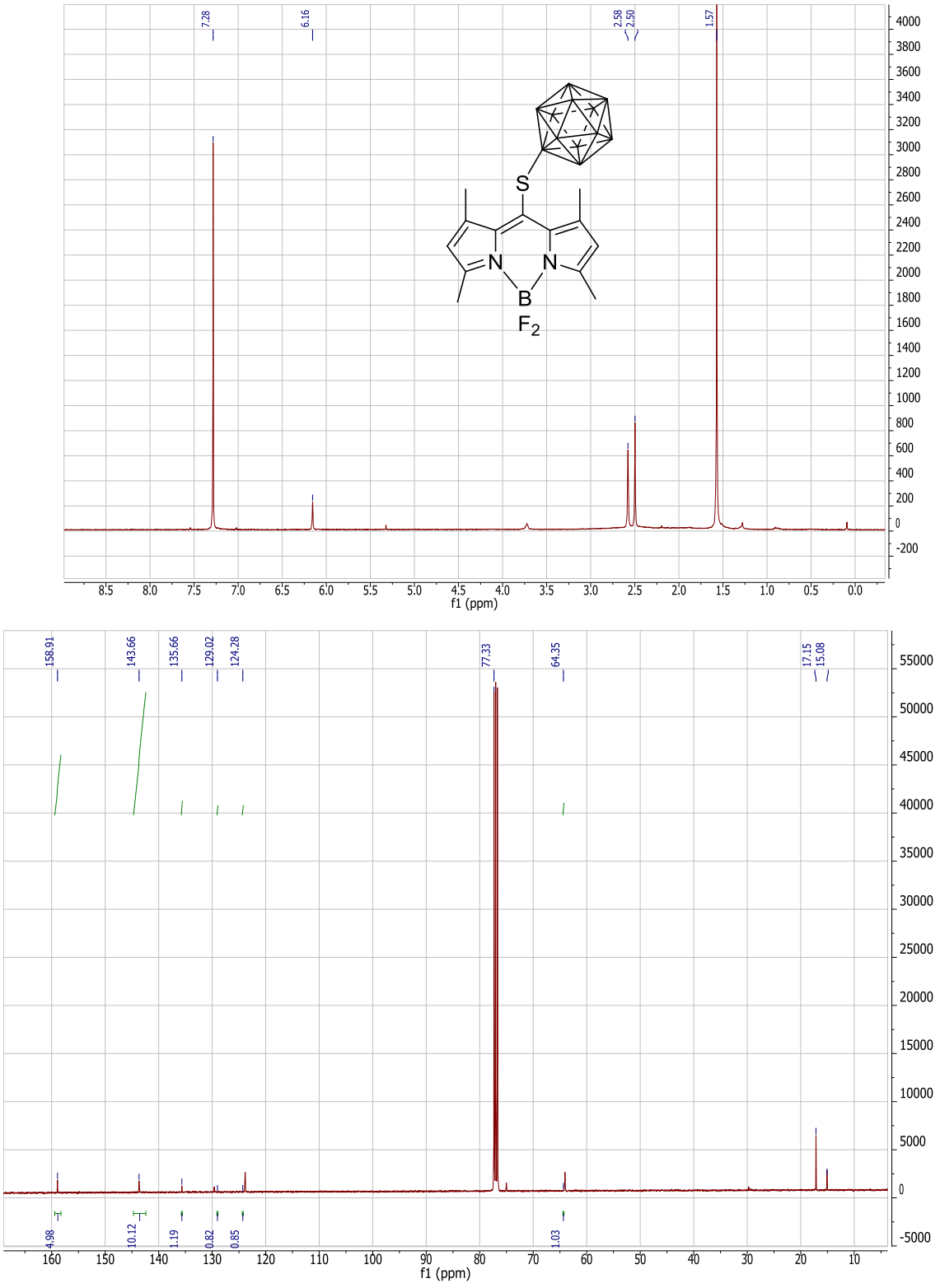

^{1}H- and ^{13}C-NMR of BODIPY **83** in $CDCl_3$

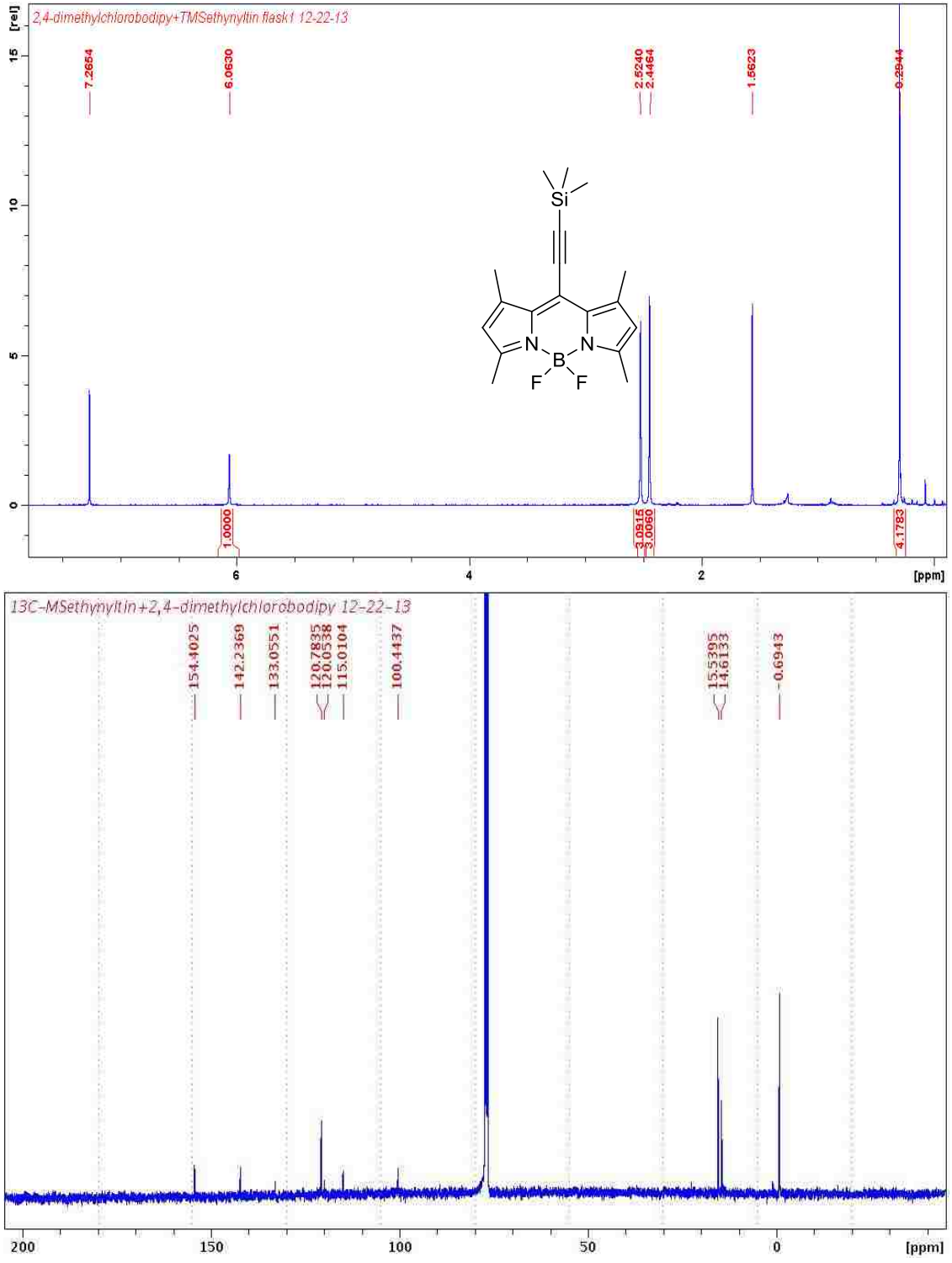

^{1}H- and ^{13}C-NMR of BODIPY **86** in $CDCl_3$

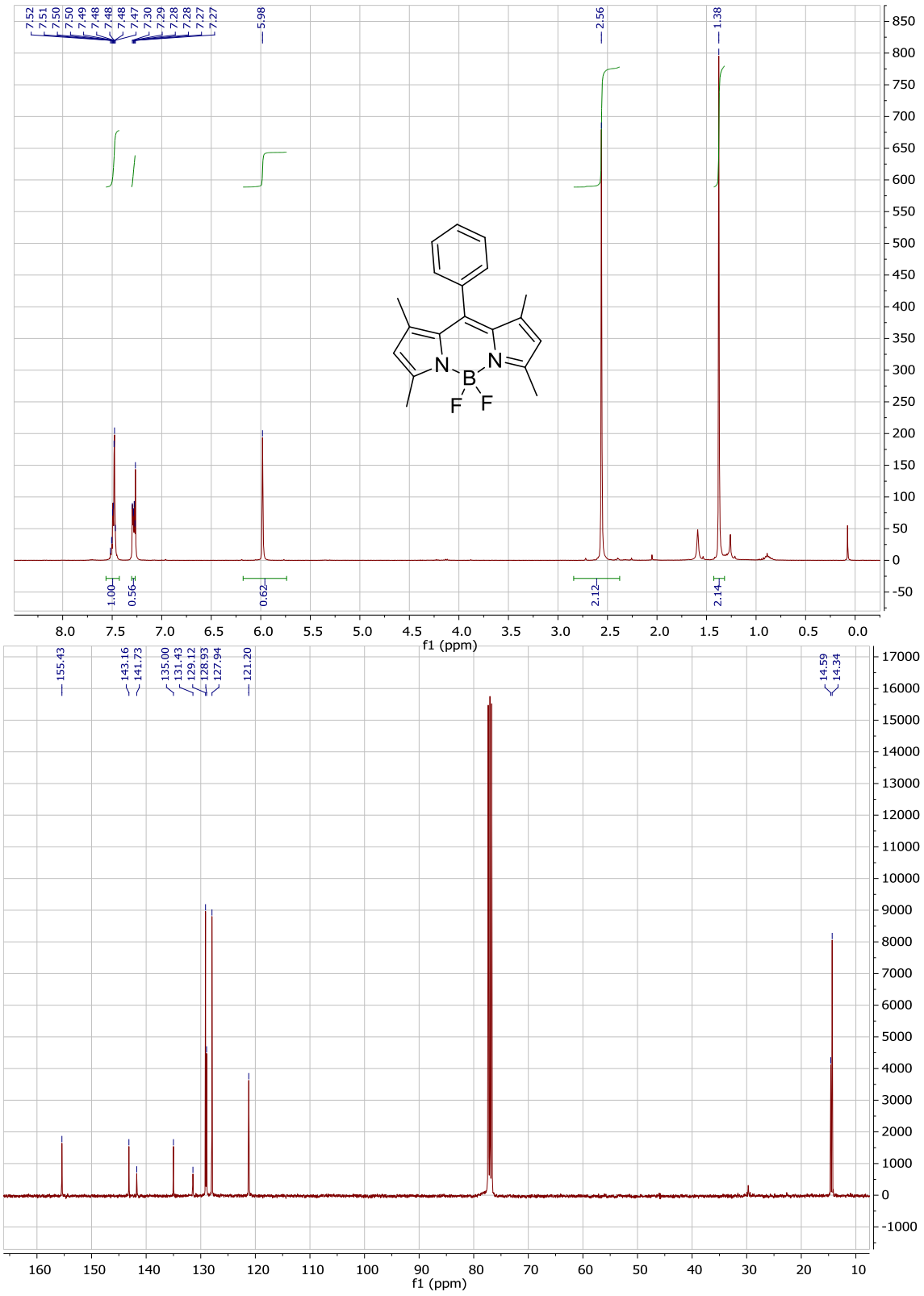

^{1}H- and ^{13}C-NMR of BODIPY **85** in $CDCl_3$

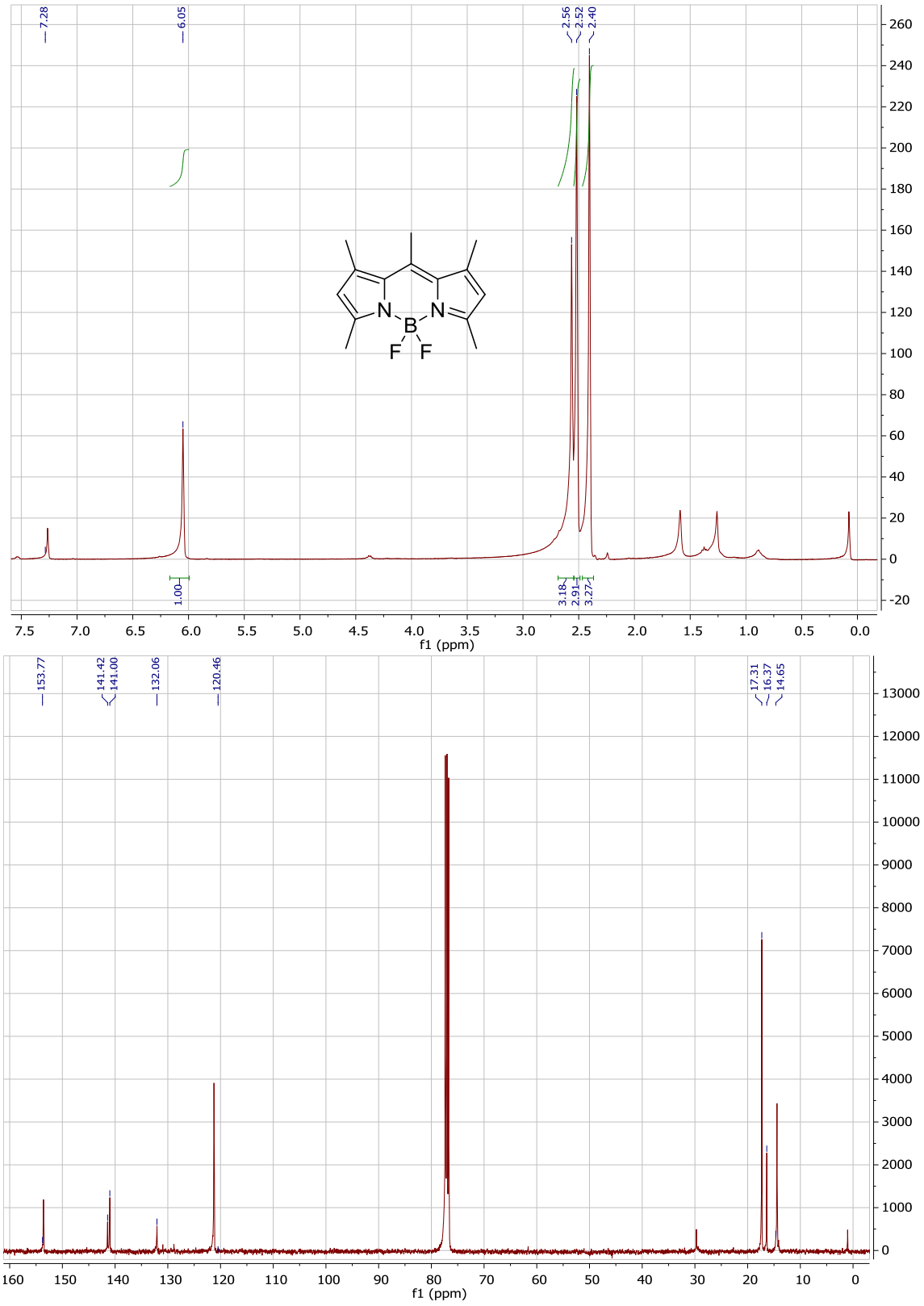

^{1}H- and ^{13}C-NMR of BODIPY **88** in $CDCl_3$

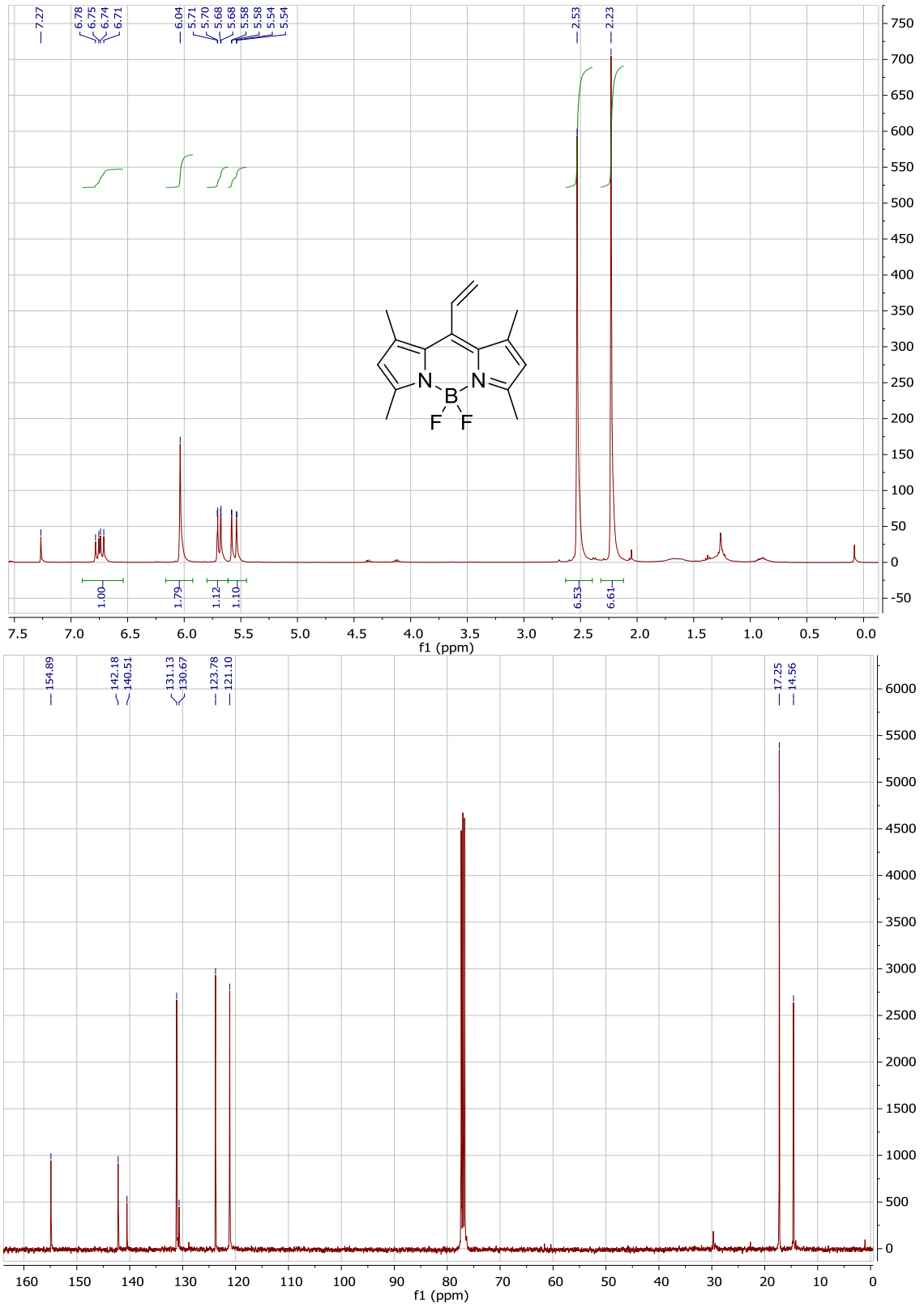

^{1}H- and ^{13}C-NMR of BODIPY **89** in $CDCl_3$

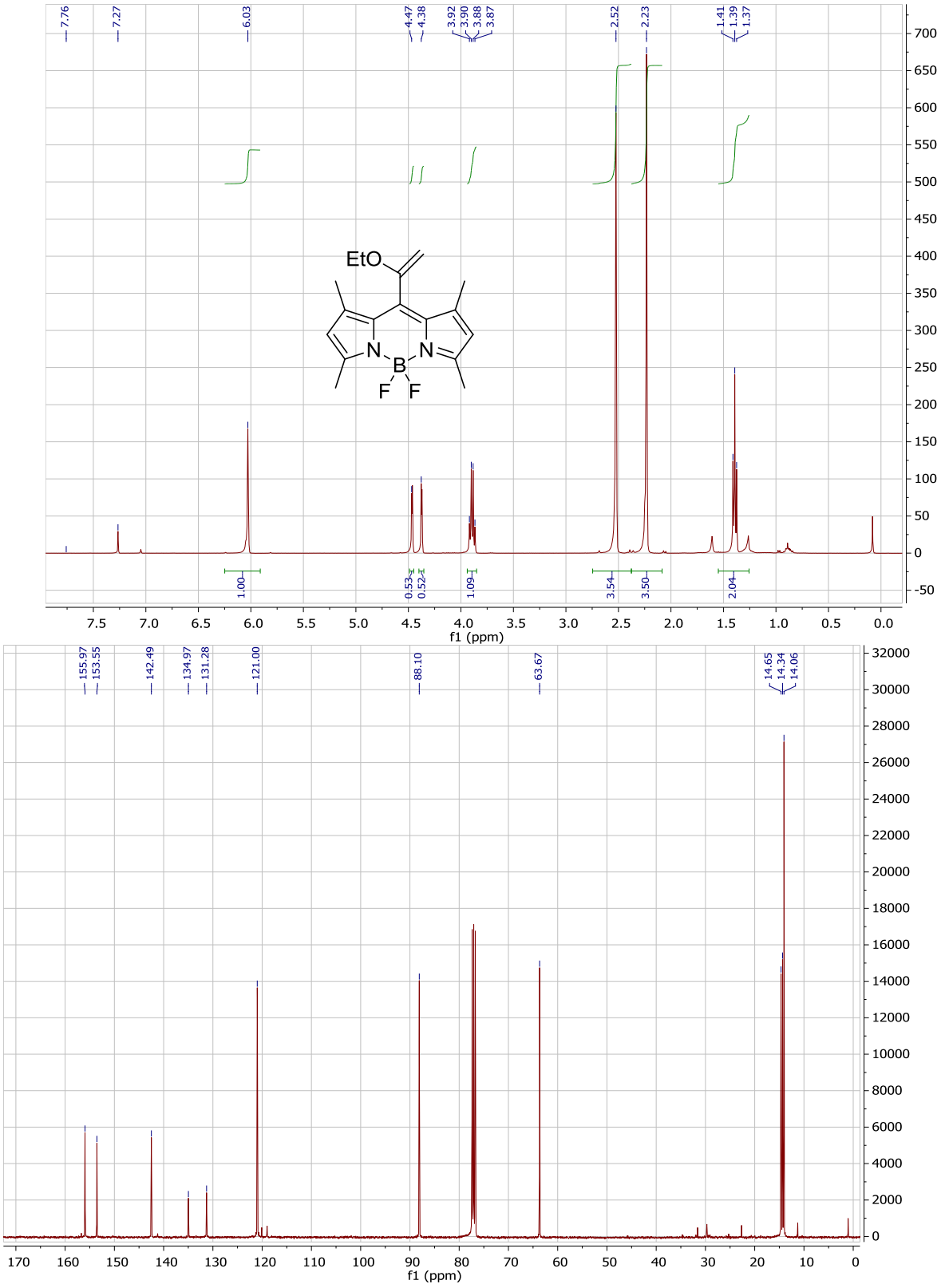

^{1}H- and ^{13}C-NMR of BODIPY **90** in $CDCl_3$

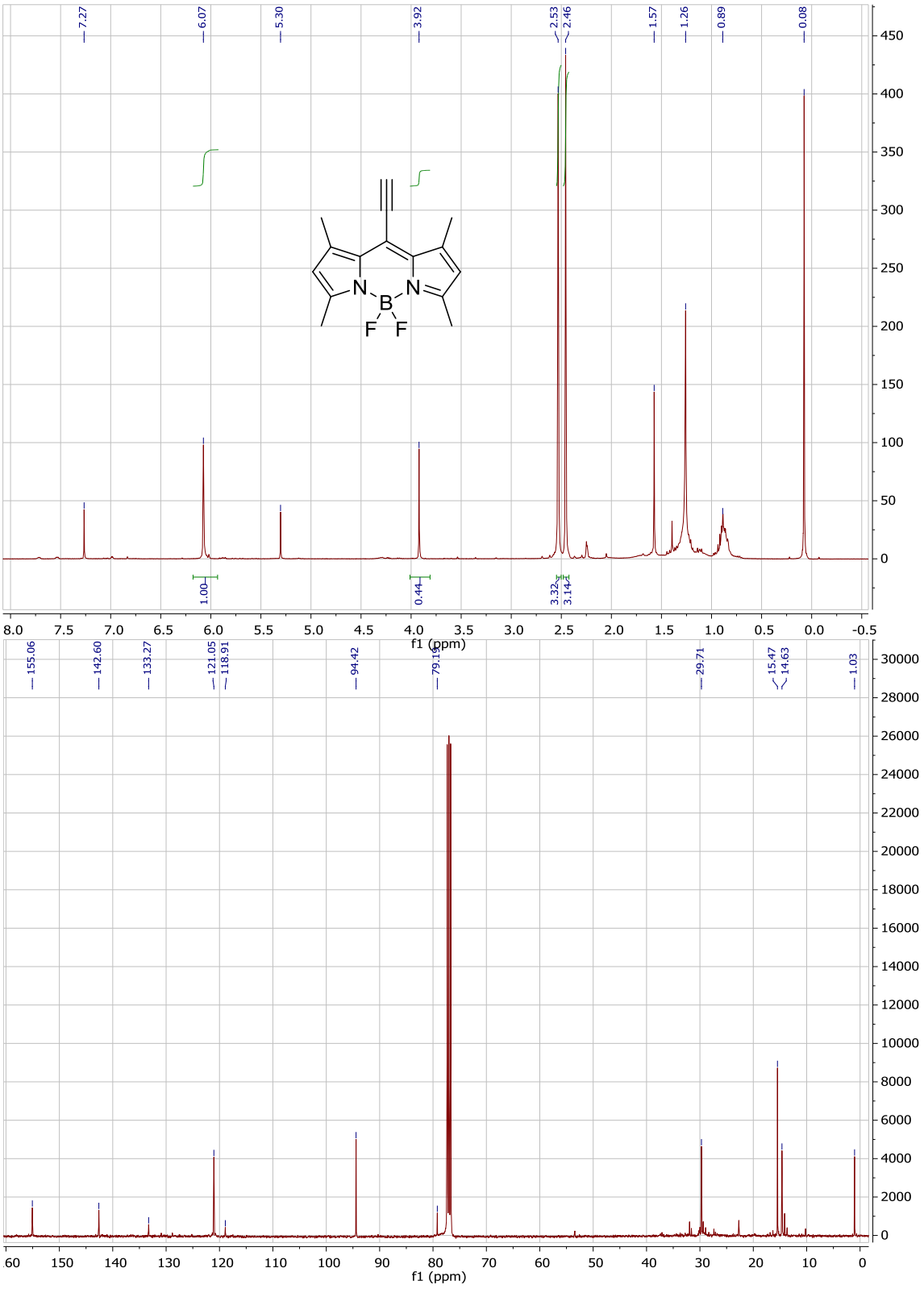

^{1}H- and ^{13}C-NMR of BODIPY **91** in $CDCl_3$

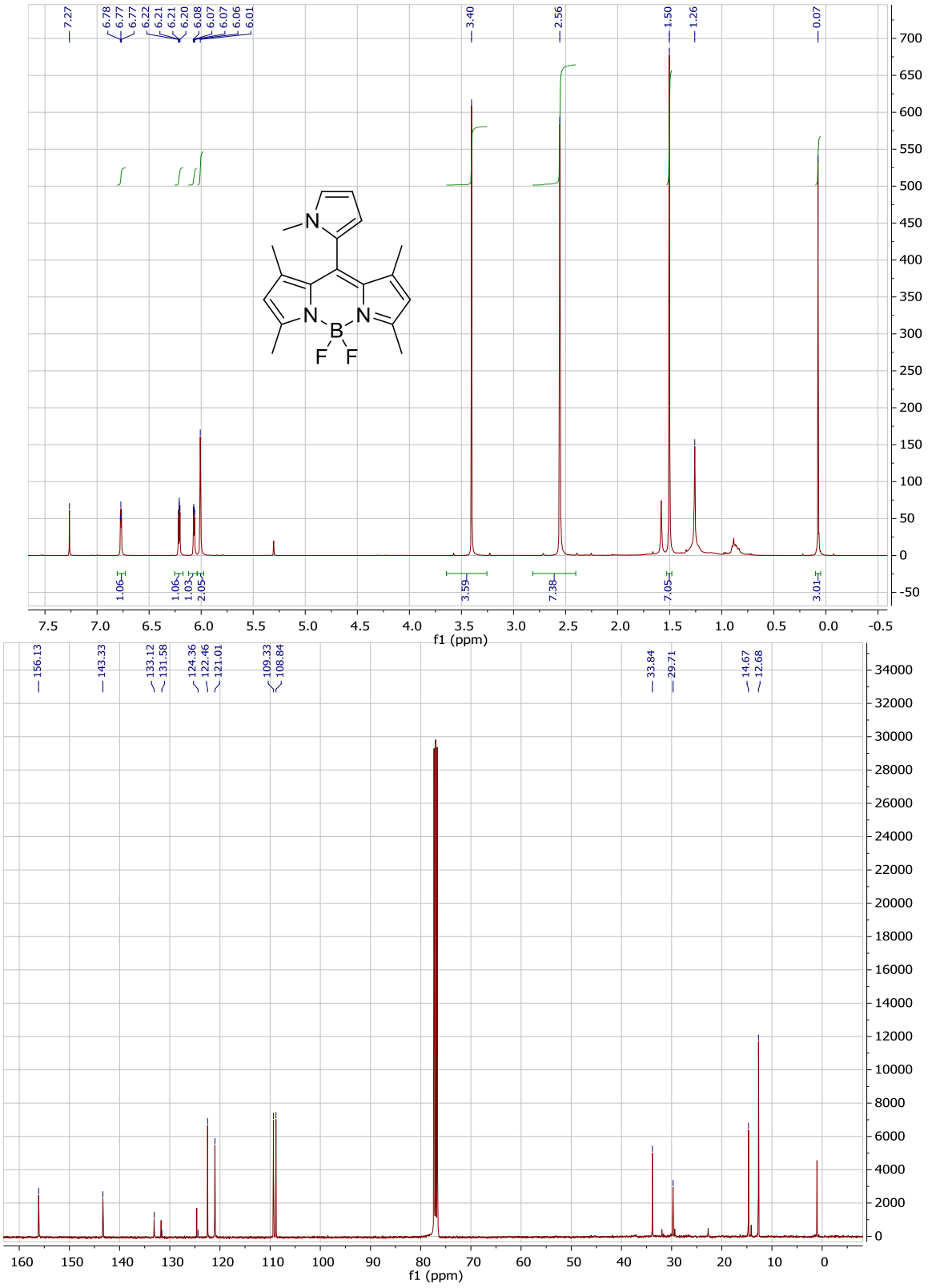

^{1}H- and ^{13}C-NMR of BODIPY **92** in $CDCl_3$

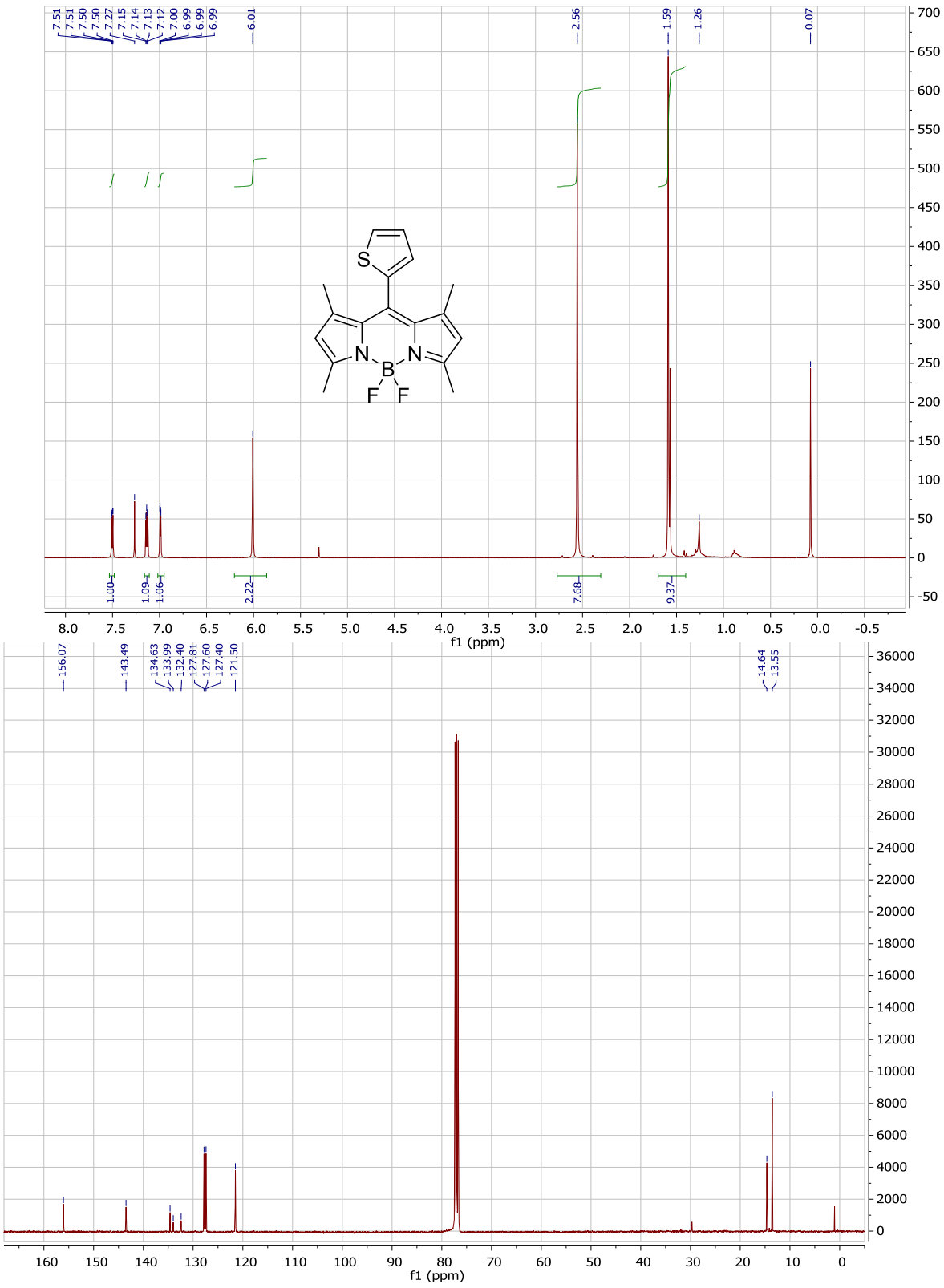

^{1}H- and ^{13}C-NMR of BODIPY **93** in $CDCl_3$

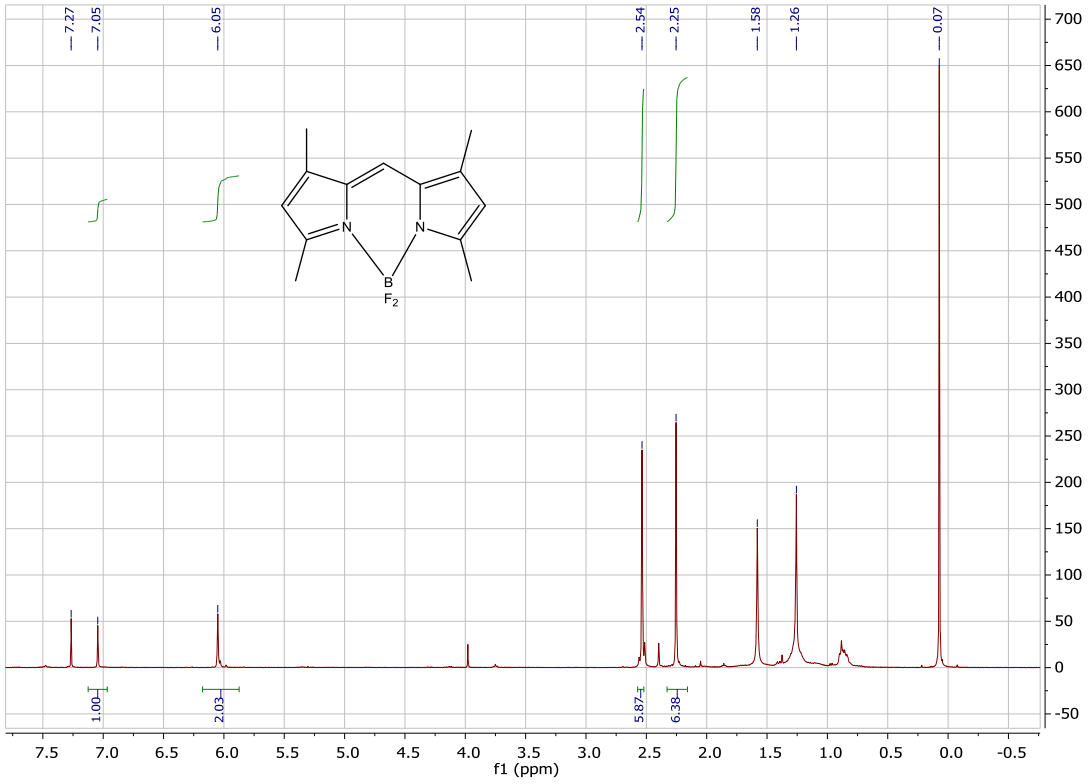

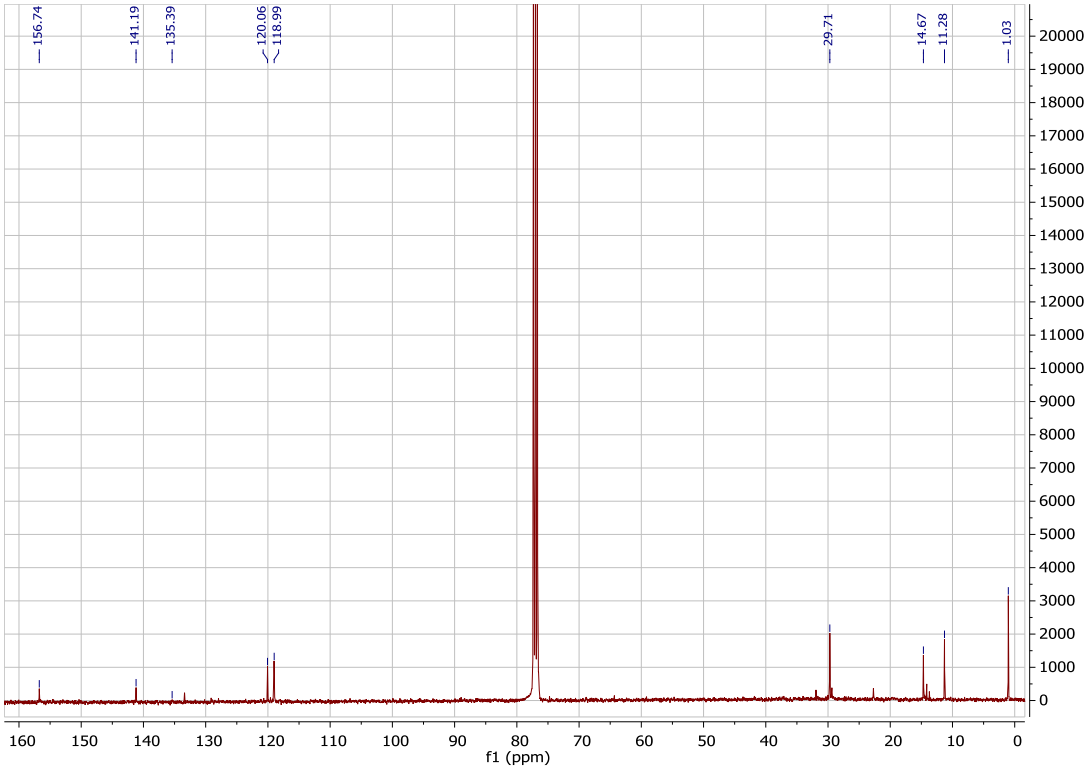

^{1}H- and ^{13}C-NMR of meso-unsubstituted BODIPY in $CDCl_3$

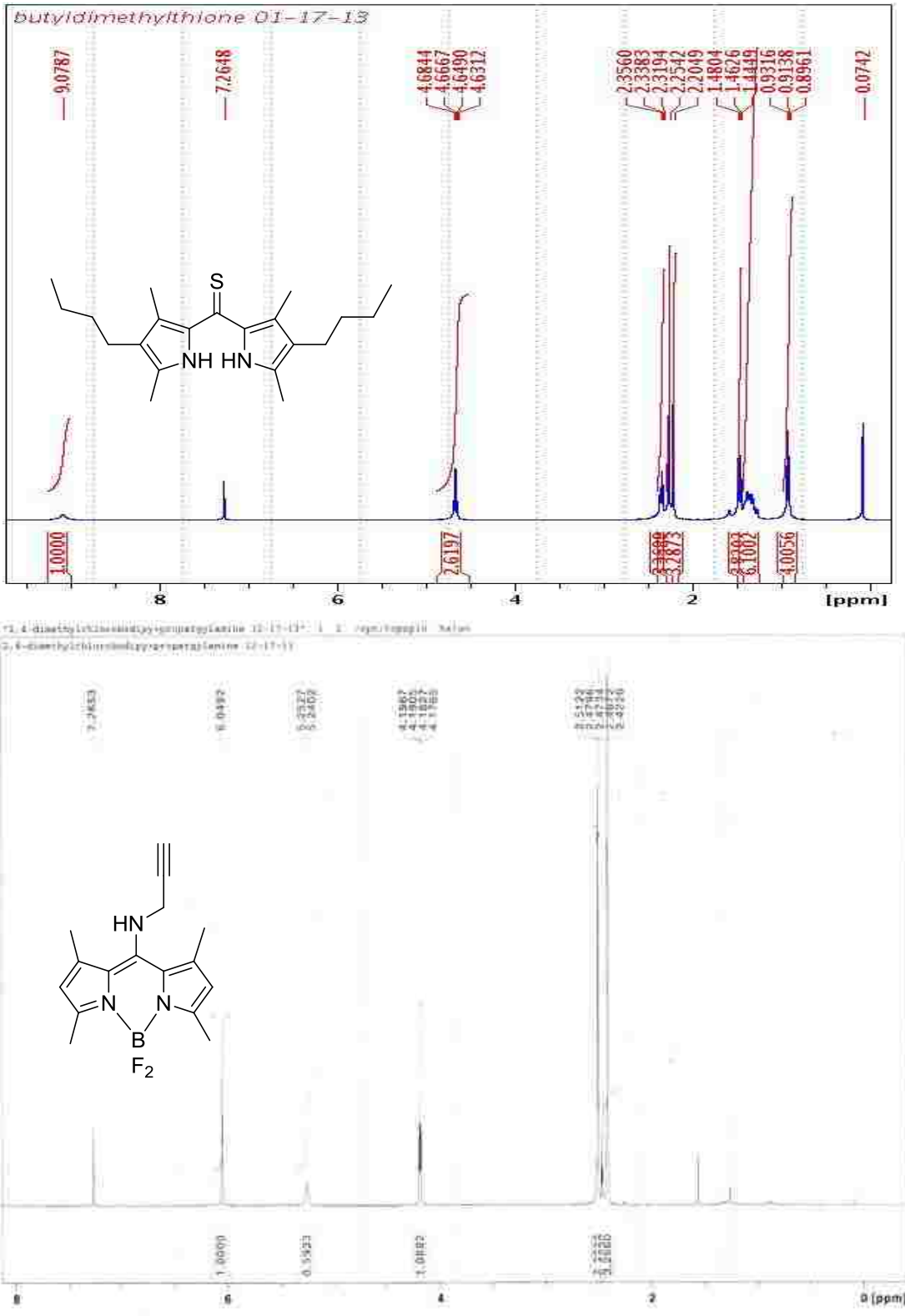

^{1}H-NMR spectra of dipyrrothione **56** and BODIPY **84** in $CDCl_3$ at 400 MHz

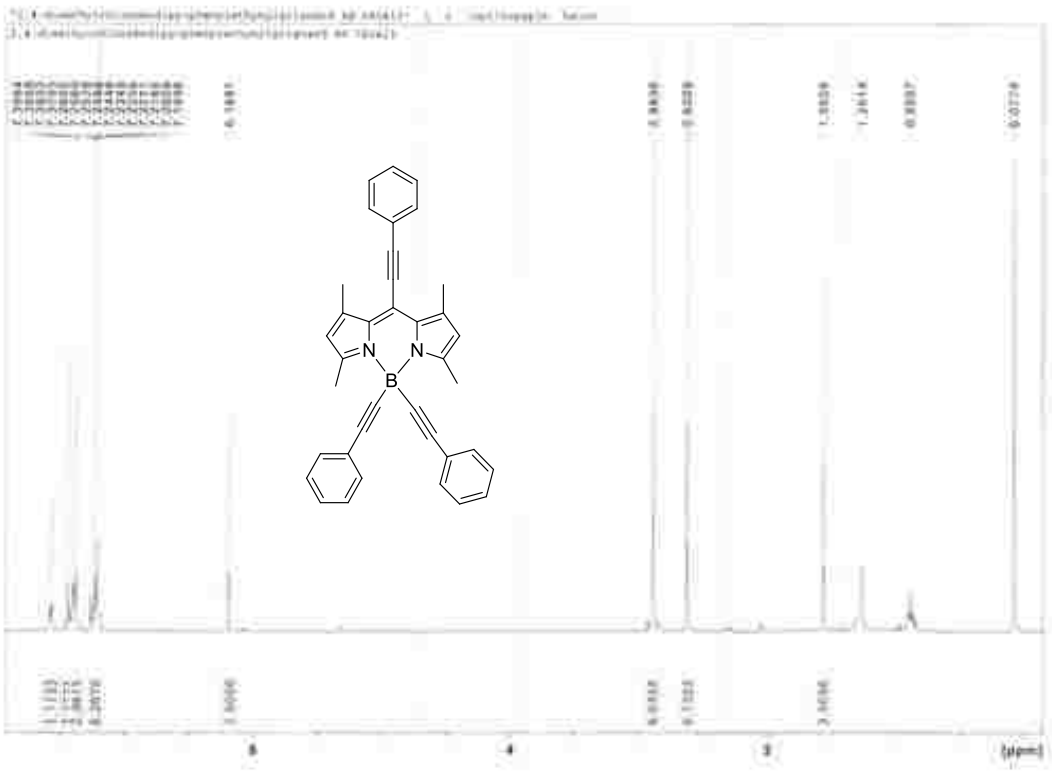

^{1}H-NMR spectrum of BODIPY **87** in $CDCl_3$ at 400 MHz

4.6 References

1. Treibs, A.; Kreuzer, F.-H. *Justus Liebigs Ann. Chem.* **1968**, *718*, 208.

2. Falk, H.; Hofer, O.; Lehner, H. *Monatsh Chem* **1974**, *105*, 169.

3. Loudet, A.; Burgess, K. *Chem. Rev.* **2007**, *107*, 4891.

4. Ulrich, G.; Ziessel, R.; Harriman, A. *Angew. Chem. Int. Ed.* **2008**, *47*, 1184.

5. Karolin, J.; Johansson, L. B. A.; Strandberg, L.; Ny, T. *J. Am. Chem. Soc.* **1994**, *116*, 7801.

6. Tan, K.; Jaquinod, L.; Paolesse, R.; Nardis, S.; Di Natale, C.; Di Carlo, A.; Prodi, L.; Montalti, M.; Zaccheroni, N.; Smith, K. M. *Tetrahedron* **2004**, *60*, 1099.

7. Goze, C.; Ulrich, G.; Mallon, L. J.; Allen, B. D.; Harriman, A.; Ziessel, R. *J. Am. Chem. Soc.* **2006**, *128*, 10231.

8. Lee, C.-H.; S. Lindsey, J. *Tetrahedron* **1994**, *50*, 11427.

9. Ulrich, G.; Ziessel, R. *J. Org. Chem.* **2004**, *69*, 2070.

10. Wang, D.; Fan, J.; Gao, X.; Wang, B.; Sun, S.; Peng, X. *J. Org. Chem.* **2009**, *74*, 7675.

11. Wood, T. E.; Thompson, A. *Chem. Rev.* **2007**, *107*, 1831.

12. Wu, L.; Burgess, K. *Chem. Commun.* **2008**, 4933.

13. Buyukcakir, O.; Bozdemir, O. A.; Kolemen, S.; Erbas, S.; Akkaya, E. U. *Org. Lett.* **2009**, *11*, 4644.

14. Coskun, A.; Akkaya, E. U. *Tetrahedron Lett.* **2004**, *45*, 4947.

15. Rurack, K.; Kollmannsberger, M.; Daub, J. New J. Chem. **2001**, *25*, 289.

16. Saki, N.; Dinc, T.; Akkaya, E. U. *Tetrahedron* **2006**, *62*, 2721.

17. Sathyamoorthi, G.; Wolford, L. T.; Haag, A. M.; Boyer, J. H. *Heteroat. Chem* **1994**, *5*, 245.

18. Boyer, J. H.; Haag, A. M.; Sathyamoorthi, G.; Soong, M.-L.; Thangaraj, K.; Pavlopoulos, T. G. *Heteroat. Chem.* **1993**, *4*, 39.

19. Sathyamoorthi, G.; Boyer, J. H.; Allik, T. H.; Chandra, S. *Heteroat. Chem.* **1994**, *5*, 403.

20. Goud, T. V.; Tutar, A.; Biellmann, J.-F. *Tetrahedron* **2006**, *62*, 5084.

21. Leen, V.; Yuan, P.; Wang, L.; Boens, N.; Dehaen, W. *Org. Lett.* **2012**, *14*, 6150.

22. Kee, H. L.; Kirmaier, C.; Yu, L.; Thamyongkit, P.; Youngblood, W. J.; Calder, M. E.; Ramos, L.; Noll, B. C.; Bocian, D. F.; Scheidt, W. R.; Birge, R. R.; Lindsey, J. S.; Holten, D. *J. Phys. Chem. B.* **2005**, *109*, 20433.

23. Ziessel, R.; Ulrich, G.; Harriman, A. *New J. Chem.* **2007**, *31*, 496.

24. Li, L.; Nguyen, B.; Burgess, K. *Bioorg. Med. Chem. Lett.* **2008**, *18*, 3112.

25. Gabe, Y.; Ueno, T.; Urano, Y.; Kojima, H.; Nagano, T. *Anal. Bioanal. Chem.* **2006**, *386*, 621.

26. Jiao, L.; Yu, C.; Li, J.; Wang, Z.; Wu, M.; Hao, E. *J. Org. Chem.* **2009**, *74*, 7525.

27. Pavlopoulos, T. G.; Boyer, J. H.; Shah, M.; Thangaraj, K.; Soong, M.-L. *Appl. Opt.* **1990**, *29*, 3885.

28. Wories, H. J.; Koek, J. H.; Lodder, G.; Lugtenburg, J.; Fokkens, R.; Driessen, O.; Mohn, G. R. *Recl. Trav. Chim. Pays-Bas.* **1985**, *104*, 288.

29. Shah, M.; Thangaraj, K.; Soong, M.-L.; Wolford, L. T.; Boyer, J. H.; Politzer, I. R.; Pavlopoulos, T. G. *Heteroat. Chem.* **1990**, *1*, 389.

30. Thivierge, C.; Bandichhor, R.; Burgess, K. *Org. Lett.* **2007**, *9*, 2135.

31. Smith, K. M. *Q. Rev. Chem. Soc.* **1971**, *25*, 31.

32. Ballantine, J. A.; Jackson, A. H.; Kenner, G. W.; McGillivray, G. *Tetrahedron* **1966**, *22, Supplement 7*, 241.

33. Smith, K. M., Vicente, M. G. H. Science of Synthesis; Georg Thieme Berlag, **2004**, *17.8*, 5084.

34. Jackson, A. H.; Kenner, G. W.; McGillivray, G.; Sach, G. S. *J. Am. Chem. Soc.* **1965**, *87*, 676.

35. Jackson, A. H.; Kenner, G. W.; McGillivray, G.; Smith, K. M. *J. Chem. Soc. C.* **1968**, 294.

36. Challis, B. G.; Challis, J. A. *The Chemistry of Amides*; John Wiley & Sons, inc., New York, 1975, P 731.

37. Julio Alvavez-Buila, J. J. *Modern Heterocyclic Chemistry*; Wiley-VCH Verlag GmbH & Co. KGaA, 2011; Vol. 1.

38. Van den Haak, H. J. W.; Van der Plas, H. C. *T. J. Org. chem.* **1982**, *47*, 1673.

39. Xiao, K.-J.; Wang, A.-E.; Huang, P.-Q. *Angew. Chem. Int. Ed.* **2012**, *51*, 8314.

40. Charette, A. B.; Grenon, M. Can. J. Chem. **2001**, *79*, 1694

41. Matsumura, Y.; Aoyagi, S.; Kibayashi, C. *Org. Lett.* **2004**, *6*, 965.

42. Alhaique, F.; Cozzani, R. G.; Riccieri, F. M. *Farmaco. Sci* **1976**, *31*, 845.

43. Arnott, E. A.; Chan, L. C.; Cox, B. G.; Meyrick, B.; Phillips, A. *J. org. chem.* **2011**, *76*, 1653.

44. Speziale, A. J.; Smith, L. R. *J. org. chem.* **1962**, *27*, 4361.

45. Haveaux, B.; Dekoker, A.; Rens, M.; Sidani, A. R.; Toye, J.; Ghosez, L. *Org. Syn.*; John Wiley & Sons, Inc. New York, 2003.

46. Baraldi, P. G.; Tabrizi, M. A.; Preti, D.; Bovero, A.; Fruttarolo, F.; Romagnoli, R.; Zaid, N. A.; Moorman, A. R.; Varani, K.; Borea, P. A. .*Med. Chem.* **2005**, *48*, 5001.

47. Lash, T. D. *Tetrahedron* **1998**, *54*, 359.

48. Smithen, D. A.; Cameron, T. S.; Thompson, A. *Org. Lett.* **2011**, *13*, 5846.

49. Mula, S.; Ray, A. K.; Banerjee, M.; Chaudhuri, T.; Dasgupta, K.; Chattopadhyay, S. *J. Org. Chem.* **2008**, *73*, 2146.

50. Osorio-Martínez, C. A.; Urías-Benavides, A.; Gómez-Durán, C. F. A.; Bañuelos, J.; Esnal, I.; López Arbeloa, I.; Peña-Cabrera, E. *J. Org. Chem.* **2012**, *77*, 5434.

51. Plater, M. J.; Aiken, S.; Bourhill, G. *Tetrahedron* **2002**, *58*, 2405.

52. Diem, M. J.; Burow, D. F.; Fry, J. L. *J. Org. Chem.* **1977**, *42*, 1801.

53. Fischer, H.; Orth, H. *Justus Liebigs Ann. Chem.* **1933**, *502*, 237.

54. Leen, V.; Braeken, E.; Luckermans, K.; Jackers, C.; Van der Auweraer, M.; Boens, N.; Dehaen, W. *Chem. Commun.* **2009**, 4515.

55. Ulrich, G.; Goze, C.; Guardigli, M.; Roda, A.; Ziessel, R. *Angew. Chem. Int. Ed.* **2005**, *44*, 3694.

56. Miyaura, N.; Suzuki, A. *Chem. Rev.* **1995**, *95*, 2457.

57. Stille, J. K.; Lau, K. S. Y. *J. Am. Chem. Soc.* **1976**, *98*, 5841.

58. Heck, R. F. *J. Am. Chem. Soc.* **1968**, *90*, 5518.

59. Sonogashira, K.; Tohda, Y.; Hagihara, N. *Tetrahedron Lett.* **1975**, *16*, 4467.

60. Rohand, T.; Qin, W.; Boens, N.; Dehaen, W. *Eur. J. Org. Chem*. **2006**, *2006*, 4658.

61. Jiao, L.; Yu, C.; Uppal, T.; Liu, M.; Li, Y.; Zhou, Y.; Hao, E.; Hu, X.; Vicente, M. G. H. *Org. Biomol. Chem.* **2010**, *8*, 2517.

62. Miyaura, N.; Suzuki, A. *Chem. Commun.* **1979**, 866.

63. Miyaura, N.; Yamada, K.; Suzuki, A. *Tetrahedron Lett.* **1979**, *20*, 3437.

64. Miyaura, N.; Yanagi, T.; Suzuki, A. *Syn. Commun.* **1981**, *11*, 513.

65. Miyaura, N.; Yano, T.; Suzuki, A. *Tetrahedron Lett.* **1980**, *21*, 2865.

66. Chinchilla, R.; Nájera, C. *Chem. Rev.* **2007**, *107*, 874.

67. Sonogashira, K. *J. Organomet. Chem.* **2002**, *653*, 46.

68. Chinchilla, R.; Najera, C. *Chem. Soc. Rev.* **2011**, *40*, 5084.

69. Graf, K.; Korzdorfer, T.; Kummel, S.; Thelakkat, M. *New J. Chem.* **2013**, *37*, 1417.

70. Stille, J. K. *Angew. Chem. Int. Ed.* **1986**, *25*, 508.

71. Milstein, D.; Stille, J. K. *J. Am. Chem. Soc.* **1978**, *100*, 3636.

Chapter 5: Syntheses of Symmetrical and Asymmetrical BODIPYs Through Functionalization of Halogenated BODIPYs

5.1 Introduction

4,4-Difluoro-4-bora-3a,4a-diaza-s-indacene (BODIPY) is a class of very versatile fluorophore recognized in the last several decades and that are used widely as labeling reagents, sensors, and photoelectronic devices.[1-3] Compared with other fluorophores, BODIPY has a lot of advantages, such as strong absorption and fluorescent bands in the visible region, relatively high thermal and photochemical stability, and easy functionalization, thus enabling variations in properties such as absorption wavelength and amphiphilicity.[4] Due to their relatively low molecular weight, BODIPY conjugates with biomolecules tend to have good permeability to living cells. Another advantage of BODIPY dyes is their low tendency for self–association, which means they have negligible aggregation because of the lack of intermolecular interactions.

Various methods have been developed to functionalize BODIPYs to change their long wavelength absorption or hydrophobicity and hydrophilicity. These methods include coupling reactions, replacement reactions and Knoevenagel reactions.[5-9] Coupling reactions and Knovenagel reactions are usually used to increase the absorption wavelength by introducing extended conjugation into the BODIPYs, while replacement reactions are used to modify the amphiphilicity by introducing heteroatom-based groups. Halogenated BODIPYs are very versatile substrates for functionalization purposes and applicable halogens include iodide, bromide and chloride which have already been introduced into all the positions of BODIPYs[11-17] (Figure 5.1). Coupling and replacement reactions were explored on these BODIPYs since different positions of the BODIPY core have different reactivity toward coupling reagents and nucleophiles. The coupling reactions explored on BODIPYs[5] include palladium-catalyzed Suzuki, Stille, Sonogashira

and Heck coupling reactions, all of which worked at the 3,5-positions of the BODIPY; Heck coupling reactions have not yet worked on the 8-position. For the 2,6-positions, Suzuki and Stille coupling reactions have been reported.[16] These coupling reactions significantly facilitated the functionalization of BODIPYs and a number of compounds were synthesized using these methods.

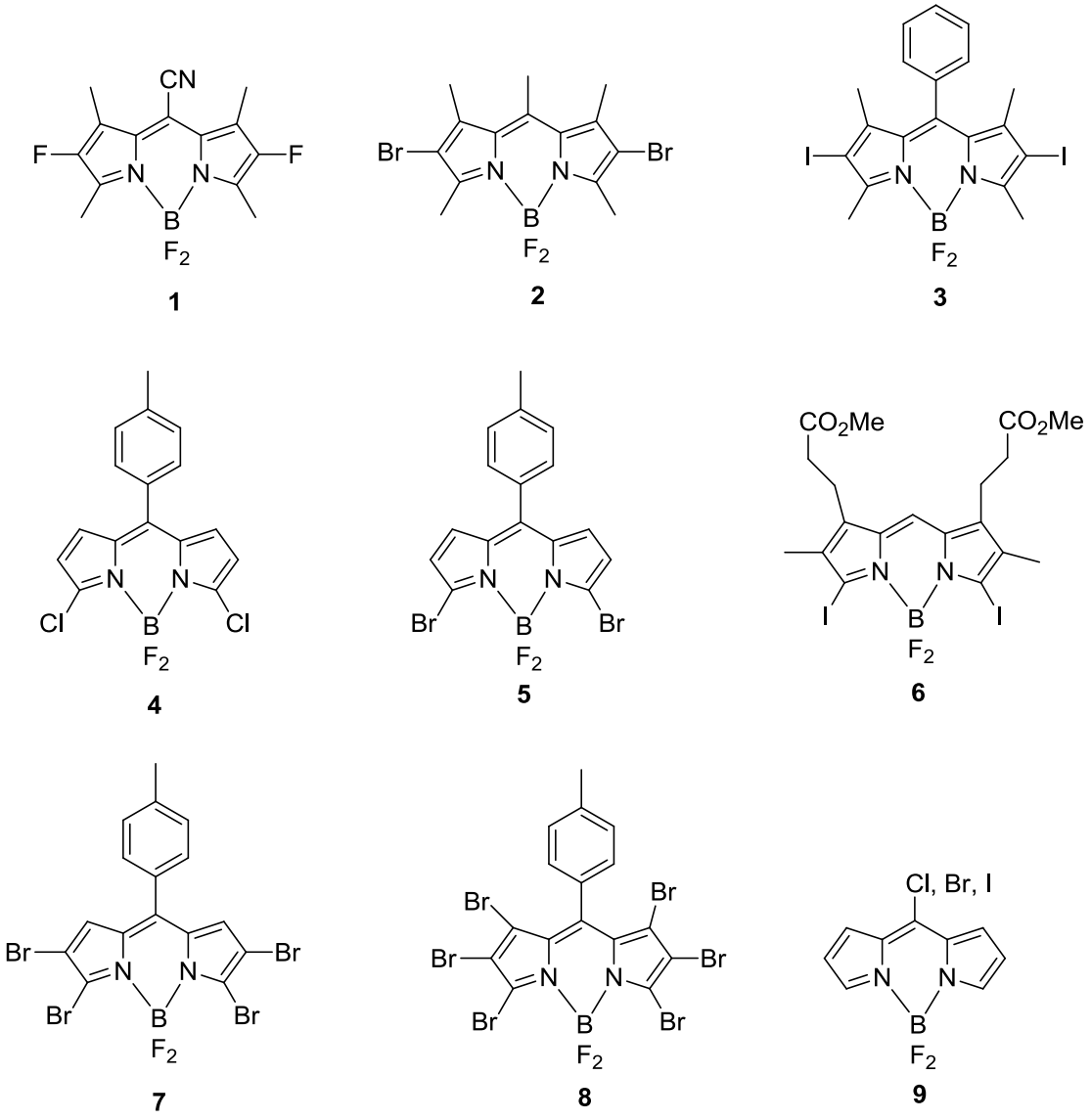

Figure 5.1: The halogenated BODIPYs.

5.2. Syntheses of Halogenated BODIPYs

In Chapter 4, we initially used pyrroketones **10** and **11** as starting material to synthesize BODIPYs; however, the reactions such as chlorination using various chlorinating reagents did not work on these two pyrroketones due to the presence of the two electron-withdrawing ester groups on the α-positions. To avoid this problem, we switched from these two pyrroketone to alkylated pyrroketones possessing no electron withdrawing groups and as a result the halogenation reactions worked very well. When we came back to reinvestigate at the reactions of these two pyrroketones **10** and **11**, we devised another strategy to make them useful by elimination of the two ester groups and subsequent introduction of some other functional groups such as halogens. It was surmised that if the chlorination reaction works on pyrroketone **12**, we can introduce halogens to the 3, 5, and 8-positions of BODIPYs at the same time, or maybe even sequentially(Scheme 5.1).

Based on this idea, the pyrroketone **10** was subjected to hydrogenation using Pd/C as catalyst in THF, and the dipyrroketone dicarboxylic acid was obtained in 90% yield. Then an electrophilic iodination reaction[15] under basic conditions using iodine gave diiodopyrroketone **12** in 75% yield. Diiodopyrroketone **12** was treated with phosgene[18] in chloroform and the reaction was monitored by UV/visible absorption spectroscopy. A peak around 480 nm indicated the fully conjugated dipyrromethene was obtained. Complexation with $BF_3.OEt_2$ using DIEA as base gave a reddish solution, which had an absorption maximum at 538 nm. This absorption wavelength is a little lower than expected for 3,5-diiodo-BODIPYs.[15] Chromatographic separation showed the product to a mixture of di-and tri-chloro-BODIPYs **15** and **16**, and this conclusion was confirmed by an X-ray crystal structure (Scheme 5.2).

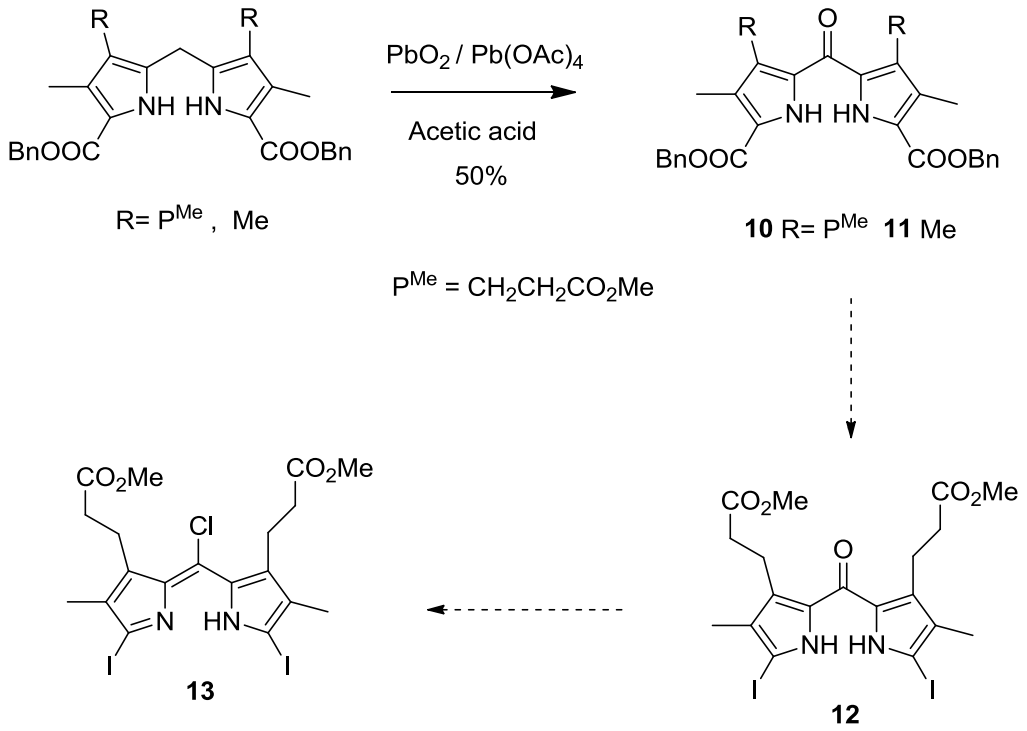

Scheme 5.1: The strategy to access halogenated BODIPYs.

10 R = P^{Me}, 11 R = Me

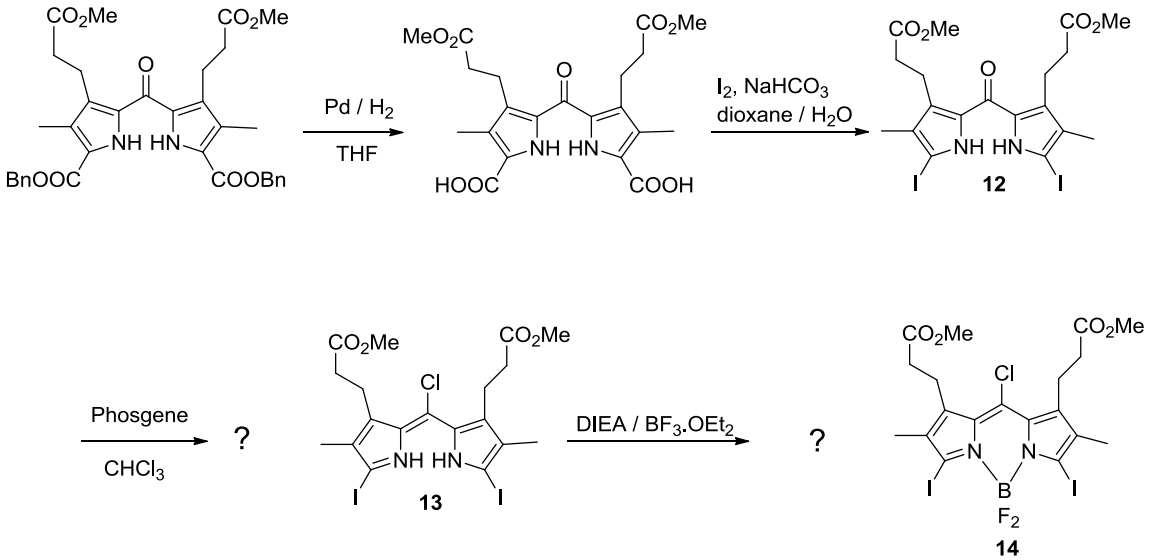

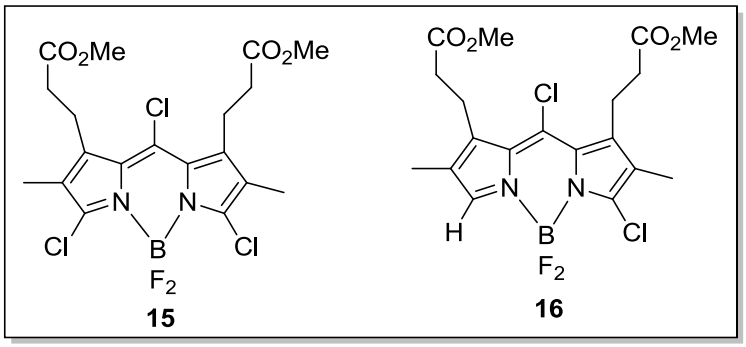

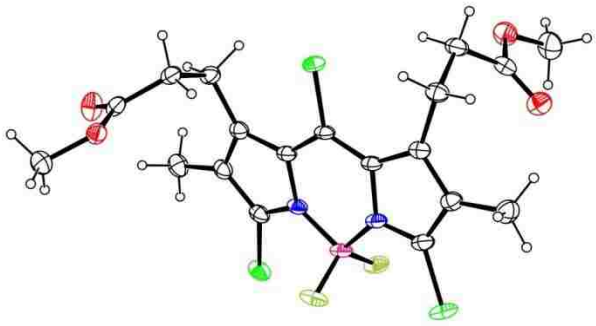

15

Scheme 5.2: Synthesis of halogenated BODIPYs **15** and **16**, and X-ray crystal structure of **15**.

5.3. Global and Selective Stille Coupling Reactions

According to the resonance structure of BODIPY, the meso-position is more electrophilic than the other positions such as the 3,5 or 2,6-postions; a computational study of the BODIPY by Mulliken charge distribution, and reactivity studies also reached same conclusion.[19] Therefore, the 8-chloro-position is more reactive than the 3,5-positions of BODIPY **15** and selective coupling reactions on 8-position over 3,5-position are possible in this case. Since we found that the Stille coupling reaction is very efficient on meso-chloro-BODIPYs (Chapter 4), we hoped that selective and global coupling reactions could both work if stoichiometric amounts of excess coupling reagents are used.

The global coupling reaction was tried first with excess organotin reagents including 2-(tributylstannyl)thiophene, tributylphenylstanne and trimethyl[(tributylstannyl)ethynyl]-silane (Scheme 5.3). A typical reaction procedure followed the Stille coupling reaction conditions we used in Chapter 4. In all cases, when the solutions were heated to 110 ^{o}C,

the reaction solution started to change color and became deeper in color with time. The reactions were monitored with UV/visible spectrophotometry and TLC; when the starting material was all used according TLC and the UV/visible spectrum showed a strong peak around 600 nm, the reactions were stopped. The global coupling reactions were usually left stirring overnight. The tri-thiophene-BODIPY prepared in this way with 2-(tributystannyl)thiophene has an absorption at 592 nm and tri-TMS-ethynyl-BODIPY has a very red shifted absorption at 648 nm while the corresponding tri-phenyl-BODIPY has a slight red shift at 546 nm. The 2-(tributystannyl)thiophene is the most reactive among the three reagents investigated, and gave the highest yield (83%), followed by TMS-ethynyltin, which gave a 79% yield. the phenyltin r,eagent was the least reactive one, giving a 60% yield. ^{1}H NMR spectra of these compounds showed different chemical shifts for the same group on the meso-position and 3,5-positions. For example, tri-TMS-ethynyl-BODIPY has different chemical shifts for the TMS groups at 0.30 and 0.28 ppm, although the tri-thiophene and triphenyl BODIPYs showed multiple aromatic peaks beween 7.56-7.09 ppm and 7.53-7.38 ppm, respectively. Structures of all these new BODIPYs were confirmed by mass spectrumometry with *m/z* at 639.1429 (MW+H), and 681 2970 (MW+H) for BODIPYs **17** and **19**, respectively. 1-Methyl-2-(tributylstannyl)pyrrole was also tried on the tri-chloro-BODIPY **15**; the product showed a peak in its UV/visible spectrum at 582 nm, but it was not possible to successfully separate the tin reagent from the product.

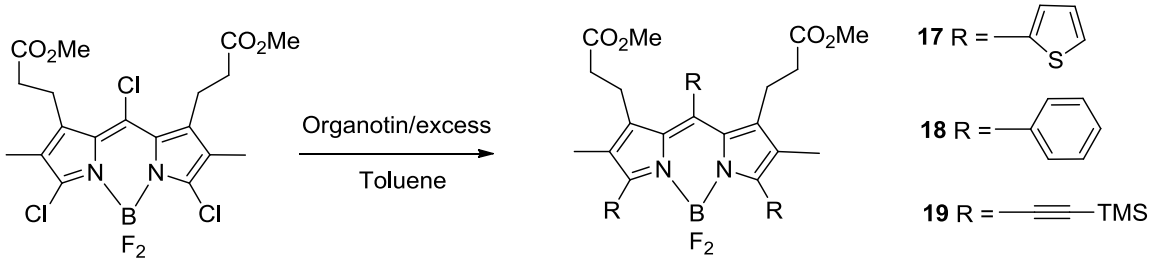

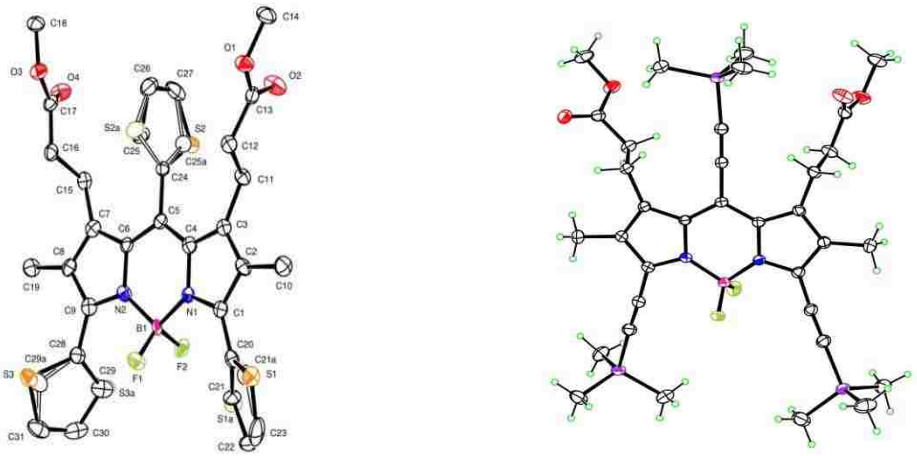

Scheme 5.3: The global Stille coupling reactions of tri-chloro-BODIPY **15,** and the X-ray structure of BODIPY **17** and **19**.

Regioselective coupling reactions were tried with the three organotin reagents above, using a reagent ratio of 1:1 (Scheme 5.4). The solutions were refluxed for five hours instead of overnight and the slight color change, compared with the tri-chloro-BODIPY, indicated that only the meso-chloro group was selectively coupled. For 2-(tributylstannyl)thiophene, the BODIPY **20** has absorption at 545 nm, a slightly red shifted compared with starting material at 538 nm. The meso-phenyl-BODIPY **21** is slightly hypsochromically shifted with an absorption at 533 nm, there is a 5 nm difference from the starting tri-chloro-BODIPY. The TMS-ethynyl-BODIPY **22** has a significant bathochromic shift at 584 nm, which is due to the conjugation of the triple bond of TMS-ethynyl group with the BODIPY core. ^{1}H NMR spectroscopy showed resonances at 7.11-7.58 ppm for the meso-thiophene group, 7.38-7.50 ppm for meso-phenyl group, and 0.30 ppm for the TMS-ethynyl. The structures of the three new BODIPYs were also confirmed by mass spectrometry, which showed peaks at *m/z* 523.0836 (MW+H) for the meso-thiophene-BODIPY **20** and 517.1238 (MW+H) for the meso-phenyl-BODIPY **21**

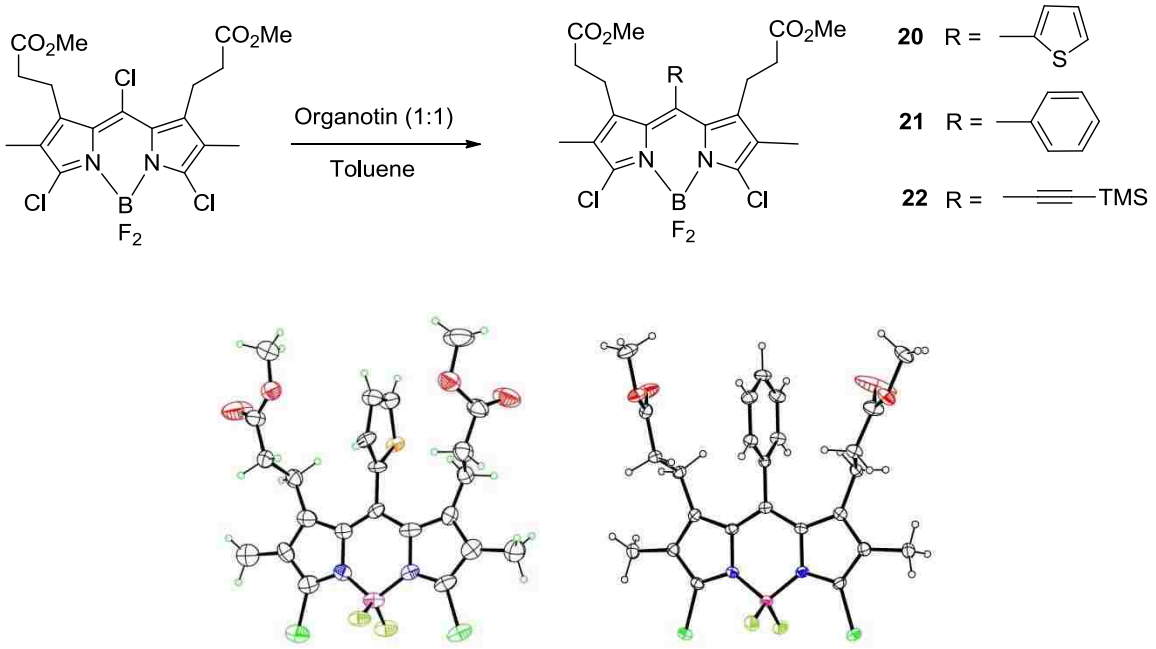

Scheme 5.4: The selective Stille coupling reactions on meso-position of BODIPY **15**, and X-ray scrystal strucyures of BODIPYs **20** and **21**.

For the three new meso-substituted BODIPYs, different functional groups were introduced at the 3,5-positions using 2.4 equivalents of organotin reagents (Scheme 5.5). For meso-thiophene-BODIPY **20**, pheny and TMS-ethynyl groups were introduced to yield the symmetrical BODIPYs **23** and **24**, which have UV/visible absorption maxima at 562 and 608 nm. ^{1}H NMR spectroscopy showed that these two compounds have chemical shift at 7.10-7.59 ppm for BODIPY **23**, which overlapped with meso-thiophene group, and 0.33 ppm for TMS group of BODIPY **24**. The identities of these two product were also confirmed with their mass spectra, with *m/z* at 607.2238 (MW-F) and 667.2473 (MW+H), respectively.

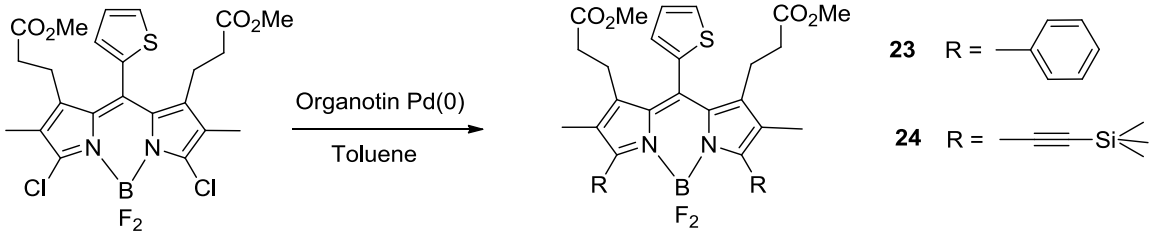

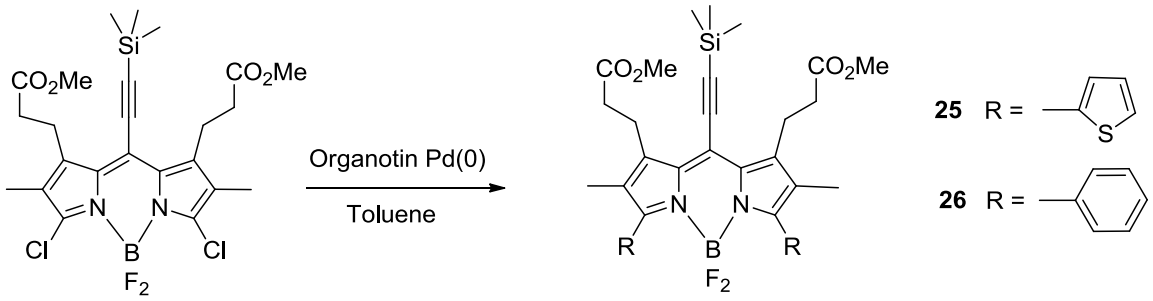

Scheme 5.5: Cross-coupling reaction on 3,5-positions of BODIPYs **23** and **24**.

Similarly, using the meso-TMS-ethynyl-BODIPY **22**, phenyl and thiophene groups were introduced at the 3,5-positions to given the BODIPYs **25** and **26.** These two BODIPYs have UV/visible absorption maxima at 601 and 631 nm, respectively. ^{1}H NMR spectroscopy showed the aromatic areas at 7.36-7.45 ppm and 7.11-7.54 ppm for BODIPYs **25** and **26**, and these two products were structurally confirmed by mass spectrometry, with *m/z* at 651.1888 (MW+H) and 663.2634 (MW+Na). For the meso-phenyl-3,5-dichloro-BODIPY **21**, the thiophene group and TMS-ethynyl group have not been efficiently introduced due to the low yields observed in the reaction. We are optimizing the conditions to achieve better yield for the selective coupling reaction of meso-chloro-BODIPY **21**.

Syntheses of unsymmetric BODIPYs through Stille coupling reactions were also attempted (Scheme 5.6). When two equivalents of organotin reagents were used, the meso-position and one of α-positions (3 or 5-positions) could react with the organotin reagent but leave the other α-position untouched and available for introduction of a third (different) group using a different organotin reagent. However, the generated di-substituted product could continue to react with organotin reagent to give a tri-substituted product as a side product, which should be a minor one due to the electronic and steric effect compared with meso-substituted BODIPY intermediate. Therefore, we tried TMS-ethynyltin first, and the di-substituted product **27** was the major product, a

small fraction was separated and was proven to be tri-substituted product. The BODIPY **27** has an absorption at 615 nm in its UV-visible spectrum. ^{1}H NMR spectroscopy showed two different chemical shifts for the two TMS groups at 0.27 and 0.30 ppm. The identity of the product was also confirmed with its mass spectrum, with *m/z* at 619.2185 (MW+H).

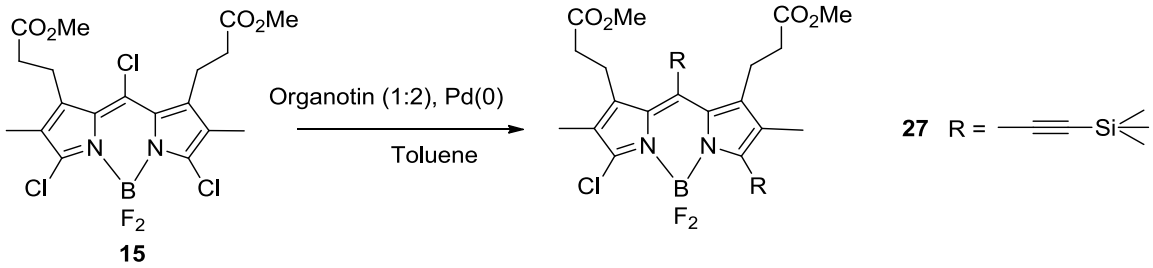

Scheme 5.6: Synthesis of asymmetric BODIPYs through Stille coupling reactions of BODIPY **15**.

5.4. Conclusion

Tri-chloro-BODIPY **15** was synthesized by phosgenation of di-iodopyrroketone **12**, and with this cmpound global and regioselective Stille coupling reactions were explored. Coupling reactions can take place selectively on meso-position (over the 3,5-positions) of BODIPYs. Therefore, the same group can be introduced to the 8, 3, and 5-positions of a BODIPY once, or one group can be selectively introduced to the meso-position, followed by the different groups on the 3 and 5-postions. We also explored the synthesis of asymmetric BODIPYs through Stille coupling reactions by introducing the same group to the meso and one of α-positions simultaneously, followed by introduction of a different group on the one remaining α-position. Some new products were synthesized and characterized by ^{1}H NMR, ^{13}C NMR and mass spectrometry. The results above indicate that it should be possible to introduce one Stille substituent to the meso-position, followed by another to an α–position, and yet a third to the second (remaining) α – position (see below).

5.5 Near Future and Future Work

1. **Syntheses of asymmetric BODIPYs by Stille coupling reactions**.

We already tried the synthesis of asymmetric BODIPYs by changing the ratio between tri-chloro-BODIPYs and organotin reagents (1:2). Another way to synthesize asymmetric BODIPY is to introduce three different groups to 8, 3, and 5-positions one by one accordingly. For example, the meso-position could be substituted by introduction of a pheny group first, followed by introducing a thiophene group to the 3-position, and then the 5-position could be substituted with a TMS-ethynyl group. All these three steps should use one equivalent of organotin reagents. Another route to synthesize

Method I

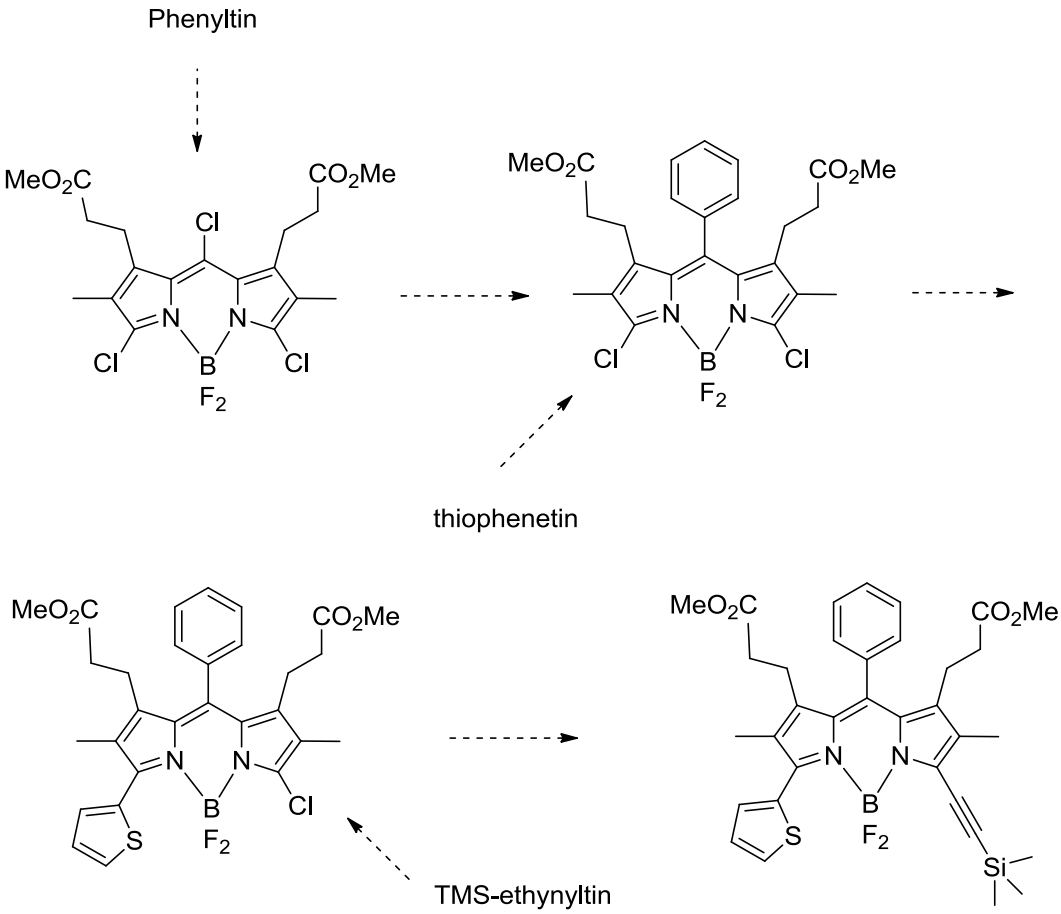

asymmetric BODIPY is by using dichloro-BODIPY **16**; two groups can be introduced to the BODIPY, followed by halogenation (such as bromination) on the 5-position; then another Stille coupling reaction can be performed on the molecule.

Method II

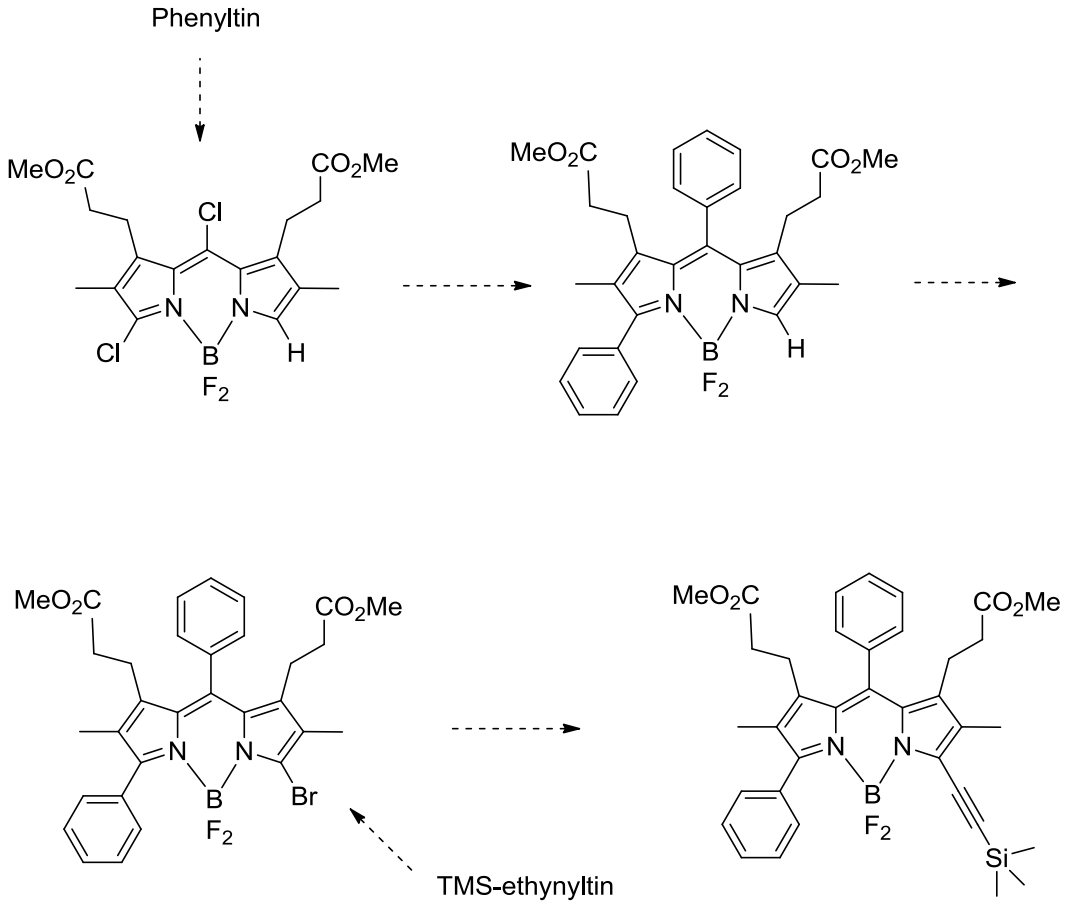

2. Replacement reactions

Selective or global replacement reactions by using various nucleophiles could be explored on tri-chloro-BODIPYs to see if there is selectivity between the meso-position and the 3 and 5-positions of BODIPYs.

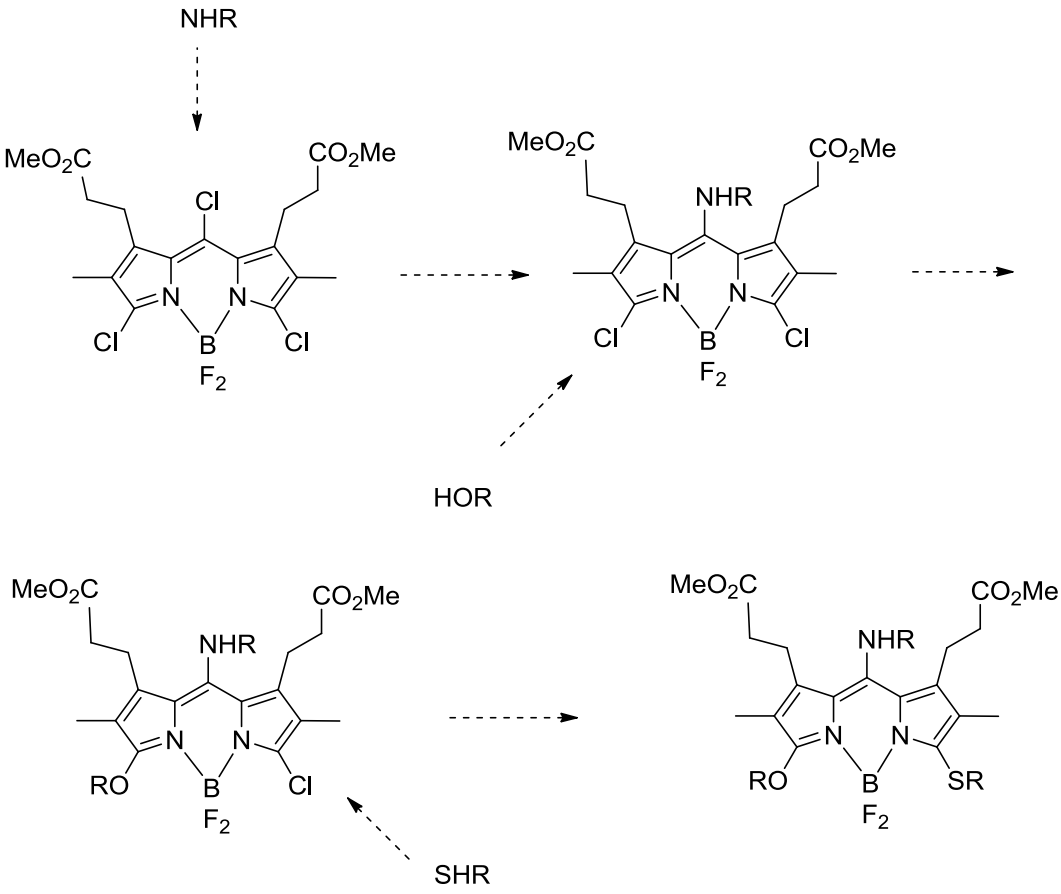

3. Introducing carboranes to BODIPYs.

We already synthesized several BODIPYs which contained TMS-ethynyl group at different postions; the TMS-protective groups can be cleaved and then reacted with decarborane to introduce carboranes to BODIPYs. In this way, one, two or three carboranes could be introduced onto the BODIPY core, and their potential as BNCT reagents can be investigated. The In addition, an ester group can be functionalized to introduce biomolecules such as lysine, etc, polyamines and PEFs to improve their biological properities.

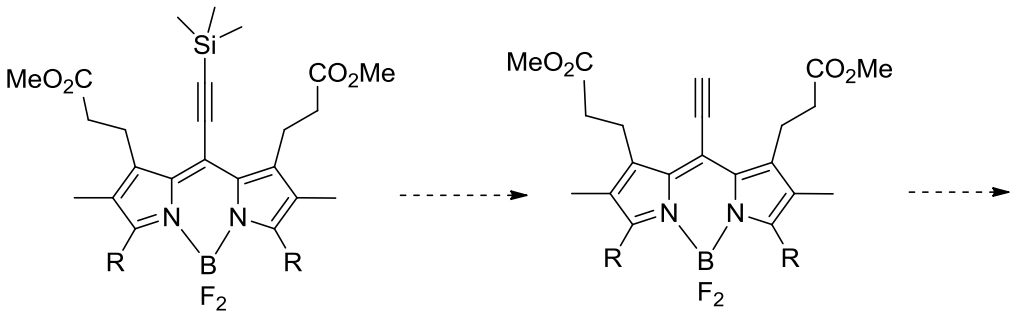

R = Ph, or thiophene

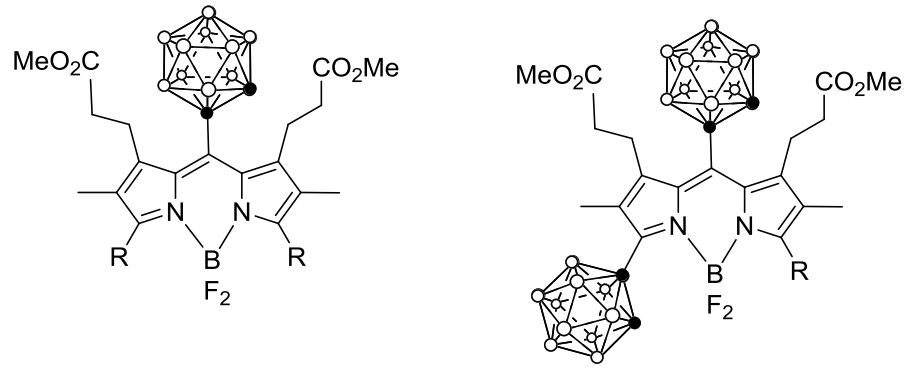

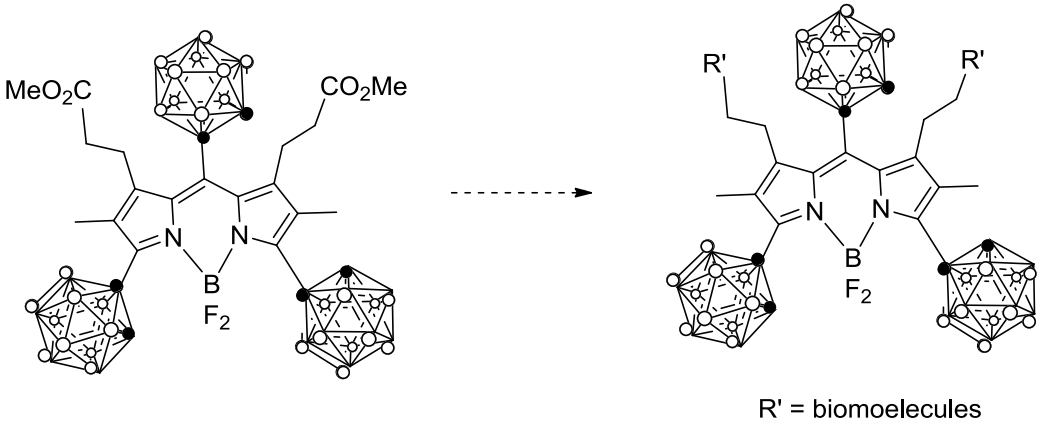

R' = biomoelecules

5.6 Experimental Part

Dimethyl3,3'-(2,2'-carbonylbis(5-iodo-4-methyl-1H-pyrrole3,2diyl))dipropanoateCompound 12: Dipyrromethane **17** (6.14 g, 0.01 mol) was dissolved in 300 ml THF, and then 5% Pd/C (350 mg) catalyst was added. The suspension was stirred under a H_2 atmosphere overnight. After TLC showed that reaction was complete, it was stopped and the reaction solution was passed through a Celite cake to remove the catalyst. The sticky solid on the top of Celite cake was redissolved and neutralized in water with aqueous ammonia and the solution was passed through the Celite cake again. The filtrate was acidified with acetic acid and a precipitate appreared from the aqueous solution. The solid was collected by filtration. The THF part was evaporated and combined with the solid to give total (4.0 g, 92%) of debenzylated product. Then the dicarboxylic acid was suspended in a solution of H_2O (250 ml)/MeOH (100 ml) and $NaHCO_3$ (4.48 g, 51.2 mmol) was added to the solution, which was sonicated to form a slurry, and then a clear solution. Then a solution of I_2 (3.84 g, 14.72 mmol) in methanol (60 ml) was added to the mixture dropwise at room temperature with vigorous stirring and some brown solid was formed during the addition. When the addition of iodine was finished, the stirring was continued for another 2 h and the precipitate was filtered and washed with water, saturated aqueous $NaHCO_3$ and water, followed by hexane to remove excess I_2 to obtain a yellowish solid. The product was left to air dry or dissolved in CH_2Cl_2 and dried over anhydrous Na_2SO_4 before removal of the solvent to give di-iodopyrroketone **10** (4.2 g, 75%). ^{1}H NMR (400 MHz; $CDCl_3$): 9.47 (s, 2H), 3.65 (s, 6H), 2.70 (t, 4H), 2.61 (t, 4H), 2.04 (s, 6H); ^{13}C NMR (100 MHz; $CDCl_3$): 173.81, 173.48, 132.72, 128.49, 126.44, 51.78, 33.91, 20.89, 12.19; HRMS (ESI): *m/z* Calcd for $C_{19}H_{23}I_2N_2O_5$ ($MW+H^+$): 612.9691; found: 612.9697

BODIPYs 15 and 16:

Diiodopyrroketone **12** (1.0 g, 1.63 mmol) was dissolved in $CHCl_3$ (150 ml) and excess phosgene in toluene solution was added to the reaction solution, which turned deep red with time; the reaction was monitored by UV/visible spectrophotometry and the reaction was stopped when a sharp peak appeared at about 480 nm. Then nitrogen gas was passed through solution to purge it of excess phosgene into an aqueous $NaHCO_3$ solution trap. Solvent was removed in vacuo to give a reddish solid, which was dissolved in 150 ml of $CHCl_3$, followed by addition of DIEA (2 ml, 7.0 equiv). The solution was stirred for 30 min, then $BF_3.OEt_2$ (2.1 ml, 10 equiv) was added and the solution turned bright red with a yellow fluorescent under UV long wavelength light. The reaction was monitored by UV/visible spectroscopy which showed a sharp peak at 538 nm. The mixture was left stirring for 24 h before being washed with water, saturated $NaHCO_3$ and brine, and then dried over anhydrous Na_2SO_4 to give a red solid. The product was purified by silica gel column chromatography, eluting with ethyl acetate/hexane (1:4) to give the product **15** as the major fraction and **16** as a minor product. BODIPY **15**: ^{1}H NMR (400 MHz; $CDCl_3$): 3.72 (s, 6H), 3.20 (t, 4H), 2.57 (t, 4H), 2.05 (s, 6H); ^{13}C NMR (100 MHz; $CDCl_3$): 172.50, 143.99, 142.31, 134.94, 128.45, 127.33 51.97, 33.80, 22.78, 8.87; HRMS (ESI): *m/z* Calcd for $C_{19}H_{19}BCl_3F_2N_2O_4$ (MW-H^+): 493.0581; found: 493.0574; BODIPY **16**: ^{1}H NMR (400 MHz; $CDCl_3$): 7.57 (s, 1H), 3.71 (s, 3H), 3.71 (s, 3H), 3.20 (m, 4H), 2.58 (m, 4H), 2.07 (s, 3H), 2.04 (s, 3H); ^{13}C NMR (100 MHz; $CDCl_3$): 172.50, 172.54, 143.54, 142.59, 142.39, 136.82, 130.12, 129.12, 128.67, 127.33, 126.83, 51.95, 51.89, 33.94, 33.87, 22.78, 22.19, 9.86, 8.87; HRMS (ESI): *m/z* Calcd for $C_{19}H_{121}BCl_3FN_2O_4$ (MW-F): 441.0955; found: 441.0935.

General Procedure for Stille Coupling Reactions:

Global coupling reactions: BODIPY **15** (15 mg, 0.03 mmol) and $Pd(PPh_3)_4$ (3.0-5.0 mg, 8%) and were added to a round bottomed flask. The flask was flushed with argon and

then anhydrous toluene (15 ml) was injected, followed by injection of the organotin reagent (0.045 mmol). The solution was refluxed for 12 h until the starting material disappeared from TLC and the UV/visible spectrum gave a sharp peak around 600 nm. Then toluene was removed and the residue was taken up in CH_2Cl_2 and washed with water, brine and then dried over anhydrous Na_2SO_4. The crude product was purified by chromatography to give the fully (tri-) substituted products.

BODIPY 17: ^{1}H NMR (400 MHz; $CDCl_3$): 7.56-7.49 (m, 5H), 7.20-7.09 (m, 4H), 3.63 (s, 6H), 2.33-2.22 (m, 6H), 2.00 (s, 6H), 1.94-1.86 (m, 2H); ^{13}C NMR (100 MHz; $CDCl_3$): 172.53, 149.74, 142.43, 134.43, 133.20, 132.97, 131.69, 129.72, 128.78, 128.02, 127.35, 127.23, 51.63, 35.08, 21.41, 10.62. HRMS (ESI): *m/z* Calcd for $C_{31}H_{30}BF_2N_2O_4S_3$ ($MW+H^+$): 638.146; found: 638.143.

BODIPY 18: ^{1}H NMR (400 MHz; $CDCl_3$): ^{1}H NMR (400 MHz; $CDCl_3$): 7.53-7.38 (m, 15H), 3.60 (s, 6H), 2.12 (t, 4H), 2.00 (m, 4H), 1.80 (s, 6H).

BODIPY 19: ^{1}H NMR (400 MHz; $CDCl_3$): 3.69 (s, 6H), 3.25 (t, 4H), 2.25 (t, 4H), 2.08 (s, 6H). 0.32 (s, 9H), 0.28 (s, 9H); ^{13}C NMR (100 MHz; $CDCl_3$): 172.84, 140.51, 135.96, 134.72, 132.80, 118.30, 113.96, 113.33, 99.15, 96.43, 51.67, 34.20, 21.39, 14.11, 9.52; HRMS (ESI): *m/z* Calcd for $C_{34}H_{48}BF_2N_2O_4Si_3$ ($MW+H^+$): 680.3014; found: 680.680.3001.

Selective Stille Coupling Reactions:

The selective coupling reactions followed the procedure of general coupling reactions. The only difference was that 1.0 equiv of organotin reagent was used instead of excess organotin reagents.

BODIPY 20: ^{1}H NMR (400 MHz; $CDCl_3$): 7.56 (dd, 1H), 7.15 (dd, 1H), 7.09 (dd, 1H), 3.62 (s, 6H), 2.28-2.02 (m, 6H), 1.96 (s, 6H), 1.89-1.83 (m, 2H); ^{13}C NMR (100 MHz; $CDCl_3$): 172.14, 145.04, 143.34, 133.48, 132.80, 130.97, 129.12, 128.48, 127.41, 126.92,

51.72, 34.84, 21.45, 8.83; HRMS (ESI): *m/z* Calcd for $C_{23}H_{23}BCl_2FN_2O_4S$ (MW-F): 523.0833; found: 523.0836

BODIPY 21: ^{1}H NMR (400 MHz; $CDCl_3$): 7.56-7.38 (m, 5H), 3.58 (s, 6H), 2.04 (t, 4H), 1.95 (m, 10H); ^{13}C NMR (100 MHz; $CDCl_3$): 171.93, 144.35, 143.17, 141.09, 133.25, 130.07, 129.90, 129.03, 128.11, 126.49, 51.59, 34.29, 21.35, 8.74; HRMS (ESI): *m/z* Calcd for $C_{25}H_{25}BCl_2F_2N_2O_4$: 517.1268; found: 517.1278.

BODIPY 22: ^{1}H NMR (400 MHz; $CDCl_3$): 3.71 (s, 6H), 3.30 (t, 4H), 2.59 (t, 4H), 2.04 (s, 6H), 0.30 (s, 9H); ^{13}C NMR (100 MHz; $CDCl_3$): 172.58, 143.02, 142.12, 131.69, 126.43, 119.32, 114.82, 98.36, 51.76, 34.15, 21.65, 8.78.

Cross Stille Coupling Reactions:

BODIPY **23** (10 mg, 0.018 mmol) and $Pd(PPh_3)_4$ (2.0 mg, 10%) were added to a round bottomed flask and flushed with argon several times. Anhydrous toluene (10 ml) was added, followed by injection of tributylphenyltin (17 µl, 3.0 equiv); the solution was refluxed for 12 h until a sharp peak appeared in the UV/visible spectrum at 562 nm in CH_2Cl_2. The reaction was stopped and the toluene was removed; the residue was taken up in CH_2Cl_2 and washed with water, brine and the dried over anhydrous Na_2SO_4. The crude product was purified by silica gel column chromatography, eluting with ethyl acetate/hexane (1:4) to give the product as a purple-red solid. All the other cross Stille coupling reaction followed this procedure.

BODIPY 23: ^{1}H NMR (400 MHz; $CDCl_3$): 7.59-7.14 (m, 13H), 3.65 (s, 6H), 2.29-2.27 (m, 6H), 2.07-1.96 (m, 2H), 1.86 (s, 6H); ^{13}C NMR (100 MHz; CDCl3): 172.61, 157.21, 142.46, 134.46, 132.27, 131.85, 129.63, 128.85, 128.67, 128.33, 127.89, 127.78, 127.19, 51.61, 35.08, 21.48, 9.81; HRMS (ESI): *m/z* Calcd for $C_{35}H_{33}BFN_2O_4S$ (MW-F) :607.2238 ; found: 607.2234.

BODIPY 24: ^{1}H NMR (400 MHz; $CDCl_3$): 7.54 (dd, 1H), 7.14 (dd, 1H), 7.08 (dd, 1H), 3.63 (s, 6H), 2.19 (m, 6H), 2.02 (s, 6H), 1.90 (m, 2H), 0.33 (s, 18H); ^{13}C NMR (100 MHz; $CDCl_3$): 172.39, 141.68, 137.79, 133.96, 133.58, 133.24, 129.01, 128.07, 127.21, 113.65, 96.17, 51.58, 34.87, 21.19, 9.54, 0.25; HRMS (ESI): *m/z* Calcd for $C_{33}H_{42}BF_2N_2O_4SSi_2$:667.2465 ; found: 667.2473.

BODIPY 25: ^{1}H NMR (400 MHz; $CDCl_3$): 7.54 (dd, 1H), 7.50 (dd, 1H), 7.11(dd, 1H), 3.72 (s, 6H), 3.39 (t, 4H), 2.64 (t, 4H), 2.09 (s, 6H), 0.32 (s, 18H);); ^{13}C NMR (100 MHz; $CDCl_3$): 172.98, 147.91, 141.22, 133.78, 131.87, 131.72, 129.13, 128.72, 127.30, 119.21, 113.57, 99.39, 51.66, 34.38, 31.59, 21.61, 10.58, 1.10; HRMS (ESI): *m/z* Calcd for $C_{32}H_{35}BFN_2O_4S_2Si$ (MW-F) :633.1885 ; found: 633.1883.

BODIPY 26: ^{1}H NMR (400 MHz; $CDCl_3$): 7.45-7.36 (m, 10H), 3.72 (s, 6H), 3.39 (t, 4H), 2.67 (t, 4H), 1.89 (s, 6H), 0.33 (s, 9H); ^{13}C NMR (100 MHz; $CDCl_3$): 173.04, 155.46, 141.29, 133.06, 131.91, 129.68, 128.78, 128.09, 127.72, 113.28, 99.30, 51.62, 34.42, 21.70, 9.74, 1.09; HRMS (ESI): *m/z* Calcd for $C_{36}H_{39}BFN_2O_4Si$ (MW-F) :621.2756 ; found: 621.2757.

Synthesis of asymmetric BODIPY 27: BODIPY **15** (15 mg, 0.03 mmol) and $Pd(PPh_3)_4$ (3.0-5.0 mmg, 8%) and were added to a round bottomed flask. The flask was flushed with argon and then anhydrous toluene (15 ml) was injected, followed by injection of the organotin reagent trimethyl[(tributylstannyl)ethynyl]silane (22.3 µl, 0.06 mmol). The mixture was refluxed until the starting material disappeared as observed by TLC and the UV/visible spectrum showed a sharp peak around 615 nm. Then the toluene was removed and the residue was taken up in CH_2Cl_2 and washed with water, brine and then dried over anhydrous Na_2SO_4. The crude product was purified by silica gel column chromatography to give the fully substituted products. ^{1}H NMR (400 MHz; $CDCl_3$): 3.68 (s, 3H), 3.68 (s, 3H), 3.25 (m, 4H), 2.56 (m, 4H), 2.07 (s, 3H), 2.02(s, 3H), 0.30 (s, 9H), 0.27 (s, 9H); ^{13}C NMR (100 MHz; $CDCl_3$): 172.79, 172.67, 143.97, 142.12, 140.47,

135.15, 133.30, 132.94, 126.60, 118.91, 114.44, 113.05, 98.73, 96.03, 51.76, 51.72, 34.24, 34.11, 21.67, 21.40, 9.53, 8.82, 0.32, 1.17; *m/z* Calcd for $C_{29}H_{39}BClF_2N_2O_4Si_2$ (MW+H) :619.2198; found: 619.2185.

5.7. Supporting Information

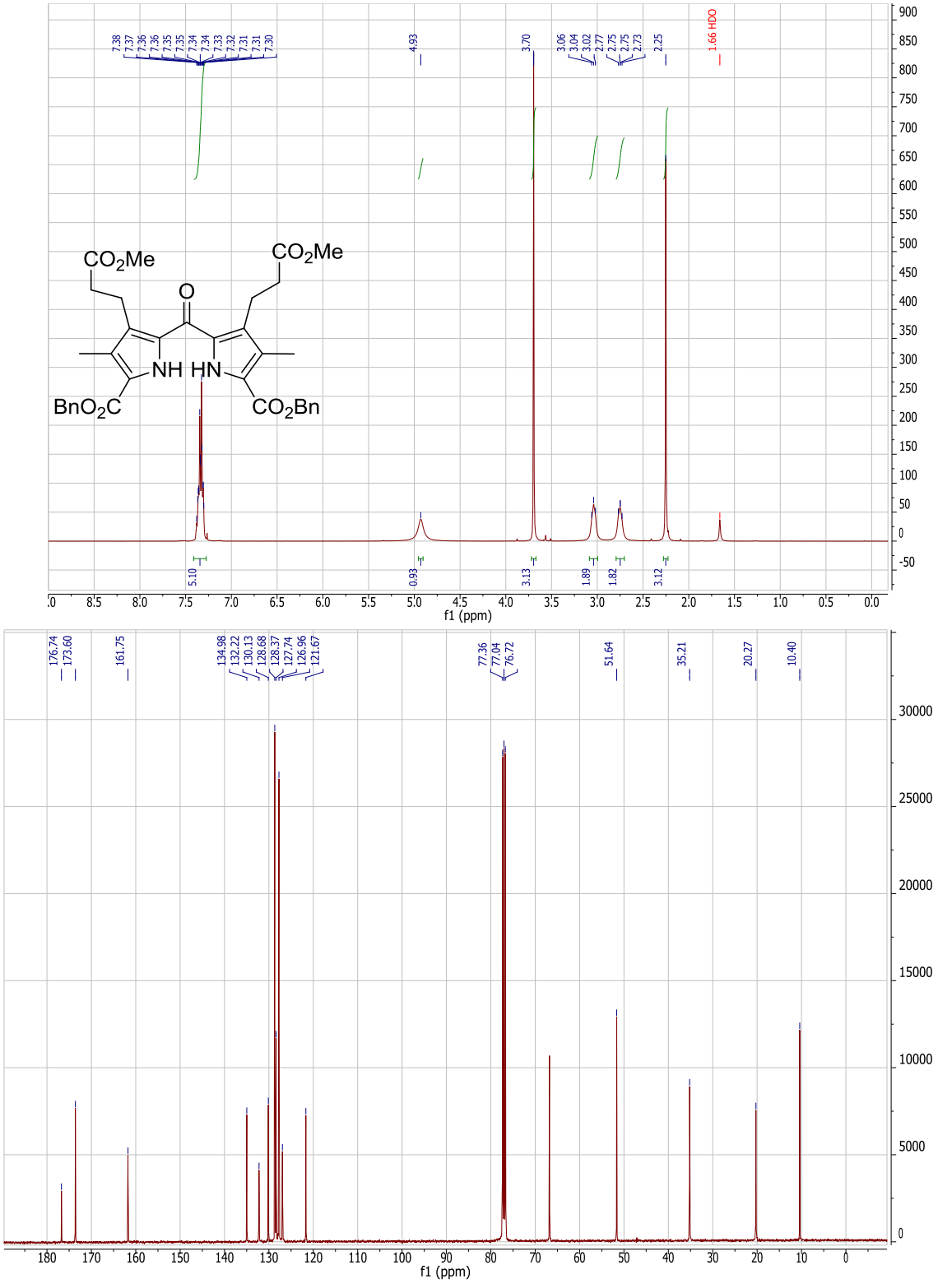

^{1}H and ^{13}C NMR spectra of dibenzyl 5,5'-carbonylbis(4-(3-methoxy-3-oxopropyl)-3-methyl-1H-pyrrole-2-carboxylate) in $CDCl_3$.

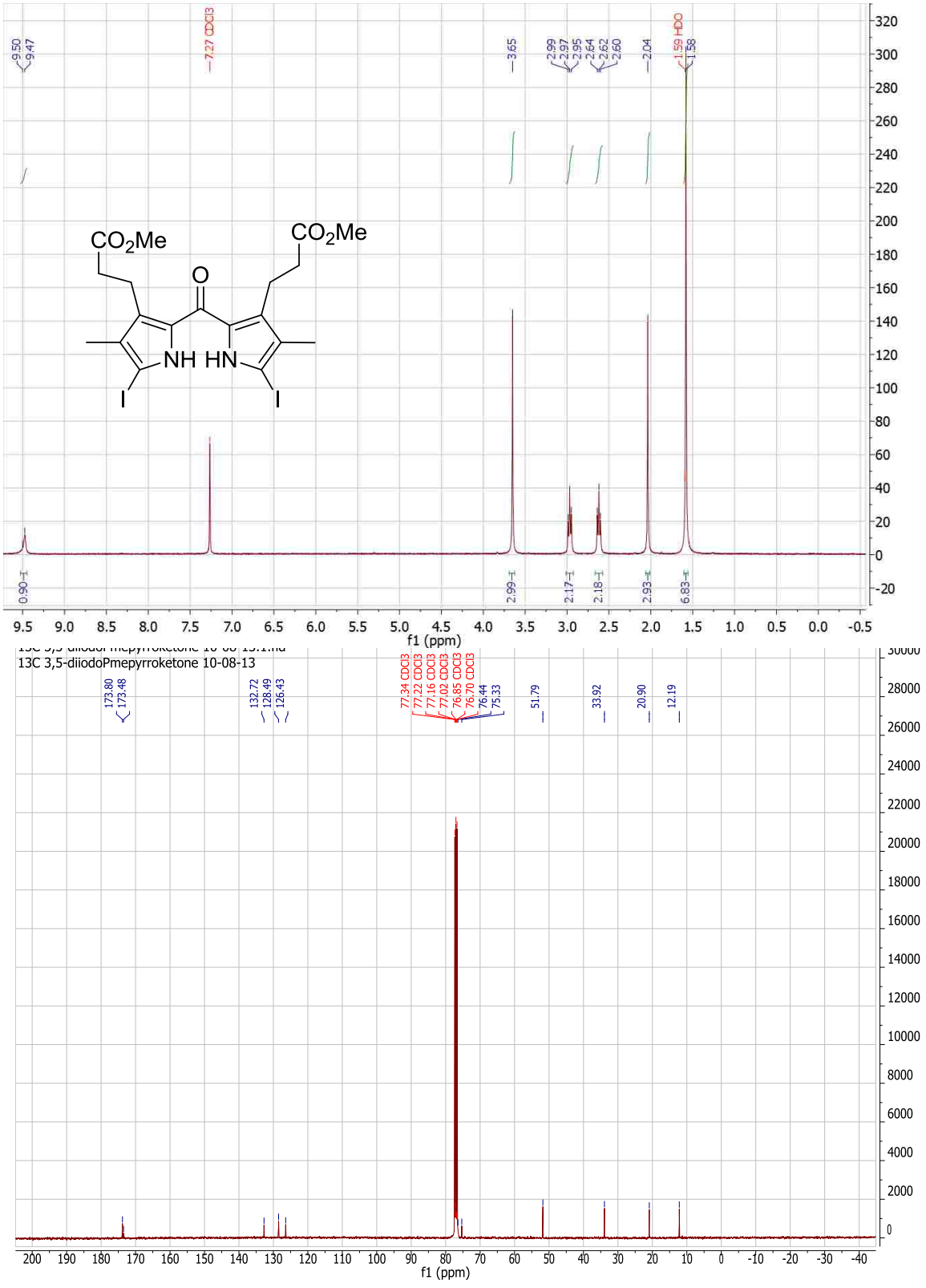

^{1}H and ^{13}C NMR spectra of dimethyl 3,3'-(2,2'-carbonylbis(5-iodo-4-methyl-1H-pyrrole-3,2-diyl))dipropanoate **12** in $CDCl_3$.

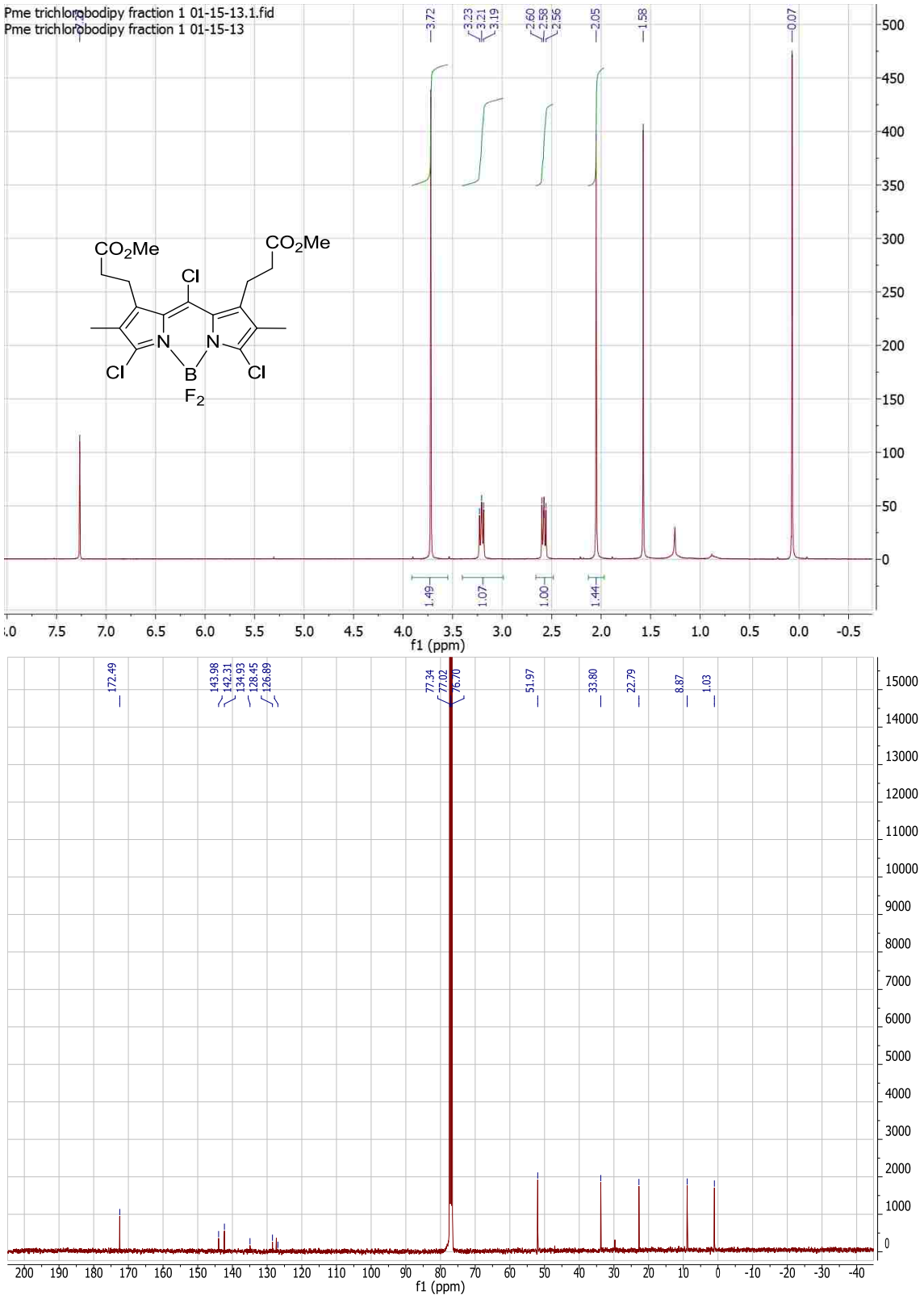

^{1}H and ^{13}C NMR spectra of BODIPY **15** in $CDCl_3$.

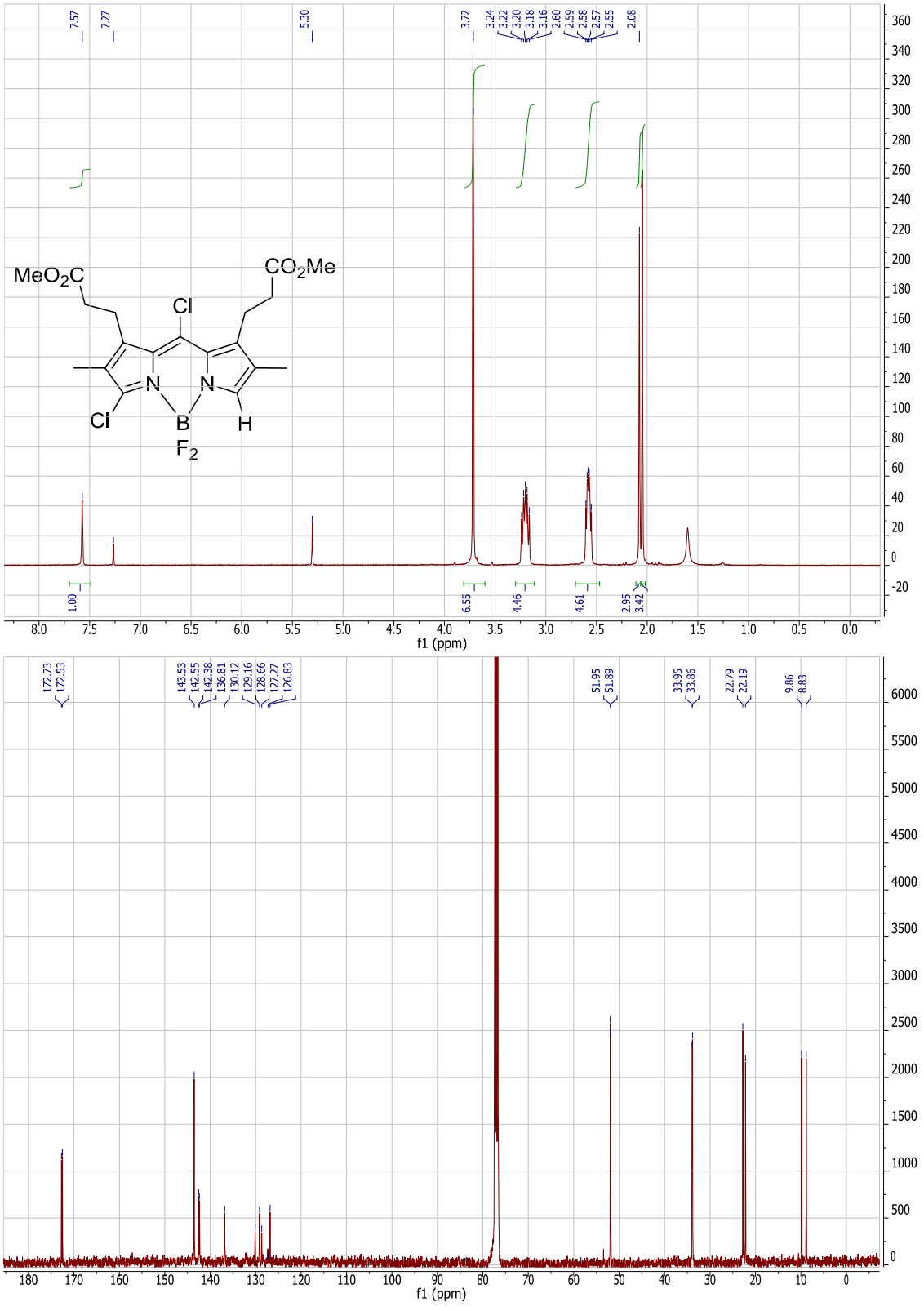

^{1}H and ^{13}C NMR spectra of BODIPY **16** in $CDCl_3$.

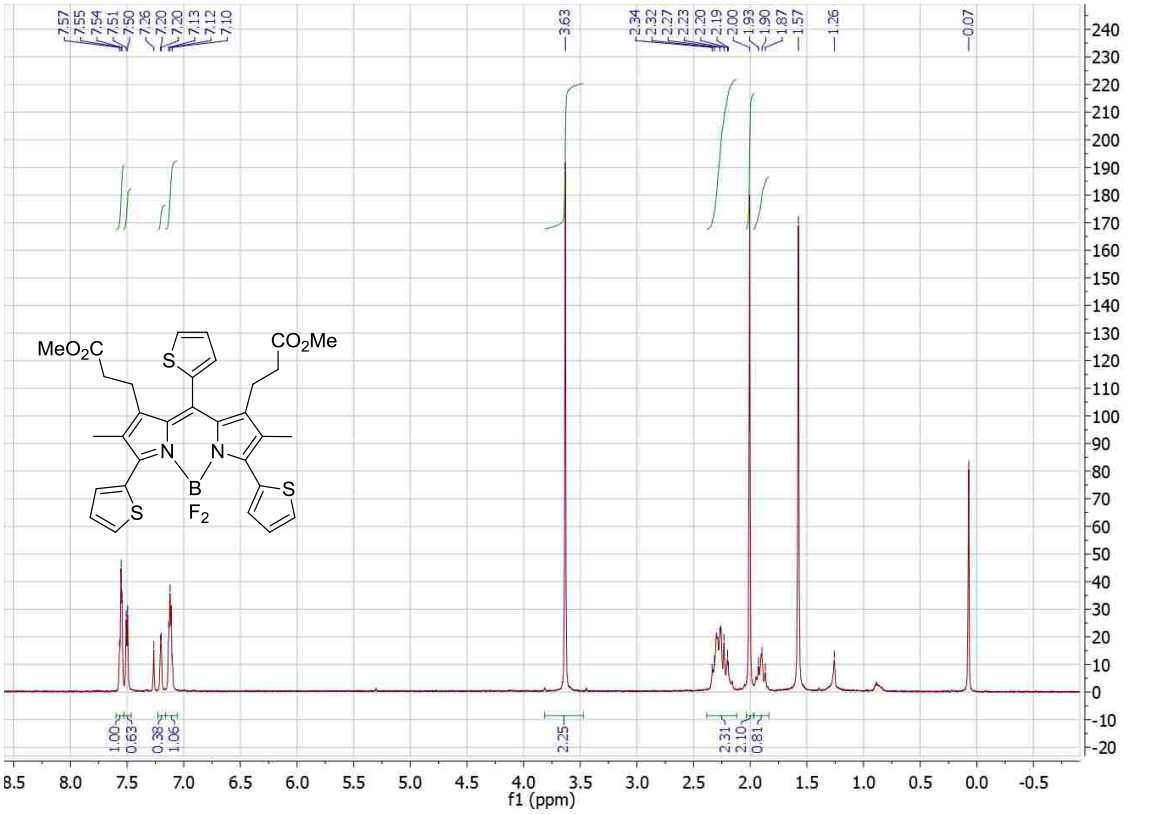

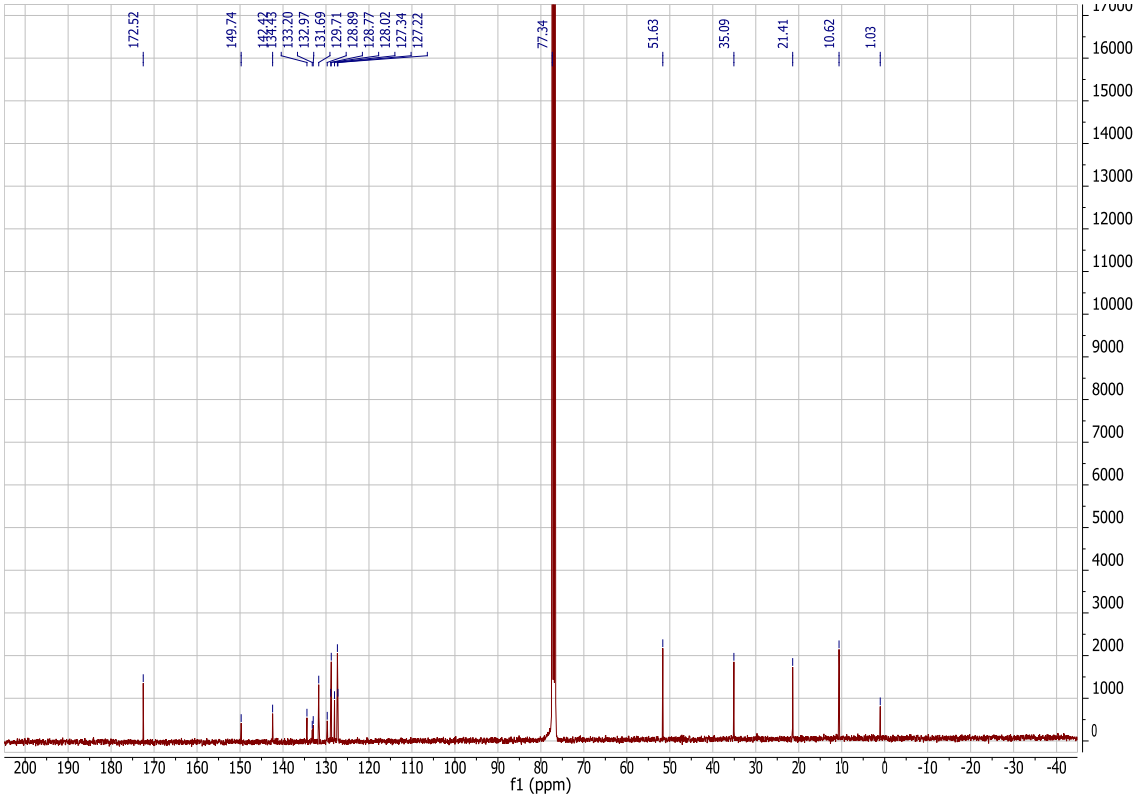

^{1}H and ^{13}C NMR spectra of BODIPY **17** in $CDCl_3$.

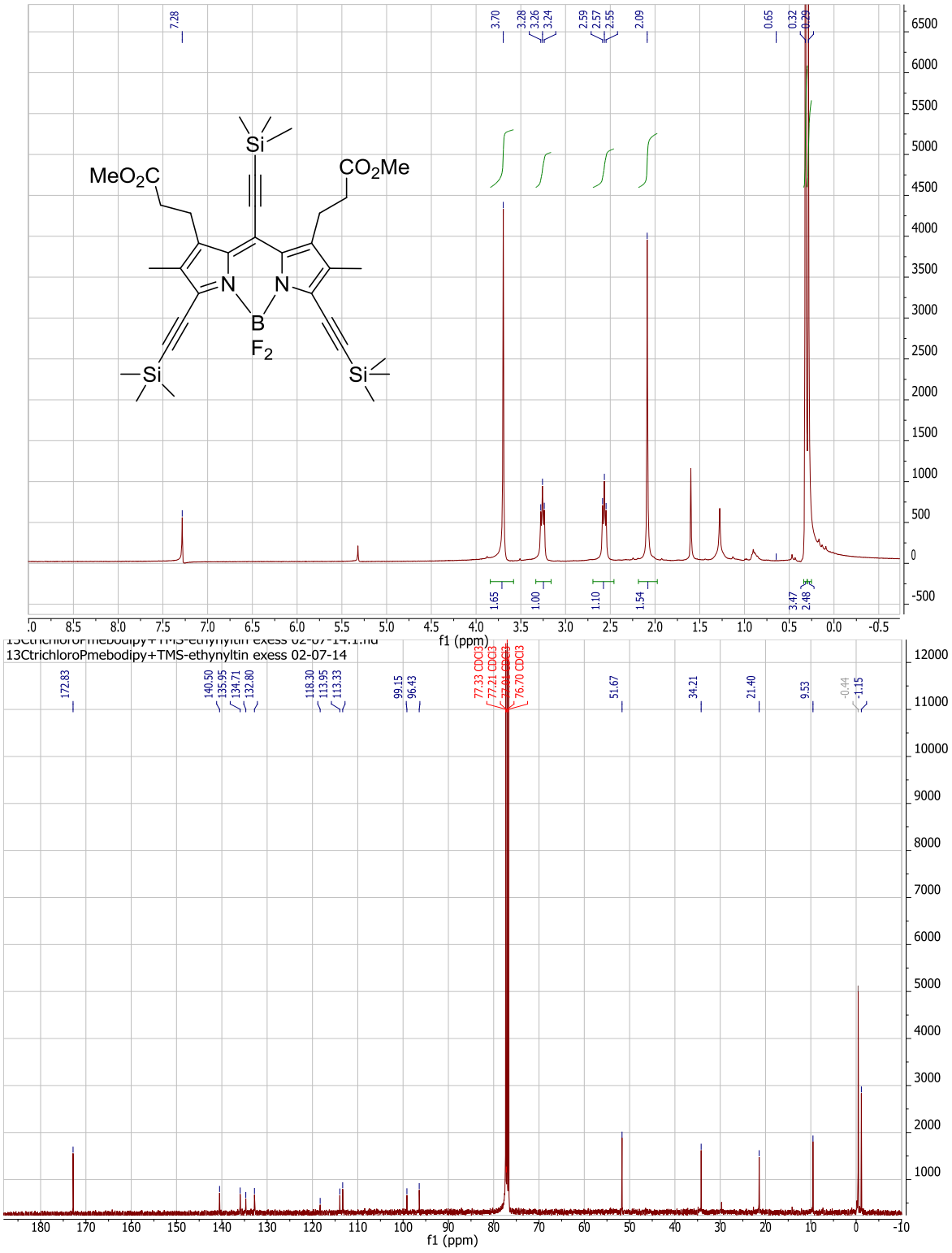

^{1}H and ^{13}C NMR spectra of BODIPY **19** in $CDCl_3$.

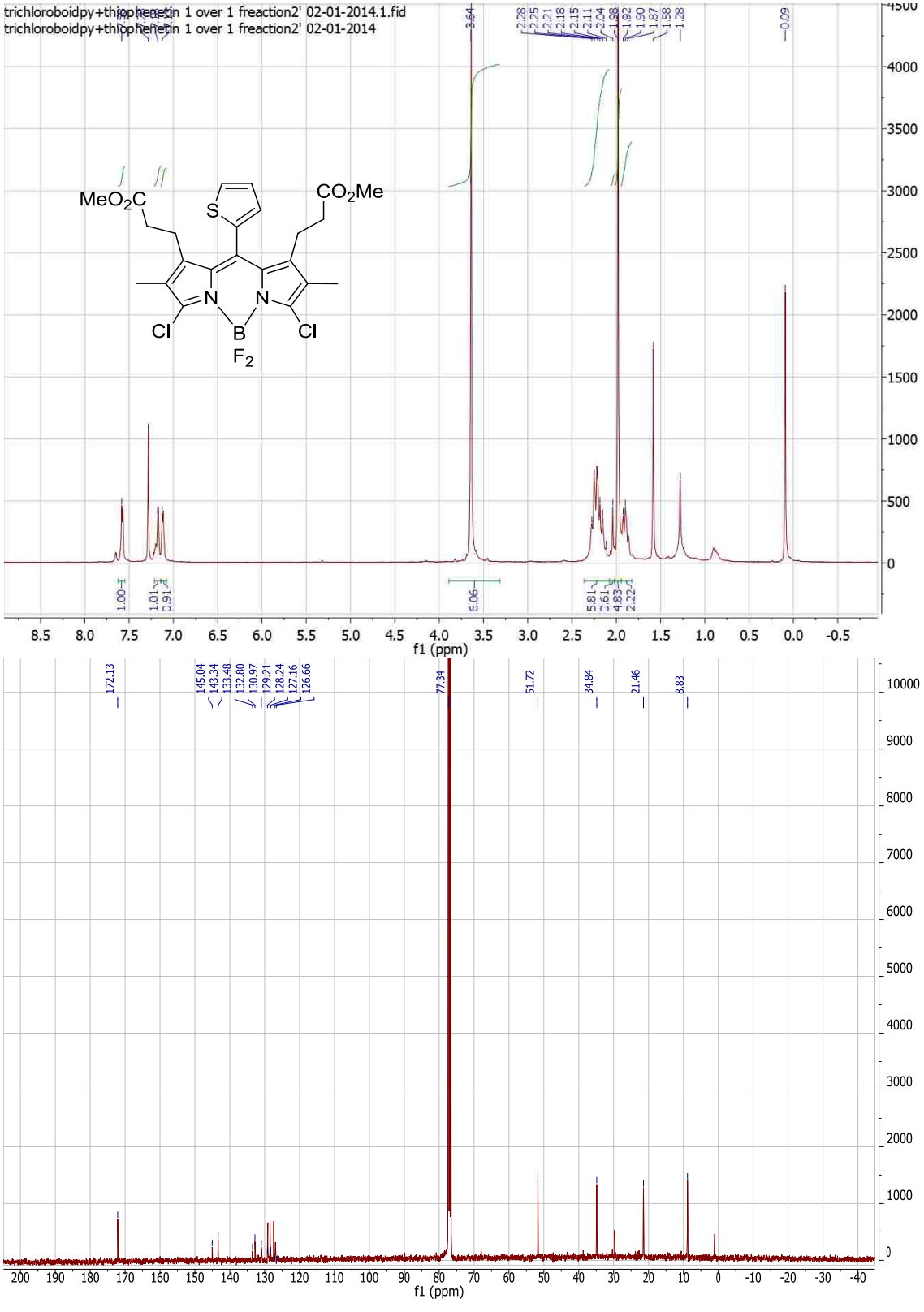

^{1}H and ^{13}C NMR spectra of BODIPY **20** in $CDCl_3$.

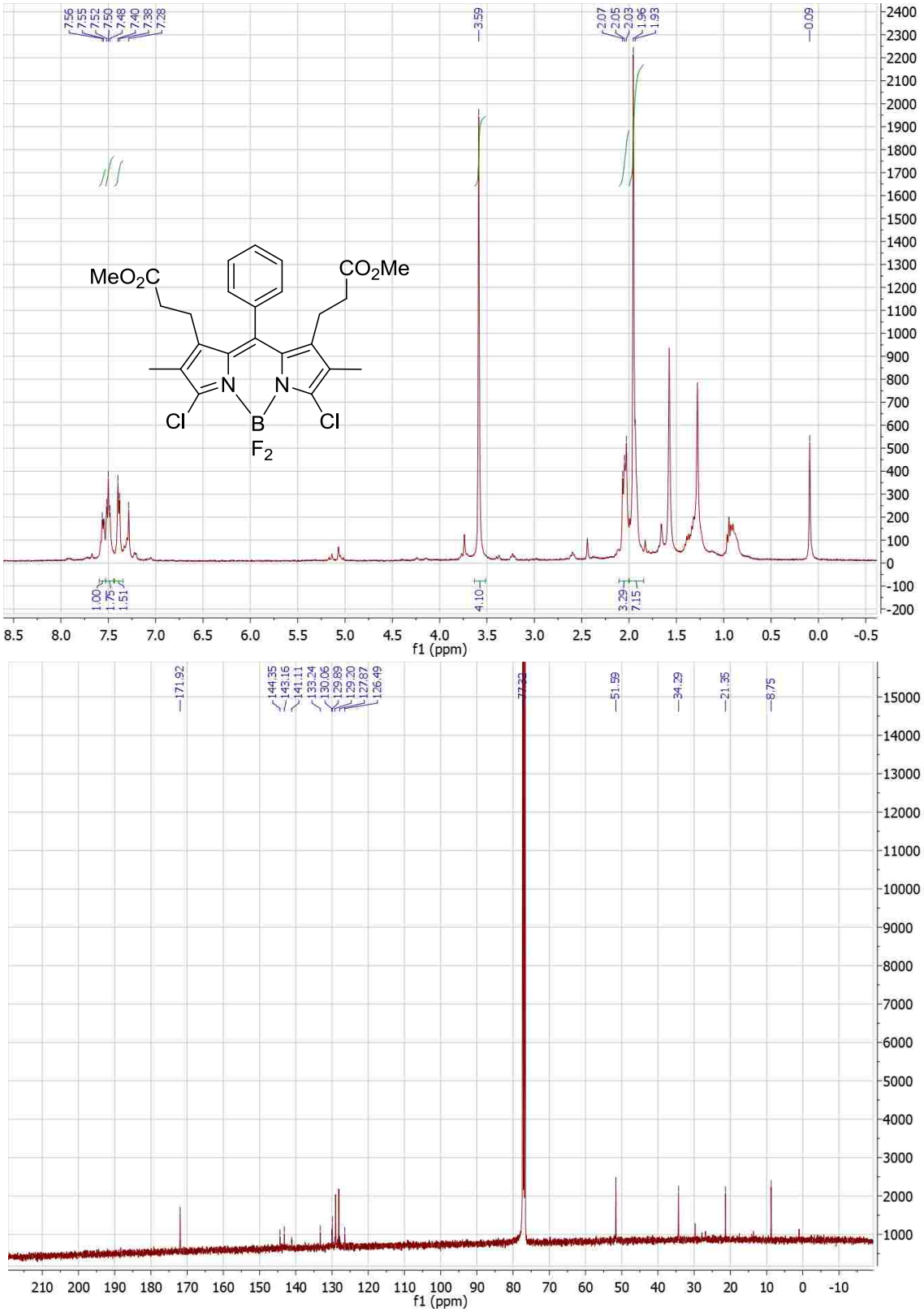

^{1}H and ^{13}C NMR spectra of BODIPY **21** in $CDCl_3$.

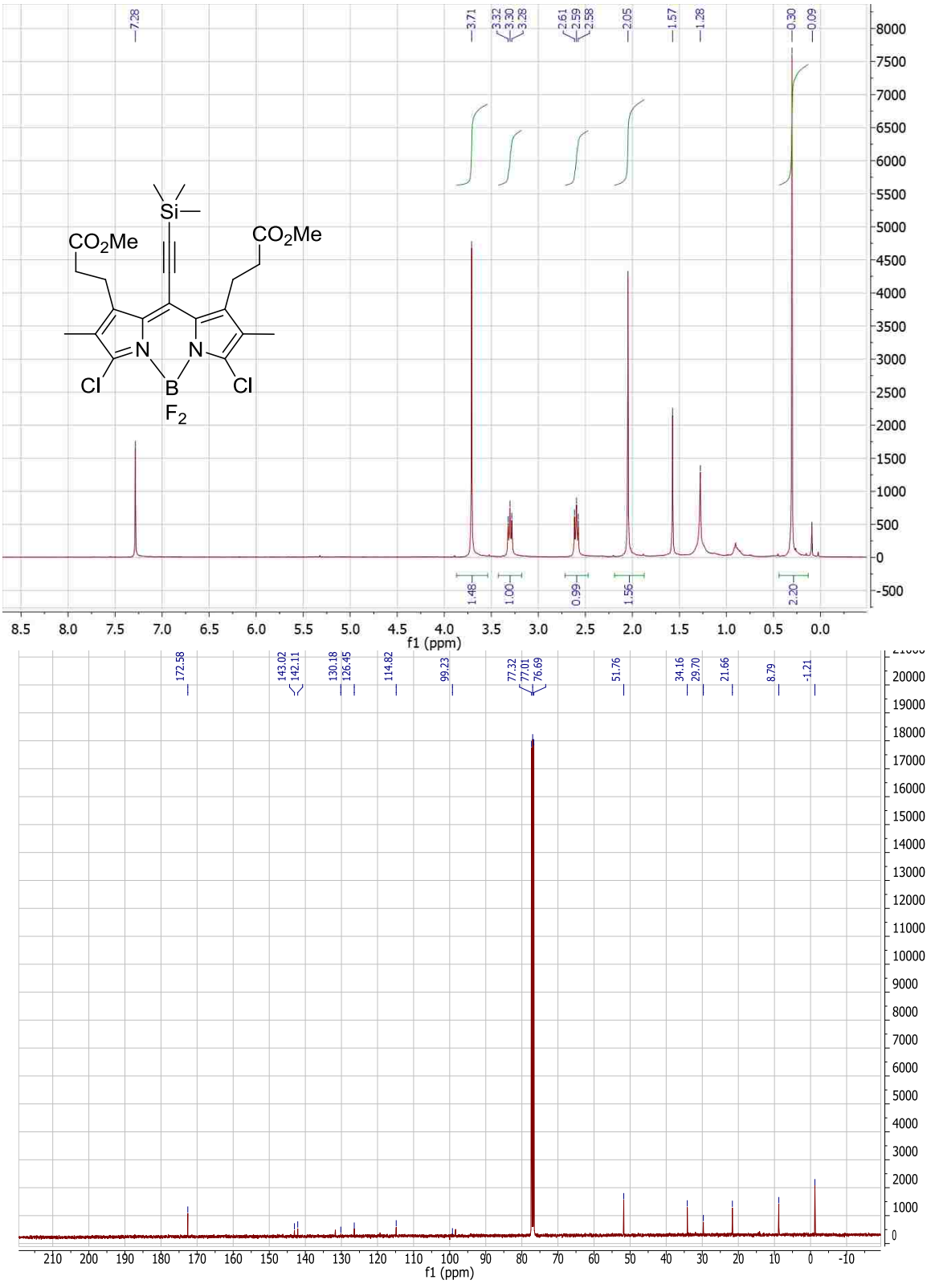

^{1}H and ^{13}C NMR spectra of BODIPY **22** in $CDCl_3$.

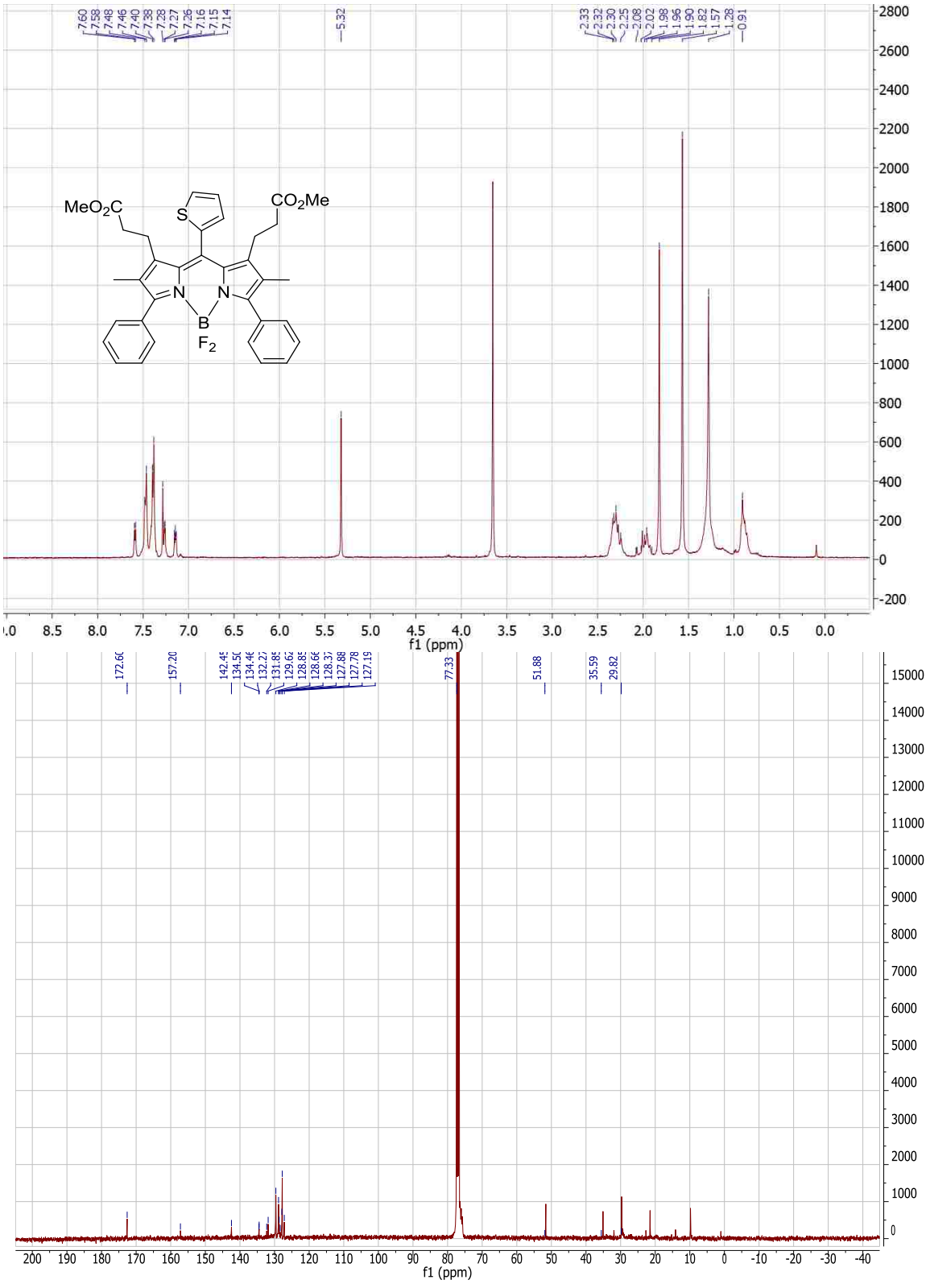

^{1}H and ^{13}C NMR spectra of BODIPY **23** in $CDCl_3$.

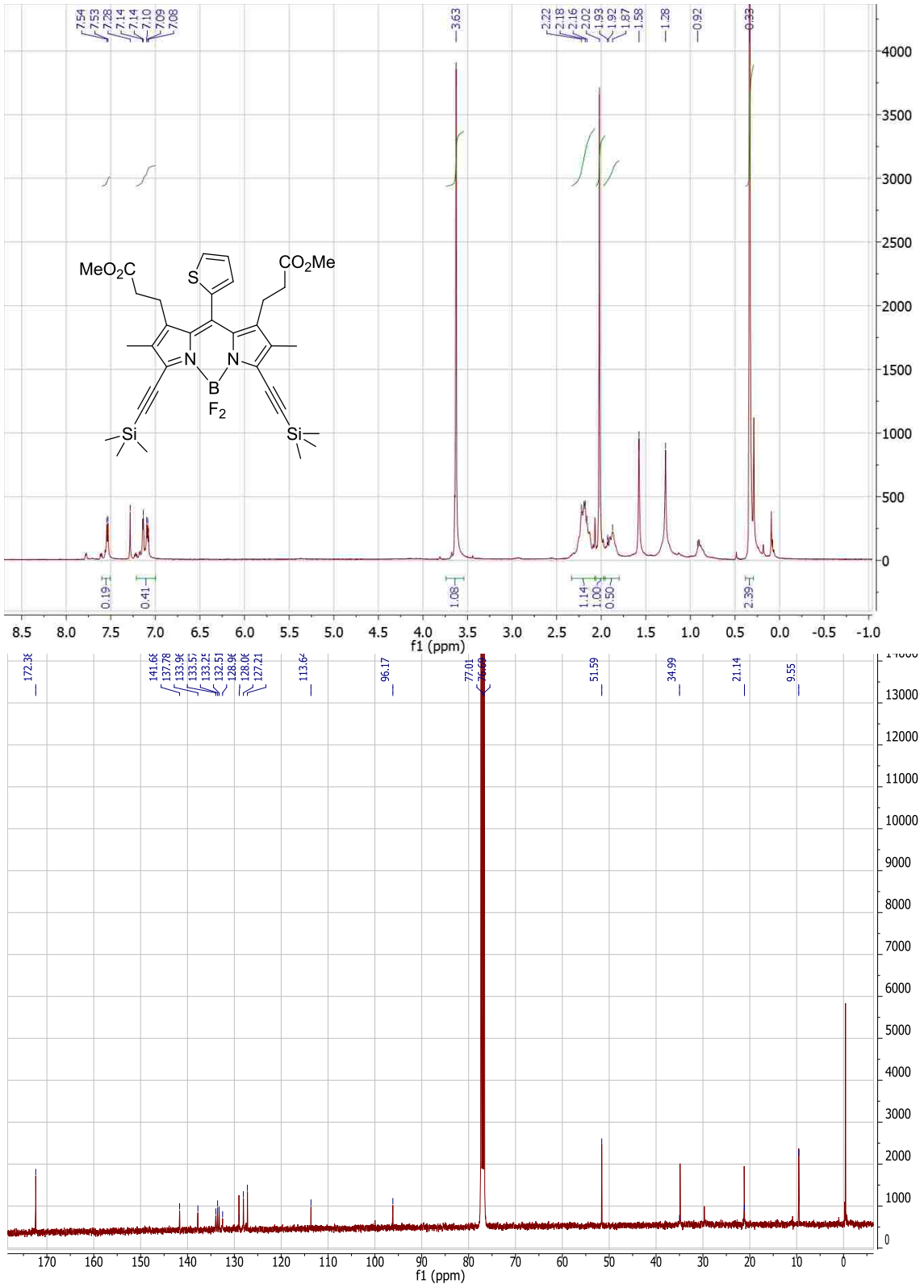

^{1}H and ^{13}C NMR spectra of BODIPY **24** in $CDCl_3$.

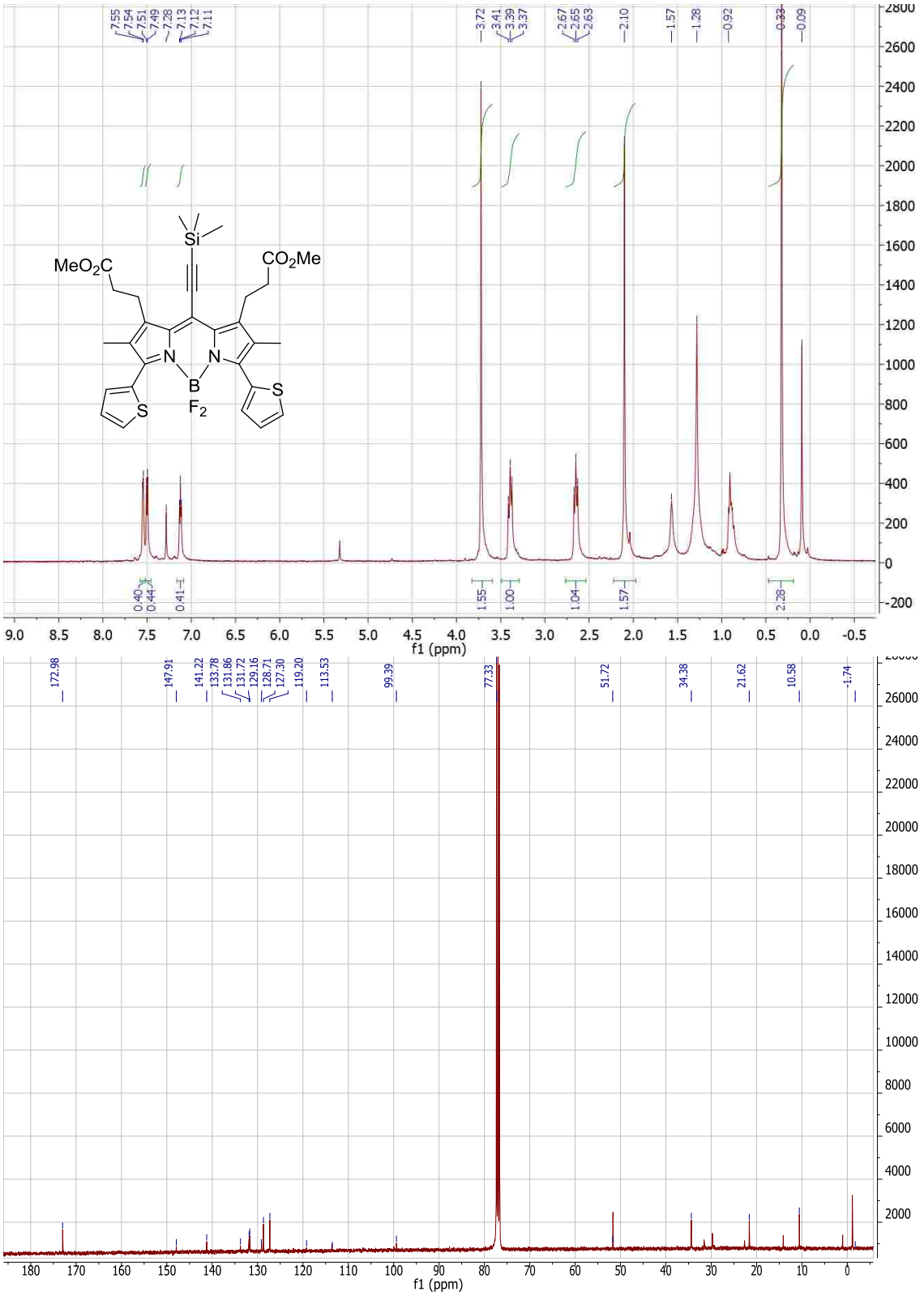

^{1}H and ^{13}C NMR spectra of BODIPY **25** in $CDCl_3$.

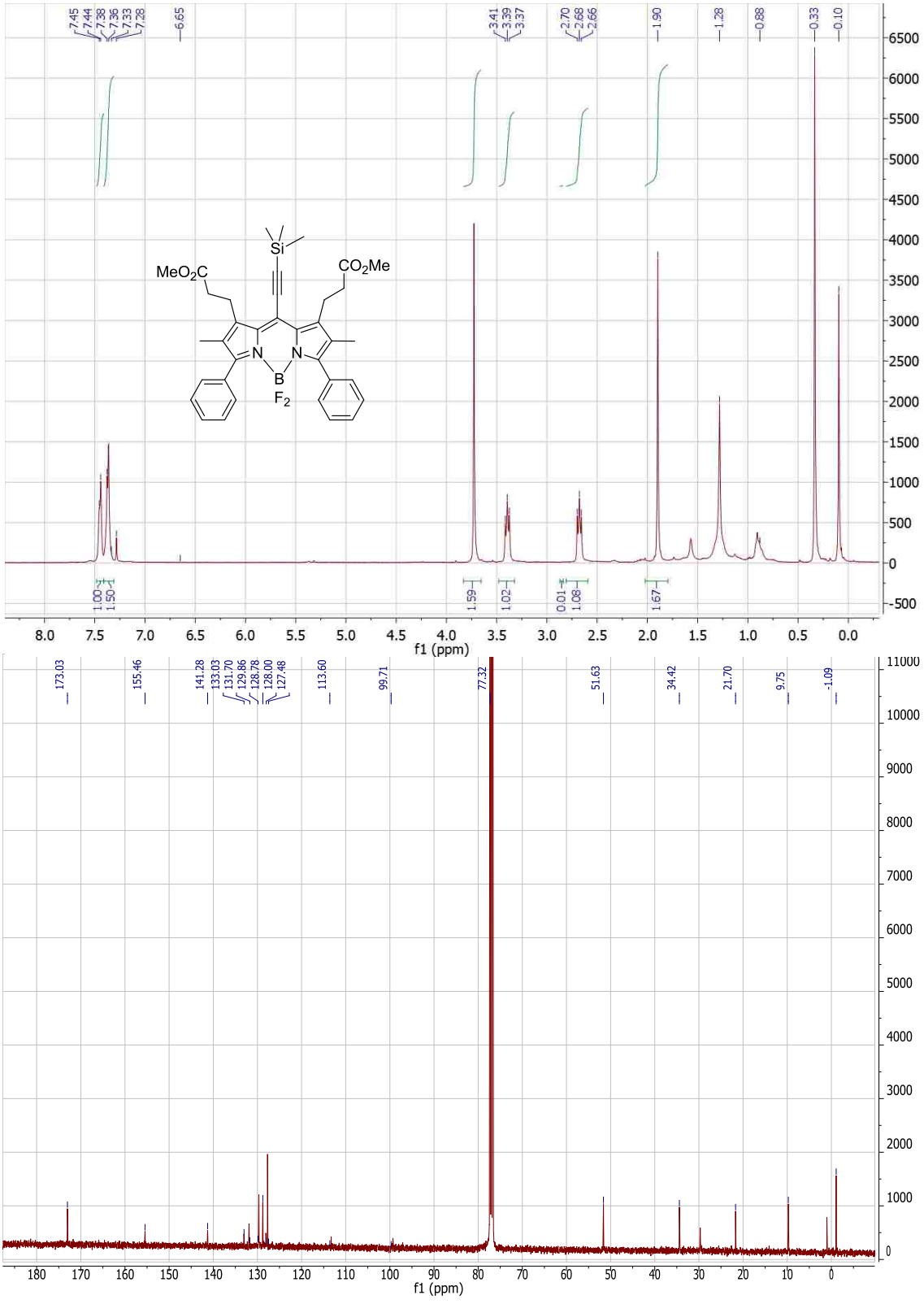

^{1}H and ^{13}C NMR of BODIPY **26** in $CDCl_3$.

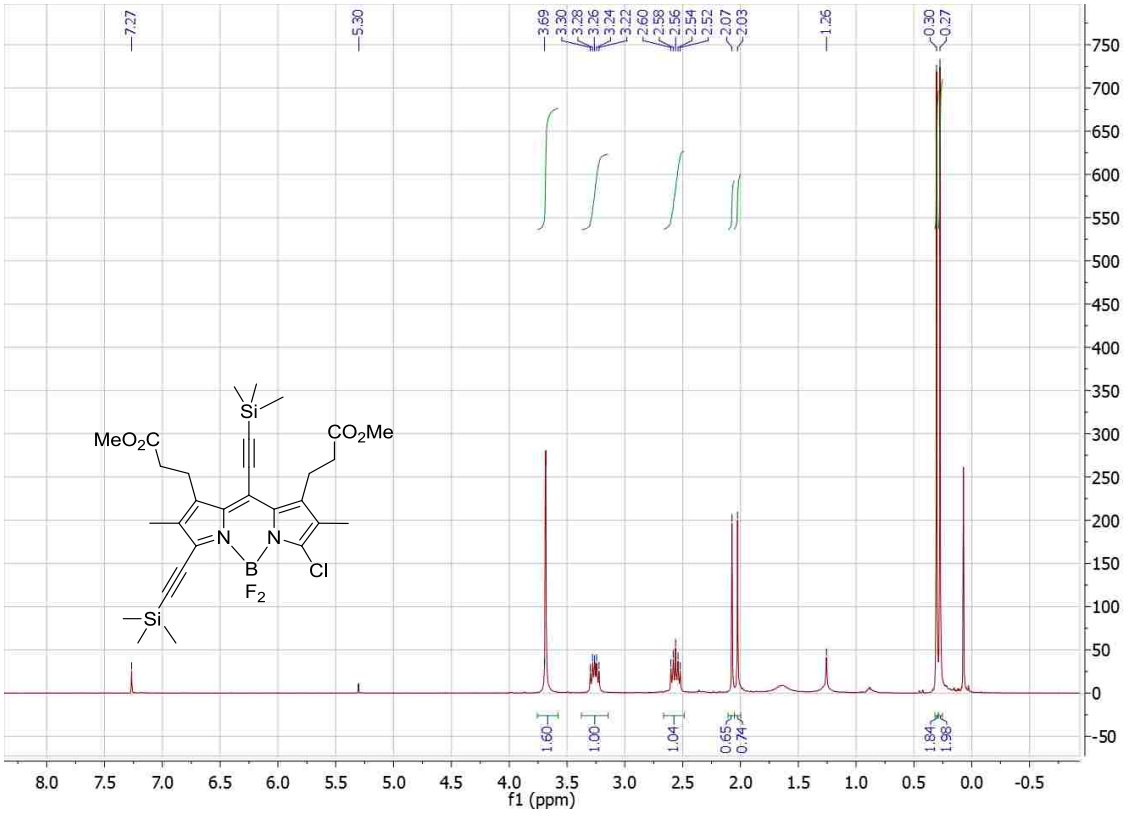

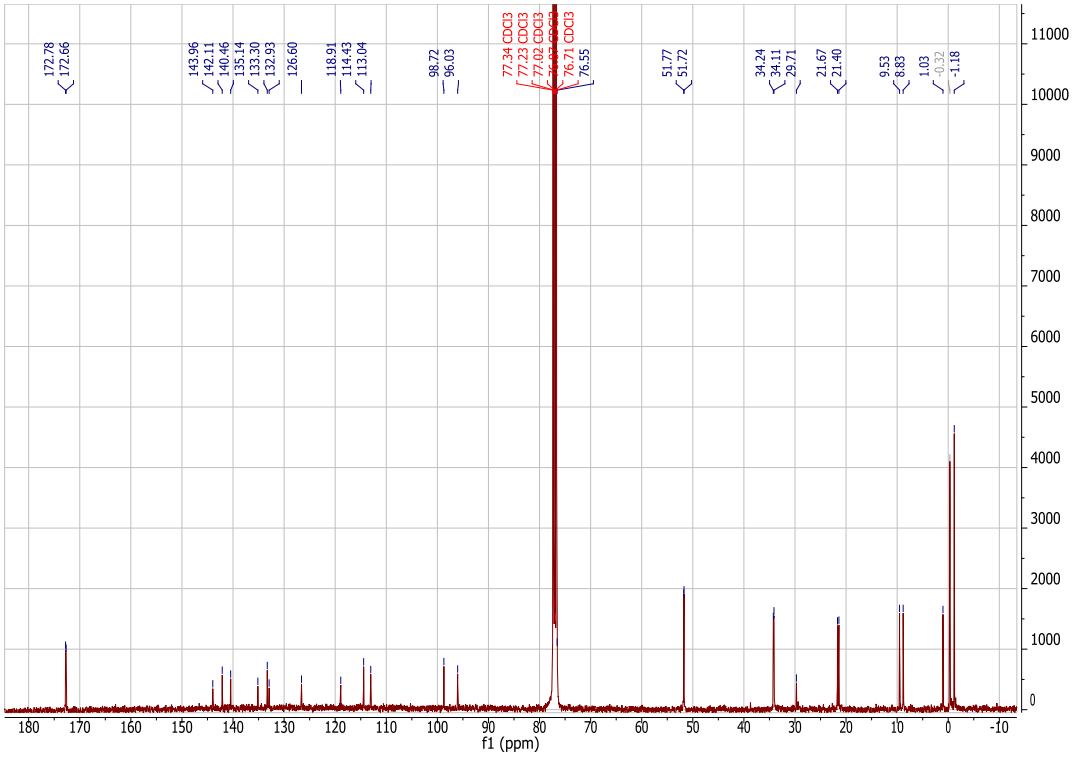

^{1}H and ^{13}C NMR of BODIPY **27** in $CDCl_3$.

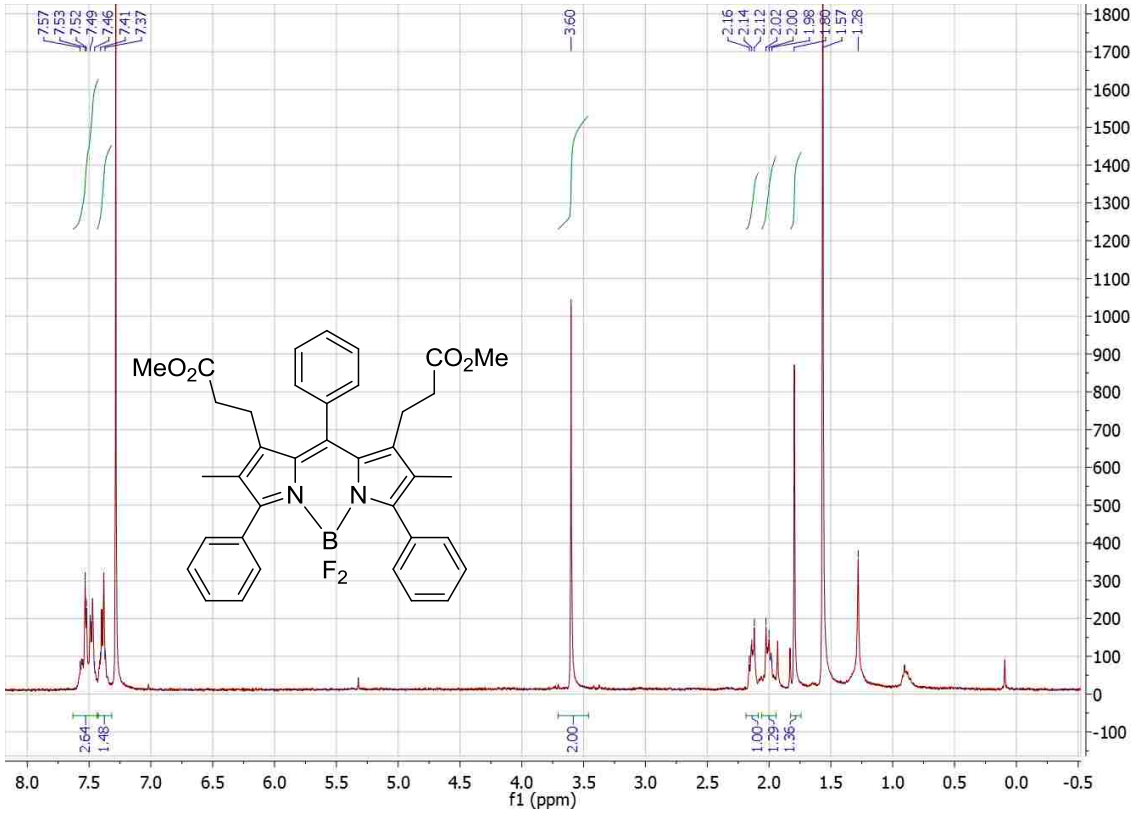

^{1}H NMR spectrum of BODIPY **18** in $CDCl_3$ at 400 MHz.

5.8. References

1. Karolin, L,; Johansson, L. B-A.; Strandberg, L.; and. Ny, T. *J. Am. Chem. Soc*. **1994**, *116* ,1994 7801.

2. Qin, W.; Baruah, M.; Van der Auweraer, M.; De Schryver, F. C.; Boens, N. *J. Phys. Chem*. A, **2005**, *109*, 7371

3 Quartorolo, A. D.; Russo, N.; Sicilia, E. *Chem. Eur. J*. **2006**, *12*, 6797

4. Loudet, A.; Burgess, K. *Chem. Rev*. **2007**, *107*, 4891.

5. Rohand, T.; Qin, W.; Boens, N.; Dehaen, W. *Eur. J. Org. Chem*. **2006**, 4658.

6. Rohand, T.; Baruah, M.; Qin, W.; Boens, N.; Dehaen, W. *Chem. Commun*. **2006**, 266

7. Baruah, M.; Qin, W.; Vallee, R. A.; Beljonne, D.; Rohand, T.; Dehaen, W.; Boens, N. *Org. Lett*. 2**0**05, *7*, 4377.

8. Rurack, K.; Kollmannsberger, M.; Daub, J. *New J. Chem*. **2001**, *25*, 289.

9. Coskun, A.; Akkaya, E. U. *Tetrahedron Lett*. **2004**, *45*, 4947.

10. Kee, H. L.; Kirmaier, C.; Yu, L.; Thamyongkit, P.; Youngblood, W. J.; Calder, M. E.; Ramos, L.; Noll, B. C.; Bocian, D. F.; Scheidt, W. R.; Birge, R. R.; Lindsey, J. S.; Holten, D. *J. Phys. Chem. B* **2005**, *109*, 20433.

11. Shah, M.; Thangaraj, K.; Soong, M.-L.; Wolford, L. T.; Boyer, J. H.; POlitzer, I. R.; Pavlopoulos, T. G. *Heteroat. Chem*. **1990**, *1*, 389.

12. Haugland, . P.; Kang, H. C. U. S. Patent 4774339, **1988**.

13. Yogo, T.; Urano, Y.; Ishitsuka, Y.; Maniwa, F.; Nagano, T. *J. Am. Chem. Soc*. **2005**, *127*, 12162.

14. Suzuki, T.; Tanaka, T.; Higashiguchi, I.; Oda, A. JP Patent 11176572, **1999**.

15. Jiao, Y.; Yu, C.; Uppal, T.; Liu, M.; Li, Y.; Zhou, Y.; Hao, E.; Hu, X.; Vicente, M. G. H. Org. Biomol. Chem*.* 2010*, 8,* 2517.

16. Jiao, L.; Pang, W.; Zhou, J.; Wei, Y.; Mu, X.; Bai, G.; Hao, E. ***J. Org. Chem*****, 2011,** *76*, 9988.

17. Leen, V.; Yuan, P.; Wang, L.; Boens, N.; Dehaen, W. *Org. Lett*. 2012, *14*, 6150.

18. Fischer, H.; Orth, H. *Justus Liebigs Ann. Chem*. 1933, *502*, 237.

19. Ortiz, M. J.; Agarrabeitia, A. R.; Duran-Sampedro, G.; Prieto, J. B.; Lopez, T. A.; Massad, W. A.; Montejano, H. A.; Garcia, N. A.; Arbeloa, I. L. *Tetrahedron* 2012, *68*, 1153.

Vita

Haijun Wang was born in Baoji, China, to Mr. Yuzhang Wang and Mrs. Guaixia Feng. He completed his Bachelars of Science in chemistry from northwest university in 2001. Then he worked as a chemist engineer in lubricating oil research and development center, PetroChina Company Limited for one year. Then he finished his Master of Science in physical organic chemistry from State Key Laboratory of Oxo Synthesis & Selective Oxidation, Chinese Academy of Sciences in 2006 and worked as a research assistant in Laboratory of Advanced Polymer Materials, Chinese Academy of Sciences for two years. In 2008, he was accepted to Graduate School Doctoral program at Louisiana State University (LSU) in the Department of Chemistry and joined prof. Kevin M. Smith research group in January 2009. Haijun Wang is currently a candidate for the Doctor of Philosophy in organic chemistry, which will be awarded to him at the May 2014 Commencement at LSU, Baton Rouge.